SEDIMENTOLOGICAL INVESTIGATIONS ON SEDIMENTS FROM THE WESTERN CONTINENTAL MARGIN OF INDIA: INFERENCES ON THE PALAEOCEANOGRAPHY DURING LATE QUATERNARY

Thesis submitted for the degree of

DOCTOR OF PHILOSOPHY

in

MARINE SCIENCE

to the

GOA UNIVERSITY

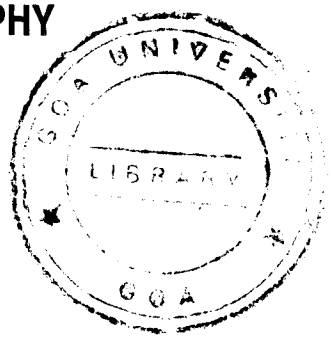

by

Thamban Meloth

National Institute of Oceanography

Dona Paula - 403 004, Goa, India

July 1998

To

My Parents

STATEMENT

As required under the University ordinance 0.19. 8. (vi), I state that the present thesis entitled **"SEDIMENTOLOGICAL INVESTIGATIONS ON SEDIMENTS FROM THE WESTERN CONTINENTAL MARGIN OF INDIA: INFERENCES ON THE PALAEOCOEANOGRAPHY DURING LATE QUATERNARY"**, is my original contribution and the same has not been submitted on any previous occasion. To the best of my knowledge, the present study is the first comprehensive work of its kind from the area mentioned.

The literature related to the problem investigated has been cited. Due acknowledgements have been made wherever facilities and suggestions have been availed of.

Thamban.M

Thamban Meloth

CERTIFICATE

This is to certify that the thesis entitled **"SEDIMENTOLOGICAL INVESTIGATIONS ON SEDIMENTS FROM THE WESTERN CONTINENTAL MARGIN OF INDIA: INFERENCES ON THE PALAEOCEANOGRAPHY DURING LATE QUATERNARY"**, submitted by **Mr. Thamban Meloth** for the award of the degree of Doctor of Philosophy in Marine Science is based on his original studies carried out by him under my supervision. The thesis or any part thereof has not been previously submitted for any other degree or diploma in any universities or institutions.

V. Purnachandra Rao

Place : Dona Paula

Date : 31.07.1998

Dr. V. Purnachandra Rao

Research Guide,
Assistant Director
Geological Oceanography Division
National Institute of Oceanography
Dona Paula - 403 004

All the corrections suggested by the Examiners have been incorporated

8.2.99

V. Purnachandra Rao

8.2.99

We shall not cease from exploration
And the end of all our exploring
Will be to arrive where we started
And know the place for the first time.
Through the unknown, remembered gate
When the last of earth left to discover
Is that which was the beginning;
At the source of the longest river
The voice of a hidden waterfall ....
Not known, because not looked for,
But heard, half heard, in the stillness
Between two waves of the sea.

- T. S. Eliot

CONTENTS

LIST OF TABLES

LIST OF FIGURES

Chapter 1

Chapter 2

Chapter 3

Chapter 4

Chapter 5

Chapter 6

Indian Ocean Monsoon

Monsoonal variations in the Indian Ocean give rise to seasonal changes in phytoplankton concentrations. Here, following a period of pre-monsoon calm (May, June, composite, left), strong summer southwesterly monsoon winds generate upwelling of nutrient-rich waters, leading to the development of bloom conditions (September, October composite, right).

PREFACE

"Upon this gifted age, in its dark hour,
Rains from the sky, a meteoric shower
Of facts .... they lie unquestioned ...."
- Edna St. Vincent Millay

The Indian Ocean summer monsoon represents one of the Earth's most dynamic interactions between atmosphere, oceans and continents. Arabian Sea is characterised by a unique, seasonally reversing monsoonal wind-induced upwelling and related high primary productivity. The high rate of surface productivity and subsequent oxidation below the thermocline is associated with a very high oxygen demand at intermediate depths, leading to an exceptionally broad and stable mid-water Oxygen Minimum Zone (OMZ). The strength of the monsoon winds, upwelling in the Arabian Sea and precipitation in the Indian subcontinent are all coupled together. Enhanced summer monsoon leads to increased continental humidity and related high riverine input to the Arabian Sea. The biological productivity, sea level and intensity of the monsoons varied regionally and also significantly in the geological past. The sediments on the continental margins of the Arabian Sea should therefore contain a geological record of these past variations. Investigations on the sediments of continental margins should not only throw light on the past climate and oceanographic changes recorded in the sedimentary environment, but also help in understanding the position and intensity of the OMZ and factors controlling the accumulation of organic carbon. Eventhough, many studies have been carried out on palaeo-monsoons using a variety of geological proxies in the western Arabian Sea (Oman margin), the eastern Arabian Sea (Indian margin) has been comparatively little studied. Palaeoceanographic studies in the western continental margin of India are very critical, since this area supports a high productivity-induced oxygen minima and high organic accumulation in the bottom sediments.

Detailed studies have been carried out on sediment cores from the western continental margin of India, in order to delineate the past climatic and oceanographic changes. A variety of geological proxies, which include grain size

parameters, organic carbon (C_{org}) and $CaCO_3$ variations, clay mineral distribution and stable oxygen and carbon isotope variations, were used. Surficial sediments were used for the distribution of authigenic green clay facies on the continental margin of India, and different facies were identified by detailed mineralogical and geochemical techniques. The results obtained and inferrences drawn on the late Quaternary palaeoceanography and palaeogeography of the westem continental margin of India forms the major theme of this Thesis and are addressed in eight chapters.

Chapter 1 presents an introduction to the study area and Arabian Sea in general. The study area lies between Ratnagiri and Cape Comorin (~17° to 7°N Latitude) at depths between ~40 and 350 m along the western continental margin of India. The scientific rationale and major objectives behind the study are highlighted here. This is followed by a brief account of previous studies on palaeoceanography and palaeoclimatology in the Arabian Sea. Physiographic and oceanographic setting of the region is discussed with special reference to Indian monsoons and related oceanic processes.

Chapter 2 gives a detailed account of samples, analytical instruments and methods used in this study. In order to achieve the objectives of this study, a total of six sediment cores and one hundred and ninety eight surficial sediment samples were selected from the western continental margin of India. Additionally, eighty two surficial sediment samples were selected from the eastern continental margin of India to compare the palaeogeography of western margin of India. Advanced analytical equipments like Isotope Mass Spectrometers, Rock-Eval Pyrolysis instrument, ICP-MS, ICP-AES and X-ray Diffractometer have been used. Details of sample preparation and treatments carried out for the precise identification and quantification of different minerals are also described.

Chapter 3 deals with the past fluctuations in nature and distribution of organic carbon (C_{org}) in six sediment cores collected from the western continental margin of India. Down core variations in carbonate ($CaCO_3$) content and grain size parameters are also discussed. Sediment cores from the upper continental slope display high C_{org}, $CaCO_3$, and sand content on core tops and in general, the values decrease with increasing depth in the Holocene and upper Pleistocene

intervals. The sediment cores from the topographic highs reveal very high C_{org}, high clay and low $CaCO_3$ content in the Holocene sediments and vice versa in the upper Pleistocene sediments. Results of Rock-Eval pyrolysis suggest that the C_{org} is immature and marine in the Holocene sediments and mostly reworked marine in the upper Pleistocene sediments. Possible controls on the past variations in C_{org} are discussed and summarised.

Chapter 4 outlines the down core variations in stable oxygen and carbon isotope ratios of both planktic (*Globigerinoides ruber* and *Globigerinoides sacculifer*) and benthic foraminifers (*Uvigerina peregrina*) in four selected sediment cores from different depositional regimes along the western continental margin of India. The results reflect the late Quaternary fluctuations in monsoons, productivity and denitrification rates. The amplitude of oxygen isotope values ($\delta^{18}O$) between the Last Glacial Maximum (LGM) and Holocene as revealed in the records of planktic foraminifers is very high and exceeds the global 'ice volume effect', suggesting significant variations in the precipitation and sea surface temperature in the region since LGM. The abrupt deglacial climatic reversals observed in the oxygen isotope records suggest that the tropical monsoon climate is very sensitive to the subtle changes in its forcing mechanisms. The carbon isotope records ($\delta^{13}C$) of planktic foraminifers are complex and many factors like variations in the upwelling intensity, productivity, nutrient availability and the variations in $\delta^{13}C$ of atmospheric CO_2 could have contributed towards their fluctuations. Carbon isotope records of infaunal benthic foraminiferal species *Uvigerina peregrina* may be representative of past changes in oceanic denitrification rates. The carbon isotope ratios of bulk organic matter ($\delta^{13}C_{org}$) are used for identifying the relative significance of terrestrial and marine organic carbon inputs.

Chapter 5 comprises the down core variations of clay mineral assemblages in four selected cores. Clay mineral abundance and the ratios of certain climatic proxies like K/C (kaolinite/chlorite), S/I (smectite/illite) and C/I (chlorite/illite) and illite chemistry are used for the palaeoclimatic interpretations during the late Quaternary. The past variations in the intensity of monsoons deduced from clay mineral proxies are in accordance with the interpretations

based on the oxygen isotope and organic carbon variations and also the climatic fluctuations reported from the monsoon dominated regions around south Asia.

A comprehensive study on the authigenic green marine clays (verdine and glaucony facies) from the western continental margin of India between Ratnagiri and Cape Comorin, forms **Chapter 6**. Detailed mineralogical and geochemical studies indicate the presence of phyllite V and phyllite C of the verdine facies and glauconitic smectite of glaucony facies in the study area. The distribution of major and minor elements in the authigenic green grains are analogous to that of verdine and glaucony grains reported from the world oceans. Shale-normalised REE pattern of the green grains are characteristically 'flat', suggesting that the authigenic clays do not act as a 'sink' for REEs. The verdine-bearing facies covers over an area of ~100,000 km^2, nearly equal to that of Amazon basin in size, and represents the largest verdine bearing sedimentary basins in the world, associated with low fluvial inputs. It is evident that the size of the verdine deposit is related to the influx of iron from the continental sources rather than the amount of fluvial discharge.

Chapter 7 contains a brief description of the authigenic green grains along the eastern continental margin of India. The distribution of verdine and glaucony facies from this margin is compared with that of western continental margin of India and also with other world occurrences. It appears that the palaeogeography of the southwestern continental margin of India is different from the others, implying late Quaternary neotectonic activity and related subsidence along this margin.

A summary of the work carried out and the salient findings of the study are outlined in **Chapter 8**.

This chapter is followed by a complete list of references cited in the text, tables and figures in alphabetical order.

ACKNOWLEDGEMENTS

I am greatly indebted to **Dr. V. Purnachandra Rao**, my research supervisor, who has not only introduced and inspired me to the field of scientific research, but also meticulously guided me during the entire study. From the conception of this research problem, through all of its rigors to the thesis completion, he encouraged, supported and motivated me to pursue good science. He never failed to share his interest in new vistas of science. He provided an atmosphere where I felt free to work, experiment, think, and grow: an ideal environment any researcher could ask for.

I am extremely grateful to **Dr. R. R. Nair**, former Deputy Director and Head, Geological Oceanography Division, National Institute of Oceanography (NIO), Goa, for his inspiring influence on my research career, continuous support and encouragement. I sincerely thank him for his scholarly insights and keen interest in my research work. He was instrumental in getting done the radiocarbon and chemical analyses for me. I am also thankful to him for directing me to the right person to work with in the beginning of my research career.

Sincere thanks to **Dr. E. Desa**, Director, NIO, Goa, for providing the necessary research infrastructure, communication facilities and encouragement. **Dr. M. Veerayya**, Head, Geological Oceanography Division is thanked for his encouragement and keen interest in my work.

I thank **Prof. G. N. Nayak**, Head, Department of Marine Sciences & Marine Biotechnology, Goa University, for his valuable advice and vital administrative support.

I am obliged to **Prof. S. Krishnaswami**, Physical Research Laboratory (PRL), Ahmedabad, who provided me with the much needed ^{14}C dates on sediment cores and was kind enough to permit me to use his laboratory and other analytical facilities. **Mr. Ravi Bhushan** helped me out with ^{14}C measurements. **Dr. M. M. Sarin** made available the ICP-AES and AAS equipments, without any formal request. **Mr. Sunil Singh** taught me the techniques and tricks of chemical analyses and carried out the ICP-AES and AAS measurements, keeping aside his own research work.

Dr. S. V. Raju of Oil India Limited (OIL), Duliajan, Assam, provided the Rock-Eval pyrolysis data and **Dr. V. Balaram** of National Geophysical Research Institute (NGRI), Hyderabad, carried out the REE and minor element chemistry on ICP-MS and I am grateful to them.

I learned the fundamentals and new frontiers in stable isotope palaeoceanography at the University of Bremen, Germany, and my sincere thanks to **Prof. Gerold Wefer** and **Dr. Ralph Schneider**, whose expertise in the field made my learning much easier. Prof. Wefer was very considerate and encouraging and introduced me to all his scientific and administrative colleagues who made my research and stay at Bremen a delightful experience. Ralph guided me with patience and found time in his busy schedule for my personal problems and needs as well. **Dr. Peter Müller** generously provided me with the organic carbon isotope data. I thank **Ms. Monika Segl** and **Ms. Birgit Meyer-Schack** for the stable isotope analyses and **Ms. Barbara Donner** and **Ms. Martina Pätzold** for teaching me the intricacies of foraminiferal taxonomy. **Ms. Grimm-Geils**, Secretary to Prof. Wefer, was ever willing to help me out of my difficulties. **Mr. Helge Arz** gave me strong friendship and the stimulating discussions with him on advances in palaeoceanography were very beneficial to me. Of all my friends, who made my life in Bremen comfortable and memorable, my sincere thanks to: **Helge Arz, Frank Lamy, Yasser Mustafa, Chris Moos, Thomas Felis, Henning Kunz, Sylke Drakshba, Georg Kirst, Dörte Budziak** and **Birger Schünlz. Dr.** and **Mrs. D. Subramanian** (LIT, Nagpur) were very affectionate and were like family during my Bremen days. **Mr.** and **Mrs. Prakash Babu** are thanked for moral support and encouragement during my stay at Bremen.

I would like to acknowledge the financial assistance provided by the **Council of Scientific and Industrial Research (CSIR)**, New Delhi, in the form of Junior and Senior Research Fellowships (CSIR-NET).

Financial support from **Deutscher Akademischer Austauschdienst (DAAD)**, Germany, in the form of a short-term fellowship under the auspice of Indo-German Cultural Exchange Programme, made it possible for me to visit Germany and carry out the necessary isotopic work at the University of Bremen. Thanks are also due to **University Grants Commission (UGC)**, New Delhi, for

selecting me for the above award and **Council of Scientific and Industrial Research (CSIR)**, New Delhi, for granting me six months of leave to visit Germany.

I am very grateful to **Mr. Albert Gouveia** of Information Technology Group, NIO, Goa, for providing the computer facilities and his valuable support in the hour of need. He also allowed me to utilise his fine collection of Coastal Zone Colour Scanner (CZCS) images to insert in this thesis. **Mr. Vinod Jacob** and **Ms. Ann Thomas** provided instinct support with software bugs.

Sincere thanks to **Dr. J. N. Pattan** and **Dr. B. N. Nath** for making available their collection of papers on REEs and helpful discussions and **Dr. S. W. A. Naqvi** for fruitful discussions on stable isotope data. **Dr. A. A. Fernandes** helped me out with R-mode factor analysis. **Dr. F. Sirocko** of Geo Forschungs Zentrum, Potsdam, Germany, provided the digital isotopic data of his core 74KL from Arabian Sea.

Thanks are due to **Dr. B. G. Wagle** and **Dr. A. R. Gujar** for allowing me use their computer, when I was in need and **Dr. Shyam Gupta** and **Dr. M. V. S. Guptha** for encouragement.

Mr. Girish Prabhu is thanked for XRD analyses. **Mr. Md. Wahidullah** and his team helped in preparation of illustrations and **Umesh Sirsat** and **Sheik Karim** with photography. **Mrs. Alison Sudakar** is thanked for providing administrative assistance. **Mr. S. Jayakumar** helped with HP Laser printer for thesis printing.

My hearty thanks are due to **Mr. Shyam Prasad**, whose words of wisdom, patience and timely support helped me to smoothly sail through the critical junctures in my research career. His door was always open to me and my problems (silly at times!).

A special note of thanks is due to **Ms. Sheeba John** for her help in many little things which were vital for the completion of this thesis.

I greatly appreciate the friendship, goodwill and support of my colleagues **Balakrishnan, Rajkumar, Prakash Babu, Saji, Sudheesh, Areef Sardar** and many others at the National Institute of Oceanography, Goa.

And to my friends, **Rahul Mohan, T. G. Prasad** and **Vijay Govindan** who have provided the critical mass necessary to sustain the cheerful moments in Goa, and through lively letters over long distances, my heartful thanks.

I would like to apologise to **all** those I have not mentioned by name, and thank them as well.

Finally, thanks to **my family members** for their patience, love and encouragement, and for not having any unrealistic expectations of me.

Chapter 1

Chapter 1

INTRODUCTION

1. 1 General introduction

The oceans, which cover more than 70% of the Earth, are inextricably involved in the physical, chemical and biological processes that regulate the total Earth system. Climate is a major component of the Earth system and consists of coupled interactions involving the atmosphere, oceans, ice sheets, land surface and biota. Global changes in climate may be either due to astronomical or man-made factors. The recent rise in atmospheric concentration of greenhouse gases on earth and predictions of global warming and regional climate change in the future underline the requirement for developing a coherent and rational approach to understand the climate system. The earth's climate undergoes natural variations from year to year and also on longer timescales. Any anthropogenic influences on the climate will thus be superimposed on a background of the natural climatic variations and therefore, understanding the variability and predictability of global and regional climate are of prime importance. In order to predict the future climatic changes more precisely, it is necessary to have an understanding of past changes in climate.

With an aim to study the interactive Earth system processes and its relevance to global change, the International Council of Scientific Unions (ICSU) constituted the 'International Geosphere-Biosphere Programme' (IGBP) in the year 1988. The major objectives of the IGBP include, developing improved understanding of the interactive physical, chemical and biological processes that regulate the Earth system and changes that are occurring in the Earth system. One of the core projects of IGBP is the 'Past Global Changes' (PAGES) programme, which focuses mainly on two streams: Stream I concerns the last 2,000 years with a temporal resolution of at least 10 years and Stream II focuses on glacial-interglacial cycles of the last several thousand years.

The Quaternary period has been the most eventful among all other geologic periods. The late Quaternary period (<130 ka-BP) has witnessed large changes in global climate. Eustatic sea level fluctuated significantly in accordance

with the waxing and waning of continental ice sheets. Our understanding of Quaternary climate and oceanographic conditions has been revolutionised by the study of sediments that have accumulated on the ocean bottom. The climatic and sea level changes recorded in the sediments during the late Quaternary can be distinguished using several proxies which bear clear signals of the past climate and oceanography. Biological, biogeochemical, geochemical and sedimentological proxies are the most commonly employed ones for this purpose. The sedimentary records from the continental margins may provide a better understanding on the past variations, because their sediments are contributed by the inputs of coastal rivers as well as from coastal processes such as upwelling and biological productivity and are sites of high organic matter burial and high sedimentation.

1. 2 Scientific rationale and scope of the study

Arabian Sea represents one of the northernmost embayments of the Indian Ocean (Fig. 1.1). It is a semi-enclosed basin surrounded by arid land masses to the west and north and by coastal highlands of western India to the east. There is no outlet to the north, but the basin's waters and sediments are influenced by inflow from Persian Gulf and the Red Sea, and by exchange across the equator. A major freshwater input from the north through Indus river, brings in a large amount of terrigenous sediments and a major influx of dust plumes from the Arabian peninsula during the SW monsoon period. The Arabian Sea experiences extremes in both atmospheric forcing and oceanic circulation that lead to the greatest seasonal variability in many surface water properties observed any where in the world oceans (Lal, 1994). Thus, the Arabian Sea experiences spectacular changes, both in space and time. Most important among them is the upwelling of nutrient-rich subsurface waters both along the western and eastern margins. The resultant high productivity and subsequent bacterial decay of organic matter, lead to extremely low dissolved oxygen concentration and related intense water column denitrification along the continental margins of the Arabian Sea (Naqvi, 1987). In addition, the Arabian Sea is found to be a perennial source of greenhouse gases like carbon dioxide to the atmosphere (Sarma *et al.*, 1998). Finally, proximity to the landmass makes the biology and chemistry of the Arabian Sea quite susceptible to continental influences both through fluvial and atmospheric inputs of

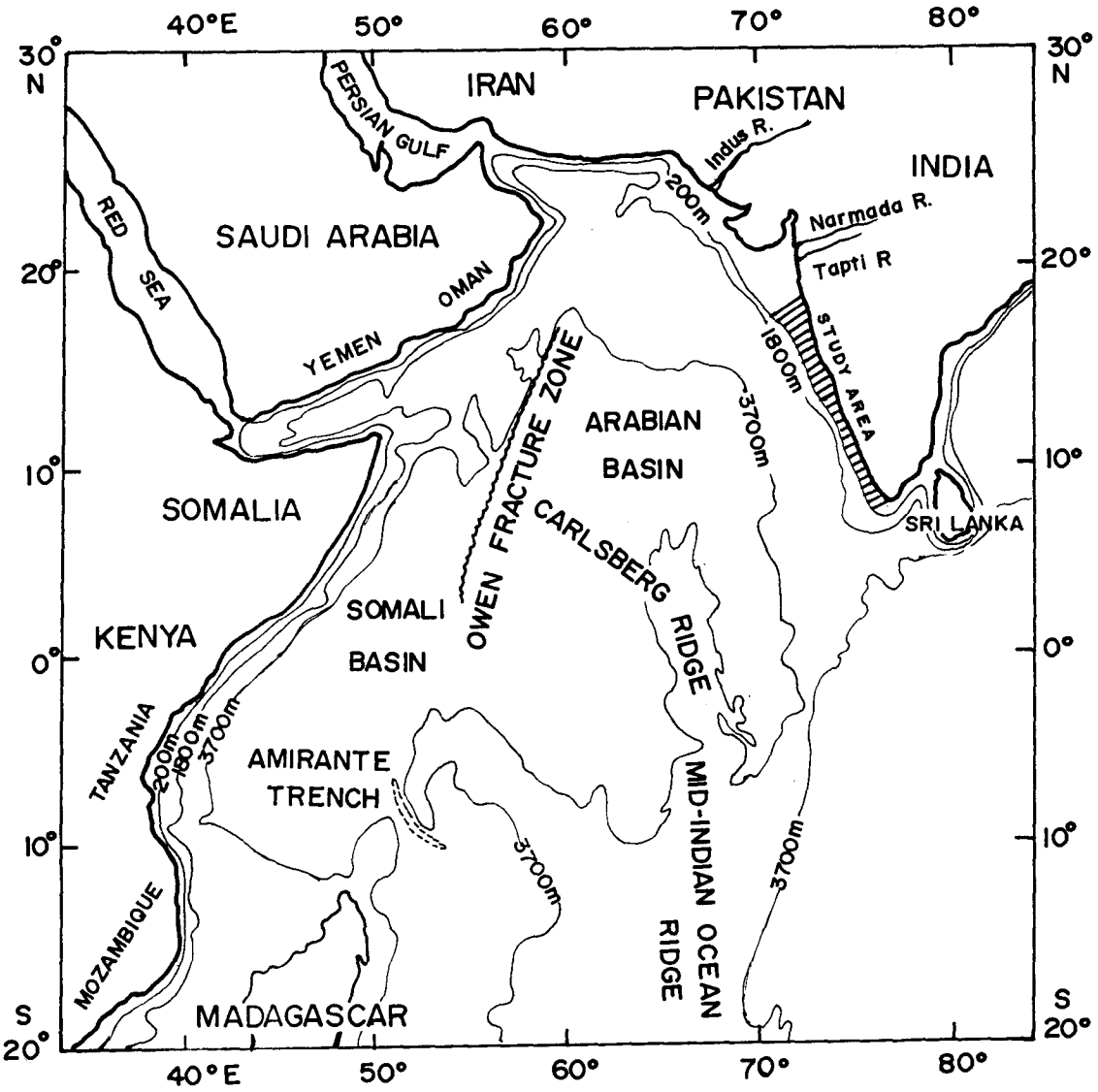

Fig. 1. 1 Physiographic features of the Arabian Sea. The hatched region off western India represents the study area (modified after National Geographic Society Atlas, 1981).

trace metal, nutrients and other elements that can affect ocean productivity and climate. In view of its unique oceanographic and climatic features, the Arabian Sea is considered as a natural laboratory to look at past climate and possible future climatic changes (see Smith *et al.*, 1991). Hence scientists from several countries have concentrated their studies on various aspects of the Arabian Sea. Should the climate become more monsoonal and upwelling more widespread under the influence of global warming, it is expected that the present Arabian Sea can be used as an analog for studying possible trends and changes in other parts of the world ocean.

The area selected for the present study is the eastern margin of Arabian Sea (i.e., the western continental margin of India) between ~17° and 7°N Latitude (Fig. 1.1). It is away from the Indus, Narmada and Tapti river discharges and from the major influx of dust plumes from the Arabian peninsula. Organic carbon content in the surficial sediments of the upper continental slope of the west coast of India has been reported to be high and causes for its enrichment (productivity/preservation models) are being discussed and debated widely and are yet to be clearly resolved. The down core variation of the organic carbon in the gravity cores collected from different topographic domains and regions of moderate to high productivity and oxygen minimum zone would help in better understanding the controls on its enrichment. Little work has been done on stable isotope studies in the sediment cores from the western continental margin of India. Since moderate to intense seasonal upwelling occurs in the study region (as in the western Arabian Sea), such studies on sediment cores may provide better signals on monsoonal variability and would be useful in understanding its influence on oceanic processes (upwelling and intensity of denitrification) during the late Quaternary. Similarly, the variations in down core distribution of clay mineral assemblages and clay mineral proxies may be in accordance with climatic changes during the late Quaternary and are expected to augment the results obtained from stable isotope studies.

Tropical continental margins are the best sites for the formation of authigenic green marine clays. Sources of iron, temperature and depth appear to be the major factors controlling the formation of green clay facies, verdine and glaucony. Verdine occurs at shallow depths (<60 m) and is replaced by glaucony

at deeper levels (>60 m). Sea level variations of the order of 120 m have been reported during the late Quaternary (Fairbanks, 1989). Palaeogeography of the continental margins has been established based on the depth distribution of green grain facies (see Odin, 1988). Here, the distribution of green grain facies from the western continental margin of India is compared with that of the eastern continental margin and the factors responsible for their differential distribution are discussed.

1. 3 Objectives of the study

Sedimentological and palaeoceanographical studies were carried out on the sediment cores and surficial sediments along the western continental margin of India. The major objectives of the present study are:

1. To examine down core variations in the nature and distribution of organic carbon, stable isotope composition of planktic and benthic foraminifers and clay mineral assemblages and to document the oceanic processes and climatic factors responsible for their variation during the late Quaternary.
2. To investigate the distribution and composition of authigenic green marine clays in the surficial sediments of the western continental margin of India and compare their distribution with that of the eastern margin of India so as to delineate the palaeogeography of the margins during the late Quaternary.

1. 4 Previous studies

The origins of "ocean science" in the Arabian Sea date back to about 2,300 BC, when trade between the Mesopotamian peoples in the Persian Gulf and peoples of the Indus valley was established (c.f. Warren, 1987). Marine geological investigations in the Arabian Sea started with the *Challenger* Expedition during 1872-76. This was followed by *Vityaz* (1889), *Valdivia* (1889-99), *Mabahiss* - *John Murray* (1933-34) and *Albatross* (1947-48) Expeditions. The International Indian Ocean Expedition (IIOE: 1962-65) is an important landmark in the history of exploration of the continental margin geology of India. During IIOE, 20 countries and 54 vessels participated and collected vast amount of scientific data. Subsequently, the Indian research vessels *INS Darshak* (1973-74), *RV Gaveshani*

(1976-89), *ORV Sagar Kanya* (since 1983), *RV Samudra Manthan* and *RV Samudra Shaudikama*, collected sediment samples and contributed significantly towards the understanding of the geology of the Indian continental margins. Rao and Wagle (1997) made a comprehensive review of the available information on the surficial geology and geomorphology of the western continental margin of India.

Several workers reported the distribution of organic carbon in sediments along the western continental margin of India and also the adjacent Arabian Sea (von Stackelberg, 1972; Slater and Kroopnick, 1984; Paropkari *et al.*, 1987; Paropkari *et al.*, 1992; Calvert *et al.*, 1995; 1996). Organic carbon (C_{org}) content in the inner shelf sediments along the west coast of India ranges from 1 to 4% and is associated with clayey sediments (Paropkari *et al.*, 1987). High C/N ratios (10-30) indicate that it is mainly of terrestrial in nature. On the outer shelf, C_{org} values are low (<1%) and are associated with relict sandy sediments. Higher levels of organic carbon (1-4 wt% and up to 16%) has been reported in the continental slope sediments of the eastern Arabian Sea ([redacted] Paropkari *et al.*, 1987), and the C/N ratios and $\delta^{13}C_{org}$ values indicate that the C_{org} is mostly of marine origin (Calvert *et al.*, 1995). The causes for high C_{org} content in the slope sediments is still a matter of debate. Some workers considered that anoxia is the most important deciding factor (Demaison and Moore, 1980; Paropkari *et al.*, 1992, 1993), while others (Pedersen and Calvert, 1990; Pedersen *et al.*, 1992; Calvert *et al.*, 1995) suggested that productivity in conjunction with factors like sediment characteristics and texture, rather than anoxia, are important for the high organic content. All these studies were carried out on surficial sediments and as such there was no significant attempt to study the fluctuations in C_{org} through time, especially on the western margin of India. Since monsoons, upwelling, organic productivity and C_{org} burial in the sediments are all interrelated, any change in the intensity of Indian monsoons would have had an impact on the C_{org} buried simultaneously.

Although the studies on stable oxygen and carbon isotope composition of calcareous marine organisms in the world oceans date back to the early 1950's, such studies in the Arabian Sea began only in the late 1970's. CLIMAP (1976) made the first attempt to reconstruct the sea surface temperature during the Last

Glacial Maximum (LGM ~18 ka-BP), using oxygen isotope variations in planktic foraminifers. Since then numerous isotopic studies were carried out on both living and fossil foraminiferal tests to delineate the past variations in climatic conditions, circulation, upwelling and water mass characteristics (e.g., Prell *et al.,* 1980; Duplessy *et al.*, 1981; Prell and Curry, 1981; Duplessy, 1982; van Campo *et al.*, 1982; Fontugne and Duplessy, 1986; Brummer and Kroon, 1988; Sarkar *et al.*, 1990; Sirocko *et al.*, 1993; 1996; Naqvi and Fairbanks, 1996). High resolution studies on the cores collected during the Ocean Drilling Programme (ODP- Leg 117) (Shimmield *et al.*, 1990; Prell, Nitsuma *et al.*, 1991) have significantly enhanced our knowledge on past variations in Asian monsoon and its effect on oceanic upwelling along the western Arabian Sea. These and numerous other studies from the Arabian Sea have suggested that the intensity of Indian monsoon had fluctuated greatly during the late Quaternary; this includes the intensification of SW monsoon around 9 ka-BP and a respective weakening at 18 ka-BP (e.g., van Campo *et al.*, 1982; Clemens and Prell, 1990; Sarkar *et al.*, 1990; Zahn and Pedersen, 1991; Clemens *et al.*, 1991; Sirocko *et al.*, 1993; 1996; Naidu, 1995; Zonneveld *et al.*, 1997). Most of these studies were restricted to the western Arabian Sea margin and very few studies have been carried out on the eastern Arabian Sea margin (western continental margin of India).

Clay mineral studies on surficial sediments in the Arabian Sea have so far been used mainly to characterise the provenance and transport pathways of fine-grained sediments (Stewart *et al.*, 1965; Biscaye, 1965; Griffin *et al.*, 1968; Goldberg and Griffin, 1970; Kolla *et al.*, 1976 & 1981; Nair *et al.*, 1982 a&b; Rao, 1989; Rao and Rao, 1995). Besides, there are a few other studies on sediment cores from the western Arabian Sea, reporting the past variations in clay mineral distribution in relation to changes in atmospheric circulation and continental climate during the Late Quaternary (Sirocko *et al.*, 1991; Sirocko and Lange, 1991). No such studies were conducted on the eastern Arabian Sea margin (western continental margin of India), to deduce the palaeoclimatic conditions using clay mineral proxies.

Earlier workers who reported the authigenic green grains in the sediments of the continental margins of India referred to them as 'glauconite' (Subbarao,

1964; Mallik *et al.*, 1976; Thrivikramji and Machado, 1982). Verdine has been recognised as a new mineral facies only in 1985 (Odin, 1985). The world occurrences of this mineral facies indicate that its distribution and abundance appear to be directly proportional to the river discharge (Odin, 1988). Subsequently, Rao *et al.* (1993) made detailed studies on the distribution of verdine and glaucony facies on the Kerala continental shelf and slope (from 9° to 10.5°N Latitude). Since there are large number of small rivers and streams cutting through the coastal belt all along the west coast of India, it is possible that the verdine bearing basin may be much larger and a regional study is necessary all along the continental margins of India to document its distribution.

1. 5 Physiographic setting

The Arabian Sea covers an area of about 3,863,000 km^2 and is surrounded by arid landmasses to the west and north and by coastal highlands of western India to the east. The Indus, Narmada and Tapti rivers are the major sources of terrigenous sediments to the Arabian Sea (see Fig. 1.1). The Indus Fan, formed by the sediments brought by Indus river, is one of the largest submarine fans in the world. The most impressive topographic feature of the Arabian Sea is the broad active mid-ocean ridge system which starts in the Gulf of Aden and trends southwest as Carlsberg Ridge, into an en echelon pattern of transform faults called Central Indian Ridge. The Carlsberg Ridge separates the deep basin of Arabian Sea into two major sedimentary basins: the Arabian Basin and Somali Basin (Fig. 1.1).

The western continental margin of India is characterised by numerous diverse geological and geomorphological features and is considered to be a passive margin. The width of the continental shelf is about 130 km off Ratnagiri and narrows down to 80 km off Cochin (c.f. Rao and Rao, 1995). It is again wider (120 km) at the southern tip of India, off Cape Comorin. Accordingly, the width of the inner shelf also varies: it is relatively wide and extends up to 60 m water depth in the northern part and narrows down to 30 m water depth in the southern part (off Cochin). The shelf break occurs at about 120 m in the northern part and at about 80 m in the southern part. The morphology of the continental slope also

varies from north to south. Isolated topographic highs rising from about 2000 to 3000 m water depth are characteristic of the upper continental slope between Goa and Cochin.

Two distinct sediment types occur on the continental shelf of western India: Modern clastic clays on the inner shelf and relict sandy sediments on the outer shelf (Nair and Pylee, 1968; Hashimi *et al.*, 1982). The continental slope is covered by silty clays which is an admixture of dominant terrigenous and biogenic components. The outer shelf sediments are Holocene carbonate sands between Ratnagiri and Mangalore, and are terrigenous sands between Mangalore and Cochin. Biogenic sediments are again predominant between Quilon and Cape Comorin.

1. 6 Geological setting

The study area lies in the tropical belt and experiences a humid tropical climate. The Western Ghats mountain chains are the major physiographic feature along the coast with elevations up to ~1000 m. Down south of Bhatkal to Quilon, the Ghats tend to recede 50 to 80 km from the coast (Krishnan, 1968). Although no major river traverses through this area, there are several medium (~85 to 250 km long) and minor rivers, and numerous streams which are seasonal in nature. They originate from and drain through the steeper slopes of the Western Ghats, covering an area of about 54,000 km^2, and discharge about 95.58 km^3 water annually into the Arabian Sea (Rao, 1979). The hydrological characteristics of all major, medium and minor rivers debouching to the eastern Arabian Sea margin are given in Table 1.1.

The hinterland geology consists mainly of Deccan Trap basalts in the northern part (up to Goa) and Precambrian gneisses, schists and charnockites in the southern part. The Precambrian rocks are extensively lateritised at places. The coastal region of southwest India consists of Miocene Warkala and Quilon beds (mainly ferruginised sandstones with clay intercalations) and Recent alluvium.

Table 1. 1 Hydrological characteristics of major, medium and minor rivers discharging to the eastern Arabian Sea (source: Rao, 1979).

Serial No.	Rivers	Drainage Area (km^2)	Average annual discharge (million m^3)
	Major		
1	Indus	468,068	50,000 @
2	Narmada	98,796	40,705
3	Tapti	65,145	17,982
	Medium		
4	Mandovi *	2,032	1,320
5	Kali *	5,179	6,537
6	Gangavati *	3,902	4,925
7	Sharavati *	2,209	4,545
8	Netravati *	3,657	4,615
9	Beypore *	2,788	5,200
10	Ponnani *	5,397	8,800
11	Periyar *	5,243	12,300
12	Pamba *	1,961	6,300
	Minor		
13	Maharashtra, Goa & Karnataka region *	2,146	966
14	Kerala region *	19,489	40,073

@ - revised value given by Milliman *et al.* (1984). * indicates rivers from the study area.

1. 7 Oceanographic setting

1. 7. 1 Monsoons

The Arabian Sea experiences extremes in atmospheric forcing that leads to the greatest seasonal variability observed in any ocean basin. The Indian monsoon, which extends from Tibet to the southern Indian Ocean and from eastern Africa to Malaysia, represents one of the Earth's greatest and most dynamic weather systems (O'Hare, 1997). Monsoons are the seasonally reversing

winds which bring rain to the Indian subcontinent and cause upwelling along the continental margins. This seasonal reversal of the wind direction between summer and winter drives the southwest (SW) and northeast (NE) monsoons in the Indian Ocean and precipitation over south Asia.

In summer, differential heating of the continental and oceanic regions leads to low atmospheric pressure above the Asian Plateau and high atmospheric pressure over the relatively cool southern Indian Ocean (Fig. 1.2). This results in a strong low-level jet stream, the Findlater Jet (Smith *et al.*, 1991) (see Fig. 1.3). Much of the intensity of this jet derives from the direct heating of the troposphere above Asia and through latent heat collected over southern subtropical ocean which is transported across the equator and released by precipitation over south Asia (Clemens *et al.*, 1991). The winter monsoon (NE monsoon) is characterised by low seasonal insolation over Asia and relatively high albedo due to seasonal snow cover. These boundary conditions produce a high pressure cell in the low-level atmosphere over Asia which results in a northeasterly wind flow over the Arabian Sea (Fig. 1.3). The winter monsoon is relatively weak and less significant in the Arabian Sea.

1. 7. 2 Circulation and water masses

The surface circulation in the Arabian Sea is modulated by the seasonal variation of the monsoonal wind system. The seasonal reversals of the surface wind field over the tropical Indian Ocean are far more dramatic than in other regions of low latitudes, and these reversals have profound impact on the seasonal variation of the surface current system (Wyrtki, 1971; Hastenrath and Greishar, 1991).

The generalised surface circulation in the northern Indian Ocean is shown in Fig. 1.4. During the summer monsoon (June-September), the low level southeasterly trade winds of the Southern Hemisphere extend across the equator to become southerly or southwesterly in the Northern Hemisphere. The frictional stresses of these in turn drive the Somali current (SC) (the fastest open ocean current on earth with a speed up to 7 knots; Smith *et al.*, 1991), the westward flowing South Equatorial Current (SEC), and the eastward flowing southwest

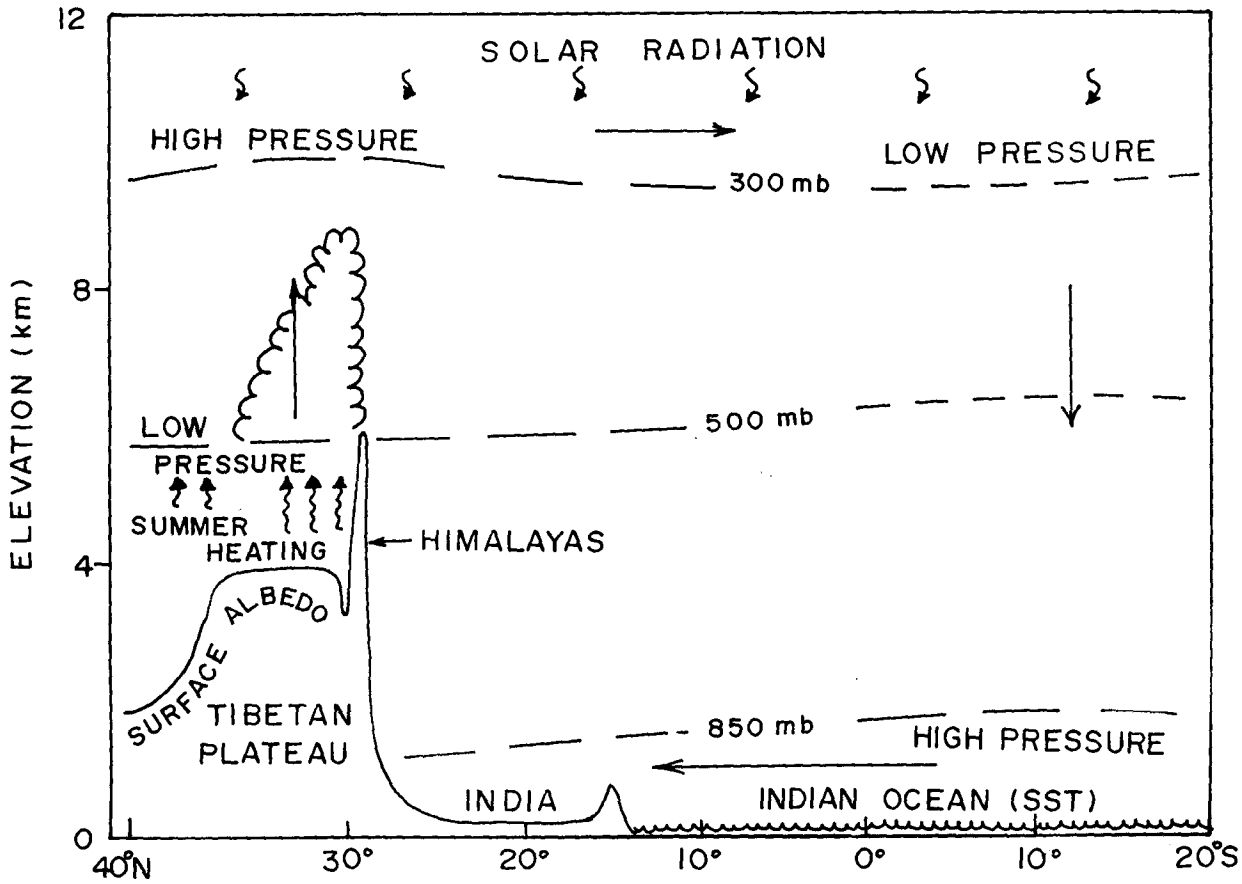

Fig. 1. 2 Conceptual model of the climatic processes and boundary conditions controlling the SW Indian monsoon (after Prell, 1984a).

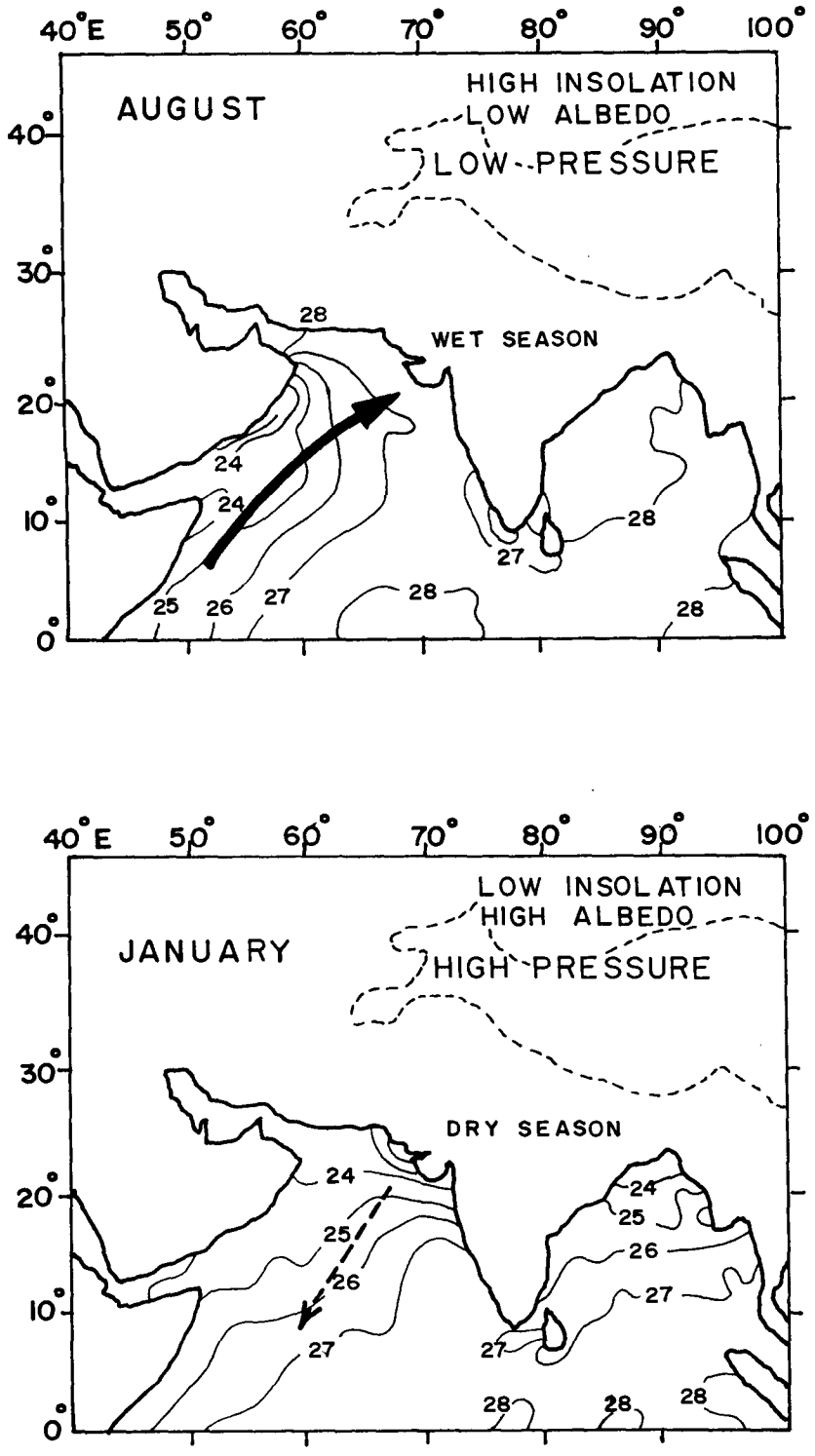

Fig. 1. 3 Modern sea surface temperature (°C) and general wind pattern during SW monsoon and NE monsoon period. The thick arrow represents the axis of Findlater Jet. Boundary conditions during this season are also illustrated. The dashed line over Asia indicates elevations >3,000 meters. Dashed arrow indicates direction of relatively weak winds during NE monsoon period (after Prell, 1984a).

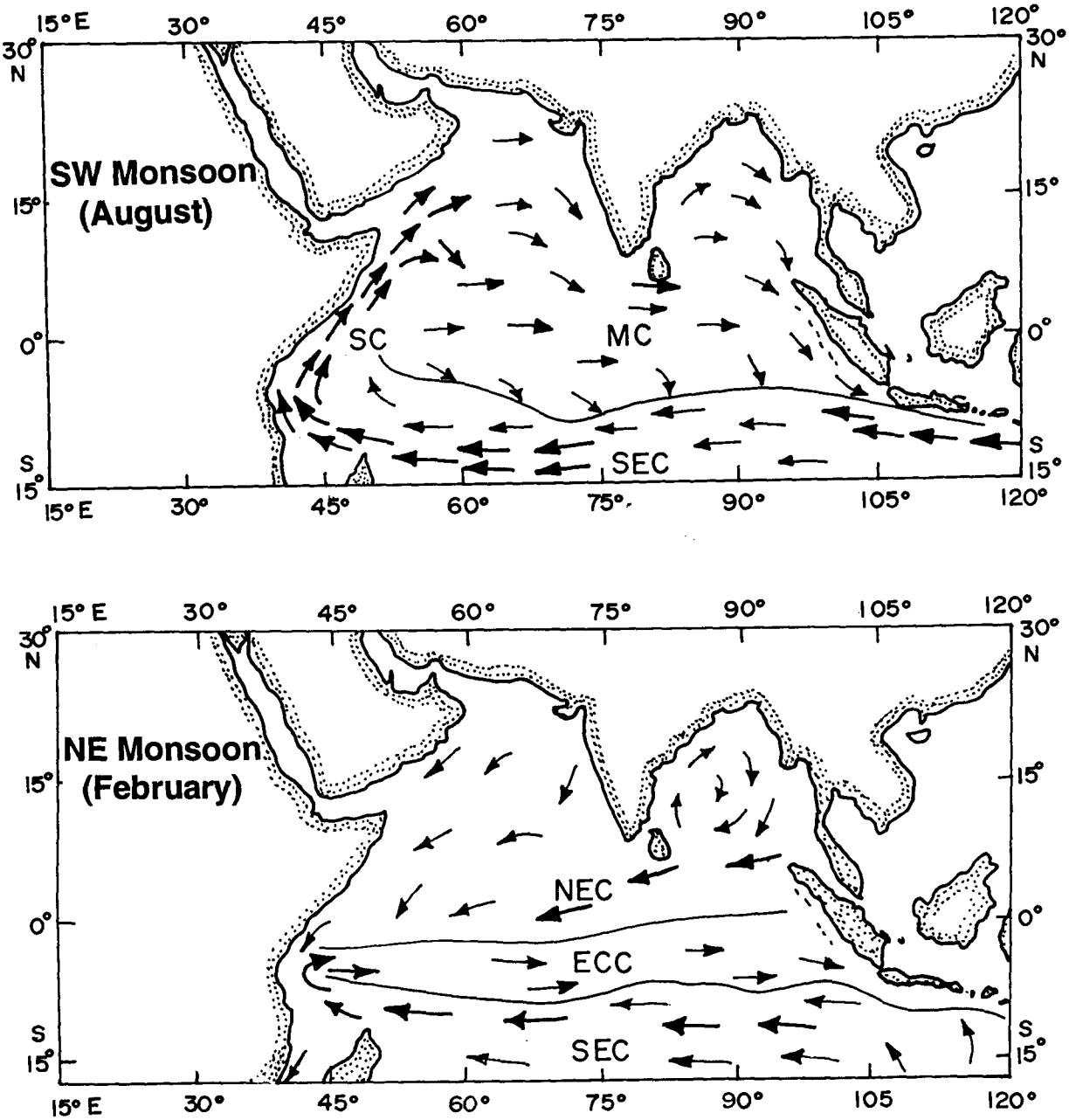

Fig. 1. 4 Surface circulation in the Indian Ocean during the SW monsoon and NE monsoon period (after Wyrtki, 1973). MC - Monsoon Current, SC - Somali Current, SEC - South Equatorial Current, NEC - North Equatorial Current, ECC - Equatorial Counter Current.

Monsoon Current (MC) (Fig. 1.4). Oceanic circulation during the NE monsoon season is relatively weak and is characterised by the North Equatorial Current (NEC), an eastward flowing Equatorial Counter Current (ECC), and a moderately developed anticyclonic gyre (Fig. 1.4).

The surface water layer of the Arabian Sea is characterised by a dense, high saline water mass called Arabian Sea High Salinity Water (ASHSW), which originates as a result of high evaporation in the northern part of the Arabian Sea (Shetye *et al.*, 1994). The present day water mass distribution along the intermediate water depths of Arabian Sea include mainly the Arabian Sea Water (ASW) which is influenced to a large extent by Persian Gulf Water (PGW) outflow (You and Tomczak, 1993). The Persian Gulf Water outflow is found at depths between 200 and 400 m with deeper levels to the south. As it moves southward, it loses its identity due to mixing with the Red Sea Waters (RSW), which is the outflow from Red Sea and South Indian Central Waters, which originate south of the equator (You and Tomczak, 1993; Kumar and Prasad, 1996). The core of the RSW outflow occurs at ~600 m water depth in the Arabian Sea. The outflows of RSW and PGW are effectively blocked by the continuation of strong northward jet of Somali Current along the western Arabian Sea during the summer, giving a rather small contribution of only up to 20% to the Arabian Sea (You, 1997).

1. 7. 3 Upwelling, productivity and oxygen minima

The response of the Arabian Sea to the atmospheric forcing is most clearly observed in the sea surface temperature (SST) patterns. Seasonal SST maps generally reflect these circulation patterns (Fig. 1. 3). During summer, as a result of the strong surface currents and the orientation of the coastlines, upwelling of deeper waters occur on both sides of the Arabian Sea. The northward flowing Somali Current invokes intense upwelling along the coast of Somalia and Arabia (Schott, 1983). Off India, upwelling occurs mainly during the summer monsoon, propagating from south to north along the coastline (Shetye *et al.*, 1990). The upwelling is apparently driven by the adjustment of the system to the anticyclonic monsoonal circulation, which causes the isopycnals to slope up towards the coast, and this effect is augmented by the equatorward component of the wind stress, blowing surface water offshore (Longhurst and Wooster, 1990).

The strong and regularly alternating monsoon winds drive all processes of production in the Arabian Sea. The resultant biological productivity shows strong seasonal variations in relation to the seasonal monsoon cycles. The eastern Arabian Sea is a region of high productivity with high values (>1.0 g C/ m^2/ day) off southwest coast of India and moderate to high values (0.25-0.5 g C/ m^2/ day) off central India coast (Qasim, 1977; Bhattathiri *et al.*, 1996).

The high rate of input of organic matter and its subsequent oxidation below the thermocline is associated with a very high oxygen demand at intermediate depths. The resulting oxygen deficiency is fostered by the sluggish intermediate water circulation, leading to a pronounced Oxygen Minimum Zone (OMZ) between 150 to 1500 m water depth (Sen Gupta and Naqvi, 1984).

Recent sediment trap studies in the Arabian Sea indicate that both biogenic and lithogenic fluxes are much higher during the SW monsoon period (Nair *et al.*, 1989). These studies show that more than 70% of the calcareous, siliceous and lithogenic material is supplied to the Arabian Sea during the SW monsoon period, suggesting that SW monsoon accounts for most of the total annual productivity. Also nearly 80% of the lithogenic flux is transported to the seafloor during the SW monsoon months (June-September), indicating an instantaneous transfer of the atmospheric signal into the sedimentary record (Nair *et al.*, 1989). The biological, geochemical and sedimentological records of the Arabian Sea should therefore reveal the structure and intensity of the Indian monsoon system in the past.

Chapter 2

Chapter 2

MATERIALS AND METHODS

To achieve the scientific objectives underlined in the Chapter 1, both sediment cores and surficial sediment samples were selected from the western continental shelf and slope of India and studies were carried out using a variety of analytical techniques.

2.1 SEDIMENT CORES

The gravity cores used in this study were collected in October 1994 during the sixth cruise of *M/V A. A. Siderenko*, a Russian research vessel chartered by the Department of Ocean Development (D.O.D), New Delhi. Six sediment cores were collected from three different physiographic settings on the western continental slope of India at depths ranging from 280 to 350 m, between Goa and Cochin: three cores are from the upper continental slope between Goa and Cochin, two from the topographic highs off Goa and one from the terrace off Cochin. All these cores fall within the Oxygen Minimum Zone (OMZ- between 150 and 1500 m water depth). Details of core location, depth of collection and length of the sediment cores recovered are given in Table 2.1.

Table 2.1 Location and details of sediment cores collected from the Arabian Sea.

Cruise No.	Core No.	Latitude °N	Longitude °E	Water Depth	Length of the cores
AAS -VI	GC - 1	14°. 56.534'	72°. 57.596'	286 m	3.60 m
AAS -VI	GC - 2	14°. 49.613'	72°. 38.823'	323 m	4.30 m
AAS -VI	GC - 3	14°. 24.423'	72°. 54.855'	355 m	4.45 m
AAS -VI	GC - 4	13°. 05.855'	73°. 46.816'	335 m	4.00 m
AAS -VI	GC - 5	10°. 22.537'	75°. 33.901'	280 m	3.33 m
AAS -VI	GC - 6	09°. 09.862'	75°. 47.600'	340 m	4.10 m

Colour and lithology of the sediments were noted shortly after the recovery of the core onboard. Careful visual examinations were also made for identifying the presence of turbidites and sediment slumping. Subsampling of all cores was done onboard at 2 cm interval for the top 20 cm and 5 cm interval for the rest. The samples were oven-dried at 60°C temperature and utilised for all further studies.

2. 1. 1 Textural analysis

Textural studies were carried out on 18 to 28 representative sediment intervals in each core (a total of 143 samples). About 10-13 g of dried sediment samples were weighed accurately and transferred into a clean 1000 ml beaker. The samples were made salt-free by repeated washings using distilled water. 25 ml of dispersing agent (10% Sodium Hexametaphosphate solution) was added to this salt-free sediment and dispersed for about 4 hours. Subsequently, the samples were wet sieved through a 63 μm sieve. The sand fraction (>63 μm) retained in the sieve was dried and weighed, while the mud fraction was collected in a 1000 ml measuring glass cylinder and subjected to pipette analysis (Folk, 1968). Percentage distribution of sand, silt and clay fractions in each sample was determined and textural classification was made based on the grain size variation (Folk, 1968).

2. 1. 2 Organic carbon analysis

The organic carbon (C_{org}) content of the sediment samples was determined by the wet oxidation method (El Wakeel and Riley, 1957). The principle behind this method is based on the oxidation of organic carbon with chromic acid and titrimetric determination of the oxidant consumed. This method is widely used and reported to produce reliable results when the availability of organic carbon is ≥1%.

About 0.3-0.15 g of the powdered sample was accurately weighed out in a boiling tube and 10 ml of chromic acid added, using a wide-tipped pipette. The tube was covered with aluminium foil wrapper and heated in a water bath for 15 minutes. It was allowed to cool and the contents of the tube were transferred into a 250 ml conical flask containing 200 ml distilled water. About 2-3 drops of ferrous-

phenanthroline indicator was added and titrated with 0.2 N ferrous ammonium sulphate solution until a pink colour just persists. A blank determination was also carried out in the same manner. Then, the concentration of the organic carbon available in the sediment was estimated as: 1 ml of 0.2 N ferrous ammonium sulphate consumed = 1.15 × 0.6 mg of carbon. The percentage of organic carbon in the sample = 0.6 × {[(Blank reading - Sample reading)] / (Weight of the sample in mg)} × 1.15 × 100. The reproducibility of the organic carbon measurements was checked by running replicates of sediment samples and it was found to be better than ±5%. Cross checking with the organic carbon values obtained during the Rock-Eval pyrolysis and the stable isotope study of organic carbon at certain intervals of the cores suggests that the relative accuracy of the measurements are better than ±10%. A total of 150 samples were analysed for organic carbon distribution in six sediment cores.

2. 1. 3 $CaCO_3$ determination

The $CaCO_3$ content of the sediment sample was determined by the rapid gasometric technique, following Hülsemann (1966). Exactly 0.5 g of the 99.5% standard $CaCO_3$ weighed out into a 50 ml conical flask. About 5 ml of concentrated HCl was taken into a small glass vial and carefully kept inside the conical flask. The flask was then fitted to a simple apparatus for producing and trapping the CO_2 evolved. The $CaCO_3$ was allowed to react with HCl by shaking the flask vigorously. The CO_2 produced by the reaction was then allowed to pass through a distilled water column where it displaces a certain amount of distilled water. The amount of distilled water displaced was collected in a standard measuring cylinder, which is directly proportional to the CO_2 produced during the reaction with carbonate and in turn to the percentage of $CaCO_3$ available in the sample. The experiments were repeated for the sediment samples and volume of the displaced liquid noted each time. Then, the percentage of $CaCO_3$ available in the sediment sample = (concentration of the standard $CaCO_3$ × volume of liquid displaced for sediment sample) / volume of liquid displaced for standard $CaCO_3$. A total 150 samples were analysed for $CaCO_3$ measurements. Replicate analyses of

both the samples and carbonate standards showed that the analytical reproducibility was better than ±5%.

2. 1. 4 Rock-Eval pyrolysis

Rock-Eval pyrolysis studies were carried out on 24 representative samples from six sediment cores at the Oil India Limited, Duliajan, Assam, using a Rock-Eval III apparatus, following the procedures of Espitalié *et al.* (1985). Pyrolysis method consists of programmed heating (25°C/ minute on average) in an inert atmosphere (helium) of a small sample of rock/ sediment (~100 mg). This method determines the following components quantitatively and selectively: (a) the free hydrocarbon in the form of gas and oil contained in the rock/ sediment sample, and (b) the hydrocarbon- and oxygen- containing compounds (CO_2) that are expelled during the cracking of the unextractable organic matter in the rock (kerogen). Rock-Eval III apparatus also determines the total organic carbon (TOC) content of the sample. Different parameters of Rock-Eval pyrolysis (HI, T_{max}, S_1 and S_2) are useful in understanding the type, degree of preservation and maturity of organic matter and hydrocarbon generation potential (Dean *et al.*, 1994). Hydrogen index (HI) is defined as the yield of hydrocarbons normalised to the percent organic carbon (C_{org}) content (expressed as mg HC/ g C_{org}). The quantity of free hydrocarbons (oil and gas) that is thermally distilled from the sediment is denoted as 'S_1' (mg HC/ g rock), and 'S_2' (mg HC/ g rock) represents the hydrocarbons generated by pyrolytic degradation of insoluble organic matter (kerogen) (Calvert *et al.*, 1992). T_{max} (°C) is the temperature at which the maximum amount hydrocarbons is generated and is used as maturity index (Espitalié and Joubert, 1987). The reproducibility of these measurements are ±8% for HI, ±8% for S_2 and S_3 values and ±1% for T_{max} values.

2. 1. 5 Coarse fraction studies

The sand fraction (>63 μm) obtained by wet sieving was further split into >500, 500-250 and 250-125 μm fractions. The 500-250 and 250-125 μm fractions were examined under a binocular microscope for the relative abundance of the

components (such as planktic and benthic foraminifers, pyritised grains, and terrigenous particles).

2. 1. 6 Stable isotope studies

Stable oxygen and carbon isotope ratios of the carbonate skeletal remains are widely used in palaeoceanography (for details, see Chapter 4). Eventhough oxygen has three stable isotopes (^{16}O, ^{17}O & ^{18}O), because of higher abundance and greater mass difference, the $^{18}O/^{16}O$ ($\delta^{18}O$) is normally used. Carbon has two stable isotopes (^{12}C & ^{13}C) and the ratio of $^{13}C/^{12}C$ ($\delta^{13}C$) is widely used. Stable isotope ratios are commonly measured using Mass Spectrometers. The present isotope study was carried out at the Isotope Laboratory of Faculty of Geosciences, University of Bremen, Germany, when the author was on a DAAD short-term fellowship.

Basic principles of Mass Spectrometers

Mass spectrometric methods are by far the most effective means of measuring isotope abundances. A mass spectrometer separates charged atoms and molecules on the basis of their masses based on their motions on magnetic and/or electric fields. In principle, a mass spectrometer may be divided into four different parts (Fig. 2.1): (1) the inlet system, (2) the ion source, (3) the mass analyser, and (4) the ion detector (for details, see Hoefs, 1987).

The *inlet system* has special arrangements for creating high vacuum, which is necessary for the stability of the ions produced and the mass separation. Purification of the gas (CO_2 in case of carbonates) before feeding to the mass spectrometer is also done here, through a trapping system which removes the moisture content and other unwanted gases produced from the sample materials during the reaction with acid.

The *ion source* is that part of the mass spectrometer, where ions are formed, accelerated, and focused into a narrow beam. Ions of gaseous samples are produced most reliably by electron bombardment. A beam of electrons is emitted by a heated filament and is directed to pass between two parallel plates. The beam is collimated by means of a weak magnetic field.

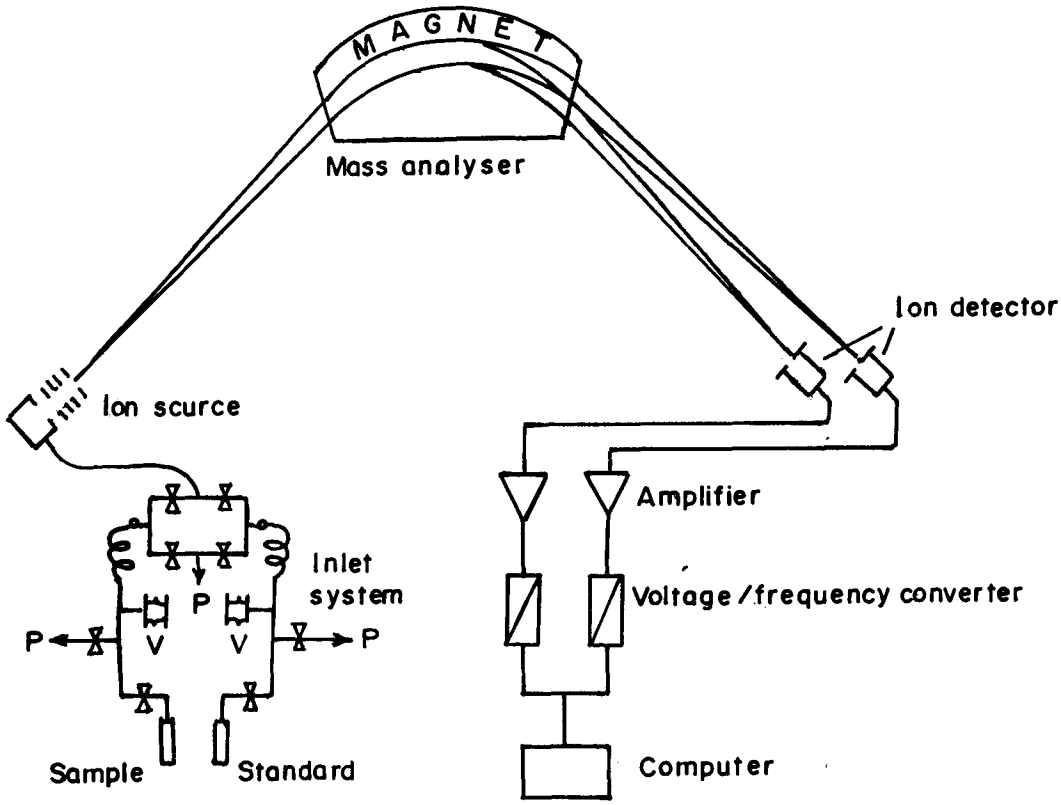

Fig. 2. 1 Schematic diagram of a mass spectrometer for stable isotope measurements. *P* denotes pumping system, *V* denotes a variable volume (from Hoefs, 1987).

The *mass analyser* separates the ion beams emerging from the ion source according to their mass/charge (M/e) ratios. This is done by using a strong magnetic field. As the ion beam passes through the magnetic field, the ions get deflected into circular paths, the radii of which are proportional to the square root of M/e. Thus the ions are separated into beams, on the basis of their masses.

After passing through the magnetic field, the separated ion beams are collected in the *ion detector* and converted into an electrical impulse, which is then fed into an amplifier. In the oxygen and carbon isotope measurements, seperate Faraday cups detect the different masses of ions simultaneously. With simultaneous collection, the isotope ratios of two different elements (O and C) can be compared quickly under nearly identical conditions. Today, in the new generation mass spectrometers (such as that of University of Bremen - Finnigan 251 and 252), the whole system is fully automated and computerised, leading to significant improvement in the accuracy and reproducibility of measurements.

Isotope measurements

Stable isotope measurements (both oxygen and carbon) were carried out on surface dwelling planktic foraminifers *Globigerinoides ruber* (white variety) and *Globigerinoides sacculifer* (the one without sac-like final chamber) and benthic foraminifer *Uvigerina peregrina*. For planktic foraminifers, only those of the 400-450 μm size ranges were used in order to avoid the size fraction effect (Duplessy *et al.*, 1981). About 10-12 specimens of 'clean' foraminifers were hand-picked under a microscope. Specimens having any fine grained material (like coccolithophorids) attached on them were avoided while picking. The entire isotope measurements reported in this study were carried out on a Finnigan MAT 252 Mass Spectrometer attached with an automated CO_2 preparation system (Carbo-Kiel, Carousel 48). The isotopic composition of the carbonate sample was measured on the CO_2 gas evolved by the treatment of foraminiferal shells with 98% Orthophosphoric acid at a constant temperature of 75°C. The standard gas was then calibrated against the international carbonate standard - Pee Dee Belemnite (PDB), using National Bureau of Standards (NBS) 19 and 20. The accepted unit of isotope ratio measurements is the delta value (δ). The δ- value is defined as:

$$\delta^{18}O = \{[(^{18}O/^{16}O)_{sample} / (^{18}O/^{16}O)_{standard}] -1\} \times 1000$$

The δ- notation represents per mil (‰) deviations from the isotopic standard PDB, prepared from the rostrum of the belemnite *Belemnitella americana* from the Cretaceous Pee Dee Formation of South Carolina. The PDB standard is defined as 0 per mil for carbon and oxygen. The isotopic composition of water is reported as per mil deviations of the sample, from Standard Mean Ocean Water (SMOW), a hypothetical water close to average ocean water (Craig, 1957). Since the sample supply of PDB is exhausted, calibrations are normally done through the analysis of National Bureau of Standards (NBS) samples. The NBS 19 is a homogenised standard of marble and NBS 20 is a homogenised standard of Jurassic Solnhofen limestone from Southern Germany. The analytical standard deviation, (i.e., the long term measurement precision) based on replicate analyses of internal laboratory standards for $\delta^{18}O$ were better than ± 0.07‰ and that for $\delta^{13}C$ was better than ± 0.04‰. Stable isotope studies were carried out on 85 samples for both planktic and benthic foraminiferal species.

For the stable isotopic composition of the organic carbon ($\delta^{13}C_{org}$), 20-30 mg of powdered sediment samples were accurately weighed in silver foil crucibles. These were then wetted with few drops of ethanol to suppress the foaming during decalcification. The sample was decalcified by drop-wise addition of 6M HCl and dried on a hot plate at about 80°C and was pressed into pellets. These samples were then combusted at 950°C in a HERAEUS CHN - Rapid elemental analyser interfaced by an automated CO_2 trapping box. Isotopic measurements were performed using a Finnigan delta-E Mass Spectrometer. The overall analytical precision, based on duplicates and repeated analyses of a laboratory internal reference sediment sample WST2 (North Sea Tidal Sediment), was better than 0.1‰. The isotopic data are reported as δ- value with reference to the PDB standard. The $\delta^{13}C_{org}$ analysis was conducted on 46 samples from two sediment cores.

2. 1. 7 Clay mineralogy

Clay mineral studies were conducted on 2 μm fraction of the sediment which was separated from the total sample based on the settling velocity principle

(Stoke's law) after removing the >63 μm fraction by wet sieving. The sample was made free of carbonate and organic matter by treating the sample solution with 5 ml acetic acid and 10 ml hydrogen peroxide, respectively. Excess acid was removed by washing with distilled water. Oriented slides were then prepared by pipetting 1 ml of the concentrated clay suspensions on glass slides and allowing them to dry in air.

X-ray diffraction studies were carried out on the air dried samples from 3° to 22° 2θ at 1.2° 2θ/minute on a Philips X-ray diffractometer (1840 Model) using nickel-filtered Cu Kα radiation, operated at 20 mA and 40 kV. The samples were then glycolated by exposing the slides to ethylene glycol vapours at 100°C for 1 hour and rescanned the slides under the same instrumental settings. The peaks for different clay mineral groups like kaolinite, chlorite, illite, smectite and gibbsite were identified. The areas of major clay minerals were calculated by using the glycolated X-ray diffractograms. The principal peak areas of kaolinite+chlorite, illite and smectite were multiplied by the weighting factors 2, 4 and 1, respectively and weighted peak area percentages were calculated following the semi-quantitative method of Biscaye (1965). Clay mineral ratios were also calculated, which are less affected by the sample treatments and ambiguity of relative abundance. In order to differentiate the kaolinite and chlorite peaks, the samples were also scanned from 24° to 26° 2θ at 1/2° 2θ/ minute. Additionally, illite chemistry was assessed using the ratio of integrated 5Å and 10Å peak areas of illite in the X-ray diffractograms, following Gingele (1996). Ratios below 0.5 represent Fe, Mg-rich illites, which are characteristic for physically eroded, unweathered rocks. Illite 5Å/Illite 10Å ratios above 0.5 are found in Al-rich illites, which are formed by strong hydrolysis. Clay mineral analyses were carried out on 50 samples from 4 sediment cores.

2. 1. 8 Radiocarbon dating

In addition to stable isotope stratigraphy, two sediment cores (GC-4 & GC-2) were radiometrically dated by ^{14}C method at the Physical Research Laboratory (PRL), Ahmedabad. The ^{14}C dating was carried out on bulk carbonates at three intervals on each core.

2. 2 SURFICIAL SEDIMENTS

Surficial sediments along the continental shelf and upper slope of western India between Ratnagiri in the north and Cape Comorin in the south and water depths between 25 and 500 m, were used for investigations on authigenic green marine clays. One hundred and ninety eight (198) sediment samples selected from different cruises of *R/V Gaveshani* (G- 17, 18, 30, 71 & 167) and *M/V Nand Rachit* (NR- 2A), were used for the study. Coarse fraction (>63 µm) of the sediment was separated by wet sieving, split into different sizes and the 125-250 and 250-500 µm size fractions were used for the present study. Coarse fraction components were identified under a binocular microscope and major sediment constituents (such as terrigenous, biogenic and authigenic green grains) were counted by spreading the sample over a gridded tray and counting about 400 grains in each sample. The percentage distribution of these constituents was obtained.

Similarly, eighty two (82) surficial sediment samples collected during the 76th and 77th cruises of *R/V Gaveshani* were selected for the distribution of authigenic green clays along the eastern continental margin of India. These samples were from the continental shelf and upper slope between the Mahanadi and Godavari river mouths and their depth varies from 18 to 247 m. Texture of the sediment was determined following standard procedures. Percentages of terrigenous, biogenic and authigenic grains were estimated.

2. 2. 1 Separation of green grains

Green grains were then separated by using a Frantz Isodynamic magnetic separator with a longitudinal slope of 25° and a lateral slope of 17° using 0.6 to 0.8 mA current, following Odin (1988). The magnetically separated fraction was examined under a binocular microscope and pure green grains were obtained by hand picking. Morphology of the green grains was also noted.

2. 2. 2 X-ray diffraction studies

Pure green grains thus obtained were powdered to fine size and both unoriented and oriented slides were prepared. The slides were scanned from 3° to

15° 2θ and 3° to 40° 2θ (selected samples) at 1.2° 2θ/ minute on a Philips X-ray diffractometer (1840 Model) using nickel-filtered Cu Kα radiation. Subsequently, nineteen samples from the west coast and five samples from the east coast of India were selected based on the geographic location and depth distribution and analysed for detailed mineralogy. The samples were subjected to ethylene glycol solvation (100°C/1 hour) and 1 N acetic acid (70°C for 2 hours) treatments separately. The slides were thermally heated on a muffle furnace at 250°C (for 1 hour), 490°C (for 2 hours) and 600°C (for 4 hours). X-ray diffractograms were obtained at each stage under the same instrumental settings.

2. 2. 3 Geochemical studies

Geochemistry of the pure green grains was carried out on only 13 samples, owing to the difficulty in obtaining enough material. For silica determination, the samples were decomposed by fusion with NaOH at a comparatively low temperature for 5 minutes in nickel crucibles (Shapero and Brannock, 1962). After cooling, the melts were leached with distilled water and the solutions were acidified with HCl. Elemental analysis was carried out on a Perkin Elmer Spectrophotometer (Lambda 11 Model). Sample digestion for other major, minor and trace elements and REEs were done using a mixture of HCl, $HClO_4$, HNO_3 and HF in an open digestion system. The resulting dried residue was then dissolved in HNO_3. Al, Fe, Mg, Mn and Ca were analysed on an Inductively Coupled Plasma - Atomic Emission Spectrometry (ICP-AES; Jobin Yvon JY-385) and Na and K by Atomic Absorption Spectrophotometer (AAS) at the Physical Research Laboratory (PRL), Ahmedabad. Minor, trace and REE analyses were carried out on an Inductively Coupled Plasma- Mass Spectrometer (ICP-MS) using a VG PlasmaQuad (FI Elemental, UK), at the National Geophysical Research Institute (NGRI), Hyderabad. The details of methods and instrumental settings are given in detail by Balaram and Saxena (1988). In contrast to ICP-AES, which generally requires prior chromatographic separation from the matrix for REEs, ICP-MS offers very low detection levels and relatively fast turnaround. The analytical accuracy was checked by analysing international standards [MAG-1 (Marine Mud), SO-3 (Soil-Canadian) and a glaucony mineral standard GL-O

(Glaucony-Odin; Odin and Matter, 1981)]. The analytical accuracy of the measurements were better than ±2% for Si, Al, Fe, Mg, K and Ca; better than ±15% for all minor and trace elements and REEs, except for Cr, Cu, Gd, and Ho where it is >15%. Sodium (Na) showed a greater uncertainty which may be due to some systematic error.

Chapter 3

Chapter 3

CONTROLS ON ORGANIC CARBON DISTRIBUTION IN SEDIMENT CORES FROM THE WESTERN CONTINENTAL MARGIN OF INDIA

3. 1 INTRODUCTION

The origin of organic carbon enrichment in Quaternary marine sediments has been a subject of intense and renewed interest during the past decade. Organic carbon is supplied to marine sediments from both marine and terrestrial sources. Studies on carbon isotopic composition of the sedimentary organic matter (Sacket, 1964; Fontugne and Duplessy, 1986) suggested that the influence of terrestrial sources is limited to areas within a few tens of kilometres of the coastline so that marine organic matter is the dominant component in most of the marine sediments.

Primary production of marine organic matter in the ocean is done by a wide range of unicellular planktonic organisms whose activities are governed by nutrient supply and solar radiation. Only a fraction of the organic matter produced in the euphotic zone is exported and settles into deeper waters. Part of this material is oxidised during settling, part is used as food by benthic organisms, part undergoes further degradation in the sediments, and the remainder is buried. The continental margins are generally much more productive than open ocean regions and a high settling flux of organic matter occurs here. Also a substantial portion of the carbon produced over the continental shelves is exported to deeper water beyond the shelf edge, thereby augmenting the settling flux of organic carbon to these areas (Walsh *et al.*, 1981). The upper parts of the continental slope could, therefore, constitute important sinks for organic carbon. Today over 90% of all organic carbon burial in the ocean occurs in continental margin sediments (Hedges and Keil, 1995). This burial represents the dominant removal pathway of reduced carbon from the oceans and hence on a geological time scale, determines the oxygen content of the atmosphere (Hedges, 1992). Thus, studies on past variations in organic carbon and factors responsible for their burial and preservation in the marine environment are of prime importance.

The amount and type of organic matter in marine sediments are responses to the supply and preservation of organic materials from marine and terrestrial sources (Summerhayes, 1981; Tissot *et al.,* 1980). Investigations on the Quaternary sediments of the Pacific and Atlantic oceans indicated that primary productivity is the principal control for the formation of organic-rich deposits (see Calvert *et al.*, 1992; Calvert and Pedersen, 1992). Hartnett *et al.* (1998) suggested that organic preservation in the continental margin sediments is influenced by the length of time, the accumulating particles are exposed to molecular oxygen in sediment pore water rather than direct influence of oxygen on organic carbon burial. The Arabian Sea is a classic example of an 'anoxic open ocean' (Demaison and Moore, 1980), with upwelling-induced high primary productivity in the surface waters and a permanent oxygen minimum zone at intermediate depths. Higher levels of organic carbon (1-4 wt.% and up to 16 wt.%) occur in the continental slope sediments of the eastern Arabian Sea (Paropkari *et al.*, 1987; Paropkari *et al.*, 1992), and its distribution is still a matter of debate. Some workers consider that anoxia is the most important deciding factor (Demaison and Moore 1980; Paropkari *et al.*, 1992; 1993), while others (Pederson and Calvert 1990; Pederson *et al.,* 1992; Calvert *et al.,* 1995) suggest that productivity in conjunction with factors like sediment characteristics and texture, rather than anoxia, are important for the high organic carbon preservation.

In this Chapter, an attempt is made to examine the distribution of organic carbon in the sediment cores retrieved from three physiographic settings on the upper continental slope and the factors responsible for its preservation are discussed.

3. 2 RESULTS

3. 2. 1 Age control and lithology

The six sediment cores used in this study were collected from the western continental margin of India (Fig. 3.1).With the exception of GC-1, all these cores have chronological control either by continuous $\delta^{18}O$ records of surface dwelling planktic foraminifers (*Globigerinoides ruber* and/or *Globigerinoides sacculifer*), or

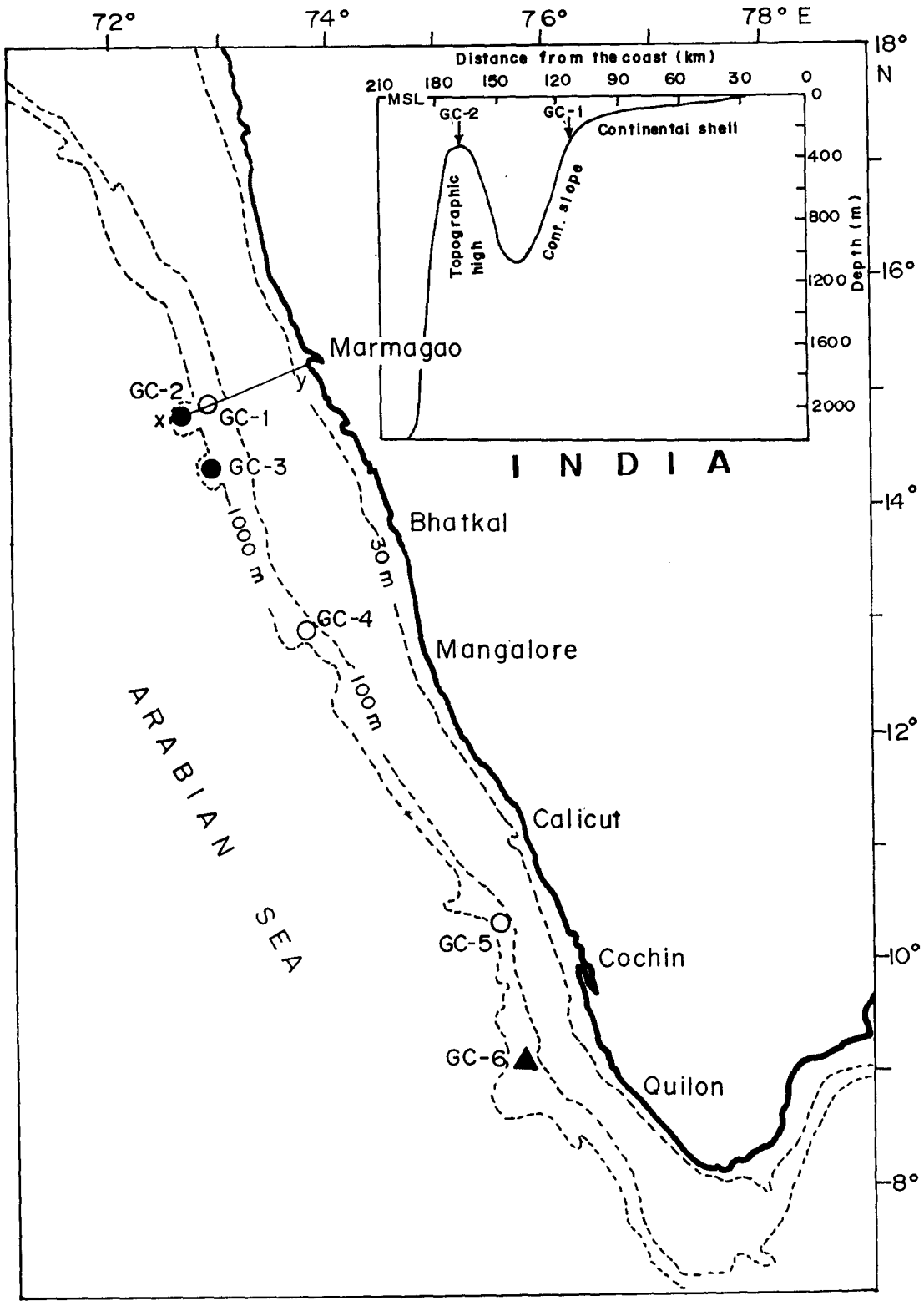

Fig. 3. 1 Locations of the Gravity Cores (GC) along the continental slope of western India. (continental slope- O; topographic high- ●; continental terrace- ▲). *Inset*: A schematic cross section (off Goa) showing the location of topographic high on the slope (transect x - y); arrows indicate the locations of the cores.

by ^{14}C (bulk carbonate) dates. Core GC-5 has a continuous high resolution record of oxygen isotope Stages 2 and 1 (i.e., the late Pleistocene and Holocene period). Core GC-4 has three ^{14}C dates (Table 3. 1) and a low resolution $\delta^{18}O$ stratigraphy till the end of Stage 3. Core GC-6 has $\delta^{18}O$ stratigraphy up to ~310 cm interval, which may include the isotope Stages 1, 2 and 3. In GC-3, $\delta^{18}O$ measurements were conducted only for the top ~200 cm of the core, representing the isotope Stages 1, 2 and part of Stage 3. For core GC-2, there are three ^{14}C dates in the upper 35 cm thick sediment column (Table 3. 2). The $\delta^{18}O$ records obtained were subsequently correlated with the stacked SPECMAP record of Imbrie *et al.* (1984) to obtain an age model for the cores. Detailed age assignments for individual cores is described in Chapter 4. In this chapter, only the age controls between the late Pleistocene and Holocene are used.

The colour of sediments in all the cores varied from olive grey in the upper portions to brown black/ greyish black in the lower portions. The grain size parameters, C_{org}, $CaCO_3$ and constituents in the coarse fraction of the sediments in all cores show distinct changes in the upper portions of the cores and the sediments below. Based on the available age controls and variations in the above parameters, each core was divided broadly into Unit 1 and Unit 2 sediments and the boundary between the two are considered as the boundary between the late Pleistocene and Holocene (around ~10 ka-BP). The length of the Unit 1 (Holocene) sediments varied between ~160 cm in GC-5 to ~25 cm in GC-2. For core GC-1, eventhough chronological control was not available, the sediment column was divided into two units based on the lithological, C_{org} and $CaCO_3$ variations.

Table 3. 1 ^{14}C ages (bulk carbonate) for the core GC - 4.

Sl. No.	Core No.	Core depths	Age in years
1	GC - 4	16 - 20 cm	6425 ± 55 years
2	GC - 4	25 - 30 cm	7465 ± 55 years
3	GC - 4	50 - 55 cm	11,850 ± 60 years

Table 3. 2 ^{14}C ages (bulk carbonate) for the core GC - 2.

Sl. No.	Core No.	Core depths	Age (years)
1	GC - 2	8 - 12 cm	2600 ± 120 years
2	GC - 2	16 - 20 cm	4640 ± 75 years
3	GC - 2	30 - 35 cm	13,990 ± 60 years

3. 2. 2 Grain size parameters

Grain size parameters measured for the sediments in all cores are given in Tables 3.3 - 3.8. Cores from the upper continental slope (GC-5, GC-4 & GC-1) revealed that sand content increased considerably in the Unit 1 sediments, eventhough silt and clay dominates throughout the core (see Figs. 3.2-3.4). It varied from a lowest value of ~1% at the base of Unit 1 to ~22% at the top in GC-5. Similarly, both GC-4 and GC-1 exhibited very low sand content (<1-2%) in Unit 2 and progressively higher values (31 - 33%) in Unit 1.

Sand content dominates the Unit 1 sediments of core GC-6 from the terrace, although higher values of sand content are also obtained in the upper parts of the Unit 2 (Fig. 3.5). Increase in sand content started from ~125 cm depth interval, corresponding to LGM, according to the isotope age estimation.

The cores from the topographic highs off Goa (GC-2 & GC-3) have high silt and clay contents in Unit 1 (silt+clay ranges between 92 and 97%), and high sand content in Unit 2. It is up to ~64% in GC-2 (Fig. 3.6). The distribution of sand content is more complex in GC-3, with higher values between 420-325 and 120-30 cm intervals and relatively low values in between (Fig. 3.7).

3. 2. 3 Organic carbon (C_{org}) and $CaCO_3$ contents

C_{org} content varies from 0.94% to 8.7% with relatively higher values (8.7%-1.2%) in Unit 1 than Unit 2 sediments of all the cores, except in GC-1 (Table 3.3-3.8; Fig. 3.2-3.7). The $CaCO_3$ content closely follows the sand content and ranges from ~13 to 80% and its distribution varies in each physiographic setting. The C_{org} and $CaCO_3$ contents are high in the core tops and gradually decrease with

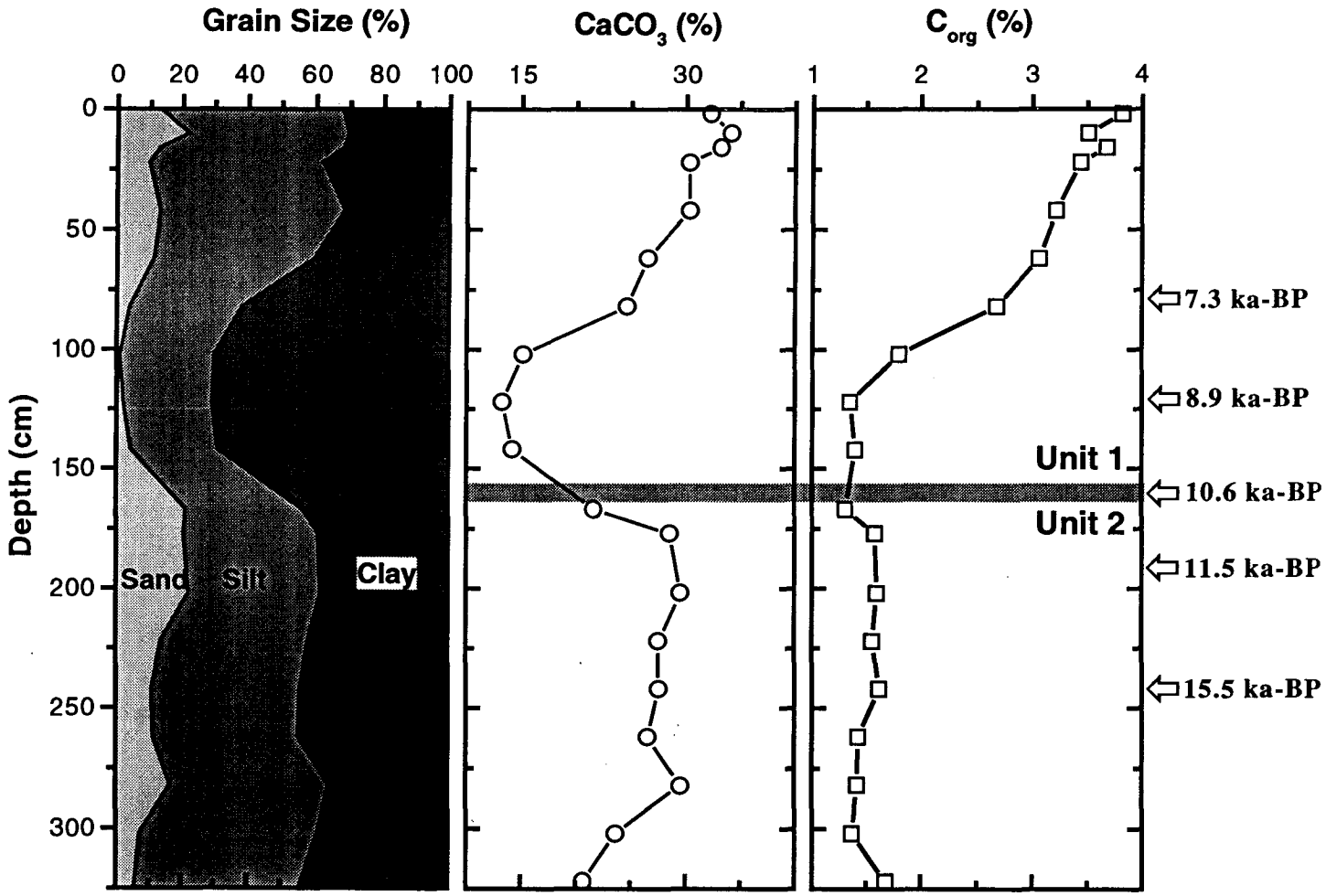

Fig. 3. 2 Downcore distribution of grain size parameters, $CaCO_3$ and C_{org} content in the core GC-5. Age estimation is based on $\delta^{18}O$ records of *G.ruber* (see Chapter 4).

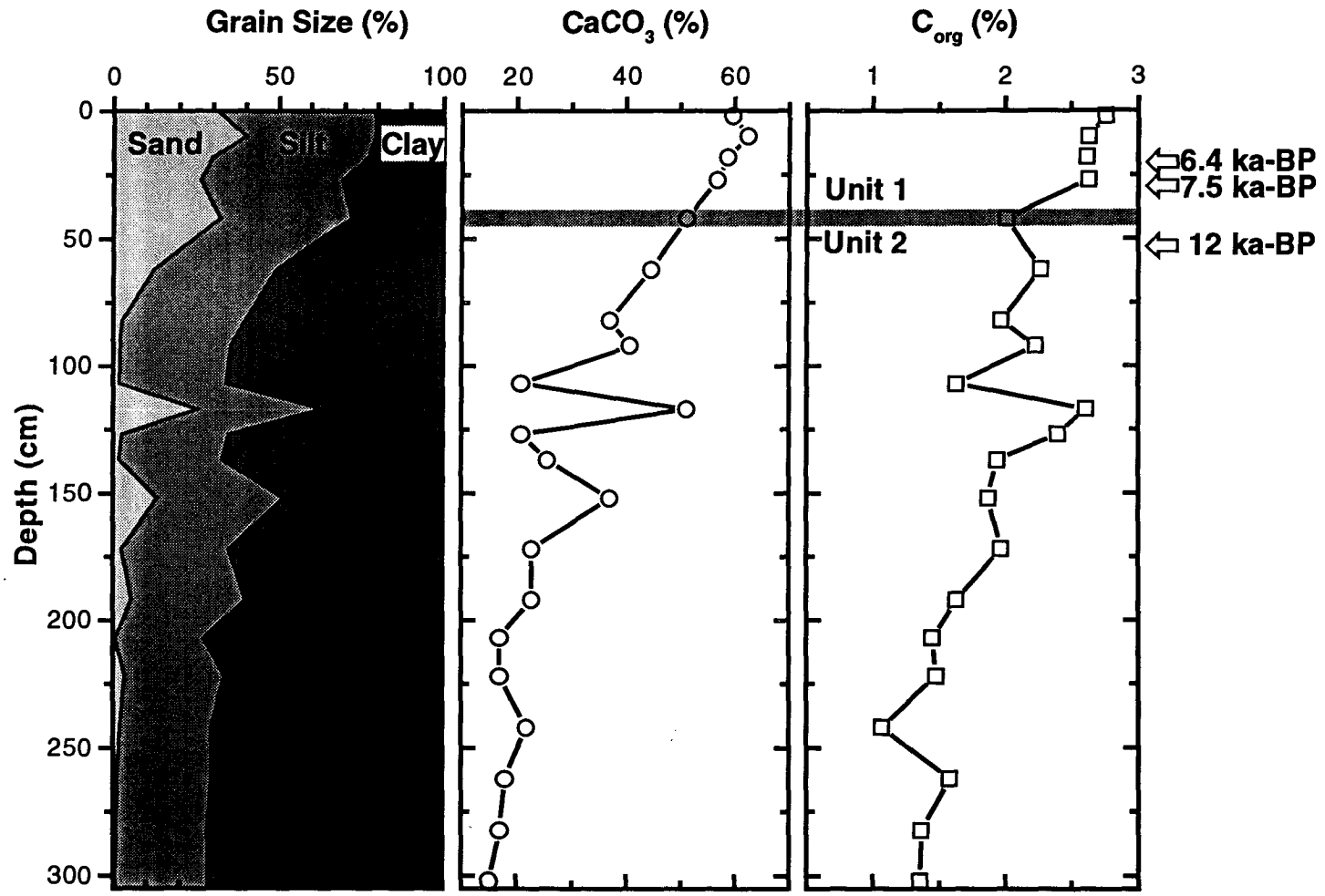

Fig. 3. 3 Down core distribution of grain size parameters, $CaCO_3$ and C_{org} content in the core GC-4. Age estimation is based on ^{14}C dating (arrows).

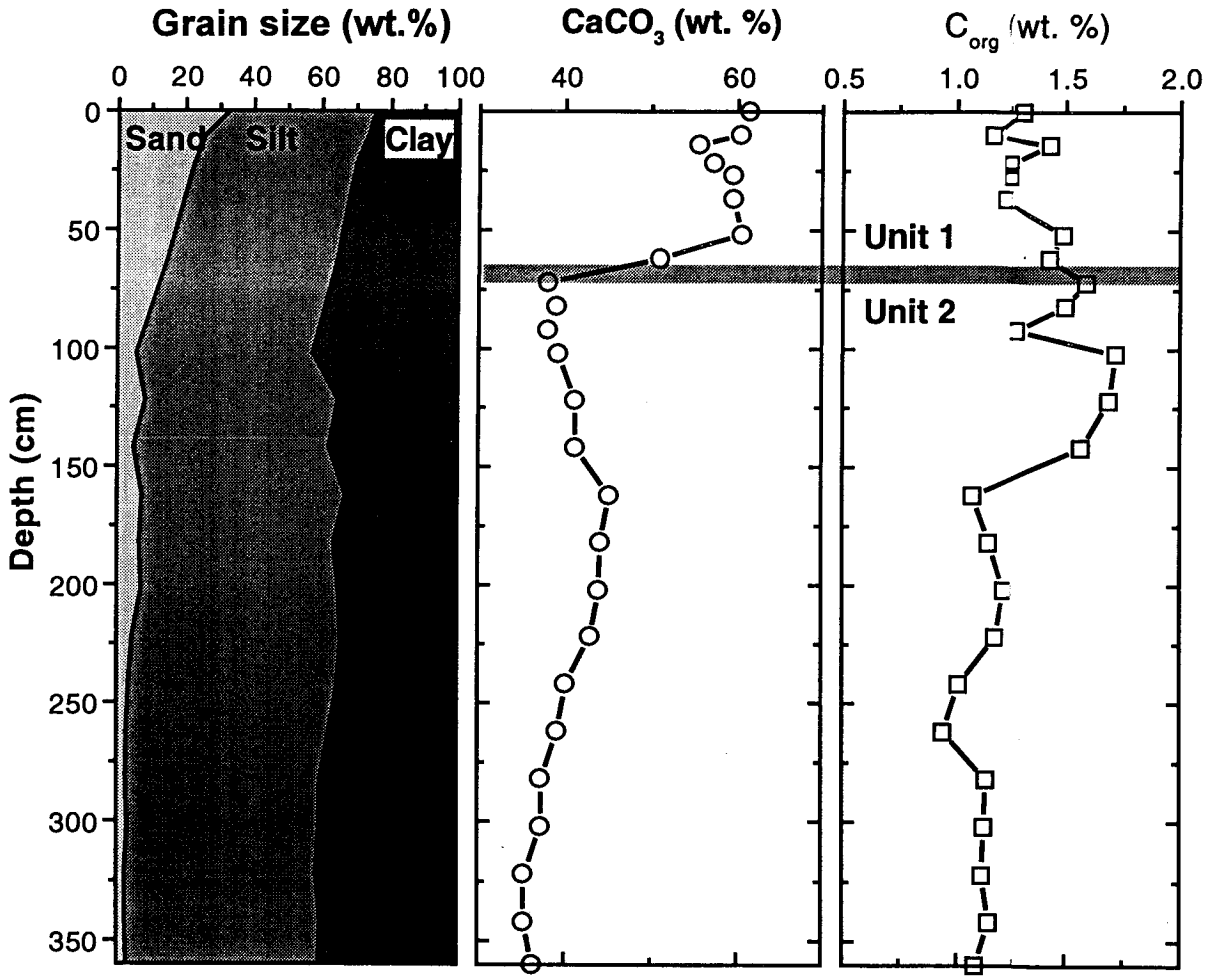

Fig. 3. 4 Downcore distribution of grain parameters, $CaCO_3$, and C_{org} content in the core GC-1.

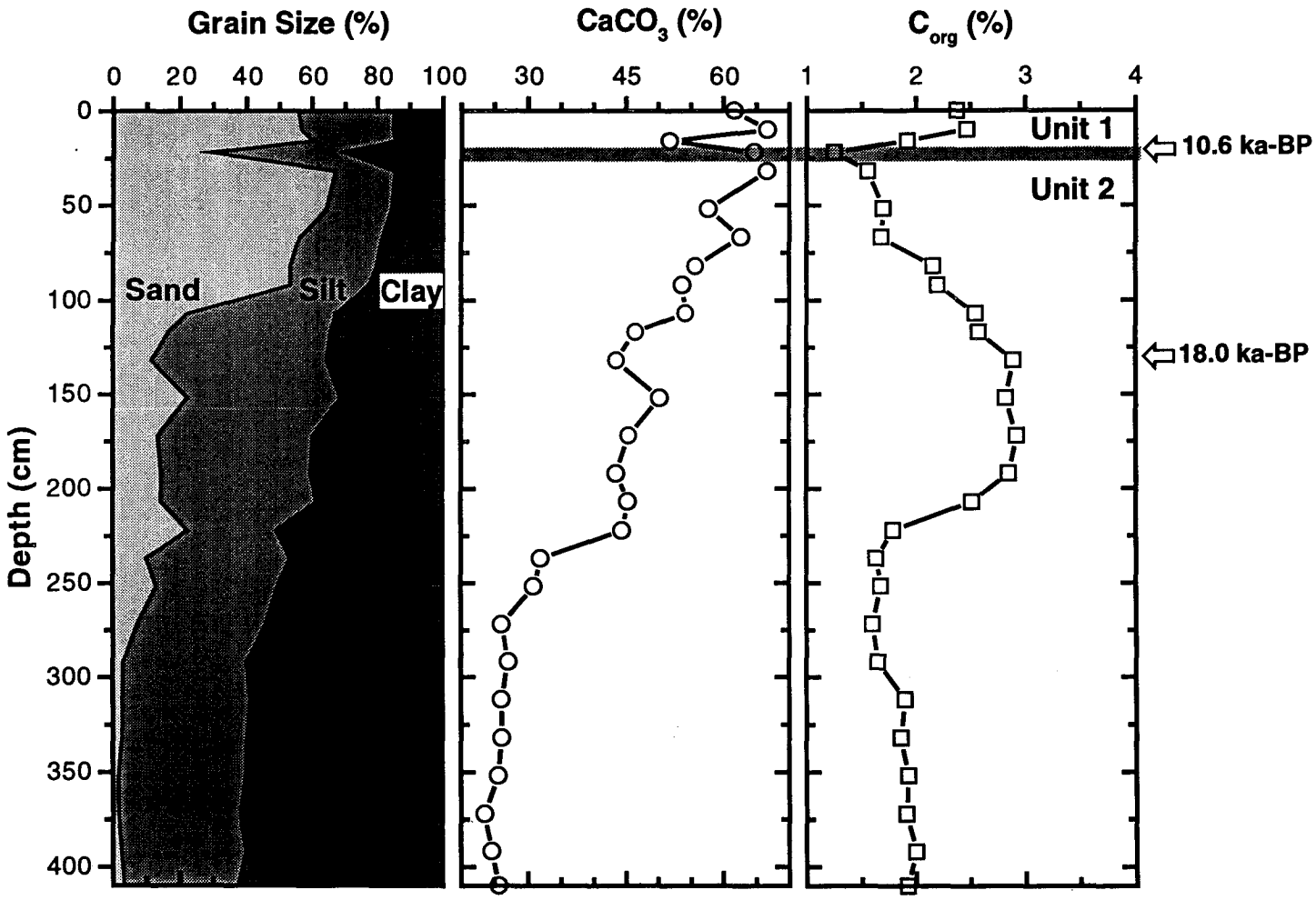

Fig. 3. 5 Downcore distribution of grain size parameters, $CaCO_3$ and C_{org} content in the core GC-6. Age estimation is based on $\delta^{18}O$ records of *G.ruber*.

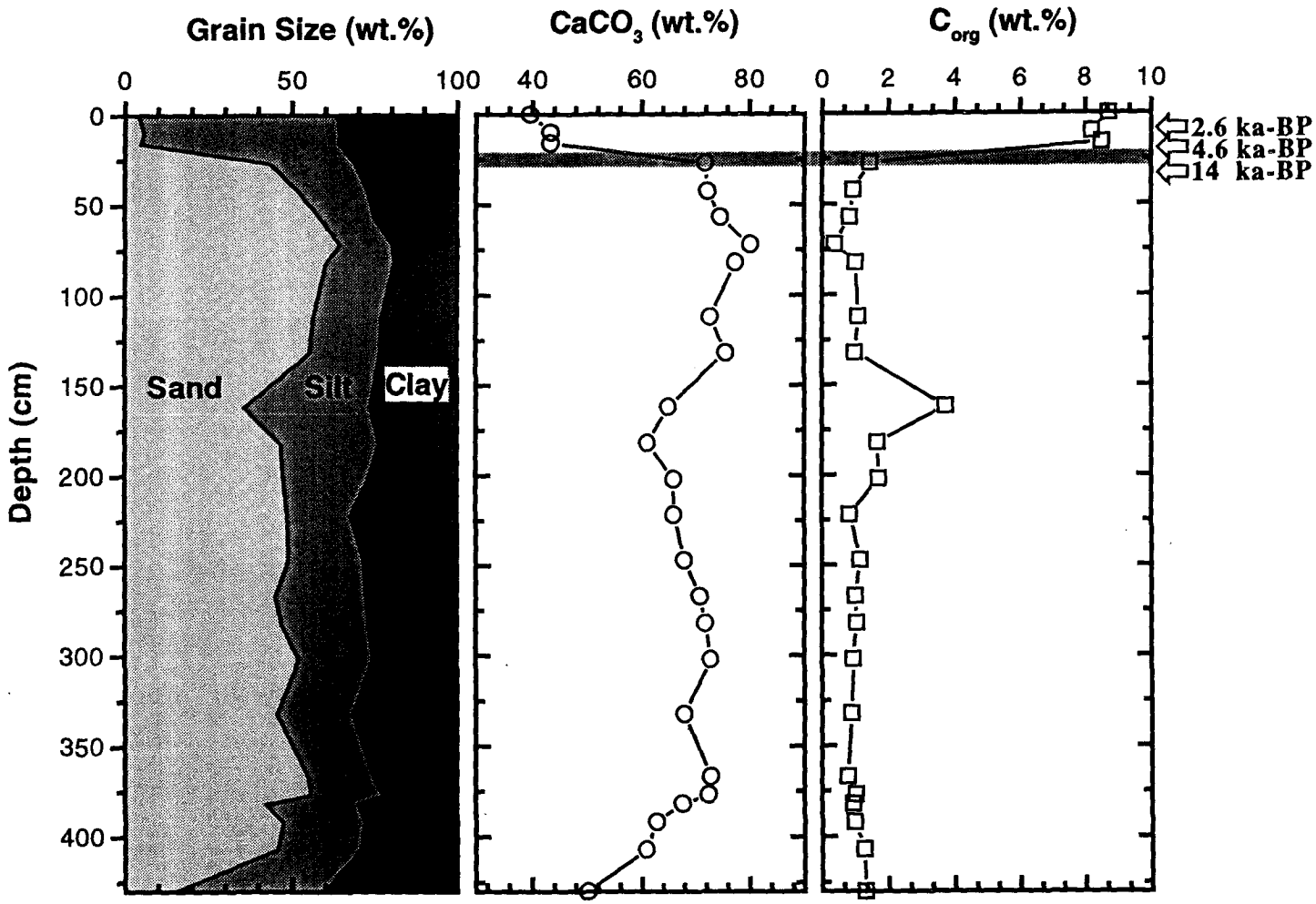

Fig. 3. 6 Down core distribution of grain size parameters, $CaCO_3$, and C_{org} content in the core GC-2. Age estimation is based on ^{14}C dating (arrows)

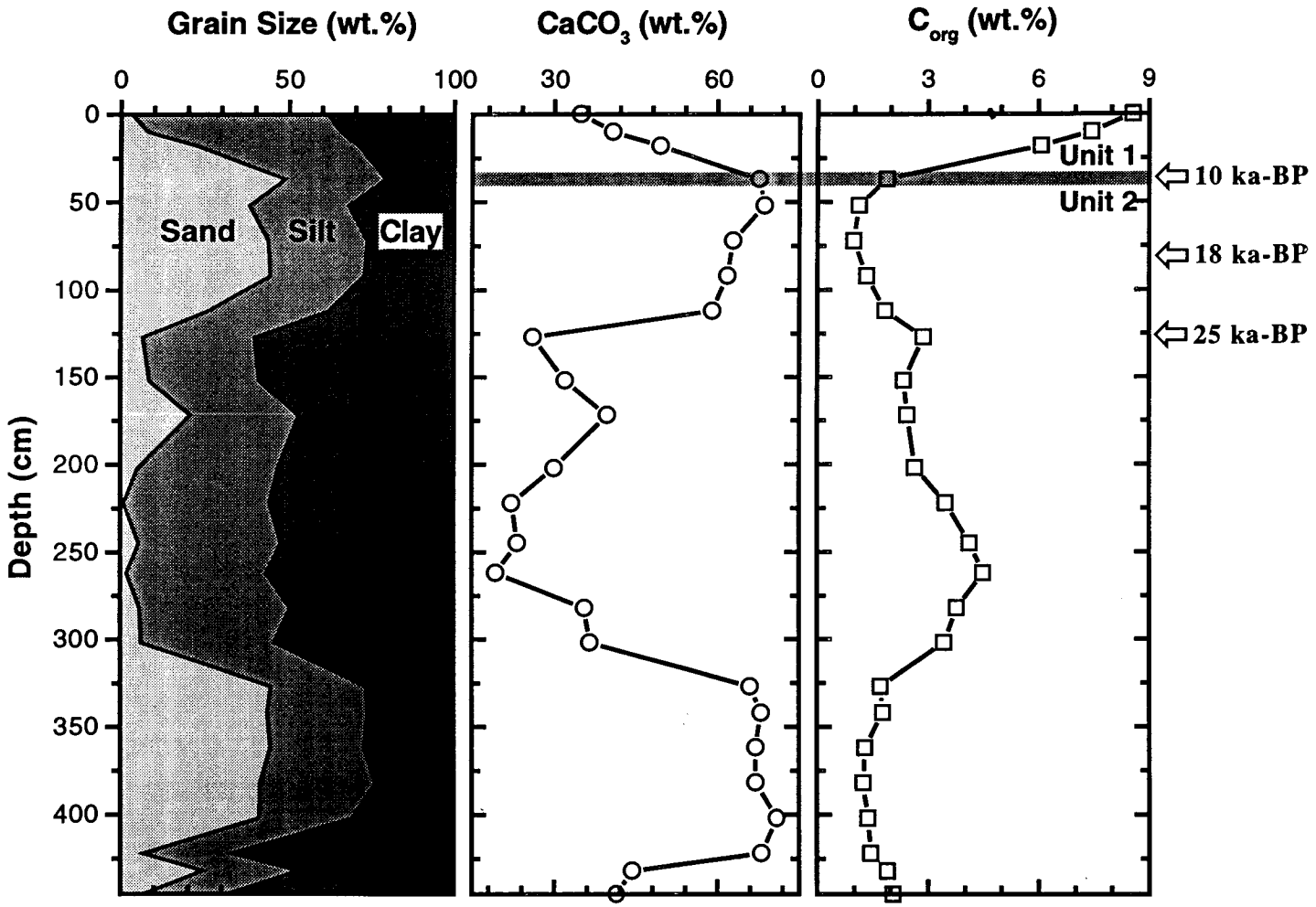

Fig. 3. 7 Down core distribution of grain size parameters, $CaCO_3$, and C_{org} content in the core GC-3. Age estimation is based on the $\delta^{18}O$ records of *G.sacculifer*.

increasing depth levels in Unit 1 sediments of the cores from the continental slope (Fig. 3.2-3.4). Within the Unit 2 sediments, these parameters decreases from the top to the bottom or remains uniformly low, inspite of the increase in $CaCO_3$ and sand content at certain levels.

The C_{org} and $CaCO_3$ content in Unit 1 sediments of the cores from the terrace follow the same trend, except that the $CaCO_3$ content is initially high (Fig. 3.5). But in the Unit 2 sediments, C_{org} initially increases with increasing depth and a broad hump of high C_{org} can be seen in the middle portions and uniformly low C_{org} values in the lower portions. This increase in C_{org} content coincides with a gradual decrease in $CaCO_3$ and sand content (Fig. 3.5).

The C_{org} content shows an inverse relationship with $CaCO_3$ and sand content of the sediments in the cores from the topographic highs. Highest C_{org} content (7.9-8.7%) corresponds to lowest $CaCO_3$ (35-49%) and high silt and clay content in the Unit 1 sediments and vice versa in Unit 2 sediments (Tables 3.7 & 3.8; Figs. 3.6 & 3.7).

3. 2. 4 Coarse fraction studies

Coarse fraction (125-250 μm size) observations under binocular microscope indicate that, the cores from the slope contain abundant planktic foraminifers, keels and traces of pyrite (as encrustations on skeletal fragments) in the Unit 1. Coarse fraction content is very less in the lower portions of Unit 1 of GC-5 (100-140 cm) and composed of mostly shell fragments of shallow water origin. Unit 2 sediments are characterised by dominant skeletal fragments of shallow water origin, benthic foraminifers *Bolivina* and *Uvigerina*, pyritized grains and infillings and a few planktic foraminifers.

Planktic foraminifers are abundant both in Unit 1 and Unit 2 sediments of the terrace; followed by keels of planktic foraminifers, *Bolivina*, *Uvigerina* and brown/black (phosphate/ pyrite) infillings and pellets in the Unit 1 sediments. While in Unit 2 sediments, abundant shell debris of shallow water origin, *Bolivina*, *Uvigerina* and pyrite infillings correspond to high organic carbon. Pyrite moulds and a few planktic foraminifers continued to dominate in the lower parts of Unit 2 sediments.

Unit 1 sediments of the cores from topographic highs contain mainly keels and few planktic foraminifers. Although planktic foraminifers dominate Unit 2 sediments, *Uvigerina*, otoliths, coiled mollusks, pelecypods, gastropods and shell debris become prominant both in 125-250 and 250-500 μm fractions. Borings on shells and a few cemented foraminiferal aggregates are common. Phosphatized coprolites and corals encrusted on small gastropods were also reported (Rao *et al.*, 1995) at certain sediment intervals of the core GC-2.

3. 2. 5 Rock-Eval pyrolysis

Hydrogen Index (HI) and 'S_2' values are found to be higher in Unit 1 sediments than in Unit 2 sediments of all the cores (Table 3.9). Highest HI (445-892 mg HC/ g C_{org}) and S_2 values (38.7-76.3) correspond to the highest organic carbon content (8.6-8.7%) in Unit 1 sediments of the cores of topographic highs. S_1 and S_2 values are low (0.17-0.39 and 0.63-1.55 respectively) in Unit 2 sediments of the cores from the topographic highs. HI values are moderate (121-198 mg HC/ g C_{org}) and low (~97 mg HC/ g C_{org}) in Unit 1 sediments of the cores from the slope and terrace, respectively. S_1 and S_2 values followed the same trend with higher values in Unit 1 (0.41-1.64 and 1.98-7.56, respectively) and lower values (0.1-0.6 and 0.3-1.8, respectively) in Unit 2 sediments. T_{max} values in all the samples varied between 390 and 441°C, without showing any significant pattern among different cores and different depth intervals within the cores (Table 3.9).

3. 3 DISCUSSION

3. 3. 1 Nature of the organic carbon

The hydrogen index (HI) and C_{org} contents show significant positive correlation ($r = 0.86$, $n = 7$) with each other in the Holocene (Unit 1) and poor correlation ($r = 0.17$, $n = 17$) in the Pleistocene (Unit 2) sediments of all cores (Fig. 3.8). The low T_{max} values of all sediment samples (390-441°C) (Table 3.9), suggests that the organic matter is thermally immature. A HI-T_{max} plot (Fig. 3.9) shows that the Holocene sediments of the slope and terrace fall above and on the Type III boundary while those of the topographic highs fall close to the Type II boundary suggesting that the C_{org} is a mixture of Type II and III in the former and

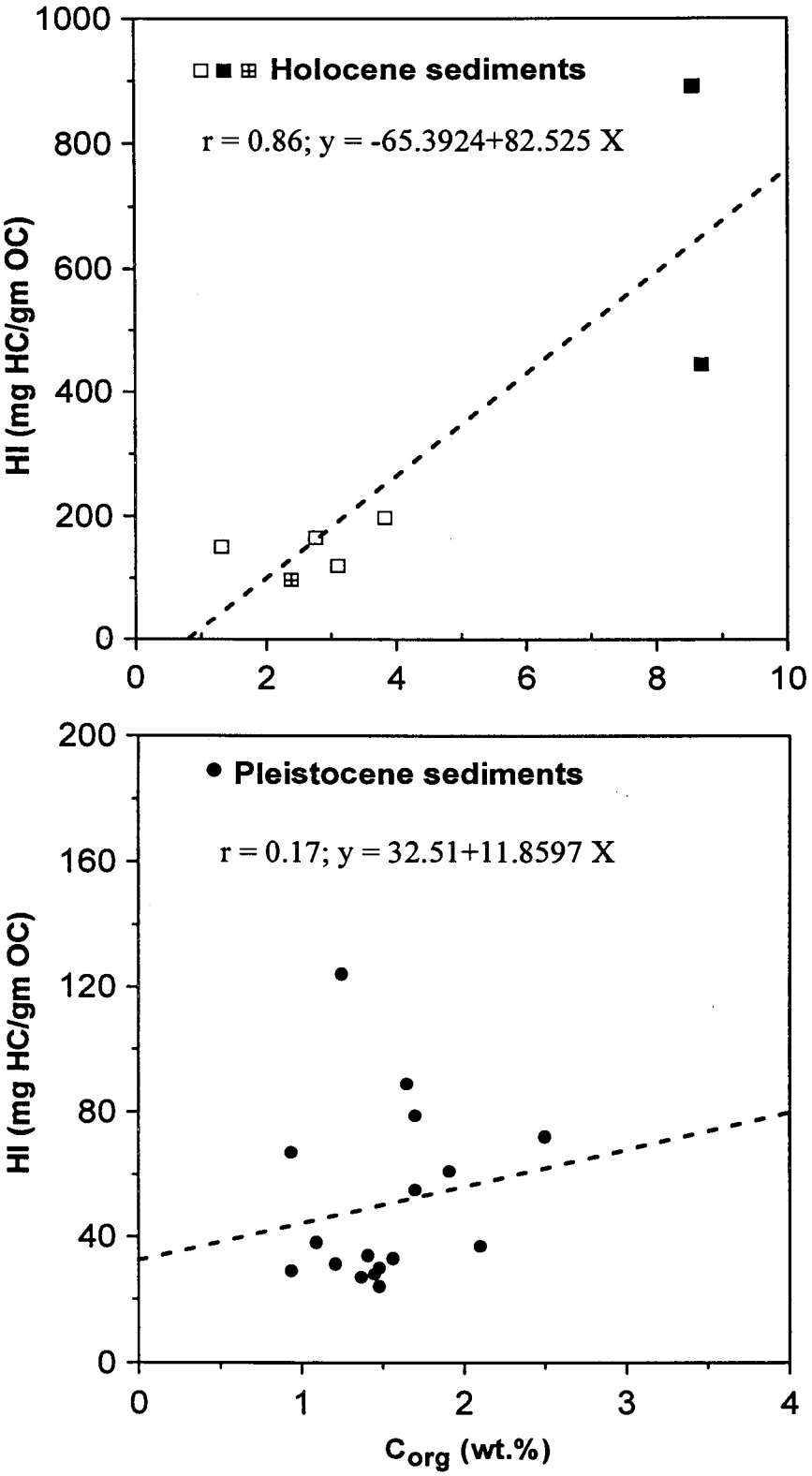

Fig. 3. 8 Relationship between C_{org} and hydrogen index (HI) for all samples.
□ - slope samples;■ -topographic high samples; ⊞ - terrace samples.

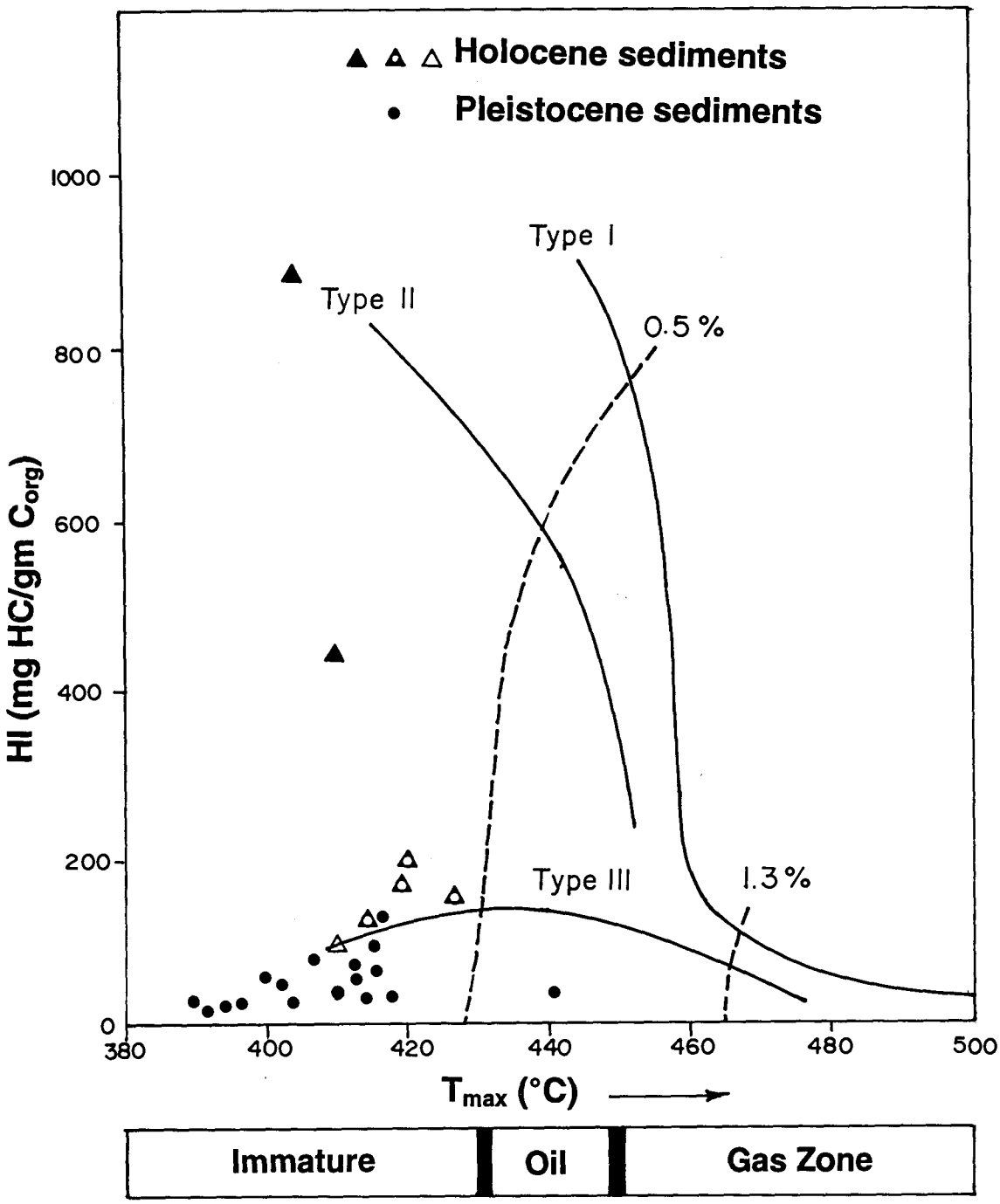

Fig. 3. 9 Relationship between HI and T_{max}. Solid lines are the boundaries for Type I, II, and III kerogens. Dashed lines represent the iso- reflectance curves.

mostly Type II in the latter (see Espitalié and Joubert, 1987). The Pleistocene sediments of all cores fall below the Type III limit (Fig. 3.9), suggesting that it is either reworked marine (Type II) and/or terrestrial (Type III). The carbon isotope ratios of organic matter on two sediment cores from the upper slope (GC-5 & GC-4) revealed that eventhough the HI values are low, the organic matter is dominantly marine throughout the cores ($\delta^{13}C_{org}$ values varied between -19.5‰ to -21.5‰; see Chapter 4). So the low HI values of the Unit 2 sediments may be mainly due the reworking of the original marine organic matter. The genetic potential (S_1+S_2) (see Tissot and Welte, 1984) is high (S_1+S_2 = 2.4 -91.2) for the Holocene and low (0.4 - 2.2) for the Pleistocene sediments.

Figure 3.10 shows the plot between C_{org} and S_2. The boundaries for Type I-II and Type II-III organic matter are also inserted in these plots, following Langford and Blanc-Valleron (1990). The C_{org} content and S_2 value of the Holocene sediments show strong positive correlation (r = 0.9, n = 7) and the values fall above and on the Type II-III boundary line or just below the boundary line. Since these sediments have high hydrogen index and positive x- intercept on C_{org} vs. S_2 (Fig. 3.10), the sample points falling just below the boundary line may represent low-hydrocarbon end members of Type II kerogen (i.e., reworked organic matter) (see Langford and Blanc-Valleron 1990). S_2 also shows positive correlation with C_{org} (r = 0.6, n = 17) in all Pleistocene samples which fall below the Type II-III boundary line (Fig. 3.10), suggesting that the organic carbon is mostly terrestrial and/or reworked marine. The slope of the regression equations (see Fig. 3.10) indicates that the Holocene and Pleistocene sediments contain about 85% and 7.5% pyrolysable hydrocarbons, respectively. The x- intercepts for the Holocene and Pleistocene sediment samples are ~2.0 and 0.5% C_{org}, respectively (Fig. 3.10), indicating that higher amounts of organic materials were available in the Holocene sediments before the hydrocarbons released by pyrolysis. The high x- intercept in Holocene sediments are due to clayey sediments in the topographic highs. Katz (1983) and Espitalié *et al.* (1985) suggested that the effect of high rock matrix adsorption for clays results in high x-intercept. The y- intercepts for Holocene and Pleistocene sediments are 17.83 and 0.35 respectively, suggesting that the adsorption capacity of 1 gram sediment

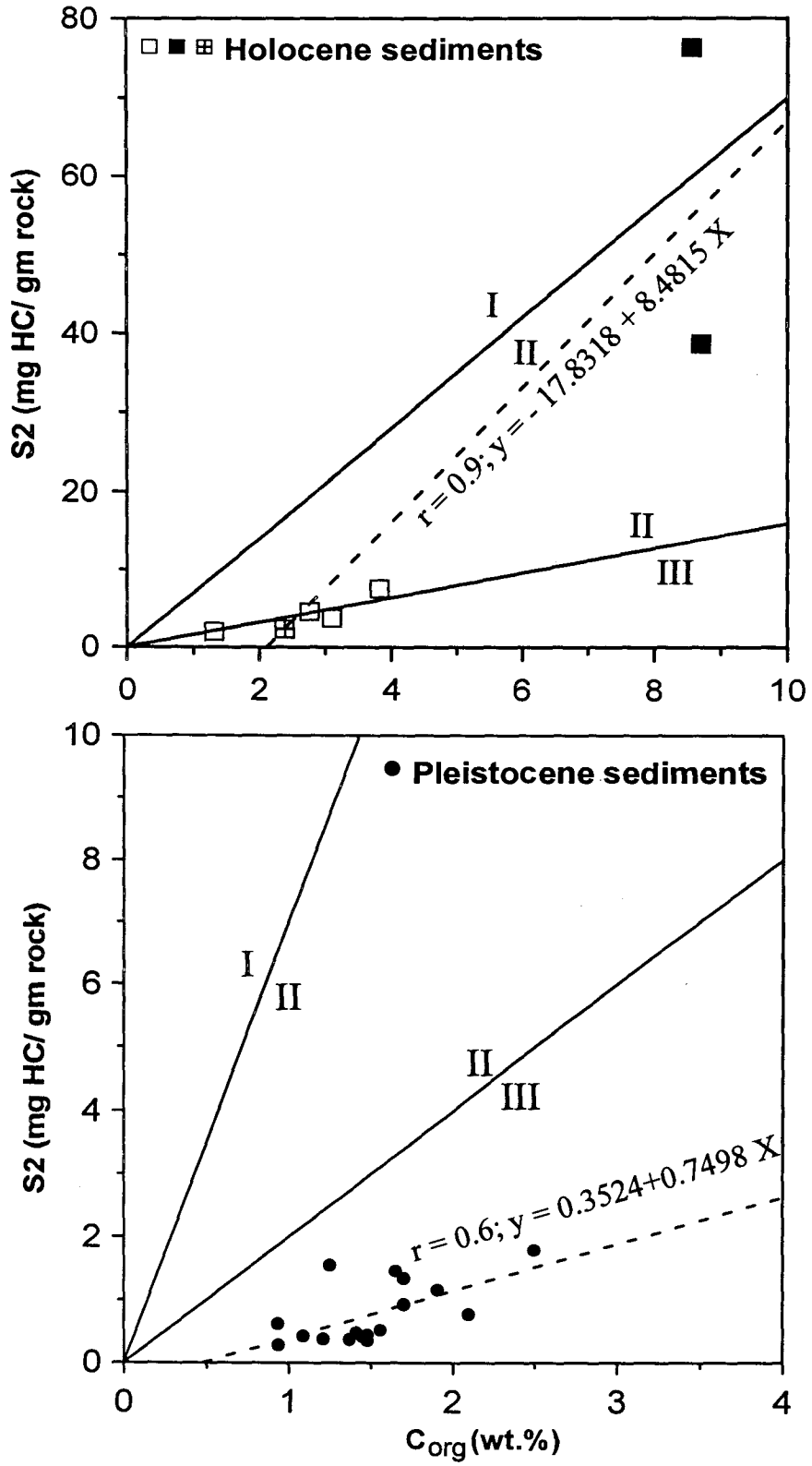

Fig. 3. 10 Relationship between C_{org} and S2 for all samples.

sample is 17.83 and 0.35 mg of pyrolysable hydrocarbons for the respective sample populations.

3. 3. 2 Sediment cores from the upper continental slope

The C_{org}, $CaCO_3$ and sand contents progressively increase from the base of the Unit 1 to the top of the cores (Fig. 3.2 - 3.4). They show strong positive correlation with each other except in GC-1. Sheu and Huang (1989) and Paropkari *et al.* (1991) suggested that the direct covariance between $CaCO_3$ and C_{org} indicate control by primary productivity. Although HI and C_{org} shows positive correlation in both Unit 1 and Unit 2 sediments, the low C_{org} in the Unit 2 sediments and its increasing trend towards the surface may indicate the enhanced productivity of the overlying waters since the beginning of the Holocene. Several workers studied palaeoproductivity fluctuations and monsoonal variations in the Arabian Sea and in the adjacent landmass and reported weakest monsoons and associated low productivity during the Last Glacial Maximum (LGM, ~18 ka-BP) and increased monsoonal wind systems and enhanced upwelling induced productivity from ~12 to 5 ka-BP (Street and Grove, 1979; Duplessy, 1982; Prell, 1984 a; van Campo *et al.*, 1982; Prell and Kutzbach, 1987). Reducing conditions in the sediments are indicated by the presence of *Bolivina, Uvigerina*, and pyrite encrustations. Weak correlation of C_{org} with $CaCO_3$ together with abundant shell fragments and benthic fauna in the Holocene part of the core (GC-1) may indicate dilution of C_{org} by reworked material from the shelf. Low values of C_{org} around the lower part of the Unit 1 sediments of GC-5 (see Fig. 3.2), correlate with high amount of clay, suggesting dilution effects due to terrigenous clay input during ~11-7 ka-BP, when the monsoonal intensity was maximum (see Chapter 5 on 'Clay minerals').

Fewer planktic foraminifers in the coarse fraction, abundant terrigenous mud (Figs. 3.2 - 3.4) and relatively low or poor correlation of C_{org} with $CaCO_3$ and sand contents of the Pleistocene sediments suggest less productivity in the overlying waters and C_{org} derivation from more than one source. Eventhough the C_{org} may be dominantly marine in nature (as revealed by the $\delta^{13}C_{org}$ records; see Chapter 4), a low productivity during glacial periods transported less C_{org} to the

bottom sediments. As a consequence, the C_{org} concentration is very low during the glacial periods compared to the Holocene sediments. Also during the lowered sea levels, reworking could have lead to degradation of the existing C_{org}, as shown by the low HI values. So the principal sources of C_{org} in the Unit 2 sediments may be from less productive overlying waters and reworked C_{org} mixed with the terrigenous flux from the adjacent shelf. Coarse fraction studies indicate that reducing conditions on the continental slope developed either due to the local depletion of the oxidising agents in oxidising conditions or due to the impingement of oxygen minimum zone. Pyritized grains and infillings suggest that part of the C_{org} was used for the pyrite formation and part was consumed by benthic organisms associated with the sediments. Since the concentration of C_{org} content itself is less, the role of anoxic conditions in its preservation could not be distinguished in these sediments. The low C_{org} in the Unit 2 sediments may primarily be due to the low supply from primary productivity and reworked sediments and dilution by other sedimentary constituents, as suggested by Calvert *et al.* (1995).

3. 3. 3 Sediment core from the terrace

The oxygen isotope stratigraphy of this core indicates that the Holocene-Pleistocene boundary occur at ~25 cm interval and the core top age may be of ~ 5-6 ka-BP (see Fig. 3.5). Accordingly, the late Holocene sediments are not available for direct comparison with LGM. Around the LGM, a broad hump of high C_{org} coincides with a gradual increase in $CaCO_3$ and sand content (Fig. 3.5). Uniformly low C_{org} values occur in the lower part of the Unit 2.

The terrace lies seaward of the upper slope (Thamban *et al.*, 1997). Existence of open ocean conditions may have resulted in the high flux of planktic foraminifers to the bottom sediments. The sediments close to the LGM were accumulated during the lowered sea level. Low HI values throughout the core (Table 3.9) suggest reworking of organic materials (see Pedersen *et al.*, 1992). The negative relationship of C_{org} with $CaCO_3$ and sand contents (Fig. 3.5) and abundant shell fragments in the sand content between 95 and 20 cm interval may indicate that the terrace received sediments from the increased productivity as well as reworked sediments from the adjacent slope. Down slope movement of

sediment on the slope has been reported in this region (von Stackelberg, 1972). Therefore the C_{org} content is diluted by the deposition of reworked sand. The concomitant increase of C_{org} and $CaCO_3$ in the Holocene sediments in the upper parts of the core (Fig. 3.5) is similar to that in the cores of the slope (Fig. 3.2 & 3.3), indicating control by primary productivity and less influence from reworking. The broad hump of high C_{org} in the sediments close to the LGM is associated with increased mud content. This may be due to the direct accumulation of sediment during the lowered sea-level and also mass transportation and accumulation of fine-grained sediments from the adjacent slope. The distribution of C_{org}, $CaCO_3$ and sand in the lower portions of the Pleistocene sediments is similar to those on the slope.

3. 3. 4 Sediment cores from the topographic highs

Despite the fact that the lateral distance is only about 50 km between the cores of the slope and topographic high (Thamban *et al.*, 1997) (see, inset in Fig. 3.1), C_{org} and HI values are significantly high in the Holocene sediments of the topographic highs (Table 3.9). Since oxygen minimum conditions exist at both the locations, preservation alone may not account for such high C_{org} and HI values. On the other hand, Pedersen *et al.* (1992) suggested that hydrogen richness in the surface sediments may not be related to bottom water oxygen content but related to the texture of the sediments. They reported similar HI values for the C_{org} deposited under anoxic conditions and oxygenated conditions. Reworking leads to degradation of C_{org} and the C_{org} shows low HI values in coarser sediments and high HI values in finer sediments (see Pedersen *et al.*, 1992). Higher HI values in the Holocene clayey sediments and very low HI values in the Pleistocene sandy sediments (Table 3.9) in the cores of the topographic highs are in agreement with the above argument. Hence it is proposed that high HI and C_{org} values are mainly due to fine-grained sediments. High mud content and Type II organic matter indicate that these highs are probably the sites of low energy conditions and more marine C_{org} accumulated in the sediments by adsorbing onto clay particles. Abundant keels of planktic foraminifers in the sediments indicate intense test dissolution due to upwelling induced suboxic conditions. Thus, the high C_{org} in the Holocene sediments is a combined influence of high

rain of C_{org} from productivity, depositional environment and preservation in the fine-grained sediments. Calvert *et al.* (1995) suggested that the organic carbon maximum on the slope of the eastern Arabian Sea sediments is not related to the position of oxygen minima, but varies according to the productivity and a combination of other sedimentological and hydrodynamical factors.

The lowest C_{org} and low hydrogen indices are characteristic of Unit 2 sediments of the topographic highs (Table 3.9). As the topographic highs are isolated features (Fig. 3.1), the C_{org} may be marine but reworked. Sediment constituents (abundant pelecypods, gastropods and coiled molluscs with very few *Bolivina* and no pyritized grains) indicate that mostly oxic open ocean conditions existed on the topographic highs until late Pleistocene. Corals encrusted on small gastropod shells also support low sedimentation rates and oxic conditions (Rao *et al.*, 1995). Cemented forminiferal aggregates may indicate their formation is similar to conditions in hardgrounds. High sand content suggests winnowing of fine fraction. These findings suggest that unlike those on the slope and terrace, this part of the sediments of the topographic highs were bathed under oxygenated water column and current winnowing may be responsible for the low C_{org} content. Thus, the texture and winnowing of bottom sediments under oxidising conditions were responsible for low C_{org} content. Shimmeild *et al.* (1990) suggested winnowing was responsible for low C_{org} content in the sediments on bank tops. The oxygenated bottom conditions also indicate that the topographic highs were lying above the oxygen minimum zone during the late Quaternary. The sudden change in lithology of the cores at 20-25 cm (Fig. 3.6 & 3.7) from sandy sediments below to clayey sediments above may suggest that the topographic highs were subsided during the late Quaternary. This is supported by the documentation of several evidences of late Quaternary neotectonic activity and subsidence along the western margin of India (Rao *et al.*, 1996).

3. 4 CONCLUSIONS

1. Studies on organic carbon (C_{org}), grain size parameters and $CaCO_3$ in the six sediment cores collected from the Oxygen minimum Zone (OMZ) between 280 and 350 m depths reveal that the relationship of C_{org} with $CaCO_3$ and sand content is diverse in the cores collected from different depositional settings.

2. The C_{org}, $CaCO_3$ and sand contents are high on core tops in the cores from the slope and terrace and progressively decrease from surface to base of the Holocene and exhibits strong correlation with each other; this implies that productivity played a major role for the enhanced organic carbon content in the sediments.

3. The low C_{org} content in the Pleistocene sediments may be due to the low productivity and dilution by skeletal constituents from the shelf during this time. Reworking of the sediments played an important role in the enhanced C_{org} content at certain intervals in the core from the terrace.

5. The very high C_{org} content in the Holocene sediments of the topographic highs is related to the combined influence of productivity, fine-grained sediments and suboxic conditions. The low C_{org} content in the Pleistocene sediments may be due to coarser sediments and winnowing in oxidising conditions.

6. Rock-Eval pyrolysis results reveal that the C_{org} is marine and immature in the Holocene sediments and reworked marine and/or terrestrial in the Pleistocene sediments.

7. The distinct variations in C_{org} content in different cores suggest that the C_{org} distribution in the Holocene sediments is mainly controlled by primary productivity in combination with texture and reworking of sediments rather than water column anoxic conditions.

Table 3. 3 Sedimentological parameters in core GC-5 (upper slope off Cochin).

Depth (cm)	C_{org} (wt.%)	$CaCO_3$ (wt.%)	Sand (wt.%)	Silt (wt.%)	Clay (wt.%)
0	3.82	32.2	12.9	54.8	32.2
10	3.51	34.1	22.0	47.5	30.6
16	3.68	33.2	12.8	55.2	32.0
22	3.44	30.3	09.6	52.6	37.8
42	3.22	30.3	13.1	55.5	31.5
62	3.06	26.5	11.1	48.3	40.6
82	2.68	24.6	03.8	34.3	61.9
102	1.80	15.2	01.1	28.9	70.1
122	1.35	13.3	02.0	27.2	70.8
142	1.40	14.2	04.2	26.8	69.0
167	1.31	21.7	21.3	35.2	43.5
177	1.58	28.6	20.6	40.3	39.1
202	1.60	29.6	22.2	39.5	38.3
222	1.56	27.6	13.6	44.6	41.8
242	1.62	27.6	10.8	45.0	44.2
262	1.43	26.6	11.3	44.0	44.7
282	1.42	29.6	16.5	47.7	35.8
302	1.37	23.6	07.0	53.8	39.2
322	1.68	20.7	05.5	50.0	44.6
333	1.48	21.7	06.0	50.9	43.0

Table 3. 4 Sedimentological parameters in core GC-4 (upper slope off Mangalore).

Depth (cm)	C_{org} (wt.%)	$CaCO_3$ (wt.%)	Sand (wt.%)	Silt (wt.%)	Clay (wt.%)
0	2.76	59.7	31.0	48.3	20.8
10	2.63	62.5	39.9	39.4	20.7
20	2.62	58.8	29.8	47.5	22.6
27	2.63	56.9	26.1	43.2	30.6
42	2.01	51.2	32.0	40.0	28.0
62	2.27	44.6	12.4	36.9	50.7
82	1.97	37.0	02.7	37.0	60.3
92	2.23	40.8	02.0	33.3	64.7
107	1.63	20.9	02.0	32.1	66.0
117	2.61	51.2	25.5	38.1	36.4
127	2.40	20.9	02.6	32.0	65.4
137	1.94	25.6	01.8	31.0	67.2
152	1.87	37.0	13.4	38.3	48.3
172	1.97	22.7	02.5	32.2	65.2
192	1.63	22.7	05.6	34.3	60.1
207	1.45	17.1	00.7	26.6	72.8
222	1.48	17.1	03.5	30.0	66.5
242	1.07	21.8	02.0	27.5	70.5
262	1.58	18.0	01.2	28.4	70.4
282	1.37	17.1	01.0	27.3	71.7
302	1.36	15.2	00.5	28.0	71.5
312	1.45	14.2	00.5	27.2	72.3
322	1.32	14.2	00.7	28.7	70.6
342	1.42	15.2	00.6	25.9	73.5
357	1.11	14.2	00.7	27.1	72.2
372	1.57	14.2	00.5	26.3	73.2
387	1.44	16.1	00.8	25.9	73.3
400	1.48	15.2	01.6	28.4	70.0

Table 3.5 Sedimentological parameters in core GC-1 (upper slope off Goa).

Depth (cm)	C_{org} (wt.%)	$CaCO_3$ (wt.%)	Sand (wt.%)	Silt (wt.%)	Clay (wt.%)
0	1.31	61.3	32.8	42.8	24.5
10	1.16	60.3	25.7	47.7	26.6
14	1.43	55.6	--	--	--
22	1.25	57.3	22.4	47.5	30.1
27	1.25	59.5	--	--	--
37	1.22	59.5	--	--	--
52	1.49	60.5	--	--	--
62	1.43	51.0	14.6	49.9	35.5
72	1.59	38.0	--	--	--
82	1.50	39.0	--	--	--
92	1.28	38.0	--	--	--
102	1.72	39.2	05.4	51.9	42.6
122	1.69	41.2	08.1	56.6	35.3
142	1.57	41.2	04.7	57.5	37.9
162	1.07	45.2	07.2	59.9	32.9
182	1.14	44.2	06.4	57.2	36.4
202	1.21	44.0	07.0	58.1	34.9
222	1.17	43.1	04.4	61.6	34.0
242	1.01	40.2	03.4	61.5	35.1
262	0.94	39.2	02.7	59.8	37.5
282	1.13	37.3	02.6	57.4	40.1
302	1.12	37.3	03.0	56.5	40.5
322	1.11	35.4	02.3	56.6	41.2
342	1.14	35.4	02.3	57.6	40.1
360	1.08	36.4	02.6	56.7	40.7

Table 3. 6 Sedimentological parameters in core GC-6 (terrace off Cochin).

Depth (cm)	C_{org} (wt.%)	$CaCO_3$ (wt.%)	Sand (wt.%)	Silt (wt.%)	Clay (wt.%)
0	2.38	61.7	55.7	29.4	14.9
10	2.47	66.7	56.7	28.2	15.1
16	1.92	51.7	60.5	25.1	14.4
22	1.25	64.7	28.9	40.7	30.4
32	1.56	66.7	67.2	18.4	14.4
52	1.70	57.7	64.4	20.1	15.5
67	1.68	62.7	56.1	25.3	18.6
82	2.16	55.7	53.4	26.4	20.3
92	2.20	53.7	53.3	24.2	22.5
107	2.55	54.1	22.1	45.0	32.9
117	2.58	46.4	16.3	49.4	34.3
132	2.89	43.5	11.4	53.1	35.5
152	2.82	50.2	22.1	46.6	31.3
172	2.92	45.4	13.3	47.1	39.6
192	2.85	43.5	14.2	45.4	40.4
207	2.52	45.4	14.2	47.2	38.6
222	1.79	44.4	22.4	26.7	50.9
237	1.63	31.9	09.7	43.5	46.8
252	1.68	30.9	12.9	36.7	50.5
272	1.60	26.1	07.2	38.6	54.2
292	1.65	27.1	03.0	37.2	59.8
312	1.90	26.1	02.7	38.5	58.8
332	1.86	26.1	02.7	37.5	59.8
352	1.93	25.6	01.7	38.2	60.1
372	1.91	23.6	01.7	36.6	61.8
392	2.00	24.6	02.6	37.4	60.0
410	1.92	25.6	03.2	34.3	62.5

Table 3. 7 Sedimentological parameters in core GC-2 (topographic high off Goa).

Depth (cm)	C_{org} (wt.%)	$CaCO_3$ (wt.%)	Sand (wt.%)	Silt (wt.%)	Clay (wt.%)
0	8.70	39.6	03.8	59.9	36.3
10	8.20	43.3	05.7	58.5	35.8
16	8.50	43.3	04.6	59.6	35.8
27	1.44	71.9	43.3	25.7	31.0
42	0.94	72.3	51.7	21.0	27.3
57	0.83	74.6	58.5	16.3	25.2
72	0.37	80.2	64.3	15.9	19.8
82	1.00	77.4	60.0	20.6	19.4
112	1.09	72.8	56.3	20.5	23.2
132	1.00	75.6	55.3	21.2	23.5
162	3.72	65.0	35.7	37.7	26.6
182	1.66	61.1	46.6	29.6	23.8
202	1.71	66.0	47.5	25.4	27.1
222	0.83	66.0	48.6	19.0	32.4
247	1.14	68.0	48.9	22.6	28.5
267	1.00	70.9	45.1	27.1	27.8
282	1.04	71.9	46.9	26.1	27.0
302	0.94	72.9	52.1	22.3	25.6
332	0.88	68.0	45.5	22.9	31.6
367	0.78	72.9	55.0	19.5	25.5
377	1.02	72.5	55.7	21.8	22.5
382	0.94	67.6	42.4	27.7	29.9
392	0.97	62.8	47.3	24.5	28.2
407	1.26	60.9	45.7	25.0	29.3
430	1.30	50.2	14.8	44.8	40.4

Table 3.8 Sedimentological parameters in core GC-3 (upper slope of Goa).

Depth (cm)	C_{org} (wt.%)	$CaCO_3$ (wt.%)	Sand (wt.%)	Silt (wt.%)	Clay (wt.%)
0	8.56	34.8	03.0	58.6	38.4
10	7.45	40.6	07.9	57.5	34.6
18	6.07	49.3	22.6	48.4	29.0
37	1.89	67.6	48.8	30.4	20.8
52	1.13	68.6	38.2	29.8	32.0
72	0.97	62.8	43.8	29.8	26.4
92	1.34	61.8	44.4	28.3	27.3
112	1.84	58.9	26.0	36.2	37.8
127	2.88	26.1	06.5	33.3	60.2
152	2.35	31.9	08.5	32.5	59.0
172	2.44	39.6	20.7	32.3	47.0
202	2.65	30.0	05.0	41.8	53.2
222	3.48	22.2	00.9	43.3	55.8
242	4.13	23.2	05.4	42.3	52.3
262	4.50	19.3	01.8	41.5	56.7
282	3.78	35.5	05.7	44.7	49.6
302	3.44	36.5	06.1	39.6	54.3
327	1.72	66.0	44.7	28.8	26.5
342	1.78	68.0	43.6	30.2	26.2
362	1.29	67.0	44.6	28.3	27.1
382	1.25	67.0	41.5	34.8	23.7
402	1.37	70.9	41.2	28.0	30.8
422	1.46	68.0	06.7	26.6	66.7
432	1.91	44.3	24.3	28.5	47.2
445	2.06	41.4	06.5	25.2	68.3

Table 3. 9 Rock-Eval pyrolysis data on selected samples in different cores.

Core No.	Sample intervals (cm)	HI (mg HC/g C_{org})	S_1 (mg HC/g rock)	S_2 (mg HC/g rock)	T_{max} (°C)	TPI (Total Production Index)
GC-5	0-4*	198	1.64	7.56	421	0.18
GC-5	55-60*	121	0.85	3.75	415	0.18
GC-5	210-215	33	0.17	0.52	417	0.25
GC-5	295-300	27	0.14	0.37	390	0.28
GC-5	325-330	24	0.14	0.35	392	0.29
GC-4	4-6*	166	1.07	4.59	419	0.19
GC-4	50-55	37	0.26	0.77	403	0.25
GC-4	210-215	28	0.20	0.41	396	0.33
GC-4	350-355	34	0.56	0.48	411	0.54
GC-4	395-400	30	0.20	0.44	404	0.31
GC-1	2-4*	151	0.41	1.98	423	0.17
GC-1	110-115	55	0.22	0.93	0.93	0.19
GC-1	195-200	31	0.10	0.38	0.38	0.21
GC-1	260-265	29	0.09	0.28	0.28	0.25
GC-1	325-330	38	0.13	0.42	0.42	0.24
GC-6	0-2*	97	0.65	2.31	411	0.22
GC-6	45-50	79	0.33	1.35	407	0.20
GC-6	100-105	72	0.41	1.80	413	0.19
GC-6	240-245	89	0.44	1.47	416	0.23
GC-6	380-385	61	0.39	1.16	402	0.25
GC-2	0-4*	445	7.48	38.68	411	0.16
GC-2	380-385	67	0.17	0.63	417	0.20
GC-3	0-4*	892	14.84	76.33	404	0.16
GC-3	380-385	124	0.39	1.55	414	0.20

Samples showing * marks are the Unit 1 (Holocene) and others are Unit 2 (Pleistocene) sediments.

Chapter 4

Chapter 4

STABLE ISOTOPE STUDIES ON SEDIMENT CORES FROM THE WESTERN MARGIN OF INDIA

4. 1 INTRODUCTION

Stable isotope composition of the calcareous marine organisms are extensively used to reconstruct the environmental conditions during the geological past. Studies in this direction started in the early 1950s on different organisms [e.g., Epstein *et al.*, 1953 (molluscs); Emiliani, 1955 (planktic foraminifera); Shackleton, 1977 (benthic foraminifera)]. The calcareous microfossils that are commonly used for oxygen and carbon isotope measurements are those of protozoans, known as foraminifera. Isotopic composition of the planktic foraminifera provides valuable information on past ocean surface conditions, and benthic species provides information on past deep ocean environments (Dawson, 1992). Studies on oxygen isotope variations have so far been used as indicators of oceanic palaeotemperature and palaeosalinity and past fluctuations in sea level and glacial ice volumes (e.g., Duplessy, 1982; Shackleton, 1987; Sarkar *et al.*, 1990; Wefer and Berger, 1991; Sirocko *et al.*, 1993). Studies on carbon isotope ratios have provided insight into changes in the past ocean biological productivity, circulation patterns and global carbon budget (Shackleton, 1977; Berger *et al.*, 1978; Shackleton and Vincent, 1978; Brummer and Kroon, 1988; Altenbach and Sarnthein, 1989).

Oxygen isotopes

During the evaporation of sea water, different isotopes of oxygen in the water molecules (^{16}O, ^{17}O and ^{18}O) are released into the atmosphere by a process known as isotopic fractionation. Isotopic fractionation is the partial separation of isotopes during a physical or chemical process and can occur due to either kinetic or thermodynamic reasons (Savin and Yeh, 1981). This process is based on the fact that since the rate of evaporation varies according to the density (and hence atomic weight) of the respective oxygen isotopes, there is a preferential

evaporation of lighter isotopes (Dawson, 1992). During periods of glaciation, ocean surface waters, as a result of their lowered temperatures, are enriched in the denser ^{18}O isotope. Conversely, snow precipitation deposited on ice sheets during glacial age is depleted in ^{18}O (enriched in ^{16}O). During periods of deglaciation, the reverse process takes place with large quantities of lighter isotopes (mostly ^{16}O) released to the ocean with the meltwater, leading to a decrease in the isotopic ratios of $^{18}O/^{16}O$ in sea water. The oxygen isotope ratios of organisms that lived during these periods, should thus reflect the environmental conditions during their living, when they finally settled into the seafloor and eventually buried.

The environmental parameters that can be obtained by the isotopic study of microfossils deposited in the sediments include: changes in global ice volume, temperature and salinity of seawater. According to the 'palaeotemperature method' of Epstein *et al.* (1953), if $CaCO_3$ of an organism is precipitated in equilibrium with the sea water in which it grows, if the $^{18}O/^{16}O$ ratio of the sea water is known or can be estimated, and if the relationship between the fractionation factor and temperature is known, then the temperature of growth of the organism can be estimated:

$$t = 16.5 - 4.3\,(\delta_s - A) + 0.14\,(\delta_s - A)^2$$

where t is the temperature, δ_s is the $\delta^{18}O$ value of the solid carbonate, and A is the $\delta^{18}O$ value of the water in which the carbonate precipitated, measured in PDB system.

Carbon isotopes

The carbon isotope (^{12}C & ^{13}C) composition of marine surface waters is controlled by the relative importance of biologically and thermodynamically controlled processes (Savin and Yeh, 1981). The two main carbon reservoirs, organic matter and sedimentary carbonates, are isotopically quite different mainly because of the operation of two different reaction mechanisms: in organic material a kinetic effect during photosynthesis concentrate the light ^{12}C in the synthesised organic material. Whereas in sedimentary carbonates, chemical exchange effect in the atmospheric CO_2 - dissolved HCO_3^- system, leads to an enrichment of ^{13}C

in the bicarbonate (Hoefs, 1987). It is generally presumed that in low latitudes, biological processes are more important than thermodynamic ones (Kroopnick, 1985; Oppo and Fairbanks, 1989; Steinmetz, 1994).

Unlike the oxygen isotopes, carbon isotope compositions of fossil marine carbonates are more complicated. The factors leading to these complexities include: a). the $^{13}C/^{12}C$ ratio of dissolved HCO_3^- varies within the water column as a result of photosynthetic carbon fixation and oxidation of organic matter (Kroopnick, 1974); b). the $\delta^{13}C$ of calcite is relatively insensitive to changes in temperature (~0.035 ‰ / °C - Emrich *et al.*, 1970); c) most foraminifers secrete $CaCO_3$ out of carbon isotopic equilibrium with the dissolved HCO_3^- by varying amounts (Wefer and Berger, 1991). Hence the downcore variations in $\delta^{13}C$ of a marine organism should only approximately, but not precisely, indicative of variations in $\delta^{13}C$ of dissolved HCO_3^- in the waters in which they grew.

In this chapter, downcore variations of oxygen and carbon isotopes of both planktic and benthic foraminifers and bulk organic matter in the sediment cores collected from the upper continetal slope of the western margin of India are presented. The purpose of this study is to interpret the past variations in monsoon, productivity and eustatic sea levels during the late Quaternary along this margin.

4. 2 RESULTS

4. 2. 1 Core GC- 5

4. 2. 1. 1 Stratigraphy and sedimentation rates

Stratigraphy of the core has been realised by comparing the downcore variations in oxygen isotope values with that of standard records like SPECMAP (Imbrie *et al.*, 1984). The total oxygen isotope record of the core may represent the last glacial period (isotope Stage 2) and the present interglacial period (isotope Stage 1). Assigning well-constrained chronology for a high resolution sediment record using only oxygen isotope stratigraphy is a difficult task. In order to put the deglacial events observed at the core site (10. 23°N, 75.34°E) on an absolute time scale, the *G. ruber* $\delta^{18}O$ profile of this core has been correlated with the *G. ruber* $\delta^{18}O$ record of core 74 KL (14.19°N, 57.20°E) (Sirocko *et al.*, 1993; 1996) (Fig. 4. 1). Core 74 KL, located in the western Arabian Sea, off Oman margin has a tight

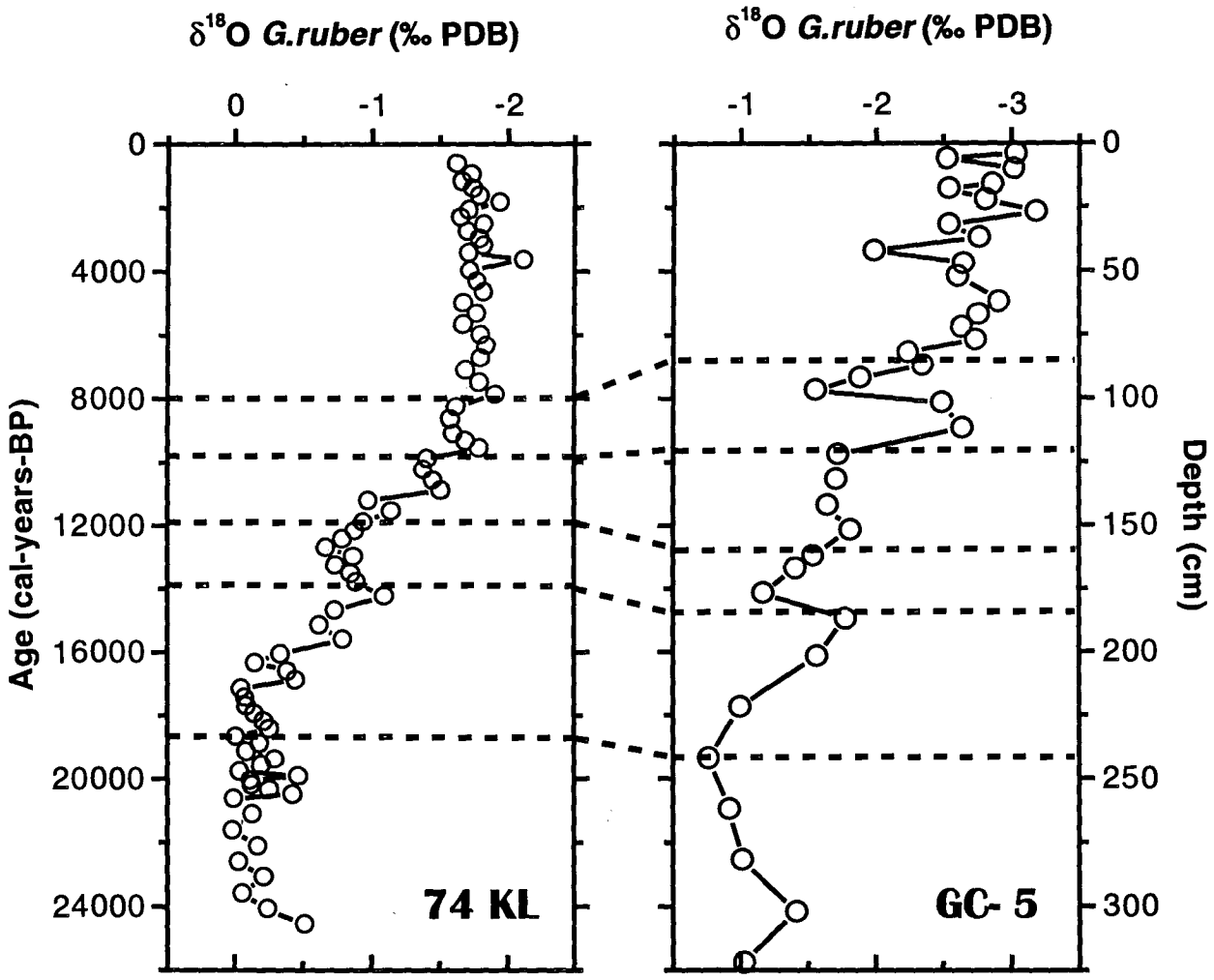

Fig. 4. 1 Age correlation between the $\delta^{18}O$ record of *G. ruber* in core GC-5 and core 74 KL from the western Arabian Sea (10.19°N, 57.20°E) (Sirocko *et al.*, 1993).

chronological control using 13 Accelerated Mass Spectrometer (AMS) ^{14}C dates and was corrected for reservoir effect and calibrated into sidereal years (calendar years) (Sirocko *et al.*, 1993). In addition, a core collected off Pakistan margin (SO 90-137KA; 23.12°N, 66.50°E), which has a very high resolution isotope stratigraphy and ten AMS ^{14}C dates (von Rad *et al.*, 1995), is also used for chronological correlations.

Several tie points were identified for core GC-5 (Fig. 4. 1). Estimated age (described as ka-BP: thousand years before present) and appropriate corrected age in calendar years (as cal-ka-BP) are given below:

Depth interval in core GC-5	Estimated ^{14}C age	Age in calendar years
120 cm	~8.8 ka-BP	~10.0 cal-ka-BP
160 cm	~10.5 ka-BP	~11.5 cal-ka-BP
180 cm	~11.5 ka-BP	~13.5 cal-ka-BP
240 cm	~15.5 ka-BP	~18.5 cal-ka-BP

The age control points thus obtained are used for both the estimation of sedimentation rates and interpreting the isotopic events at the core site.

The estimated sedimentation rates varied widely within the time duration represented by the core (approximately 24 cal-ka-BP) (Thamban, 1998). Average sedimentation rates are high with a value of ~13. 5 cm/ ka (Table 4. 1). From the core bottom to ~12 cal-ka-BP, the sedimentation rate was ~13. 7 cm/ ka. Sedimentation rates were highest (up to ~20 cm/ ka) during the period between ~12 and 8 cal-ka-BP (Table 4.1). This period coincides with maximum clay content in the core (>70%; see Fig. 4.4c) and correlates with the well known monsoonal maximum in the Arabian Sea and in the adjoining Indian subcontinent (e.g., Prell *et al.*, 1980; Duplessy, 1982; van Campo, 1986; Sirocko *et al.*, 1993). Rate of sedimentation is low (~10 cm/ ka) between ~8 cal-ka-BP and the core top (Table 4.1).

Table 4. 1 Average sedimentation rates calculated for the two cores based on interpolated isotope chronology.

Core GC - 5 (off Cochin)			Core GC - 3 (off Goa)		
Depth (cm)	**Estimated Age (kyr)**	**Sedimentation rates (cm/kyr)**	**Depth (cm)**	**Estimated Age (kyr)**	**Sedimentation rates (cm/kyr)**
0-80	0-8	10.0	0-50	0-12	4.2
80-160	8-12	20.0	50-125	12-24	6.3
160-325	12-24	13.7			

4. 2. 1. 2 Oxygen isotope ($\delta^{18}O$) variations

$\delta^{18}O$ records of planktic foraminifera

The down core $\delta^{18}O$ values of *G. ruber* varied between -3.18 and -0.76‰, with more negative (lighter) values at the core top and relatively heavier values in the lower portions (Table 4.2; Fig. 4.2). The $\delta^{18}O$ profile reveals the typical isotopic evolution from the last glacial to present interglacial period. The heaviest (increase in ^{18}O) value for *G. ruber* (-0.76‰) is found at around 242 cm interval of the core (Fig. 4.2a) and may corresponds to the last glacial maximum (LGM- ~18 ka-BP), when the global ice cover was at its maximum. The $\delta^{18}O$ values of *G. sacculifer* vary between -2.57 and -0.34‰ (Fig. 4.2b). The LGM-Holocene isotopic difference (LGM & Holocene isotope values - average values of three intervals each from LGM and Holocene sections) of *G. ruber* ($\Delta\delta^{18}O$) is ~2.1‰ (see Table 4.2; Fig. 4.2a). The $\Delta\delta^{18}O$ values of *G. sacculifer* (~2.07‰) is comparable with that of *G. ruber*, though the absolute values are relatively heavier in *G. sacculifer* (Fig. 4.2b).

The oxygen isotope records of both *G. ruber* and *G. sacculifer* follow similar trend from bottom to the core top with a step-wise deglaciation punctuated by a series of abrupt fluctuations (see Fig. 4.2a&b). The $\delta^{18}O$ values of *G. ruber* show a pronounced negative excursion from -0.76‰ at ~240 cm depth interval to -1.78‰ at ~190 cm. Between 190 and 160 cm depth interval, the values remain relatively heavy (-1.16 - 1.54‰) (Fig. 4.2a). The $\delta^{18}O$ values once again showed negative excursions, culminating at ~110 cm depth interval with a value of -2.64‰. An abrupt and large fluctuation is observed around 100 cm interval in $\delta^{18}O$ record

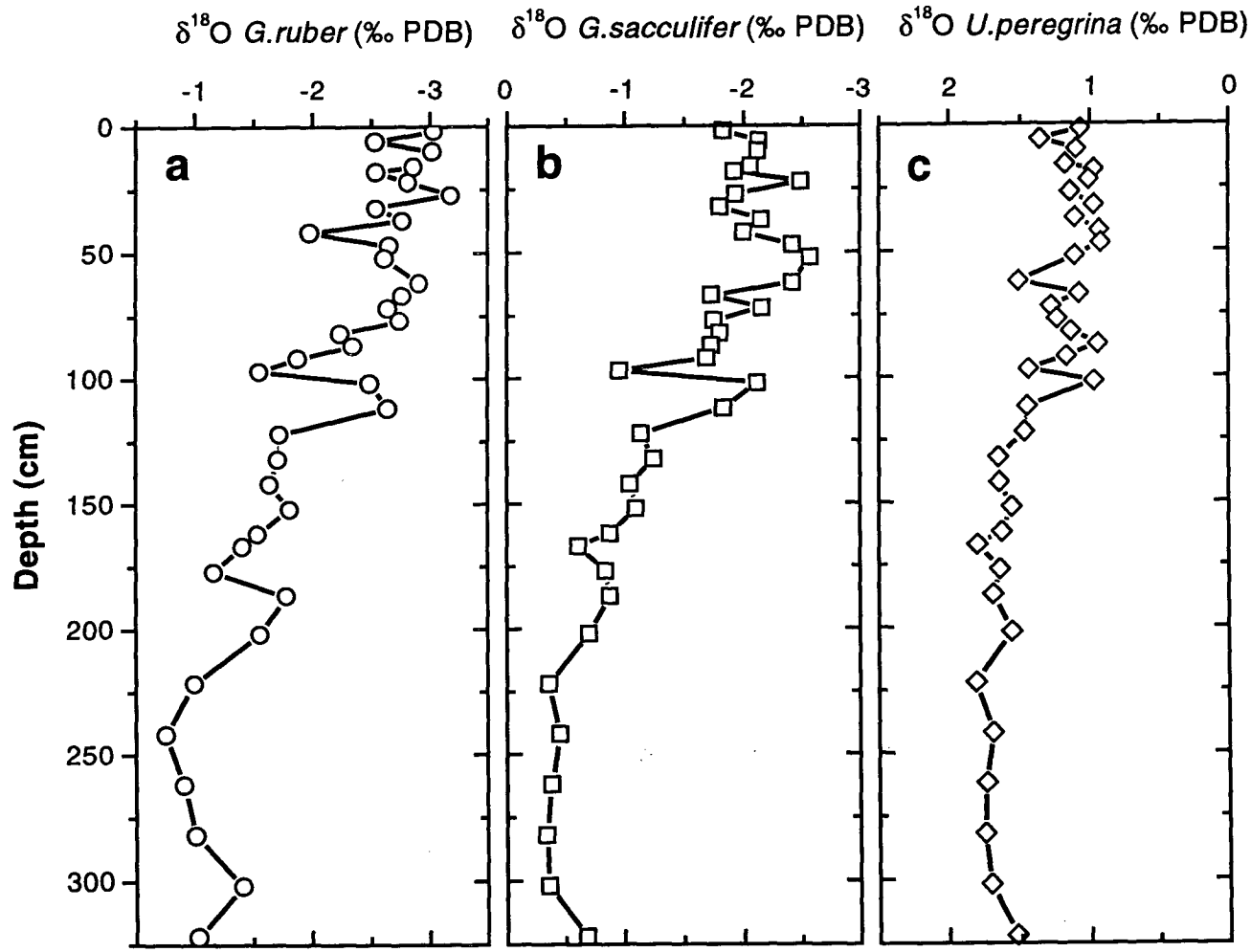

Fig. 4. 2 Down core records of $\delta^{18}O$ variations in core GC-5; (a). *G. ruber*, (b). *G. sacculifer*, (c). *U. peregrina*.

towards heavy values (from -2.5‰ to -1.55‰). Thereafter, the $\delta^{18}O$ values remained more or less constant between -2.6 and -3.2‰, except at ~45 cm depth interval where a large excursion towards heavier values is seen (-1.98‰) (Fig. 4.2a). The deglacial events discernible in the $\delta^{18}O$ record of *G. sacculifer* are relatively less abrupt than in *G. ruber* (Fig. 4.2b). The Holocene *G. sacculifer* $\delta^{18}O$ minima is observed between 60 and 45 cm interval and core top values are relatively heavy.

$\delta^{18}O$ record of benthic foraminifera

Oxygen isotope values of *U. peregrina* fluctuate between 0.92‰ and 1.81‰ (Table 4.2; Fig. 4.2c). The heaviest value (1.81‰) was obtained for the LGM interval (~220 cm depth interval). Unlike that of *G. ruber* and *G. sacculifer*, the $\delta^{18}O$ values of *U. peregrina* remained more or less constant (1.8 - 1.5‰) between 300 and 110 cm core depths. The $\delta^{18}O$ values abruptly dropped to 0.97‰ at ~100 cm. The glacial-interglacial $\delta^{18}O$ amplitude is low ($\Delta\delta^{18}O$ ~0.9‰), compared to those observed in the *G. ruber* and *G. sacculifer* records ($\Delta\delta^{18}O$ ~2.1‰).

4. 2. 1. 3 Carbon isotope ($\delta^{13}C$) variations

$\delta^{13}C$ record of planktic foraminifers

The downcore values of $\delta^{13}C$ fluctuates between 1.81 and 0.41‰ and 1.76 to 0.25‰ for *G. ruber* and *G. sacculifer*, respectively (Table 4.3; Fig. 4.3a&b). Relatively higher values occur at the core top. Although the $\delta^{13}C$ fluctuations are not clear as in the case of oxygen isotope records of the same species, a general increasing trend from glacial to interglacial period can be seen.

The $\delta^{13}C$ values of *G. ruber* show a decreasing trend from the core bottom and reach a minimum value of 0.41‰ at around 150 cm depth interval (Fig. 4.3a). These values increase towards the core top with a maximum (1.81‰) at around 70 cm depth interval. The $\delta^{13}C$ fluctuations of *G. sacculifer* do not exactly match with that of *G. ruber*, though there is a mid- Holocene maximum and a subsequent minimum of $\delta^{13}C$ (Fig. 4.3b).

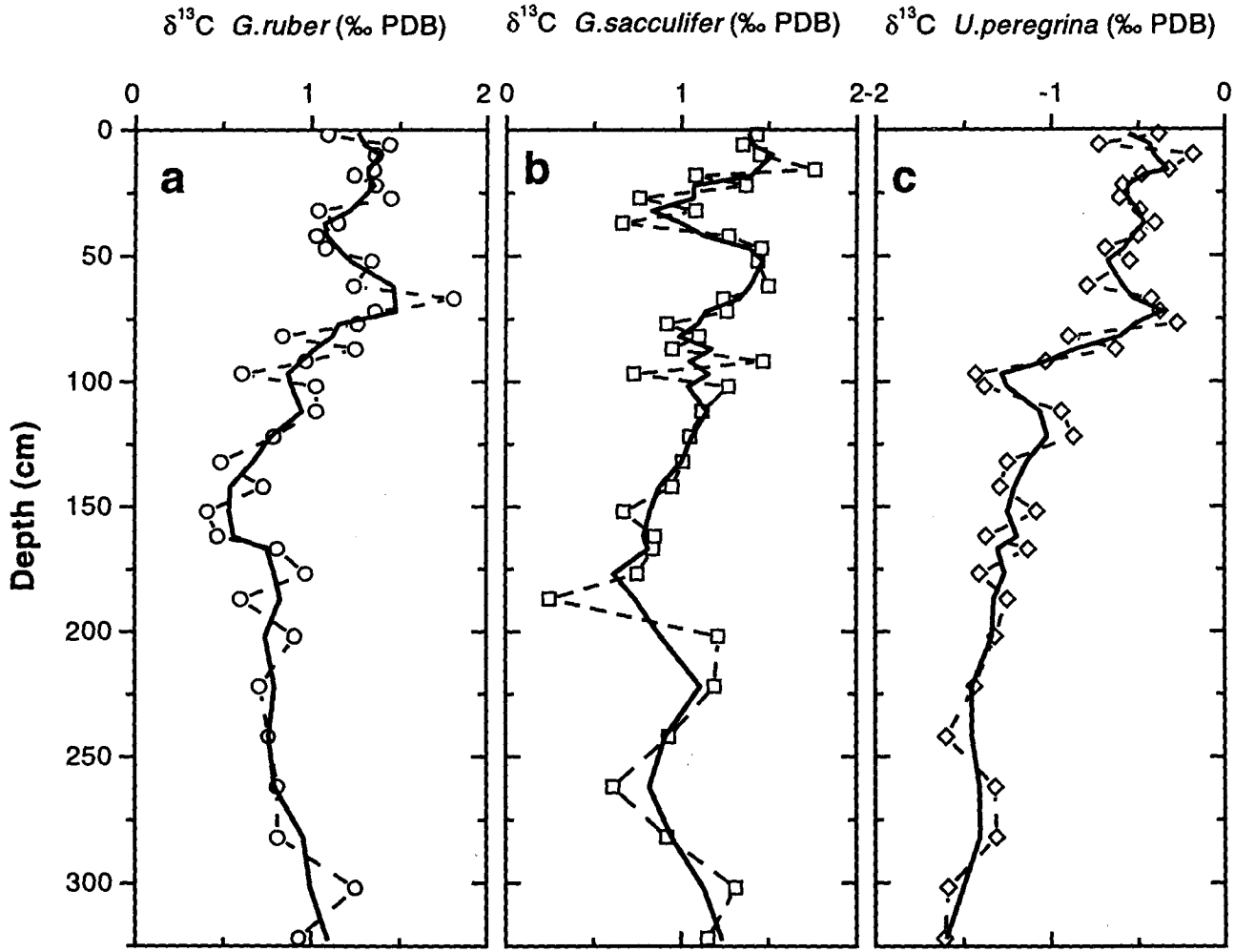

Fig. 4. 3 Down core $\delta^{13}C$ variations in core GC-5; (a). *G. ruber*, (b). *G. sacculifer*, (c). *U. peregrina*. Smoothed curves (thick line) were obtained by a three point moving average.

$\delta^{13}C$ record of benthic foraminifera

The $\delta^{13}C$ values of *U. peregrina* vary from -0.18‰ at the core top to values as low as -1.6‰ at the bottom of the core (Table 4.3; Fig. 4.3c). The isotope values remained more or less constant around -0.5‰ between 100 cm depth interval and the core top. The $\delta^{13}C$ values increased gradually from the LGM to Holocene, except a marked $\delta^{13}C$ minimum found around 100 cm depth interval corresponding to early Holocene period (Fig. 4.3c).

$\delta^{13}C_{org}$ variations

The $\delta^{13}C_{org}$ measurements in this core were made only up to 200 cm interval (corresponding to ~15 cal-ka-BP). The $\delta^{13}C_{org}$ values range between -19.54‰ at the core top and -21.55‰ at around 112 cm core depth (Table 4.4; Fig. 4.4a). There $\delta^{13}C_{org}$ values show a negative incursion between 170 and 60 cm depth intervals, with values reaching upto -21.55‰.

4. 2. 2 Core GC- 3

4. 2. 2. 1 Stratigraphy and sedimentation rates

The isotope measurements for GC-3 were carried out only up to 200 cm interval. The age control points for the core were obtained by correlating the $\delta^{18}O$ records with the stacked SPECMAP isotope records of Imbrie *et al.* (1984). As shown in Fig. 4. 5, the age control point at 200 cm depth interval corresponds to ~40 ka-BP. Using this timescale, Stage 1 and 2 and part of the Stage 3 were identified (Fig. 4.5).

Sedimentation rates calculated using the above age model, indicate relatively low average sedimentation rates for this core compared to GC-5 (see Table 4.1). Rate of sedimentation during Stage 2 (~24 - 12 ka-BP) was slightly higher (6.3 cm/ ka), than during Stage 1 (~12 - 0 ka-BP) (4.2 cm/ ka) (Table 4.1).

4. 2. 2. 2 $\delta^{18}O$ and $\delta^{13}C$ variations

The $\delta^{18}O$ values vary between -2.65 and -0.52‰ and -2.31 and -0.18‰ for for *G. ruber* and *G. sacculifer*, respectively (Table 4.5; Fig. 4.5). Lowest $\delta^{18}O$ value occur at 102 cm interval for *G. ruber* and at 82 cm for *G. sacculifer.* Both the records show the general glacial-interglacial trends. Since the isotope variations of

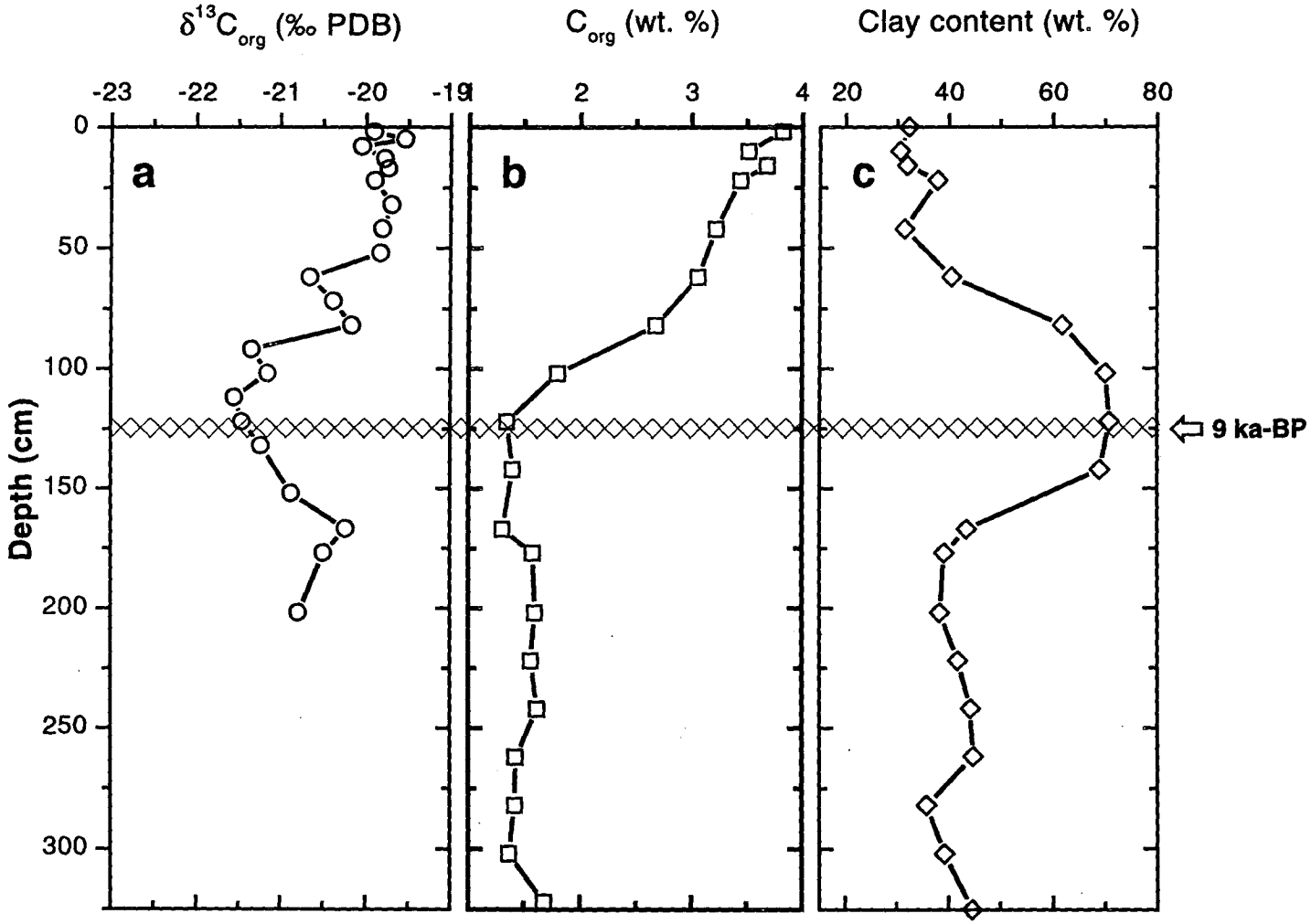

Fig. 4. 4 Down core variations of: a). $\delta^{13}C_{org}$, b). C_{org}, and c). Clay content, in GC-5.

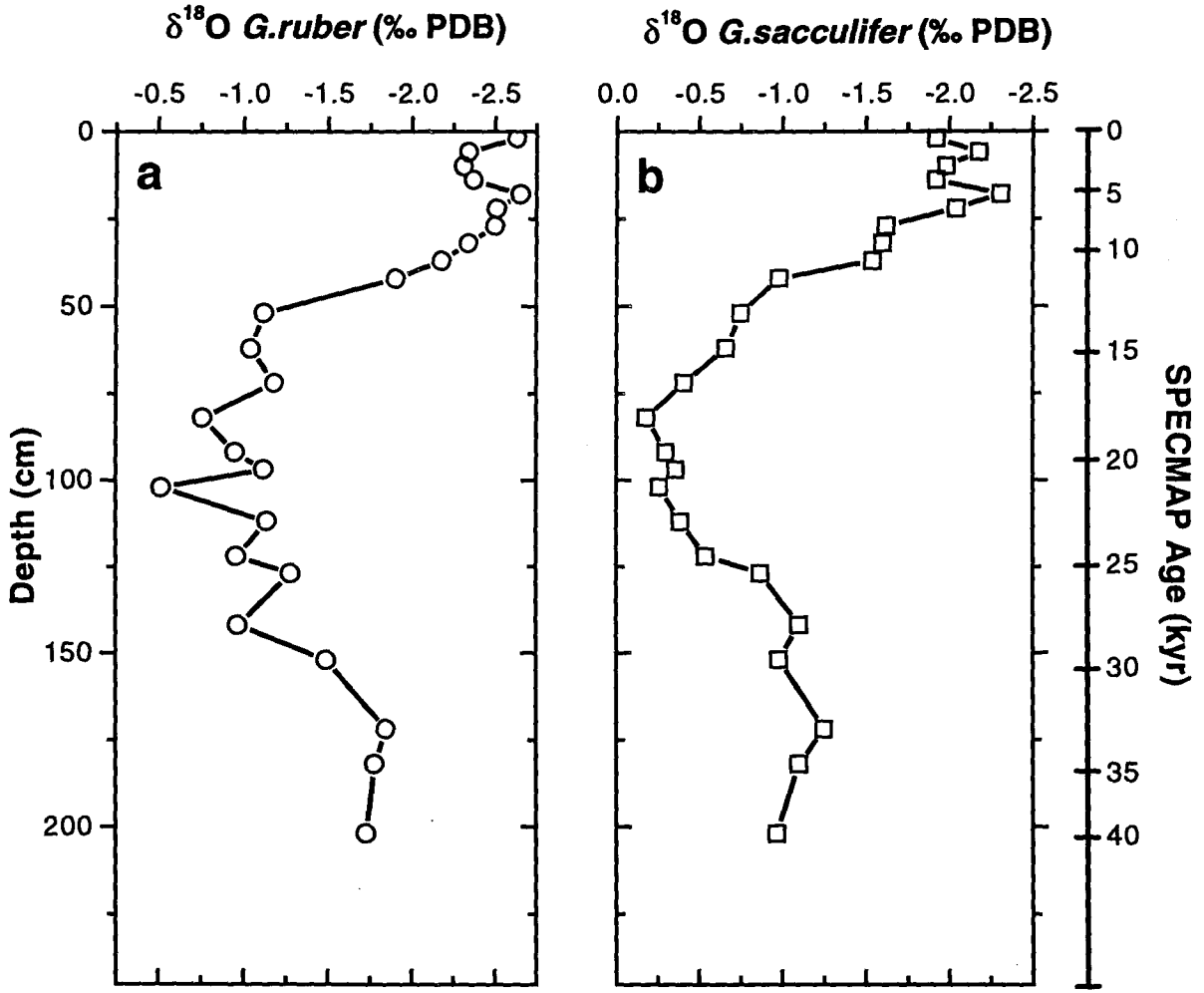

Fig. 4. 5 Down core variations of $\delta^{18}O$ values in core GC-3. The age scale on the right is obtained by correlation with SPECMAP (Imbrie *et al.*, 1984)

G. sacculifer are smoother and well-defined than that of *G. ruber*, the *G. sacculifer* records have been used here for age estimations and LGM assignment. The greater fluctuations in the *G. ruber* records may most probably be due to bioturbation effects. The glacial-interglacial $\delta^{18}O$ amplitude of *G. ruber* ($\Delta\delta^{18}O$ ~2.11‰) and *G. sacculifer* ($\Delta\delta^{18}O$ ~2.13‰) is comparable to that of core GC-5.

The downcore carbon isotopic variation in the planktic foraminifers showed wide fluctuations. The $\delta^{13}C$ values of *G. ruber* varied between ~0.9 and 1.63‰ with relatively higher values in the Holocene and low values during the glacial periods, albeit with greater fluctuations (Table 4. 5). The $\delta^{13}C$ records of *G. sacculifer* varied between ~1.0 and 2.0‰.

4. 2. 3 Core GC-4

4. 2. 3. 1 Stratigraphy

Stratigraphy of this core has been realised by the oxygen isotope record of *U. peregrina* and three bulk carbonate ^{14}C dates (Fig. 4.6; Table 4.6; Table 3.1 of Chapter 3). Using these dates and oxygen isotope curves, the LGM (~18 ka-BP) interval is placed at ~90 cm. Age model for sediments below this interval is obtained by correlation with SPECMAP standard records (Imbrie *et al.*, 1984). Since the oxygen isotope records for core GC-4 were obtained only up to 225 cm depth interval and are of very low resolution, it is very difficult to define precisely the stage boundaries and correct ages below the ^{14}C date points. Moreover, possibilities of downslope movements cannot be ruled out in this part of the slope as observed by spikes in texture, C_{org} and $CaCO_3$ content distribution around 120 cm core depth (see Fig. 3.3 in Chapter 3).

4. 2. 3. 2 $\delta^{18}O$ and $\delta^{13}C$ variations

The down core $\delta^{18}O$ record of *U. peregrina* varies from 0.8‰ in the Holocene and ~1.8‰ during the glacial periods (Table 4.6; Fig. 4.6). The $\delta^{18}O$ record of this core is not as demonstrative as in cores GC-5 or GC-3. The glacial-interglacial $\delta^{18}O$ amplitude is low ($\Delta\delta^{18}O$ ~1.0‰).

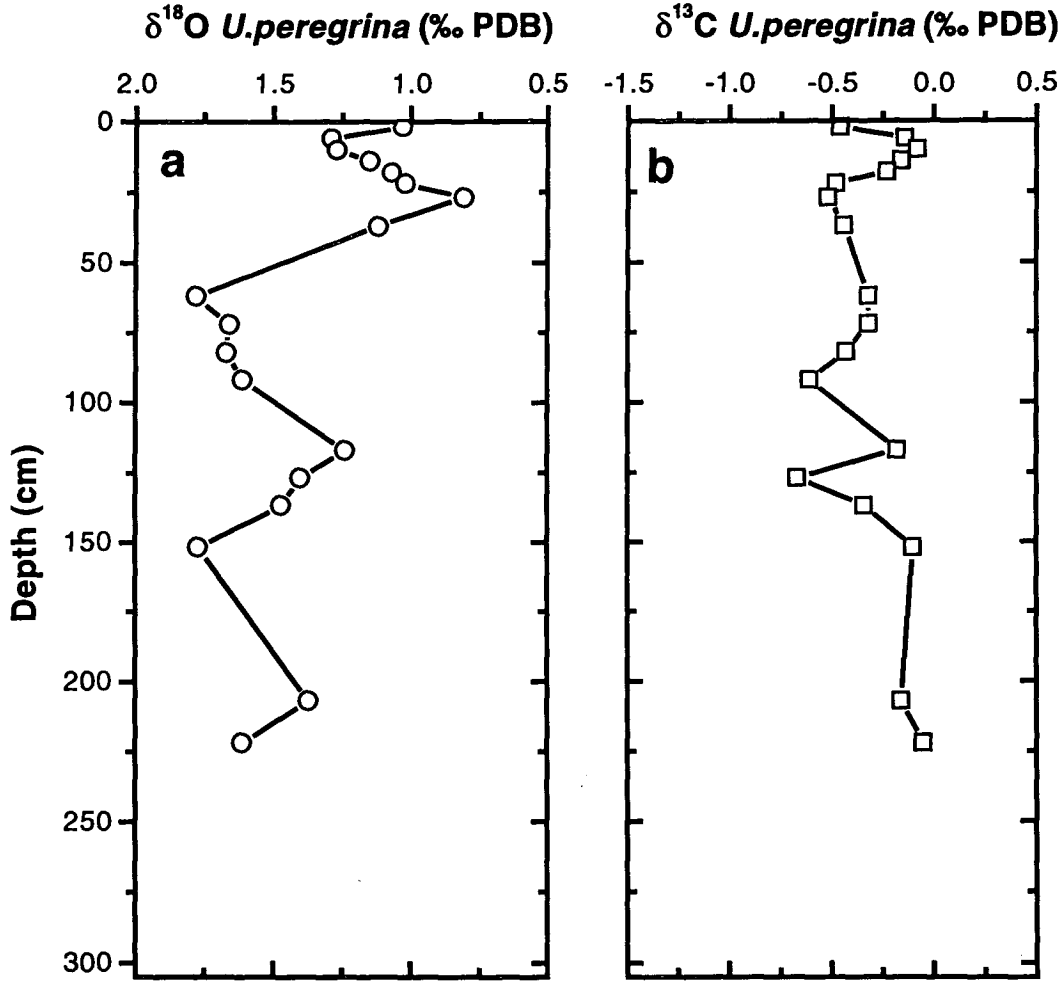

Fig. 4. 6 Down core variations in $\delta^{18}O$ and $\delta^{13}C$ values of *U.peregrina* in core GC-4.

The *U. peregrina* $\delta^{13}C$ values in this core vary between -0.61‰ during LGM period and -0.08‰ in the Holocene part. The $\delta^{13}C$ record does not show any significant variation between the glacial to interglacial period.

4. 2. 3. 3 $\delta^{13}C_{org}$ variations

The downcore $\delta^{13}C_{org}$ variations in the core GC-4 (Table 4.7; Fig. 4.7a) show a remarkably constant distribution throughout the core with values varying between -19.71 and -20.45‰ (average value of -20.14 ± 0.4‰). The $\delta^{13}C_{org}$ values are heavy and are within the range associated with marine planktic organic matter at water temperatures >20 °C (-18 to -21‰: Fontugne and Duplessy, 1981; 1986; Jasper and Gagosian, 1990). Although there is a slight decreasing trend (towards lighter values) from the core bottom to top, the difference is only <1‰ and significant variations are not found between the glacial-interglacial boundaries (Fig. 4.7a).

4. 2. 4 Core GC-6

4. 2. 4. 1 *Stratigraphy*

The $\delta^{18}O$ record of *G. ruber* in this core spans up to ~300 cm interval. Using the oxygen isotope curves, the LGM (~18 ka-BP) interval is placed at ~130 cm and the Pleistocene - Holocene boundary at ~25 cm interval (see Fig. 4.8). Apparently the upper Holocene part of the sediments is missing. Therefore, this core is not used for detailed isotopic interpretation and only the LGM and Holocene boundaries are used for further studies on this core.

4. 2. 4. 2 *$\delta^{18}O$ and $\delta^{13}C$ variations*

The down core $\delta^{18}O$ values of *G. ruber* fluctuate between -0.7‰ at LGM and -2.9‰ in the Holocene (Table 4.8; Fig. 4.8). The $\delta^{18}O$ record of this core is also not demonstrative as that of cores GC-5 or GC-3. The glacial-interglacial $\delta^{18}O$ amplitude is comparable to that of GC-5 and GC-3 ($\Delta\delta^{18}O$ ~2.2‰).

The downcore $\delta^{13}C$ record of *G. ruber* show wide fluctuations. The $\delta^{13}C$ values vary between ~0.7‰ and 1.5‰ with relatively higher values in the

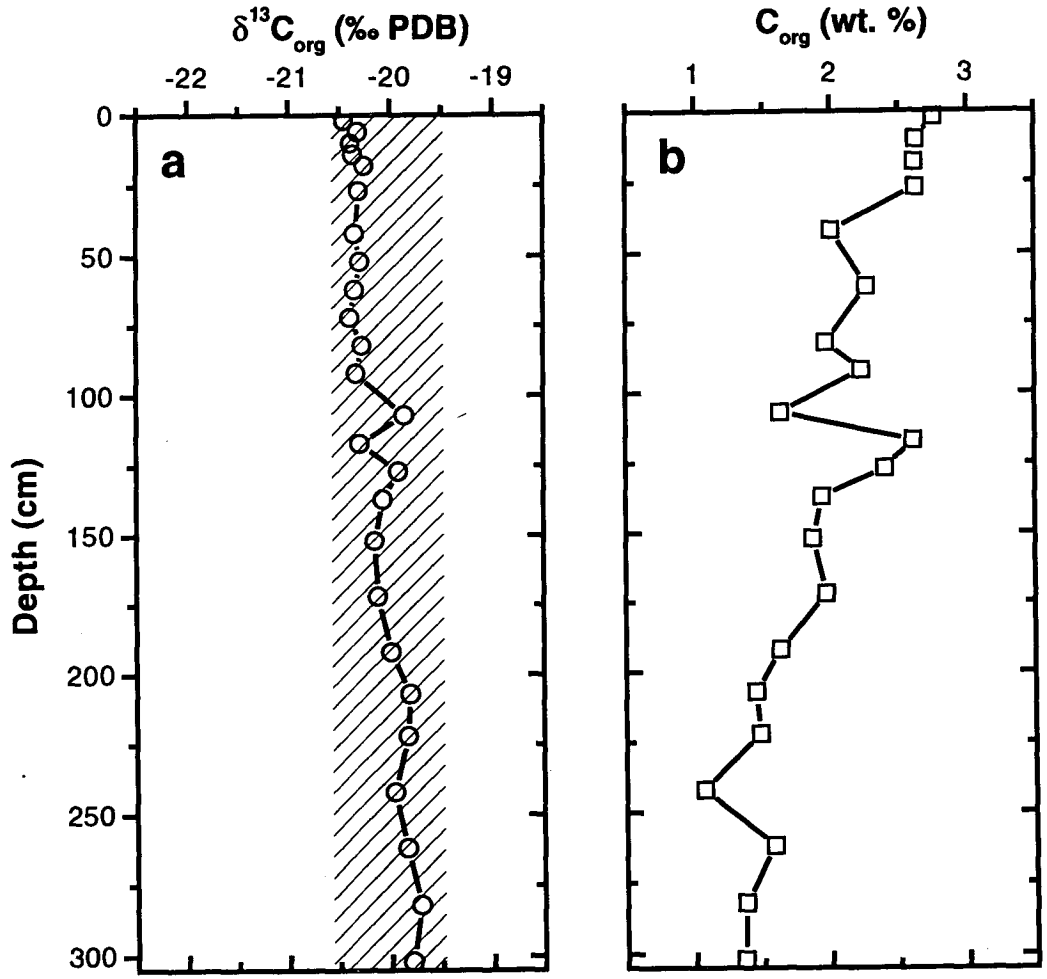

Fig. 4. 7 Down core variations of $\delta^{13}C_{org}$ and C_{org} content in core GC-4.

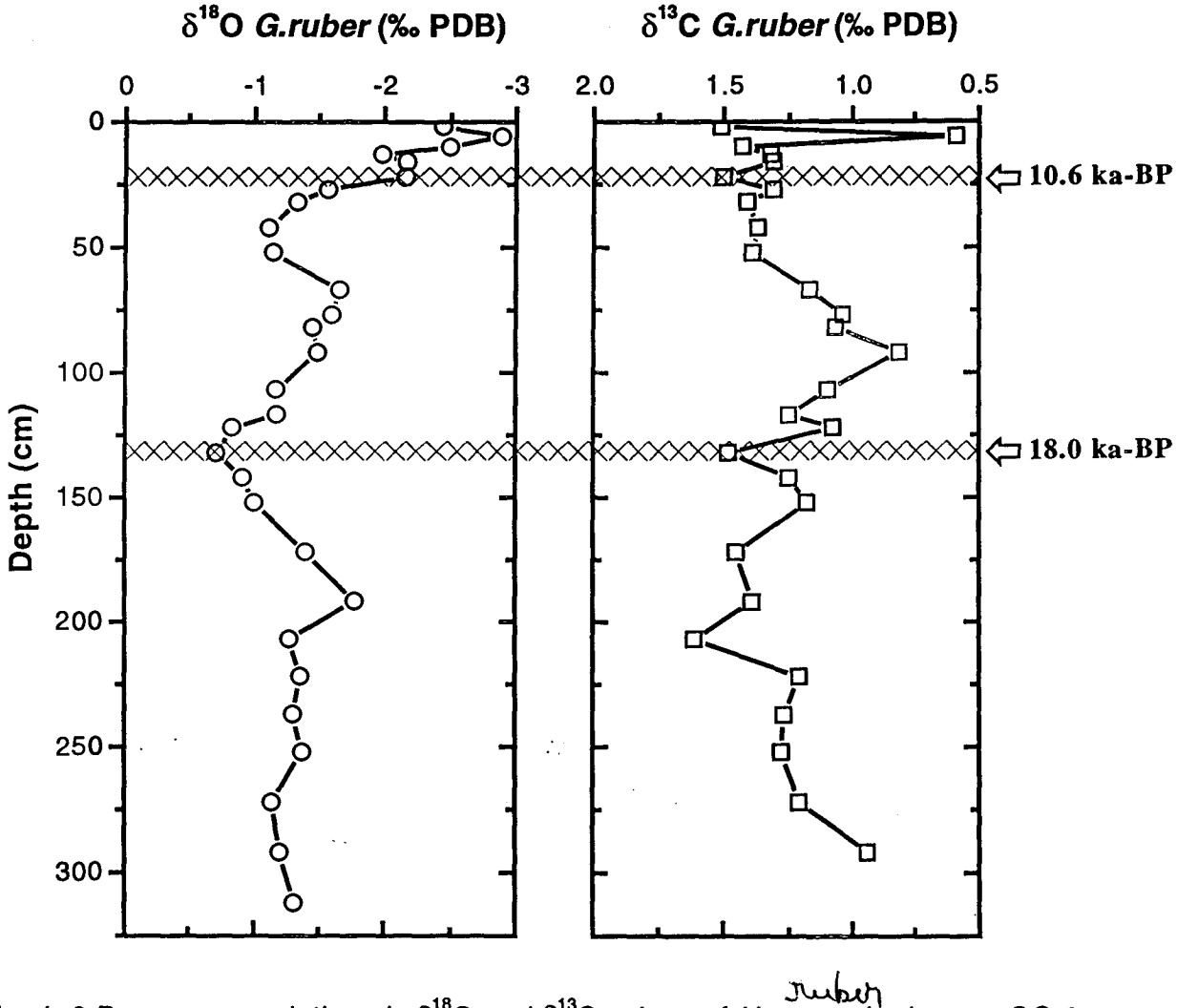

Fig. 4. 8 Down core variations in $\delta^{18}O$ and $\delta^{13}C$ values of *U. ~~peregrina~~ ruber* in core GC-6.

Holocene (except for a spike at 6 cm interval) and low values during the glacial periods (Table 4. 8; Fig. 4. 8).

4. 3 DISCUSSION

Core GC-5 has continuous high resolution oxygen and carbon isotope records of both planktic (*G. ruber* and *G. sacculifer*) and benthic (*U. peregrina*) foraminifers spanning ~24 ka-BP. Carbon isotope record of bulk organic matter is also available for this core. Palaeoceanographic and palaeoclimatic interpretations presented in this chapter are mainly based on this core.

4. 3. 1 The last deglaciation as observed in Core GC-5

Oxygen isotope values of both *G. ruber* and *G. sacculifer* exhibit a step-wise character (Fig. 4. 2a&b). The large increase (~1.0‰) towards lighter isotope values from ~18 cal-ka-BP culminating at ~14 cal-ka-BP represents a major transition between LGM and Holocene. This transition period correlates with the Event 3 of Sirocko *et al.* (1993) and also coincides with the first abrupt deglacial event in the North Atlantic called Bølling-Allerød (~14.5 cal-ka-BP) (Sirocko *et al.*, 1996). This change is more distinct in *G. ruber* records than that of *G. sacculifer*. The $\delta^{18}O$ profile reported here and the palaeo-SST record obtained using the alkenone method at MD 77194 (Sonzogni *et al.*, 1998), show similar features, indicating a significant deglacial warming phase depicted in GC-5 around ~14.5 cal-ka-BP. Between ~13.5 and 11.5 cal-ka-BP, the $\delta^{18}O$ records show a significant excursion towards heavier values (Fig. 4.1) that coincide with a decrease in SST values at MD 77194 corresponding to the Younger Dryas cooling event. This coincidence may suggest that a link exists between tropical climate and high latitude surface conditions, as argued by Sirocko *et al.* (1996). The isotope values at 160 - 180 cm (~11.5 - 9 cal-ka-BP) interval in GC-5, once again exhibit excursions towards more negative values. Similar step-wise and abrupt transitions were reported from the sediment cores collected off the Oman margin (Sirocko *et al.*, 1993; 1996).

4. 3. 2 Glacial-interglacial amplitude in $\delta^{18}O$

Fluctuations in mean isotopic composition of the oceans are mainly attributed to the amount of continental ice. In addition, evaporation, precipitation, freezing and mixing processes also change the local $\delta^{18}O$ values of the surface waters (Savin and Yeh, 1981). The global 'ice volume effect' (the isotopic effect by the building of polar ice during the glacial period and melting of the same during interglacial period) has been a controversial issue with different studies projecting different values (Emiliani, 1955; Savin and Yeh, 1981; Duplessy, 1982). Many studies however, agree upon amplitudes of $\delta^{18}O$ values around 0.8 to 1.3‰ with most estimates lying closer to 1.2‰ (Savin and Yeh, 1981). Presently the widely accepted value of 'ice volume effect' is ~1.2‰ (Labeyrie *et al.*, 1987; Fairbanks, 1989).

The observed amplitude of $\delta^{18}O$ values between the LGM and Holocene (~2.1‰) in core GC-5 is higher by ~0.9‰ than that can be explained by the ice volume effect (~1.2‰; Labeyrie *et al.*, 1987). This excess glacial-interglacial amplitude (0.9‰) has to be accounted by local changes in sea water $\delta^{18}O$.

Several workers have reported the glacial to interglacial variations in oxygen isotope values exceeding the ice volume effect from the tropical Indian and Atlantic Oceans (Duplessy, 1982; Sirocko *et al.*, 1993; Dürkoop *et al.*, 1997). These were attributed to: 1). changes in sea surface temperature (SST), 2). changes in precipitation and evaporation (i.e., sea water salinity changes), 3). mixing with other water masses, and, 4). changes in seasonality of the foraminifers (see Sirocko *et al.*, 1993). In the following paragraphs, these factors are briefly discussed and their significance in the observed $\delta^{18}O$ amplitude on core GC-5 is evaluated.

Increase in sea surface temperature (SST)

Numerous studies have indicated that temperature is a major factor leading to the isotopic fractionation of $^{18}O/^{16}O$ (e.g., Epstein *et al.*, 1953; Savin and Yeh, 1981; Wefer and Berger, 1991; Dawson, 1992). However, the quantification of tropical SST during the last glacial period has been controversial, since different palaeotemperature proxies seem to provide conflicting informations.

Palaeotemperature reconstruction by CLIMAP (1981) based on foraminiferal transfer functions (TF) suggests almost no cooling or even slightly warmer temperatures in the tropical belt during the last glacial maximum (LGM). Palaeotemperatures thus estimated have been later confirmed through the use of modern analogue technique (MAT) (Anderson *et al.*, 1989; Thunnel *et al.*, 1994). All these techniques and also the isotopic palaeotemperature method appear to be imperfect palaeothermometers as they are influenced by many factors other than temperature alone (see Sonzogni *et al.*, 1998 for details).

Alkenones (long chained, unsaturated ketones) are widely recognised as reliable palaeotemperature proxies and the unsaturation ratio of C_{37} alkenone (U^k_{37}) has been found to correlate with growth temperature in laboratory cultures of *Emiliania huxleyi* and is now used to quantify palaeotemperature (Brassel *et al.*, 1986; Prahl *et al.*, 1988; Schneider *et al.*, 1995; Bard *et al.*, 1997). A recent alkenone study on Indian Ocean cores indicated that SST values obtained by alkenone method for LGM were significantly cooler than that suggested by TF and MAT studies (Sonzogni *et al.*, 1998). The SST during LGM was found to be ~2°C cooler than today in a sediment core collected off south India (Core MD 77194 - 10.28°N and 75.14°E) (Sonzogni *et al.*, 1998). Incidentally, this core location is close to that of core GC-5.

According to Epstein *et al.* (1953) and Ganssen and Sarnthein (1983), an increase in SST by about 1°C will lead to a $\delta^{18}O$ decrease of 0.2‰. It thus seems unlikely that the observed high $\Delta\delta^{18}O$ values in all three cores (GC-5, GC-3 & GC-6) are solely due to the glacial cooling. The cooling of sea surface by about 2°C during the LGM at the core sites can account for only part of the observed high values. Hence, of the total excess isotopic LGM-Holocene variance (~0.9‰), only about 0.4‰ can be attributed to the deglacial increase in temperature alone.

Increase in precipitation

The $\delta^{18}O$ distribution in sea water also depends on the fresh water influx and in turn the salinity of sea water (Duplessy, 1982). An increased precipitation or decreased evaporation will lead to a relative increase in ^{16}O values compared to ^{18}O values resulting in a lowered $\delta^{18}O$ values in the sea water as well as the

foraminifers living in that water column. The modern $\delta^{18}O$ distribution of the *G. ruber* from core top samples of the Northern Indian Ocean is in agreement with the present day mean annual salinity conditions (Duplessy, 1982). Studies on the oxygen and carbon isotopes in plankton-tow, surface and core samples in the Northern Indian Ocean, revealed that an increase in salinity by ~1.0 p.s.u leads to an increase in $\delta^{18}O$ value by ~0.3‰ (Duplessy *et al.*, 1981). Using this $\delta^{18}O$ - salinity relationship, an LGM increase in Sea Surface Salinity (SSS) by ~2.0 p.s.u can account for an isotopic difference of ~0.6‰ at the core sites.

Palaeo-monsoonal studies using pollen proxies in the eastern Arabian Sea have revealed that monsoonal precipitation enhanced considerably since the LGM, peaking at ~9 ka-BP (van Campo, 1986). The high glacial-interglacial $\delta^{18}O$ amplitude observed in the Indian Ocean cores were used to support an increase in salinity during the LGM and subsequent lowering of salinity due to the enhanced SW monsoon (Duplessy, 1982). The observed variations in the clay mineral assemblages (see Chapter 5) and $\delta^{13}C_{org}$ records (see below) in this core also support increased river runoff during the periods of enhanced humidity that correspond to the early Holocene period. A reduced rainfall and runoff from the continent during LGM, could have caused a relative increase in surface water salinity.

So the observed high LGM-Holocene $\delta^{18}O$ amplitude can be explained by a combination of both temperature and salinity changes. This hypothesis is consistent with both the relatively low LGM cooling in the Arabian Sea (Zahn and Pedersen, 1991; Sonzogni *et al.*, 1998) and a decrease in precipitation/ increase in evaporation during LGM (Duplessy, 1982). Fluctuations in salinity are also observed as abrupt events during the deglaciation at the GC-5 core site (see section 4.3.3, 'Abrupt events').

Mixing of different water masses

Mixing of different water masses can also control the surface water $\delta^{18}O_{seawater}$ values (Shackleton and Vincent, 1978). The isotopically lighter Persian Gulf Water out flow ($\delta^{18}O$ ~ 0.7‰ SMOW; approx. 200 m depth) and Red Sea out flow water ($\delta^{18}O$ ~ 0.25 - 0.4‰ SMOW; approx. 600 m depth) may admix with the

isotopically heavier South Indian Central Waters ($\delta^{18}O$ ~ 1.3‰ SMOW, 100-200 m depth) and Arabian Sea surface waters ($\delta^{18}O$ ~ 0.9‰ SMOW, 0-100 m depth) (see Zahn and Pedersen, 1991; Sirocko *et al.*, 1993). Persian Gulf and Red Sea outflow waters originate from the western part of the Arabian Sea, whereas the cores investigated here are located on the eastern part and were retrieved from a shallow depth (280 m water depth). These points rule out the possibility that admixture from water masses as a factor leading to local increase in isotopic values during the Holocene period.

Changes in seasonality and habitat of foraminifera

G. ruber prefers warm stratified waters and is taken as a representative of surface water temperatures during the warm season (Ganssen and Sarnthein, 1983). *G. sacculifer* abundance peaks during the late summer and early autumn (Deuser *et al.*, 1981) and the $\delta^{18}O$ values of this species may represent annual mean SST, provided the range of seasonality in temperature and salinity is small. Since studies on their past changes in seasonalities are not available at this stage, it is difficult to quantify their significance in controlling the $\delta^{18}O$ variations observed in the cores.

4. 3. 3 Species-specific variation in $\delta^{18}O$ records

Absolute values of $\delta^{18}O$ in *G. sacculifer* showed a relative enrichment with respect to that of *G. ruber* (see Fig. 4.2a&b). Studies on living planktic species revealed that *G. ruber* prefers the uppermost 100 m water column and is therefore restricted to the euphotic zone (Duplessy *et al.*, 1981). Although the *G. sacculifer* secretes most of its shell calcite in the upper photic zone of the water column (Fairbanks *et al.*, 1982), shell calcite continue to precipitate below the mixed layer in association with cooler subsurface waters (Ganssen and Sarnthein, 1983). It has been estimated that about 20% of the tests of *G. sacculifer* precipitate below this top layer and the gametogenetic calcification in *G. sacculifer* occurs at depths of 300-800 m (Duplessy *et al.*, 1981; Ganssen and Sarnthein, 1983). These points suggest that the species-specific depth habitat may be responsible for the observed ^{18}O enrichment in the *G. sacculifer* compared to *G. ruber*.

4. 3. 4 Abrupt deglacial $\delta^{18}O$ fluctuations and possible mechanisms

Several high resolution palaeoclimatic studies using a large amount of continental data from the monsoon domains in Asia and Africa point to a series of abrupt short-term phases of intense aridity in the deglacial records, even after the North Atlantic climate had calmed down (Gasse and van Campo, 1994; Zahn, 1994). Accordingly, major dry spells are recorded at all sites during intervals ~11-9.5 ka-BP, ~8-7 ka-BP and ~3-4 ka-BP (Gasse and van Campo, 1994). These climatic anomalies occurred after the environmental conditions around the high latitudes became remarkably stable, indicating that the tropical climate is very sensitive to the subtle changes of its forcing mechanisms (Zahn, 1994). Eventhough numerous terrestrial sites in India, Africa and Tibetan plateau (Pant and Maliekal, 1987; Singh *et al.*, 1990; Gasse and van Campo, 1994) have shown the undoubted presence of these short-term fluctuations, their presence in marine isotope profiles have not yet been clearly established. This may be mainly due to the fact that the mixing time of ocean is relatively very large (of the order of ~1000 years; Prell *et al.*, 1986) and any abrupt fluctuation in monsoonal climate may not be imprinted in the deep sea sediments. Moreover, most of the marine cores analysed so far come from the deep sea, away from direct continental interaction. An exceptional case is a high resolution study on organic-walled dinoflagellate cysts from the western Arabian Sea (Zonneveld *et al.*, 1997), which had indicated such abrupt fluctuations in monsoon climate during the last deglaciation.

The high resolution oxygen isotope records of the core GC-5 appear to reflect these 'fast flickers' of climatic events to a certain extent (see Fig. 4.2a&b). The abrupt fluctuations observed at the core site are more distinct in the *G. ruber* $\delta^{18}O$ records than that of *G. sacculifer.* These climatic reversals occurred around ~11 ka-BP (~13.5 cal-ka-BP), ~8 ka-BP (~9 cal-ka-BP) and possibly at ~ 4 ka-BP (Fig. 4.2a). Core GC-5 was collected from the upper continental slope (~280 m water depth) off Ponnani river, which drains the Western Ghats. A heavy summer rainfall (~3000 mm/year; Krishnan, 1968) is characteristic of this region. So the changes in freshwater input can lead to changes in sea water salinity conditions and in turn the isotopic composition of the sea water. This continental monsoon connection is further corroborated by the distribution of grain size parameters and

down core $\delta^{13}C_{org}$ records (Fig. 4.4a&c), which indicate that the supply of terrigenous clays and organic matter is controlled by variations in fresh water river input (see section 4.3.9 '$\delta^{13}C_{org}$ records').

Studies on summer monsoon variability using both geological evidences and climatic models suggest that the stronger monsoons in the past were associated with increased radiation in the Northern Hemisphere summer and reduced glacial-age boundary conditions (ice-sheet extent, continental albedo and SST of the Arabian Sea) (van Campo *et al.*, 1982; Prell, 1984a; Kutzbach and Street-Perrot, 1985; Prell and van Campo, 1986). Biological, biogeochemical and lithogenic evidences from Arabian Sea sediment records indicate that the Arabian Sea summer monsoon winds responded in a strong, coherent fashion to changes in the distribution of solar radiation as determined by the cyclical variability in obliquity and precession of the Earth's orbit (Clemens *et al.*, 1991). During LGM (~18 ka-BP), the highly reflective ice sheets, generally cold oceans and equatorward advance of sea ice in both the hemispheres had a significant effect on the climate of the monsoon regions, eventhough the seasonal distribution of the insolation at the top of the atmosphere was similar to that of today (Webb III *et al.*, 1993).

Although the changes in summer solar insolation account for the general envelop of the post-glacial monsoon fluctuations, it does not explain the timing and amplitude of short-term fluctuations. These abrupt climatic reversals in monsoon intensity as revealed by continental and marine records were mainly attributed to: a). influence of sea surface conditions, b). changes in seasonal tropical land surface conditions (Gasse and van Campo, 1994), and c). a combination of mechanisms, with different factors influencing at different time intervals (Zonneveld *et al.*, 1997).

Variations in sea surface conditions and circulation patterns

Changes in the cross-equatorial heat transport by ocean surface currents in the thermohaline 'conveyor belt' circulation induced by the variations in North Atlantic Deep Water (NADW) may have influenced the short-term climatic instabilities in SW-monsoon intensity (Zahn, 1994). An abrupt monsoonal reversal around ~12.5 cal-ka-BP is attributed to the atmospheric and eventually

thermohaline ocean circulation changes related to the temperature fluctuations in the northern latitudes (Zonneveld *et al.*, 1997).

Changes in tropical land surface conditions

Gasse and van Campo (1994) suggested that tropical land surface conditions (soil moisture feedback and changes in methane production from wetlands) provide a more satisfactory explanation for the abrupt short-term climatic reversals for the past 9 ka-BP. A positive feedback mechanism in the form of expansion of vegetation cover, expansion of wetlands and enhanced soil moisture may have reduced the land albedo (thus increasing land-sea pressure gradient) and enhanced the monsoon intensity. Further, the watering of wetlands could lead to an increase in CH_4 production, amplifying the atmospheric warming effect. Methane production is however, self-limiting, as both denser vegetation cover and enhanced water levels eventually reduce the CH_4 production. Once the monsoon precipitation is fully established, methane production falls and soil moisture decreases its specific heat capacity so that more heating is required to raise the temperature. Evapo-transpiration exceeds evaporation, leading to subsequent cooling of the land, and eventually reduces the land-ocean pressure gradient (Gasse and van Campo, 1994). This negative feedback mechanism may have effectively caused abrupt monsoonal reversals, which observed as isotopic reversals in core GC-5. Zonneveld *et al.* (1997) also identified the short-term monsoonal fluctuations for the past ~9 ka as observed in a core from the western Arabian Sea and suggested the tropical land surface boundary conditions as a possible forcing mechanism.

4. 3. 5 Benthic $\delta^{18}O$ record and local temperature effects

As discussed earlier, the estimated isotopic effect due to the melting of global ice sheets ('ice volume effect') itself amounts to ~1.2‰ (Labeyrie *et al.*, 1987; Fairbanks, 1989). The LGM-Holocene $\delta^{18}O$ amplitude of *U. peregrina* ($\Delta\delta^{18}O$ ~ 0.9‰) in core GC-5 is lower than the ice volume effect and also the amplitude shown by the planktic records ($\Delta\delta^{18}O$ ~2.1‰). This observation is unique and has not yet reported in other standard benthic records (e. g., Zahn and Pedersen, 1991; Sarkar and Bhattacharya, 1992). The cause for this anomaly

should be local in nature and possibly related to the past changes in bottom water conditions.

It is generally assumed that the bottom water temperatures have not changed much during the last glacial-interglacial period (see Savin and Yeh, 1981). Accordingly the benthic $\delta^{18}O$ records should atleast represent the 'ice volume effect' (~1.2‰). Although vertical mixing by bioturbation has the potential to considerably reduce the $\delta^{18}O$ variance of downcore records (Zahn and Pedersen, 1991), the relatively high sedimentation rate (> 10 cm/ ka) at the core site negate this possibility. It is more likely that the reduced $\Delta\delta^{18}O$ value could be due to past variations in ambient water hydrography or by the downslope transfer of foraminiferal tests from shallower (hence "warmer") shelf region.

The Persian Gulf Water outflow and Red Sea Water outflow orginate from the western part of the Arabian Sea and their influence reduces as they move southward (You, 1997). Moreover, the core of the Red Sea Water outflow (~600 m water depth) (see section 1.7.2. of Chapter 1), is well below the depth of present core site. Therefore these water masses are less likely to contribute to the changes in $\delta^{18}O_{seawater}$ at the GC-5 core site.

Eustatic sea level was at about ~120 m below the present level during the last glacial maximum (LGM) (Fairbanks, 1989). Core GC-5 was collected from ~280 m water depth. Therefore, the water depth at the core site could have been about 160 m during this period. It is likely that this shallow depth of the core site could have influenced the ambient water temperature conditions. The temperature profile of the water column (Fig. 4.9) near the core site indicates that the mixed layer depth is at ~100 m water depth and below this there is a sharp decline in temperature suggesting a strong thermocline. The temperature of the sea water at about 280 m depth (present day depth of the core) is ~13°C and the temperature at 160 m depth can be as high as 2-3°C (see Fig. 4.9). This indicates that the ambient water temperature at the core site was higher due to apparent shallowing of the core site and superimposed on the lowered SST conditions during the glacial stage. Converting this temperature difference into isotope values (0.2‰ per 1°C; see Ganssen and Sarnthein, 1983), this could have lead to a reduction in isotopic values by about 0.4-0.6‰. By adding these values to the obtained value

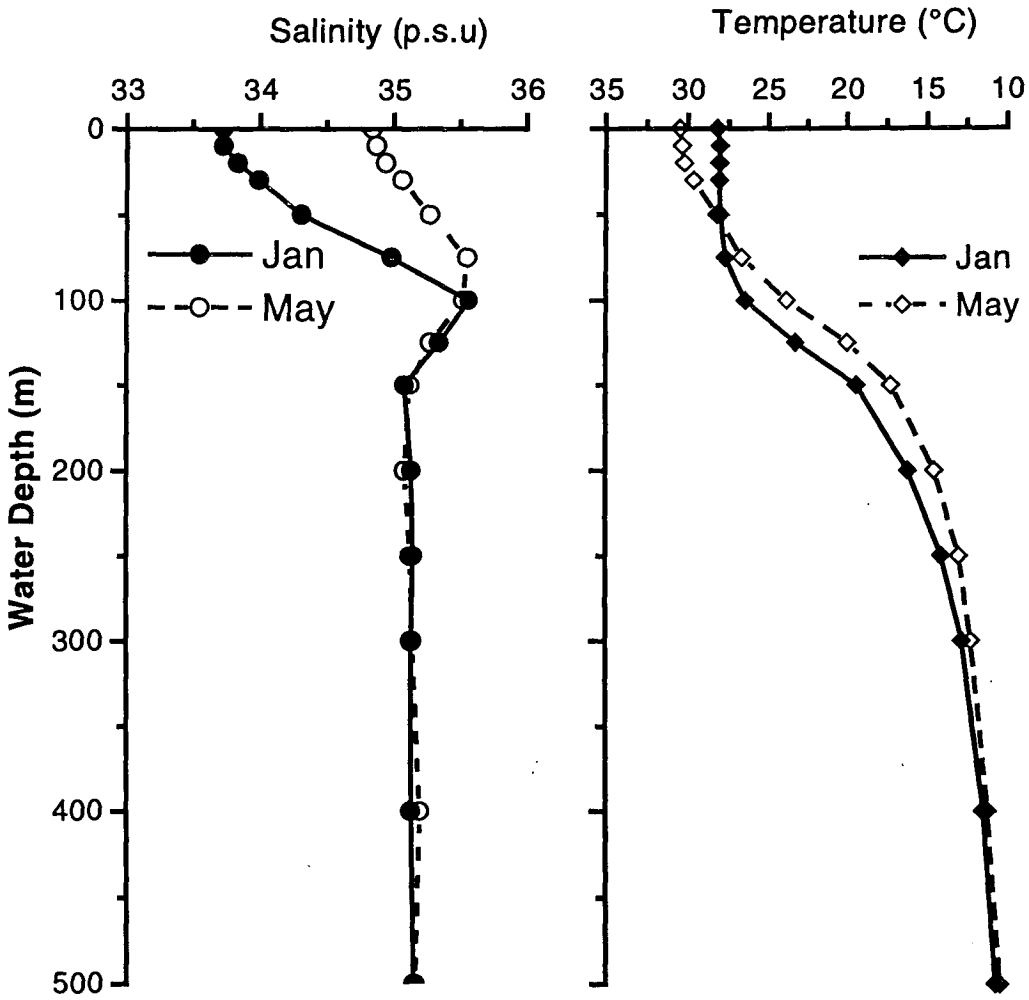

Fig. 4. 9 Temperature and salinity profile at 10.5°N 75.5°E (from NOAA, 1994)

of LGM-Holocene $\delta^{18}O$ amplitude of *U. peregrina* (~0.9‰), the $\Delta\delta^{18}O$ value will be at ~1.3-1.5‰, which is comparable with standard benthic records. Therefore, the reduced benthic $\delta^{18}O$ and $\Delta\delta^{18}O$ values can be attributed to the local temperature effects caused by lowered sea level at the core site during LGM.

The *U. peregrina* $\delta^{18}O$ profile does not show abrupt climatic reversals, as observed in planktic foraminifers. As the LGM-Holocene amplitude is relatively low (Fig. 4.2c), and influenced by local ambient water conditions, the abrupt events are not distinct. Throughout the isotope stage 2, the $\delta^{18}O$ values remained more or less constant around 1.7‰, once again suggesting the influence of enhanced water temperature due to lowered sea level at the site. After this period, a large negative excursion of $\delta^{18}O$ values coincide with highly enhanced precipitation related to monsoons (van Campo, 1986). The absence or displacement of isotopic reversals when compared with the planktic records support a continental connection for the planktic isotopic reversals in the core. Therefore, the surface water $\delta^{18}O_{seawater}$ values at the core site could have varied as a function of continental fresh water input, which is in turn monsoon driven. A similar relation between monsoon-induced precipitation and sea water isotopic changes has been suggested for the ODP site 724 (Zahn and Pedersen, 1991).

The absolute values of benthic foraminiferal $\delta^{18}O$ (1.8 - 1.1‰) are also very low compared to other similar records from the deeper regions (e.g., 2.54 to 1.18‰ - Zahn and Pedersen, 1991; 3.8 to 2.4‰ - Ahmad and Labeyrie, 1994). This also can be attributed to the relatively higher temperature (leading to enrichment of heavy isotope values) prevailing at the core site.

4. 3. 6 Controls on $\delta^{13}C$ variations in planktic foraminifers

As mentioned earlier (section 4.1.1), the carbon isotope ratios of planktic foraminifers are very complex and only a portion of the total $\delta^{13}C$ variations observed in planktic foraminifers in deep sea sediments reflect local upwelling, productivity and nutrient variations (e.g., Prell and Curry, 1981; Ganssen and Sarnthein, 1983; Wefer and Berger, 1991). Most of the foraminifers precipitate calcite out of carbon equilibrium and also the degree of disequilibrium is not constant and varies from species to species (Wefer and Berger, 1991). It has

been proposed that the $\delta^{13}C$ value of planktic foraminifers is a function of the $^{13}C/^{12}C$ ratio of the sea water ΣCO_2 and of 'vital effects' related to metabolic processes such as respiration and symbiont photosynthesis (Erez and Honjo, 1981). It is shown that the $\delta^{13}C$ and $\delta^{18}O$ values are mutually exclusive signals controlled by the environmental parameters, light and temperature, respectively (Spero and Williams, 1988).

The past $\delta^{13}C$ fluctuations in the tropical surface waters have been mainly attributed to: 1). variations in the $\delta^{13}C$ composition of the atmospheric CO_2 caused by variation in forest biomass; and 2). variations in nutrient availablilty and primary productivity.

Variation in $\delta^{13}C$ of atmospheric CO_2

Shackleton (1977) and Prell and Curry (1981) suggested that the stratigraphic variations of $\delta^{13}C$ in planktic foraminifers may be related to the changes in isotopic composition of the atmospheric CO_2, which when equilibrated with the surface ocean, transmits its $\delta^{13}C$ signal to the shallow-dwelling planktic foraminifers. On a glacial-interglacial time scale, terrestrial vegetation which is a very reactive carbon reservoir, is destroyed when it is overridden by ice sheets. Vegetation also responds to precipitation and temperature variations at low latitudes. A recent study by Street-Perrot *et al.* (1997) revealed that the increase in atmospheric CO_2 concentration during the early Holocene period was correlated to a decrease in the amount of $\delta^{13}C$ of bulk organic matter deposited in tropical lake sediments. Stable carbon isotope ratios of peats from the Nilgiris (southern India) also revealed that increased precipitation and soil moisture during ~9 ka-BP favoured spread of C_3 type terrestrial vegetation (mainly trees; $\delta^{13}C$ ~ -26 to -28‰), compared to the dominance of C_4 type vegetation (mainly grasses; $\delta^{13}C$ ~ -11 to -13‰) during LGM and late Holocene arid periods (Sukumar *et al.*, 1993; Rajagopalan *et al.*, 1997). Since the $\delta^{13}C$ of forest biomass is low (-25 to -21‰) (Craig, 1953) compared to the mean ocean $\delta^{13}C$ (~0‰) (Kroopnick, 1985), the $\delta^{13}C$ of the mean ocean water is affected by the transfer of carbon from terrestrial biosphere to the ocean (Shackleton, 1977). The $\delta^{13}C$ of the atmospheric CO_2 increased during periods of maximum vegetation (as trees preferentially use ^{12}C),

would be thus to the surface sea water. Prell and Curry (1981) concluded that the single largest forcing mechanism for the observed similarities in amplitude and timing of the past $\delta^{13}C$ events, are the variations in the $\delta^{13}C$ composition of the atmospheric CO_2 caused by variations in terrestrial biomass. The fluctuations in oceanic denitrification rate on glacial-interglacial time scales could be another factor leading to the observed glacial-interglacial CO_2 fluctuations and $\delta^{13}C$ variations (see below).

The planktic $\delta^{13}C$ record of core GC-5 may be also related to the variations in atmospheric CO_2 $\delta^{13}C$ composition. The deglacial minimum in $\delta^{13}C$ *G. ruber* (see Fig. 4.3a) is similar to that observed in many sediment cores from the tropical Atlantic Ocean (Berger *et al.*, 1978; Oppo and Fairbanks, 1989). Subsequent maximum in $\delta^{13}C$ during early Holocene may be due to the enhanced monsoonal precipitation resulting in an increase in C_3 vegetation cover and $\delta^{13}C$ of atmospheric CO_2, which in turn increase the surface sea water $\delta^{13}C$.

Variation in the upwelling intensity and productivity

The hypothesis that upwelled waters should contain a carbon isotopic signature is based on the fact that during biological productivity, ^{12}C is preferentially fixed by planktons in the surface water, leaving the surface water enriched in ^{13}C (Prell and Curry, 1981). As the organic matter sinks in the water column, gets oxidised and adds isotopically light carbon to what is already present. During upwelling, the carbon thus released by oxidation is recycled to the surface. Kroopnick (1985) suggested that the $\delta^{13}C$ of the ΣCO_2 ($\delta^{13}C_{\Sigma CO2}$) of the Arabian Sea surface waters is around 1.6‰ and it is ~0.0‰ at a depth of 100-200 m; therefore, the isotopic carbon signal in the tests of foraminifers, should register the upwelling signals.

Using high resolution sediment cores from the tropical sectors of the Pacific, Atlantic and Indian Oceans, Oppo and Fairbanks (1989) found that the deglacial $\delta^{13}C$ signal of planktic foraminifers could not be simply attributed to the changes in mean ocean $\delta^{13}C$ due to the transfer of organic carbon between the terrestrial and oceanic reservoirs. Instead they offered two hypotheses: 1). An enhanced upwelling rate could have caused the deglacial $\delta^{13}C$ minimum by

transporting more ^{12}C- enriched deeper water to the surface. If the decrease in $\delta^{13}C$ around 150 cm depth interval of GC-5 (Fig. 4.3a&b) (~11 cal-ka-BP), is due to the enhanced upwelling of colder (deep) waters, one would expect more positive (heavier) values of $\delta^{18}O$ in *G. ruber* and *G. sacculifer* for the corresponding period. Since this is not observed (see Fig. 4.2), the hypothesis may not be applicable here. The isotope data of *G. ruber* collected by sediment traps from the Arabian Sea revealed that unlike $\delta^{18}O$, the $\delta^{13}C$ values showed considerable interannual and geographical differences, suggesting the relation between $\delta^{13}C$ and upwelling intensity is complicated (Curry *et al.*, 1992). 2). Changes in $\delta^{13}C$ values could be produced by variations in the mixing of source waters or changes in the input and degradation of terrestrial organic carbon. Variations in regional input and oxidation of terrestrial organic matter (nitrogen-poor, isotopically lighter), could be an important factor leading to a deglacial $\delta^{13}C$ minimum in GC-5. Schneider *et al.* (1992) proposed similar mechanisms for the deglacial $\delta^{13}C$ minimum in the cores from the Benguela upwelling region. If the $\delta^{13}C$ variations of planktic foraminifers correspond to the above, then the $\delta^{13}C$ variations in benthic species from the same core should also indicate similar fluctuations, which are not exhibited in the $\delta^{13}C$ results of *U. peregrina*.

4. 3. 7 $\delta^{13}C$ of *U. peregrina*: oceanic denitrification record?

The marine organic matter and the CO_2 released during its oxidation in the water column are significantly depleted in $\delta^{13}C$ (Zahn and Pedersen, 1991). Hence the $\delta^{13}C_{\Sigma CO2}$ values in the mid-depth Arabian Sea are depleted when compared to the regional deep waters (Kroopnick, 1985; Zahn and Pedersen, 1991). Numerous studies on the $\delta^{13}C$ variations in *U. peregrina* revealed that it precipitates its shell calcite out of carbon isotopic equilibrium with the ambient bottom water mass (e.g., Zahn *et al.*, 1986; Grossman, 1987; McCorkle *et al.*, 1990). The departures from the equilibrium for the $\delta^{13}C$ in the benthic foraminifers are attributed mainly to "vital effects" and microhabitat effects.

"Vital effect" is manifested by disequilibrium isotopic compositions and in most cases result in the depletion of heavy isotopes (Wefer and Berger, 1991).

This disequilibrium occurs due to the incorporation of isotopically-light metabolic CO_2 into the carbonate test and the magnitude of vital effect is proportional to the amount of metabolic CO_2 in the organism's internal CO_2 pool (Erez, 1978). It appears that almost all biogenic carbonates are influenced by vital effect; however, the degree of disequilibrium varies widely and is species-specific (Grossman, 1987).

Recent studies indicate that the $\delta^{13}C$ fluctuations closely correlate with the accumulation rates of organic carbon and may reflect a species-specific response to variations in the microenvironments (Zahn *et al.*, 1986; Grossman, 1987; McCorkle *et al.*, 1990). *U. peregrina* prefers a near surface infaunal habitat with a preference for the decaying "soup" of organic matter on the sea floor (Zahn *et al.*, 1986; Altenbach and Sarnthein, 1989). Moreover, the $\delta^{13}C$ values of *U. peregrina* appear to reflect the $\delta^{13}C$ of porewater ΣCO_2 and are therefore, indirectly linked to the flux of organic carbon reaching the sea floor (McCorkle *et al.*, 1990). The $\delta^{13}C$ values of *U. peregrina* therefore record the bottom water CO_2 variations only partially and in regions of high organic carbon accumulation, these values may serve to document the palaeoproductivity changes of the ocean (Zahn *et al.*, 1986).

The down core record of *U. peregrina* $\delta^{13}C$ in core GC-5 closely matches with the C_{org} profile (compare Fig. 4.3c & 4.4b), suggesting a direct causal link between the two. Unfortunately, dry bulk density of the sediment was not determined so as to calculate the accumulation rate of organic carbon, which is a more correct and direct parameter to correlate with the $\delta^{13}C$ record (McCorkle *et al.*, 1990). Nevertheless, the very high organic carbon values in the upper 100 cm interval in the core (> 2.5 %) may point to a relatively high C_{org} accumulation rate in this section.

Highly enhanced $\delta^{13}C$ values were obtained for the upper Holocene section compared to the lower glacial and deglacial section (Fig. 4.3c). Higher productivity leads to a preferential fixing of ^{12}C in the settling organic particles and low surface productivity leads to an enrichment of ^{13}C in the organic particles settling to the depth (e.g., Zahn *et al.*, 1986; Zahn and Pedersen, 1991). It may therefore imply that the highly enriched $\delta^{13}C$ values of *U. peregrina* during the Holocene period

are mainly due to reduced productivity. But this however, may not be true, because of the following observations from this region: a). Palaeo-productivity studies in the Arabian Sea have indicated a considerable increase in the monsoon-induced upwelling intensity and productivity since the LGM with a maximum around the early Holocene (Prell and Curry, 1981; Fontugne and Duplessy, 1986; Clemens *et al.*, 1991; Sirocko *et al.*, 1993, 1996; Naidu and Malmgren, 1995 among others). b). Relatively high amplitude in C_{org} content was observed between the LGM and Holocene (up to 2%) (Fig. 4.4b). Rock-Eval pyrolysis parameters and faunal distribution attest to the significant increase in marine organic carbon with the onset of Holocene compared to the glacial period (see Chapter 3).

Sarnthein *et al.* (1988) have reported that unlike in the rest of the world oceans, there is a distinct mid-Holocene increase in new productivity (P_{new}), accompanied by a synchronous increase in $\delta^{13}C_{org}$ values in the Arabian Sea. They showed that the increase in palaeoproductivity is correlated with an increase in $\delta^{13}C$. The *U. peregrina* $\delta^{13}C$ record of GC-5 (Fig. 4.3c) is also similar to that of Sarnthein *et al.* (1988), wherein an enhanced palaeoproductivity coincides with high $\delta^{13}C$ values. The following is an attempt to explain this anomalous $\delta^{13}C$ distribution, assuming that $\delta^{13}C$ of *U. peregrina* mostly record the local organic carbon flux than the global variations in deep water ΣCO_2 (see Zahn *et al.*, 1986; McCorkle *et al.*, 1990).

Field and laboratory culture studies suggest that the carbon fixation in marine phytoplankton can be attributed to either C_3 (RuBP carboxylase) mechanism or C_4 (β-carboxylation) mechanism (Descolas-Gros and Fontugne, 1985). High $\delta^{13}C$ values are associated with C_4 mechanism and low values with C_3 mechanism. Two observations which have palaeoclimatological significance are:

1. During the initial exponential growth of the diatom population, $\delta^{13}C$ values are low, close to the values characteristic of the C_3 pathway. During the second phase of stationary growth phase, the $\delta^{13}C$ values showed a massive increase, indicative of C_4 pathway (β-carboxylation). The increase in β-carboxylation and $\delta^{13}C$ values was related to deteriorating growth conditions such as depletion of nutrients (Descolas-Gros and Fontugne, 1985). So an increase in

C_4 pathway of carbon fixation can account for the increased $\delta^{13}C$ values during the Holocene.

2. Increased $\delta^{13}C$ values are associated with the C_4 carbon fixation mechanism of dinoflagellates and Chlorophyceae. Immense blooms of dinoflagellates ("red tides"), are associated with unusual conditions leading to complete denitrification of the surface water; whereas a subsurface maxima of ammonia and phosphorus is prevalent (i.e., an unusually low N:P ratio) (Codispoti, 1983). Sarnthein *et al.* (1988) consider these dinoflagellate blooms as a possible mechanism for the anomalous $\delta^{13}C_{org}$ values in their Arabian Sea sediment cores.

Altabet *et al.* (1995) and Ganeshram *et al.* (1995) demonstrated that productivity-induced denitrification is a possible mechanism linking the ocean's nitrogen and climate cycles. The reduction in sea level and corresponding reduction in continental shelf area, together with a decrease in the intensity of water column stratification in tropical regions during recent glacial periods seem to have resulted in decreased rates of denitrification relative to nitrogen fixation. Since denitrification is closely controlled by the water column anoxia which in turn is related to biological productivity, it has been proposed that glacial decrease in denitrification can be mainly attributed to the reduced upwelling-induced productivity and fluxes of organic detritus on the continental margins (Ganeshram *et al.*, 1995). During the Holocene, the increased productivity could have lead to an enhanced denitrification.

As discussed above, if the denitrification rate increased during the Holocene, it would lead to a specific deficit in nutrient budget (unusually low N:P ratio). These short phases of nutrient depletion may lead to a situation similar to the stationary growth of diatoms (i.e., C_4 mechanism) resulting in a massive increase in $\delta^{13}C$. Alternatively, denitrification can lead to adverse environmental conditions where dinoflagellates and Chlorophyceae (carbon fixation by C_4 mechanism) can thrive, leading to an enrichment of $\delta^{13}C$ in the marine organism (Descolas-Gros and Fontugne, 1985).

If the organic matter settling down to the sea bottom during periods of enhanced denitrification is anomalously rich in $\delta^{13}C$, and if the variations in *U. peregrina* $\delta^{13}C$ are primarily influenced by the organic matter accumulation rate at

the sea bottom (see Zahn *et al.*, 1986), then the increase in $\delta^{13}C$ of organic matter would lead to an enrichment in the $\delta^{13}C$ of *U. peregrina*. The observed highly enhanced $\delta^{13}C$ records of *U. peregrina* during Holocene (LGM-Holocene amplitude in $\delta^{13}C$ >1.0‰) may be therefore indicate the influence of the above factors.

Alternatively, part of the $\delta^{13}C$ changes in core GC-5 could be attributed to the effect of alkalinity during the LGM. Because the CO_2 partial pressure (P_{CO2}) of the sea surface and the atmosphere must be in approximate equilibrium, the presumed glacial drop in atmospheric CO_2 up to 90 p.p.m.v. recorded in ice cores (Barnola *et al.*, 1987) must have been accompanied by an increase in surface water [CO_3^{2-}]. Spero *et al.* (1997), based on laboratory studies, showed that the $\delta^{13}C$ of the planktic and benthic foraminifers can indeed be affected by the changes in alkalinity of the sea water. At constant alkalinity, but varying ΣCO_2 (or varying alkalinity and constant ΣCO_2), the $\delta^{13}C$ of *Orbulina universa* tests decrease with an increase in [CO_3^{2-}]. Estimations of $\delta^{13}C$ changes suggest that a glacial rise in [CO_3^{2-}] can lead to a drop in $\delta^{13}C$ of the order of atleast ~0.25 - 0.5‰ (Spero *et al.*, 1997). So while interpretting the $\delta^{13}C$ variations, the past alkalinity variations should also be considered as significant.

4. 3. 8 $\delta^{13}C_{org}$ record and past variations in organic carbon input

Various mechanisms proposed for the glacial-interglacial variations in $\delta^{13}C$ of organic matter are: a). varying proportions of marine and terrestrial organic matter input; b). temperature-dependant isotopic fractionation during photosynthesis; c). changes in the surface water CO_2 concentrations; and d). diagenesis of sedimentary organic matter (Jasper and Gagosian, 1990; Rau *et al.*, 1991; Müller *et al.*, 1994).

Fontugne and Duplessy (1981) showed a significant correlation between sea surface temperature (SST) and carbon isotopic composition of marine planktons and suggested a positive temperature effect on carbon isotopic fractionation (an increase in $\delta^{13}C_{org}$ values with increasing temperature). Despite the fact that the complete $\delta^{13}C_{org}$ record of core GC-5 is not available for comparison of glacial-interglacial variations, significant changes within the

deglacial period itself (see Fig. 4.4a), indicate that the observed carbon isotopic variations of the sediment organic matter may not be related to the temperature factor.

The $\delta^{13}C_{org}$ records could also be affected by the pre- and post- burial diagenesis (McArthur *et al.*, 1992). In the absence of any secular changes in the downcore $\delta^{13}C_{org}$ values, the effect of diagenesis may be minimum.

Rau *et al.* (1991) suggested that the sediment $\delta^{13}C_{org}$ variations may serve as a proxy for surface water dissolved molecular CO_2 concentrations [CO_2(aq)]. This is based on the fact that the carbon isotopic fractionation during photosynthesis by plankton largely depends on the concentration of ambient dissolved CO_2(aq). As discussed above (see sections on benthic and planktic foraminiferal $\delta^{13}C$ records), the past variations in atmospheric CO_2 can influence the isotopic compositions of the organic matter and inorganic shells. As the $\delta^{13}C_{org}$ records are not complete up to the LGM, and the fact that significant variations are observed within the interglacial period itself (see Fig. 4.4a), it is not possible to correlate the $\delta^{13}C_{org}$ records with the glacial-interglacial variations in surface water CO_2 concentrations.

The observed downcore variations in $\delta^{13}C_{org}$ values may indicate more clearly the varying supply of organic matter from marine and terrestrial sources. It has been suggested that the carbon isotope ratio of the organic matter in marine sediments depends primarily on the percentage of the continental versus marine sources of carbon (Fontugne and Duplessy, 1986; Jasper and Gagosian, 1990). Since the terrigenous organic matter is depleted in ^{13}C ($\delta^{13}C_{org}$ values range from -27 to -28‰), compared to marine plankton (ideally $\delta^{13}C_{org}$ values >-21‰), a higher terrigenous contribution can lead to decrease in $\delta^{13}C_{org}$ values and vice versa.

Jasper and Gagosian (1990) presented a binary mixing model for estimating the relative proportions of marine and terrigenous organic carbon in the marine sediments which can be expressed as follows:

$$\delta^{13}C_S = F_T\,\delta^{13}C_T + F_M\,\delta^{13}C_M \qquad (1)$$

$$F_T + F_M = 1 \qquad (2)$$

Then,

$$F_M = [(\delta^{13}C_S - \delta^{13}C_T) / (\delta^{13}C_M - \delta^{13}C_T)] \qquad (3)$$

where, $\delta^{13}C_S$ = measured $\delta^{13}C_{org}$ of a given sample; $\delta^{13}C_T = \delta^{13}C_{org}$ of terrigenous end member; $\delta^{13}C_M = \delta^{13}C_{org}$ of marine end member; F_T = terrigenous fraction of total C_{org}; and F_M = marine fraction of the total C_{org}.

It is assumed that the riverine particulate organic carbon to the ocean has a mean $\delta^{13}C_{org}$ value of -26‰ (Fontugne and Duplessy, 1986). Measured $\delta^{13}C_{org}$ values of the planktons of the eastern Arabian Sea have a mean value of -19‰ (Fontugne and Duplessy, 1981). Hence the marine and terrigenous $\delta^{13}C_{org}$ end member values used in this study are -19‰ and -26‰, respectively.

The results reveal that $\delta^{13}C_{org}$ values of top levels of the core (0-50 cm) are closer to the modern plankton values (average $\delta^{13}C_{org}$ value -19.8‰). The estimated terrigenous carbon input to the core site is <15% of the total available C_{org} (Table 4.3). Hence any significant input of terrigenous C_{org} can be ruled out. These results are in accordance with the present day scenario, where the low C/N ratios and $\delta^{13}C_{org}$ values indicate that the C_{org} content in the upper continental slope sediments is mainly marine in nature (Calvert *et al.*, 1995).

Between ~60 cm and 150 cm core depths, the $\delta^{13}C_{org}$ values decreases sharply, indicating relatively higher terrigenous C_{org} input. Estimated terrigenous C_{org} input ranges between ~20 and 36% (Table 4.3). The maximum terrigenous carbon input estimated at ~100 cm core depth (~9 cal-ka-BP) coincides with a large increase in terrigenous clay input to this site (Thamban, 1998) (see Fig. 4.4c). This early Holocene maxima of terrigenous input coincides with the period of highly enhanced monsoon with very humid conditions in the Arabian Sea and Indian subcontinent (e.g., van Campo, 1986; Clemens *et al.*, 1991; Sirocko *et al.*, 1996). These observations suggest that the $\delta^{13}C_{org}$ record of GC-5 is controlled by the mechanism of varying supply of terrigenous and marine organic matter.

4. 3. 9 The last deglaciation at GC-3

The $\delta^{18}O$ range and amplitude of core GC-3 matches exceptionally well with that of core GC-5, eventhough the locations of the cores are separated by more than 4 degrees latitude. The glacial-interglacial $\delta^{18}O$ amplitude is ~ -2.1‰ for *G. sacculifer* and ~ -1.9‰ for *G. ruber*, respectively (Fig. 4.5) and are similar to that in core GC-5. As discussed for core GC-5, this may be explained by a

combination of changes in SST (by ~ 2°C; Sonzogni *et al.*, 1998) and precipitation (Duplessy, 1982) during the LGM and subsequent deglaciation period (see the section on GC-5). Slightly lower amplitude observed in the *G. ruber* $\delta^{18}O$ record (~-1.9‰) compared to that of core GC-5 (~-2.1‰) may be explained by the variation in summer SST at both the core sites. Although the upwelling induced cooling of the surface water occurs at both the sites, its effect decreases from south to north. Hence the $\delta^{18}O$ values at the core top are slightly decreased.

The glacial-integlacial events for the last ~25 ka seen in the oxygen isotope record of core GC-3 are similar to that of the high resolution record of core GC-5 off Cochin. Most characteristic among them is the step-wise character of the isotopic changes from LGM to Holocene.

4. 3. 10 Benthic $\delta^{18}O$ record of core GC-4

The amplitude of the $\delta^{18}O$ record is lower, when compared with standard isotopic curves of *U. peregrina* from the Pacific (e.g., Shackleton *et al.*, 1983), Atlantic (e.g., Zahn *et al.*, 1986) and Indian Oceans (e.g., Zahn and Pedersen, 1991; Sarkar and Bhattacharya, 1992; Ahmad and Labeyrie, 1994). It is however, comparable with that of core GC-5 (compare Fig. 4.2c & Fig. 4.6a). Since the *U. peregrina* $\delta^{18}O$ records should normally represent atleast the ice volume effect (~1.2‰; Labeyrie *et al.*, 1987), the $\delta^{18}O$ amplitude observed is unreasonable. As discussed for the core GC-5 (see above), the relatively shallow depth of the core site (<350 m water depth), could have lead to an enhanced bottom water temperature and hence a reduced glacial-interglacial isotope effect. Also the effect of bioturbation on vertical mixing of sediments at this site has to be taken into account.

4. 3. 11 $\delta^{13}C_{org}$ record of GC-4 and palaeoproductivity variations

The relatively constant heavy $\delta^{13}C_{org}$ values obtained throughout the core GC-4 (Fig. 4.7a) suggest that marine productivity was the main supplier of organic matter to the core site and very less from the terrestrial sources. This can be also observed in the isotope records of Core GC-5 (see Fig. 4.4a), wherein (except during the period around ~9 cal-ka-BP where there was significant input of terrigenous organic matter), the organic matter is mainly marine. The above

observation and taking the C_{org} content in the sediment as a palaeoproductivity indicator (see Chapter 3), would imply that productivity has increased significantly since LGM in this part of Arabian Sea. Eventhough the transport of organic matter to the sea bottom varied through time, the main supplier remained to be the surface water primary productivity. This increased productivity with the onset of Holocene at the core site is in accordance with the well established hypothesis of enhanced monsoon-induced productivity since LGM (e.g., Prell and Curry, 1981; Clemens *et al.*, 1991; Sirocko *et al.*, 1996 among others). Absence of significant terrigenous organic matter supply to the core site in the past may be mainly attributed to the absence of major rivers bringing large amount of terrigenous sediment load to this site.

4. 4 CONCLUSIONS

1. The stable isotope record of planktic and benthic foraminifers and organic matter in four sediment cores from the western continental margin of India indicates that the intensity of monsoons and related oceanic productivity fluctuated widely during the late Quaternary.
2. Down core oxygen isotope records of planktic foraminifers *Globigerinoides ruber* and *Globigerinoides sacculifer* exhibit a step-wise feature and are comparable with the deglacial warming stages reported in other regions of the Arabian Sea. The general trend of $\delta^{18}O$ record suggests that the Arabian Sea summer monsoon responded strongly to the fluctuations in solar insolation during the late Quaternary.
3. The amplitude of $\delta^{18}O$ values between the Last Glacial Maximum (LGM) and Holocene ($\Delta\delta^{18}O$ ~2.1‰) exceeds the global 'ice volume effect' (1.2‰) significantly; this is best explained by a combination of decrease in sea surface temperature (SST) and increase in salinity during LGM.
4. The abrupt fluctuations in the high resolution $\delta^{18}O$ record during the last deglacial period in a core off Cochin appear to correspond to the abrupt climatic reversals reported from the continental records during this period. Changes in tropical land surface conditions (soil moisture feedback and

changes in methane production from wet lands) may explain these abrupt reversal events.

5. The $\delta^{18}O$ record of benthic foraminifer *U.peregrina* shows that $\delta^{18}O$ amplitude ($\Delta\delta^{18}O$ ~0.9‰) is lower than the 'ice volume effect' (~1.2‰) and is not represented in any other regional records. This has been attributed to local temperature effects caused by the apparent shallowing of the core site during LGM.
6. The down core carbon isotope ($\delta^{13}C$) records of planktic foraminifers (*G. ruber* and *G. sacculifer*) are very complex and many factors like variations in upwelling intensity, productivity, nutrient availability and variations in $\delta^{13}C$ of atmospheric CO_2 could have contributed to the past variations in the total $\delta^{13}C$ values.
7. The $\delta^{13}C$ records of benthic foraminifera *U. peregrina* closely correlate with the C_{org} record and are thus against the established hypothesis that enhanced productivity leads a decrease in $\delta^{13}C$ of the organic matter produced. The $\delta^{13}C$ variations can be attributed to the glacial-interglacial variations in oceanic denitrification rate and/or sea water alkalinity.
8. The down core variations in the carbon isotope ratios of bulk organic matter ($\delta^{13}C_{org}$) in two sediment cores indicate that the C_{org} is dominantly marine in nature. The observed $\delta^{13}C_{org}$ variations may correspond to the varying supply of organic matter from terrestrial and marine sources.

Table 4. 2 Oxygen isotope records of core GC-5.

Gravity Core	Depth interval (cm)	G. ruber $\delta^{18}O$ (‰ PDB)	G. sacculifer $\delta^{18}O$ (‰ PDB)	U. peregrina $\delta^{18}O$ (‰ PDB)
GC-5	2	-3.04	-1.83	1.07
GC-5	6	-2.53	-2.13	1.36
GC-5	10	-3.02	-2.12	1.10
GC-5	16	-2.86	-2.06	1.18
GC-5	18	-2.54	-1.92	0.97
GC-5	22	-2.81	-2.49	1.01
GC-5	27	-3.18	-1.93	1.15
GC-5	32	-2.54	-1.80	0.97
GC-5	37	-2.76	-2.15	1.11
GC-5	42	-1.98	-2.00	0.93
GC-5	47	-2.65	-2.42	0.92
GC-5	52	-2.61	-2.57	1.11
GC-5	62	-2.91	-2.42	1.51
GC-5	67	-2.76	-1.73	1.08
GC-5	72	-2.64	-2.16	1.28
GC-5	77	-2.74	-1.75	1.24
GC-5	82	-2.24	-1.8	1.14
GC-5	87	-2.35	-1.73	0.94
GC-5	92	-1.88	-1.69	1.17
GC-5	97	-1.55	-0.96	1.44
GC-5	102	-2.49	-2.12	0.97
GC-5	112	-2.64	-1.83	1.53
GC-5	122	-1.72	-1.14	1.47
GC-5	132	-1.71	-1.25	1.65
GC-5	142	-1.64	-1.05	1.65
GC-5	152	-1.81	-1.10	1.56
GC-5	162	-1.54	-0.88	1.63
GC-5	167	-1.41	-0.61	1.80
GC-5	177	-1.16	-0.84	1.64
GC-5	187	-1.78	-0.88	1.69
GC-5	202	-1.56	-0.70	1.56
GC-5	222	-0.99	-0.36	1.81
GC-5	242	-0.76	-0.45	1.69
GC-5	262	-0.91	-0.38	1.74
GC-5	282	-1.01	-0.34	1.75
GC-5	302	-1.41	-0.36	1.71
GC-5	322	-1.03	-0.68	1.53

Table 4. 3 Carbon isotope records of core GC-5. The *U. peregrina* values after corrected for disequilibrium with ambient seawater are also given by adding +0.9‰ with the original values (after Mix *et al.*, 1991).

Gravity Core	Depth interval (cm)	*G. ruber* $\delta^{13}C$ (‰)	*G. sacculifer* $\delta^{13}C$ (‰)	*U. peregrina* $\delta^{13}C$ (‰)	*U. peregrina* $\delta^{13}C$ ‰ (corrected)
GC-5	2	1.09	1.43	-0.38	0.52
GC-5	6	1.44	1.35	-0.73	0.17
GC-5	10	1.36	1.45	-0.18	0.72
GC-5	16	1.35	1.76	-0.32	0.58
GC-5	18	1.24	1.08	-0.48	0.42
GC-5	22	1.36	1.37	-0.59	0.31
GC-5	27	1.45	0.76	-0.61	0.29
GC-5	32	1.04	1.08	-0.49	0.41
GC-5	37	1.15	0.66	-0.40	0.50
GC-5	42	1.03	1.27	-0.50	0.40
GC-5	47	1.08	1.46	-0.69	0.21
GC-5	52	1.34	1.44	-0.55	0.35
GC-5	62	1.24	1.50	-0.79	0.11
GC-5	67	1.81	1.24	-0.42	0.48
GC-5	72	1.13	1.26	-0.37	0.53
GC-5	77	1.26	0.92	-0.27	0.63
GC-5	82	0.84	1.10	-0.90	0.00
GC-5	87	1.25	0.95	-0.63	0.27
GC-5	92	0.97	1.47	-1.03	-0.13
GC-5	97	0.61	0.73	-1.43	-0.53
GC-5	102	1.03	1.27	-1.38	-0.48
GC-5	112	1.03	1.12	-0.94	-0.04
GC-5	122	0.79	1.05	-0.87	0.03
GC-5	132	0.49	1.01	-1.25	-0.35
GC-5	142	0.73	0.95	-1.29	-0.39
GC-5	152	0.41	0.67	-1.08	-0.18
GC-5	162	0.47	0.85	-1.37	-0.47
GC-5	167	0.81	0.84	-1.13	-0.23
GC-5	177	0.97	1.04	-1.41	-0.51
GC-5	187	0.60	0.25	-1.25	-0.35
GC-5	202	0.91	1.21	-1.32	-0.42
GC-5	222	0.71	1.19	-1.44	-0.54
GC-5	242	0.76	0.93	-1.60	-0.70
GC-5	262	0.81	0.61	-1.32	-0.42
GC-5	282	0.81	0.92	-1.31	-0.41
GC-5	302	1.25	1.31	-1.59	-0.69
GC-5	322	0.93	1.15	-1.61	-0.71

Table 4. 4 Down core $\delta^{13}C_{org}$ records of core GC-5. F_M and F_T are the estimated fraction of marine and terrigenous C_{org} (relative percentages), respectively. Estimations are based on the binary mixing model presented by Jasper and Gagosian (1990).

Gravity Core	Depth interval (cm)	$\delta^{13}C_{org}$ (‰ PDB)	F_M (%)	F_T (%)
GC-5	2	-19.91	87	13
GC-5	5	-19.54	92	08
GC-5	8	-20.05	85	15
GC-5	13	-19.78	89	11
GC-5	17	-19.74	89	11
GC-5	22	-19.90	87	13
GC-5	32	-19.70	90	10
GC-5	42	-19.81	88	12
GC-5	52	-19.83	88	12
GC-5	62	-20.65	76	24
GC-5	72	-20.38	80	20
GC-5	82	-20.16	83	17
GC-5	92	-21.34	67	33
GC-5	102	-21.15	69	31
GC-5	112	-21.55	64	36
GC-5	122	-21.46	65	35
GC-5	132	-21.23	68	32
GC-5	152	-20.87	73	27
GC-5	167	-20.23	82	18
GC-5	177	-20.49	79	21
GC-5	202	-20.78	75	25

Table 4. 5 Down core oxygen and carbon isotope records of core GC-3.

Gravity Core	Depth interval (cm)	*G. ruber* $\delta^{18}O$ (‰)	*G. sacculifer* $\delta^{18}O$ (‰)	*G. ruber* $\delta^{13}C$ (‰)	*G. sacculifer* $\delta^{13}C$ (‰)
GC-3	2	-2.63	-1.92	1.33	1.30
GC-3	6	-2.34	-2.18	1.58	1.77
GC-3	10	-2.31	-1.98	1.49	2.03
GC-3	14	-2.37	-1.92	0.86	1.74
GC-3	18	-2.65	-2.31	0.95	1.77
GC-3	22	-2.51	-2.04	0.74	1.51
GC-3	27	-2.50	-1.62	1.64	1.31
GC-3	32	-2.34	-1.60	1.28	1.32
GC-3	37	-2.18	-1.54	1.46	1.67
GC-3	42	-1.90	-0.98	1.20	1.60
GC-3	52	-1.12	-0.75	1.14	1.30
GC-3	62	-1.04	-0.66	0.90	1.27
GC-3	72	-1.18	-0.41	1.16	1.60
GC-3	82	-0.76	-0.18	1.07	1.00
GC-3	92	-0.95	-0.30	0.96	1.47
GC-3	97	-1.12	-0.36	1.04	1.59
GC-3	102	-0.52	-0.26	0.90	1.21
GC-3	112	-1.14	-0.39	1.30	1.24
GC-3	122	-0.96	-0.54	1.23	1.05
GC-3	127	-1.28	-0.87	1.44	1.40
GC-3	142	-0.97	-1.10	0.93	0.92
GC-3	152	-1.49	-0.98	1.11	1.45
GC-3	172	-1.85	-1.25	1.23	1.49
GC-3	182	-1.78	-1.10	1.28	1.48
GC-3	202	-1.73	-0.97	1.38	1.50

Table 4. 6. Down core oxygen and carbon isotope records of *U. peregrina* in GC-4.

Gravity Core	Depth interval (cm)	*U. peregrina* $\delta^{18}O$ (‰)	*U. peregrina* $\delta^{13}C$ (‰)
GC-4	2	1.03	-0.46
GC-4	6	1.29	-0.14
GC-4	10	1.27	-0.08
GC-4	14	1.15	-0.16
GC-4	18	1.07	-0.23
GC-4	22	1.02	-0.48
GC-4	27	0.81	-0.52
GC-4	37	1.12	-0.44
GC-4	62	1.78	-0.32
GC-4	72	1.66	-0.32
GC-4	82	1.67	-0.43
GC-4	92	1.61	-0.61
GC-4	117	1.24	-0.18
GC-4	127	1.40	-0.67
GC-4	137	1.47	-0.34
GC-4	152	1.77	-0.10
GC-4	207	1.37	-0.16
GC-4	222	1.61	-0.05
GC-4	242	1.76	-0.28

Table 4. 7 Carbon isotope records of the organic matter ($\delta^{13}C_{org}$) in GC-4.

Gravity Core	Depth interval (cm)	$\delta^{13}C_{org}$ (‰ PDB)
GC-4	2	-20.45
GC-4	6	-20.31
GC-4	10	-20.38
GC-4	14	-20.36
GC-4	18	-20.25
GC-4	30	-20.30
GC-4	45	-20.34
GC-4	55	-20.29
GC-4	65	-20.34
GC-4	75	-20.39
GC-4	85	-20.27
GC-4	95	-20.33
GC-4	110	-19.88
GC-4	120	-20.29
GC-4	130	-19.92
GC-4	140	-20.07
GC-4	155	-20.15
GC-4	175	-20.12
GC-4	195	-19.99
GC-4	210	-19.81
GC-4	225	-19.83
GC-4	245	-19.96
GC-4	265	-19.84
GC-4	285	-19.71
GC-4	305	-19.79

Table 4. 8 Down core oxygen and carbon isotope records of core GC-6.

Core No.	Depth (cm)	*G. ruber* $\delta^{18}O$ (‰ PDB)	*G. ruber* $\delta^{13}C$ (‰ PDB)
GC-6	2	-2.44	1.51
GC-6	6	-2.89	0.59
GC-6	10	-2.49	1.43
GC-6	13	-1.98	1.32
GC-6	16	-2.17	1.31
GC-6	22	-2.16	1.50
GC-6	27	-1.57	1.31
GC-6	32	-1.33	1.41
GC-6	42	-1.11	1.37
GC-6	52	-1.14	1.39
GC-6	67	-1.66	1.17
GC-6	77	-1.60	1.04
GC-6	82	-1.45	1.07
GC-6	92	-1.49	0.81
GC-6	107	-1.17	1.10
GC-6	117	-1.17	1.25
GC-6	122	-0.83	1.08
GC-6	132	-0.71	1.48
GC-6	142	-0.91	1.25
GC-6	152	-1.00	1.18
GC-6	172	-1.40	1.45
GC-6	192	-1.78	1.39
GC-6	207	-1.27	1.61
GC-6	222	-1.36	1.21
GC-6	237	-1.30	1.27
GC-6	252	-1.37	1.28
GC-6	272	-1.14	1.21
GC-6	292	-1.20	0.94

Chapter 5

Chapter 5

CLAY MINERAL VARIATIONS IN SEDIMENT CORES: PROXIES FOR LATE QUATERNARY MONSOONS

5. 1 INTRODUCTION

Clay minerals are the weathering products of rocks and soils and their composition largely depends on climate, geology and topography of the area. Once formed in weathering profiles, clay minerals are stable, carried away by transporting agents such as river, glacier and wind, and accumulate in sedimentary basins on land or in marine environment, i.e., continental margins and/or deep sea. Numerous studies have indicated the following: (a) Clay minerals in the marine environment are largely detrital (Biscaye, 1965); (b) There are no diagenetic effects in recent marine clays and therefore the provenance of different clay minerals can be identified (Grim, 1968); (c) Crystallinity of particular clay minerals can also be used as an evidence of climatic change (Jacobs and Heys, 1972); (d) As rainfall is the most controlling factor determining the leaching rates in weathering profiles, the composition of clay minerals in the sediments are useful indicators of palaeoclimatic conditions (Singer, 1984). Several workers have indicated that many other processes act on clay minerals simultaneously or immediately after reaching the marine environment, overlap and suppress the climate-induced differentiation of clay minerals. These processes include: size sorting of clay minerals during transportation (Whitehouse *et al.*, 1960; Gibbs, 1977), flocculation of certain clay minerals at lower salinities (Grim, 1968), selective deposition of clay minerals in relation to organo-mineral interactions (Degens and Ittekot, 1984), texture-related clay mineral variations (Maldonado and Stanley, 1981), dispersal of clay minerals due to the prevalence of regional and local currents (Kolla *et al.*, 1981; Naidu *et al.*, 1985), redistribution of settled clays during reworking and methods followed for sample preparation and quantitative clay mineral analyses (Biscaye, 1965; Pierce and Seigal, 1969). As a consequence of these factors, either selective transportation and deposition of clay minerals or mixing of clay minerals from different sources take place. It is

also possible that the distribution may not show distinctive variations to differentiate the climatic record, because changes in the relative abundance of an individual clay mineral may signify either an increase in that component, or a decrease in one or more of the other components. Therefore the interpretation of down core variations in clay mineral concentrations are difficult and clay mineral distribution alone in the stratigraphic record should be used with caution in interpreting the climatic record. Singer (1984) suggested that the information obtained on clay minerals should be used in combination with other climatic proxies.

Previous studies on clay mineral distribution in the surficial sediments of the Arabian Sea were mainly used to understand the provenance and transport pathways of fine-grained terrigenous sediments (e.g., Biscaye, 1965; Kolla *et al.*, 1976; 1981; Nair *et al.*, 1982a&b; Rao and Rao, 1995). Although a few studies were carried out on sediment cores to infer the palaeoclimatic conditions along the western margin of Arabian Sea (Sirocko *et al.*, 1991; Sirocko and Lange, 1991), no significant attempt has been made to study the same along the eastern Arabian Sea margin (western margin of India).

In this chapter, four gravity cores were analysed for clay mineral distributions. Although, these cores extend on the western margin of India over 5 degrees latitude (between Goa and Cochin), the depth at which the cores were collected (about 300 m) and the hinterland geology (predominantly Precambrian metamorphic rocks) are similar. Humid tropical climatic conditions exist in this area. Therefore, if the clay minerals are derived from a single source, the processes that dilute the climatic signals should be more or less same for all cores. Here the ratios of clay mineral assemblages were utilised rather than their relative abundance to interpret the climatic record. In this way the problem of mutual dilution can be eliminated (see Gingele, 1996; Gingele *et al.*, 1998). Most importantly, palaeoclimatic information derived from clay minerals has been correlated with that obtained from the oxygen isotope analyses of foraminifers and C_{org} variations in the core. So the interdisciplinary approach followed here helped to overcome the limitations using the clay minerals as climatic record.

Age assessment for all four cores is based on either ^{14}C (bulk carbonate) dating or $\delta^{18}O$ measurements on surface dwelling planktic foraminifers (*Globigerinoides ruber* and *Globigerinoides sacculifer*). Radiocarbon dating results on cores GC-4 and GC-2 are given in Chapter 3 (Table 3.1 & 3.2 of Chapter 3) and detailed oxygen isotope stratigraphy for the cores GC-5 and GC-3 are given in Chapter 4 (see Fig. 4.1 & Fig. 4.5).

5. 2 RESULTS

The major clay mineral groups present in all the sediment cores are: smectite (S), illite (I), kaolinite (K) and chlorite (C) (Fig. 5.1 - 5.2). Gibbsite (G) is also identified in two cores off southwest India (GC-5 & GC-4). The relative abundance of major clay minerals varied significantly within the core and among different cores. The down core variations of different clay mineral groups and the ratios of clay minerals such as K/C, S/I, C/I and Illite 5Å/Illite 10Å are shown in Tables 5.1 - 5.4 and depicted in Figures 5.3 - 5.6.

5. 2. 1 Sediment cores from the upper continental slope

Illite and kaolinite are the dominant clay minerals in the core off Cochin (GC-5) (Fig. 5.3). Illite content varies from 32.4 to 45.6% with relatively higher values towards the bottom of the core (Table 5.1). Kaolinite content varies between 22.5 and 32.2%. Smectite content is relatively low (6.8-11.4%), except at the core top (17.2%) and at around 100 cm interval (18%). Chlorite content remains uniform throughout the core, except a relatively high value (27.6%) at around 200 cm interval and low value (14.2%) around 100 cm interval. Gibbsite peaks are present in all X-ray diffractograms and prominent reflections are seen between 145 and 45 cm depth intervals (Fig. 5.1).

The K/C ratios vary between 0.81 and 2.1, with highest value at around ~100 cm (Table 5.1; Fig. 5.3). The S/I ratio varies from 0.05 to 0.55 with two maximas, one at ~100 cm and the other at the core top. The C/I ratio ranges between 0.36 and 0.61, with a minimum value at ~100 cm. Overall, the trend of K/C and S/I ratios is similar and C/I ratio is opposite to them.

Illite dominates over other clay minerals in a core off Mangalore (GC-4), and its values range between 36.9 and 46.8% (Table 5.2; Fig. 5.4). Kaolinite

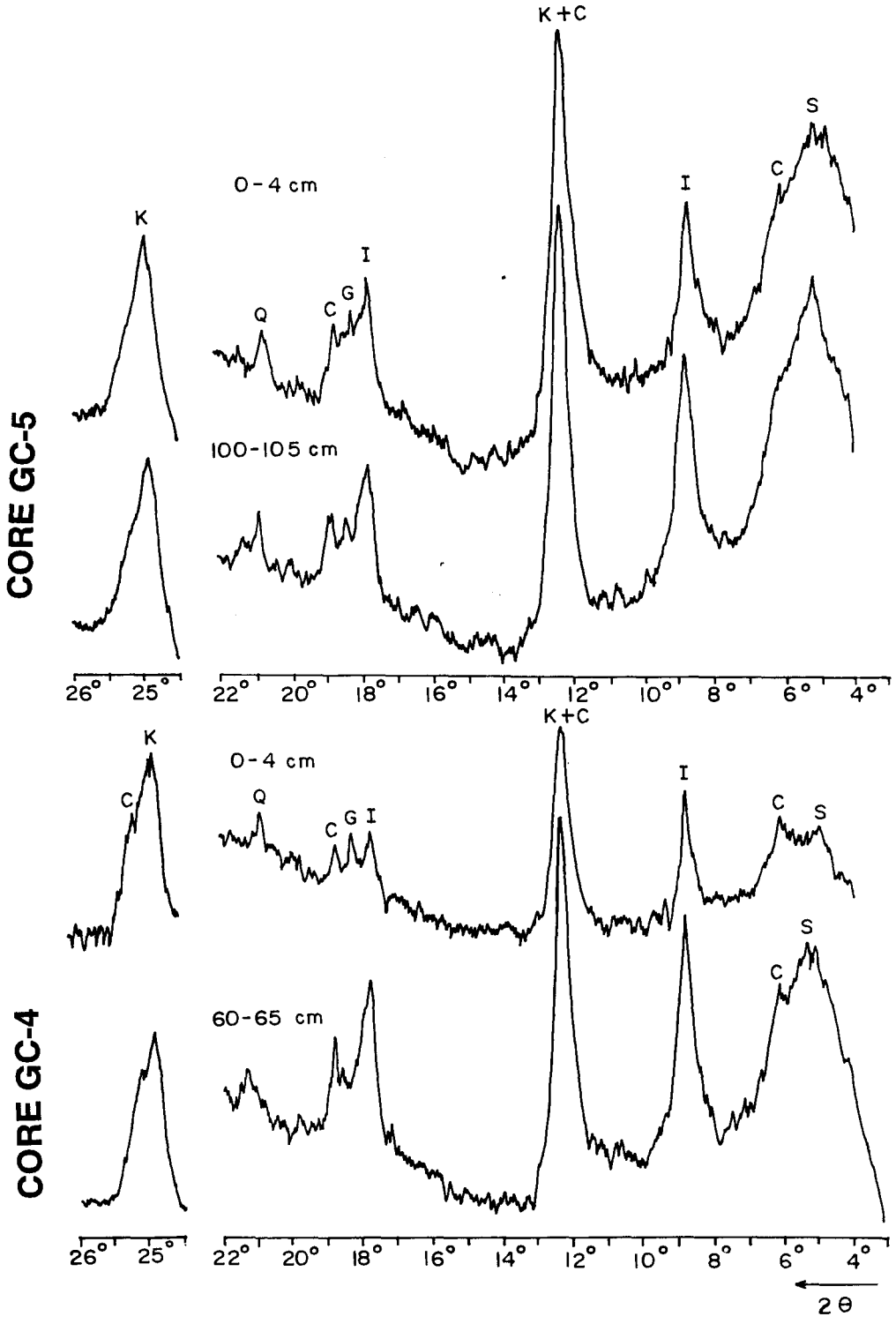

Fig. 5. 1 Representative X-ray diffractograms (glycolated) showing the presence of major clay minerals at two different depth intervals in cores GC-5 and GC-4 from the upper continental slope of India. S - smectite; I - illite; K - kaolinite; C - chlorite; G - gibbsite.

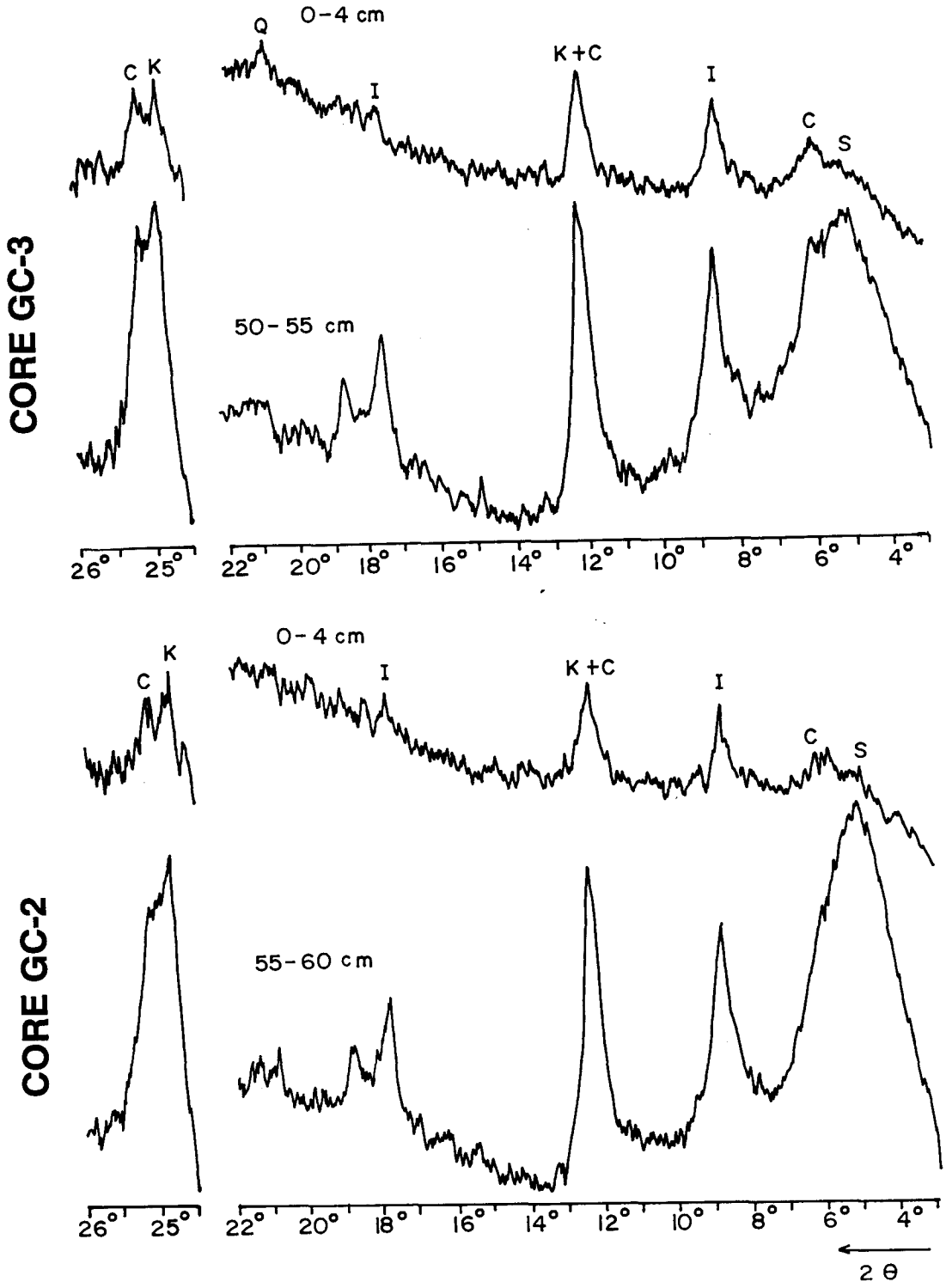

Fig. 5. 2 Representative X-ray diffractograms (glycolated) showing the presence of major clay minerals at two different depth intervals in cores GC-3 and GC-2 from the topographic highs off Goa. S - smectite; I - illite; K - kaolinite; C - chlorite; G - gibbsite.

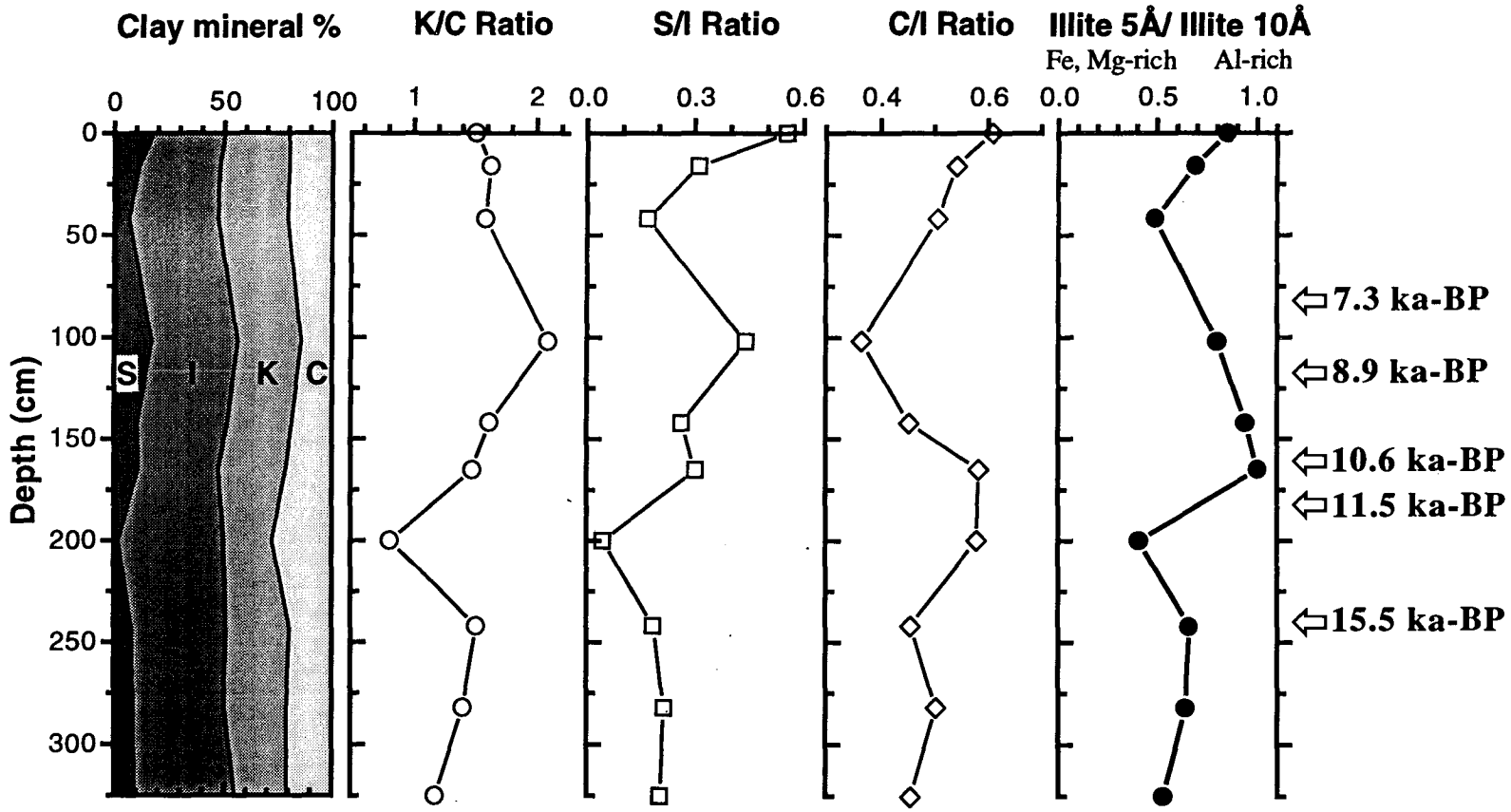

Fig. 5.3 Down core distribution of clay mineral abundances, clay mineral ratios and Illite 5Å/ Illite 10Å ratios in core GC-5. Age control points are based on the oxygen isotope stratigraphy of *G.ruber*. K - kaolinite; C - chlorite; S - smectite; I - illite.

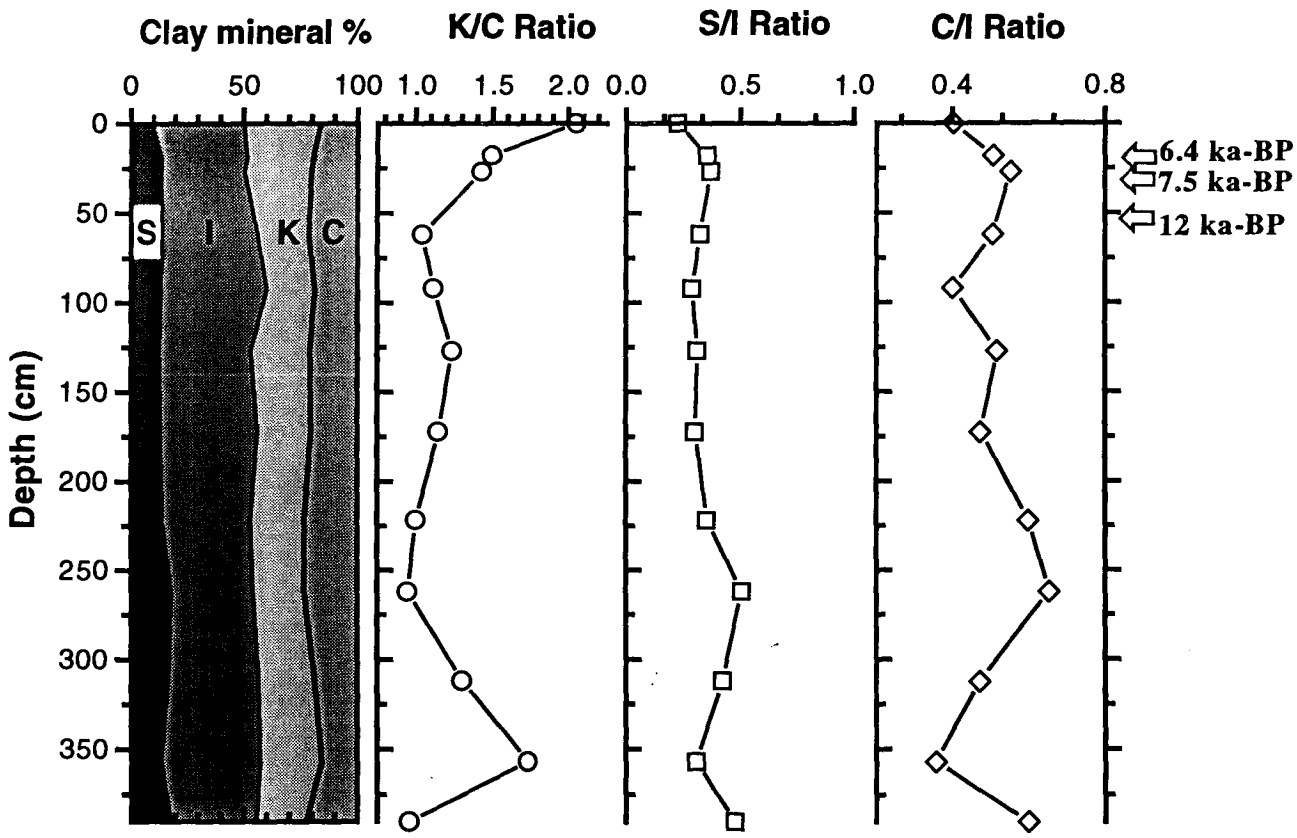

Fig. 5. 4 Down core variation of major clay mineral percentages and clay mineral ratios in core GC-4. Age control is by ^{14}C dates (arrows) on bulk carbonate. S - smectite; I - illite; K - kaolinite; C - chlorite.

values are highest at the core top (33.7%) and range between 21 and 33.7%. In contrast, the smectite content is low at the core top (9.2%) and its value is high at the bottom (18%). Chlorite content ranges between 23.6 and 16.4% and the trend is similar to that of smectite. The ratios of clay minerals indicate that K/C ratios show two maximas, one at ~360 cm interval and the other at the core top (Table 5.2; Fig. 5.4) and C/I ratio show variations exactly opposite to that of K/C. S/I ratios do not show significant down core fluctuations.

5. 2. 2 Sediment cores from the topographic highs

Illite is the most dominant clay mineral in these cores (GC-3 and GC-2) and its values are higher than in the cores of the upper slope (GC-5 and GC-4). Illite content varies from 38.1 to 58.3% in GC-3 (Table 5.3; Fig. 5.5). Kaolinite contents are lower (ranging between 6.8 and 20.5%) and smectite contents are higher, and values vary between 7.8 and 29.6% with higher values below the 20 cm interval. Chlorite content varies between 15.5 and 24.0%, and higher values correspond to low kaolinite concentrations. Gibbsite peaks are not observed in these cores (Fig. 5.2).

The K/C ratios fluctuated between 0.35 and 1.3, with higher values around 50 cm (1.3) and 330 cm (0.93) intervals and relatively lower values in between. S/I ratios also exhibit a similar trend, fluctuating between 0.15 and 0.78. Eventhough the C/I ratios showed only marginal variations, relatively higher values are obtained for 300-380 cm and ~110 cm intervals (Table 5.3; Fig. 5.5).

Highest concentrations of illite (range 41.7-62.7%) and lower concentration of smectite (5.9 - 6.9%) correspond to the upper portions of the sediments in core GC-2 (Table 5.4; Fig. 5.6). Smectite concentrations are relatively high (ranges between 14.2 and 22.2%) below this part. Chlorite content varies between 15.6 and 21.5% (Fig. 5.6). The K/C values varied between 0.61 and 1.04, with highest value at 10 cm interval. S/I and C/I ratios exhibit a low value around 10 cm interval and higher values around 50 cm interval (Table 5.4; Fig. 5.6).

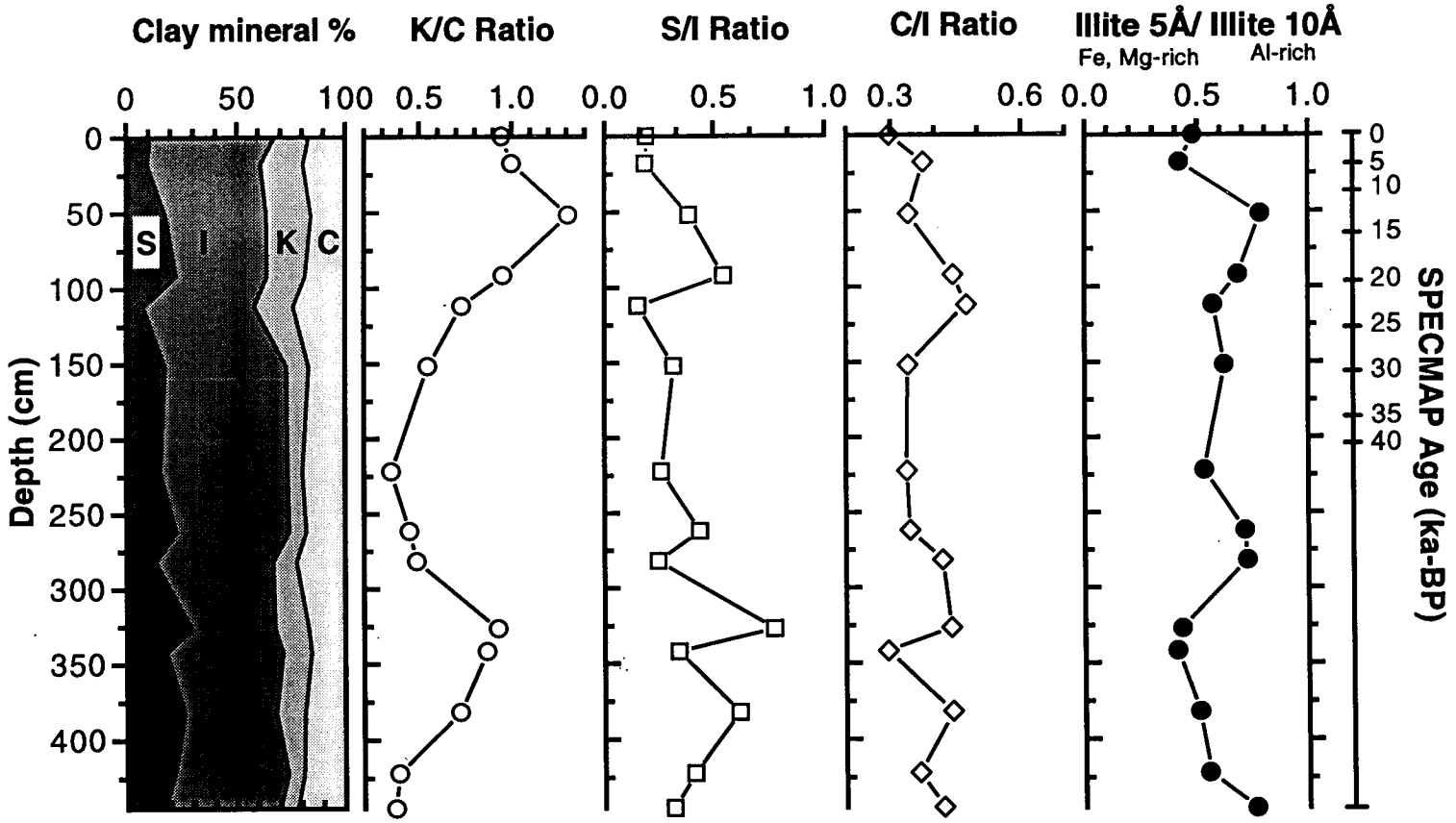

Fig. 5. 5 Down core variations in major clay mineral percentages, clay mineral ratios and illite chemistry in core GC-3. Age scale is based on the oxygen isotope stratigraphy of *G. sacculifer*. S - smectite; I - illite; K -kaolinite; C - chlorite.

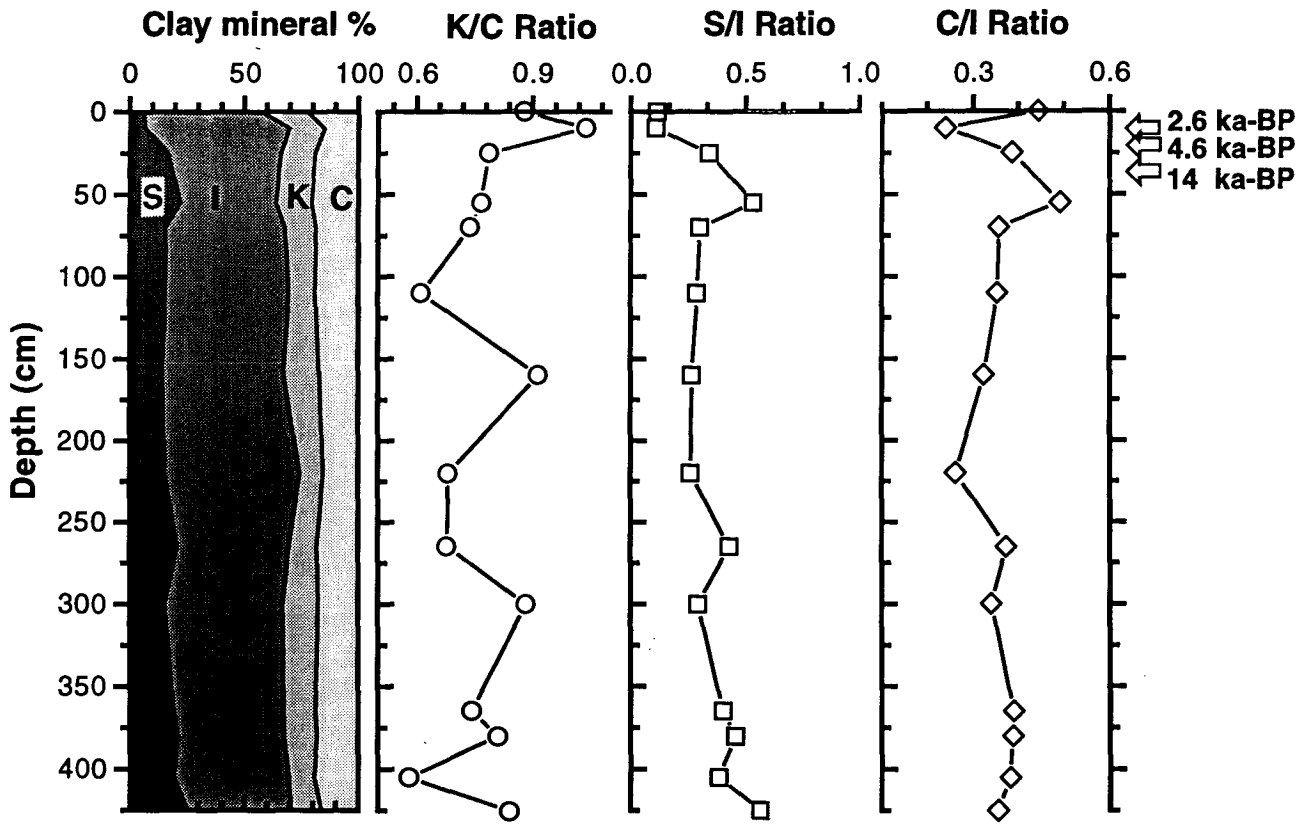

Fig. 5. 6 Down core variations in major clay mineral percentages and clay mineral ratios in core GC-2. Age control is by ^{14}C dates (arrows) on bulk carbonate.

5. 3 DISCUSSION

5. 3. 1 Provenance and transport pathways of clay minerals

River discharge and aeolian input are the two main processes, supplying the terrigenous material to the Arabian Sea (Sirocko and Lange, 1991). The Indus river constitutes the major fluvial source to the Arabian Sea (Kolla *et al.*, 1981). Rivers that drain the Peninsular India, like Narmada, Tapti and numerous other small rivers along the central and southwest coast of India, also contribute terrigenous flux to the eastern Arabian Sea. As these rivers drain different sedimentary terrains under different climatic conditions, the clay minerals brought by these rivers are also different. For example, the Indus originate in the Himalayas and carries the glacial (physical/mechanical) weathering products of Precambrian rocks and semi-arid to arid soils of Pakistan and NW India (Krishnan, 1968). Illite and chlorite are the major clay mineral assemblages in the Indus discharge (Nair *et al.*, 1982a; Konta, 1985). The Narmada and Tapti rivers drain basic volcanic rocks in the semi-arid conditions and several workers have reported smectite as an abundant clay mineral in the suspended and bed loads of these rivers (Subramanian, 1980; Naidu *et al.*, 1985). Humid climatic conditions prevail over peninsular India south of Tapti river and the hinterland geology is mostly basaltic in the northern part (north of Goa) and Precambrian gneissic rocks in the south (Goa to Cochin). Intense chemical weathering takes place in humid conditions, and the characteristic clay minerals are kaolinite and gibbsite.

Sirocko and Lange (1991) have showed that wind-borne dust loads act as major sources of clay mineral distribution in the western and central Arabian Sea. It originates from the deserts of Africa, Arabia and Mesopotamia by the northwesterly winds (the Shamal winds), which overrides the rain-bearing SW monsoon winds during the summer (Sirocko and Sarnthein, 1989). But its accumulation along the eastern Arabian Sea (western continental margin of India) is significantly less and fine grained river-borne sediments are abundant along this margin (Kolla *et al.*, 1981; Naidu *et al.*, 1985). Detailed clay mineral investigations on surficial sediments along the western continental margin of India (from Indus river mouth in the north to Cochin in the south), revealed that illite is mainly supplied by the river Indus (Rao and Rao, 1995). The Indus-borne clay minerals

are transported to the south of its source by a southerly surface current during the SW monsoon season (June-August). Hence the surficial sediments from the continental slope along the northwestern margin of India indicate a mixture of clay minerals from the Indus and from the Narmada and Tapti and dominance of illite over other clay minerals, eventhough its absolute abundance shows a decreasing trend from north to south (Rao and Wagle, 1997).

Illite concentrations in the cores from the topographic highs off Goa (up to 58.3% and 62.7% in GC-3 and GC-2, respectively) are higher than in the cores of the upper continental slope off southwest India (up to 47.7% in GC-5 and 46.7% in GC-4). This may indicate that either the sources of illite at these locations are different or physical processes may have favoured the sorting of these clay minerals and responsible for high illite content in the sediments of the topographic highs. Illite content in the inner shelf sediments between off Mangalore and Cochin is low, despite the fact that the hinterland geology is dominated by Precambrian gneissic rocks and heavy rainfall occur during the SW monsoon in this region (Rao and Rao, 1995). Obviously, illite reaching the outer shelf and upper slope would be low and cannot explain the high illite content on the topographic highs.

High illite contents on the topographic highs (at the core top samples) are associated with organic-rich (C_{org} content up to 8.7%), mud-dominated (~up to 97% silit and clay), sediments (see Fig. 3.6 & 3.7 of Chapter 3). Therefore, size sorting during transportation or reworking may not have taken place. The ratio of Illite 5Å/Illite 10Å in the core top sediments from topographic high, especially core GC-3 is low (0.48) (Table 5.3; Fig. 5.5). Relatively low values may indicate retaining of cations in its structure during the mechanical weathering process, leading towards more Fe, Mg-rich illites. In contrast, the ratios of Illite 5Å/Illite 10Å in the surface samples of core GC-5 are ~0.85, indicating an overwhelmingly Al-rich illites of alluvial nature (Table 5.1; Fig. 5.3). It could be that the illites derived from the hinterland may have undergone intense hydrolysis in the drainage area, resulting in stripping of cations from its structure and becoming Al-rich.

Slow scan X-ray diffractograms of kaolinite and chlorite clearly show that the chlorite is more in the surface sediments of the topographic high (Fig. 5.2), and kaolinite is more prominent and chlorite is indistinct in the surface sediments

of the cores from the upper slope off southwest India (Fig. 5.3). High chlorite content corresponds to high illite in the core top. These imply that the sources of illite and chlorite at the topographic highs are different from those in the cores from the upper slope. It is therefore, suggested that the clays from the topographic highs of Goa may have derived from the Indus discharge, transported by SW monsoon currents and accumulated on these highs.

Smectite values are relatively lower in the upper portions of the sediments in the cores of the topographic highs (GC-3 and GC-2; Fig. 5.5 & 5.6), compared to those in the sediment cores from the upper continental slope (GC-5 and GC-4; Fig. 5.3 & 5.4). The topographic highs are isolated features on the continental slope (see Fig. 3.1 of Chapter 3). As the sediments in the upper portions of the cores were accumulated during the Holocene transgression, it is likely that the clays transported from the hinterland of Penisnular India must have accumulated largely on the slope itself and little may have transported to the topographic highs. Moreover, high illite and chlorite in the sediments of the topographic highs (Fig. 5.2) support that these were derived from the Indus discharge. It is therefore likely that the smectite associated with them may have also been transported along with illite and chlorite or may have its source from the Narmada and Tapti river discharges. Rao and Rao (1995) reported that illite and chlorite are the most abundant clay minerals followed by minor smectite and kaolinite in the sediments of the Indus river.

The sediments in the lower portions of the cores correspond to lowered sea level. The sea level during LGM was at about 120 m below the present level (Fairbanks, 1989). As the shelf break in the study area occurs between ~110 and 120 m, the sediments transported by the rivers must have accumulated directly on the continental slope during LGM. Since high content of smectite occurs in the cores from the topographic high (Fig. 5.2) together with low illite and chlorite, it is suggested that the smectite must have derived from the discharge of Narmada and Tapti rivers. It implies that during the lowered sea levels, the fine-grained sediments accumulated on the topographic highs were a mixture of Indus and Narmada-Tapti river inputs.

Kaolinite constitutes up to 32.4% in GC-5 and up to 33.7% in GC-4 (Fig. 5.3 & 5.4) and are higher than that of topographic highs. Prominent gibbsite peaks

occur at all intervals in both the cores (Fig. 5.1). Kaolinite and gibbsite are characteristic chemical weathering products under tropical humid climate (Millot, 1970; Chamley, 1989). Precambrian gneissic rocks of the Western Ghats are capped by laterites at several places in the hinterland region of the study area (Krishnan, 1968). Moreover, kaolin deposits of the Warkala Formation outcrop near the southwest coast of India (Krishnan, 1968). Therefore the kaolinite and gibbsite on the continental slope indicate that these are transported by the dense network of mountain rivers draining the Western Ghats, which are fed by the strong SW monsoon rains. Nair (1975) reported high kaolinite content in the nearshore sediments and attributed its source to the kaolin deposits on land. Nair *et al.* (1982b) and Rao and Rao (1995) reported kaolinite and gibbsite on the continental shelf and upper slope and suggested the influence of source rock and cross shelf transport processes. The absence of gibbsite and low content of kaolinite in the cores of the topographic highs (GC-2 and GC-3) further suggest that the clay minerals derived from the hinterland are less significant than clay minerals brought by the SW monsoon currents.

5. 3. 2 Glacial-interglacial variations in the distribution of clay minerals

With the background knowledge on the sources and transport mechanisms of clay minerals and their regional distribution (Rao, 1989; Sirocko and Lange, 1991; Rao and Rao, 1995) and the distribution of clay minerals from the upper portions of cores as discussed above, the down core variations of clay minerals are used in interpreting the palaeoclimatic conditions of the Indian subcontinent during the late Quaternary. Since the lithogenic sedimentation along the western continental margin of India is mainly attributed to river runoff, the clay fraction should contain signatures of past monsoonal climate on land.

Since kaolinite is formed under warm humid conditions and chlorite under semi-arid to arid and cold climate, an increase in the ratio of kaolinite/chlorite (K/C) may indicate a prevalence of humid climate (Gingele, 1996). Illite forms under cold humid conditions and an increase in chlorite/illite (C/I) ratio would suggest an arid climate on land. As smectite is formed by intense chemical weathering of hinterland basaltic rocks under semi-arid conditions, increase in smectite/illite (S/I) ratio should also indicate increased precipitation on the

hinterland. Illite 5Å/Illite 10Å ratios provide another tool for the enhanced precipitation on land (see Gingele, 1996).

Clay mineral ratios thus obtained for all the cores were analysed on a chronological perspective, so as to identify monsoonal signals during the late Quaternary. It may be recalled that the sediments in the upper and lower portions of the cores from the topographic highs (GC-3 and GC-2) have their sources from Indus and Narmada-Tapti and Indus, respectively. These clays were transported to the site by longshore currents. As there are two sources of sediments involved, clear climatic signals are difficult to obtain from these cores. In addition, core GC-2 from the topographic high has limited chronological control, as indicated by sharp changes in age, lithology and other sedimentological parameters, suggesting a hiatus between ~14 and 4.6 ka-BP (see Table 3.2; Fig. 3.6). Reworking is evident in core GC-4 as indicated by spikes in sand, carbonate and organic content distribution (Fig. 3.3). Therefore down core clay mineral variations of core GC-5 from the upper continental slope, were mainly used for palaeoclimatic interpretations. Core GC-3 from the topographic high, which has a good chronological control, is also discussed where clay mineral assemblages from a single source reveal the climatic signals. Since chronostratigraphy in the cores is complete only for Stages 1 and 2, palaeoclimatic interpretations for the period between LGM and present interglacial are discussed here. For convenience, time intervals of ~18 to 12 ka-BP, 12 to 5 ka-BP and 5 to 0 ka-BP, are discussed separately below.

Between LGM (~18 ka-BP) and early Holocene (~12 ka-BP)

The down core variations of clay minerals in a core from the upper slope of southwest India (GC-5) indicate that both smectite and kaolinite contents are low during this period and illite is relatively high. The humidity indicators K/C and S/I ratios remained low with minimum values (0.81 and 0.58 respectively) around 200 cm interval, while the aridity indicator C/I ratio is high (0.58) during the same period (Fig. 5.3). Although illite is dominantly Al-rich throughout the core GC-5 (Illite 5Å/Illite 10Å ratios varies between 0.41 and 1.0), it tends to be more Fe, Mg-rich around this interval (Fig. 5.3).

In the core from topographic high off Goa (GC-3), kaolinite and illite contents remained relatively low during this period. Clay mineral proxies (K/C, S/I, C/I and Illite 5Å/Illite 10Å ratios) clearly suggests that the continental climate was dry with low terrigenous influx from rivers.

Downcore C_{org} variations and stable oxygen isotopes variations of foraminifers in cores GC-5 and GC-3 also support the above findings. For example, the $\delta^{18}O$ records of planktic foraminifers showed that glacial $\delta^{18}O$ values are significantly heavier than those of Holocene time and the LGM-Holocene $\delta^{18}O$ amplitude (up to 2.1‰) exceeds the global 'ice volume effect' substantially (see Chaper 4). The results suggest that during LGM, the precipitation over Arabian Sea and Indian subcontinent was minimum and/or the evaporation over Arabian Sea had increased, both indicating a weaker SW monsoon and prevalence of more arid conditions. The very low amount of C_{org} content in the glacial sediments compared to the Holocene sediments (Fig. 3.2) of these cores also suggest that the SW monsoon-induced productivity was low, transporting less C_{org} to the bottom sediments (see Chapter 3).

Several studies have suggested that during LGM, palaeoclimatic conditions on the monsoon domains of Asia differed markedly from the present one. The SW monsoon was very weak during the LGM due to the decreased solar insolation and increased land albedo (Prell *et al.*, 1980; Fontugne and Duplessy, 1986). The wide spread glaciation in the vicinity of Himalayas and Tibetan Plateau during this time must have lead to maximum snow and/or ice cover, and therefore maximum albedo. The enhanced albedo reduced the land to ocean sensible heating, resulting in a weakened monsoon circulation (Prell, 1984b). At ~18 ka-BP, the highly reflective ice sheets, generally cold oceans and equatorward advance of sea ice in both the hemispheres had a significant effect on the climate of the monsoon regions, eventhough the seasonal distribution of insolation at the top of the atmosphere was similar to that of today (Kutzbach and Street-Perrot, 1985). Evidences from numerous other studies (on palaeoclimate) such as lake level fluctuations in Africa (Street and Grove, 1979), stable isotope ratios on foraminifers and organic matter in Arabian Sea sediments (Duplessy, 1982; Fontugne and Duplessy, 1986), pollens from the marine sediments (van Campo,

1986) and climatic model simulation studies (Prell and Kutzbach, 1987), all point to a period of weak SW monsoon during LGM. Recent studies on $\delta^{13}C$ records on peats from the Nilgiri hills (which form a part of the Western Ghat mountain ranges from where most of the Peninsular rivers originate) have also indicated an arid phase during the LGM (Sukumar *et al.*, 1993; Rajagopalan *et al.*, 1997). The clay mineral data thus obtained for the Arabian Sea cores is consistent with the stable isotopic and C_{org} records of the same cores and are also in accordance with other palaeoclimatic data obtained from this region.

Between early to mid- Holocene (~12 - 5 ka-BP)

The clay mineral abundances and proxy ratios in both the cores from the upper slope (GC-5 and GC-4) reveal that there is a marked increase in smectite, kaolinite and decrease in chlorite content soon after ~12 ka-BP (Figs. 5.3 & 5.4). This trend towards more humid conditions is distinct in the GC-5 record. Here the K/C ratio increased from a value of 0.8 to 2.1 culminating at ~9 ka-BP (see Table 5.1). S/I ratio also showed a similar increasing trend and the C/I ratio showed a decreasing trend. The illite brought to the site was overwhelmingly Al-rich as indicated by the Illite 5Å/Illite 10Å ratios which increase up to 1.0 (Fig. 5. 3). Both proxies for humid conditions (K/C and S/I ratios) peak around ~9 ka-BP and showed a decreasing trend thereafter (Fig. 5.3). The arid indicator (C/I) showed a minimum value around the same period. The total clay content, which was generally low during the last glacial period, also increased dramatically during this period reaching a maximum value at ~9 ka-BP (see Fig. 3.2 of Chapter 3).

In the core of the topographic high off Goa (GC-3), K/C ratios (humidity indicator) are high (up to 1.31) during ~12 ka-BP and decreased thereafter. This again suggest an intensified monsoonal rainfall over the Indian subcontinent around 12-7 ka-BP.

The $\delta^{18}O$ records of planktic foraminifers in GC-5 and GC-3 cores showed a dramatic excursion towards more heavier values around ~9 ka-BP, suggesting local contributions of low saline water (hence more heavier $\delta^{18}O$ values) during this period (see Figs. 4.2 & 4.5 in Chapter 4). The $\delta^{13}C_{org}$ records of GC-5 also showed marked increase towards more negative values, indicating an increased terrigenous river input around this time (Fig. 4.4 in Chapter 4). These findings are

consistent with the clay mineral data and reveal that SW monsoon-induced rainfall peaked around ~9 ka-BP.

Both continental (lake levels, pollens, fluvial deposits) and marine (foraminiferal oxygen isotopes and pollens) records from the monsoon domains of Asia and Africa revealed that the intensity of the SW monsoon was maximum at about ~ 9 ka-BP, when the Northern Hemisphere insolation was at its maximum (Singh *et al.*, 1972; Street and Grove, 1979; van Campo *et al.*, 1982; Swain *et al.*, 1983; Williams and Clarke, 1984; Sirocko *et al.*, 1993). This period has been described as a very humid period with greatest abundance of monsoonal rains over Indian subcontinent (van Campo, 1986). Model simulation studies showed that at ~ 9 ka-BP, the precipitation around the Indian subcontinent was about ~ 0.75 cm/day compared to the modern value of ~ 0.5 cm/day (during summer), i.e., an increase of 50% (Kutzbach, 1981; Kutzbach and Street-Perrot, 1985). A strong humid phase with dominance of C_3 vegetation type was also reported at around ~9 ka-BP from the Nilgiri hills, based on the stable isotope ratios of tropical peats (Sukumar *et al.*, 1993; Rajagopalan *et al.*, 1997).

Between mid- Holocene and Present day (5 - 0 ka-BP)

Soon after the period of increased monsoons, both K/C, S/I and Illite 5Å/Illite 10Å ratios decreased to a minimum around 50 cm interval (~4.5 ka-BP) and C/I values increased in the core GC-5 from the upper slope (Fig. 5.3). This may be indicative of reduced monsoonal intensity in the Indian subcontinent after peaking around ~9 ka-BP. In core GC-5, the S/I ratios Illite 5Å/Illite 10Å ratios increased after this period again reaching a maximum value at the core top. K/C and C/I ratios do not exhibit this trend. The decrease in humidity conditions around ~4.5 ka-BP after the early to mid- Holocene peaking is also observed in core GC - 3.

The oxygen isotope records for cores GC-5 and GC-3 also reveal a climatic reversal around ~4.5 ka-BP and thus support the findings in clay mineral variations. Both core GC-5 and GC-3 show a significant drop in $\delta^{18}O$ values (>0.5‰) towards more negative values around 50 cm interval (corresponding to ~4.5 ka-BP), indicating a reduction in monsoonal intensity (see Chapter 4).

Pollen profiles from Rajasthan (Singh *et al.*, 1972), aggrading sedimentation records from Son valley (Williams and Clarke, 1984), monsoon upwelling records from the western Arabian Sea (Naidu, 1996) and stable isotope ratios of peats from Niligiris (Sukumar *et al.*, 1993; Rajagopalan *et al.*, 1997), showed similar weak monsoon conditions between ~4.5 and 2.5 ka-BP.

5. 4 CONCLUSIONS

1. Clay mineral studies on four sediment cores along the western continetal slope of India reveal that the detrital flux transported through rivers is the main process supplying lithogenic material to the sediments.
2. Illite and chlorite are the dominant clay minerals on the topographic highs and are apparently derived from the Indus discharge. Kaolinite and gibbsite associated clay minerals in the sediments of the cores from the upper continental slope indicate abundant detrital flux from the hinterlands of the Peninsular India.
3. Down core variations in clay mineral proxies reveal that the K/C (kaolinite/chlorite) and S/I (smectite/illite) ratios (humidity indicators) were low and the aridity indicator C/I (chlorite/illite) ratio was high during LGM. These indicate that the continental climate was dry and less amount of terrigenous material reached the Arabian Sea during this period.
4. Marked increase in K/C and S/I ratios and decrease in C/I ratio and abundant clay accumulation in the core GC-5 between ~12 and 5 ka-BP suggest intense humid conditions. Monsoonal intensity during this period was maximum, when the northern hemisphere summer insolation was at its maximum. The clay mineral proxies also indicate a late Holocene arid period around ~4.5 ka-BP.
5. The climatic variations deduced based on clay mineral proxies are in agreement with the interpretations based on $\delta^{18}O$ and C_{org} variations in the same cores and also with the climatic variations reported from the monsoon-dominated areas around the Arabian Sea and Indian subcontinent.

Table 5.1 Down core variations in major clay minerals in core GC-5.

Depth (cm)	Smectite (%)	Illite (%)	Kaolinite (%)	Chlorite (%)	S/I	K/C	C/I	Illite 5Å/ Illite 10Å
0	18.0	32.4	29.8	19.8	0.55	1.51	0.61	0.85
16	11.4	36.6	32.2	19.8	0.31	1.63	0.54	0.69
42	6.8	40.4	32.4	20.4	0.17	1.59	0.51	0.49
102	17.2	39.0	29.7	14.2	0.44	2.09	0.36	0.80
142	10.8	40.8	29.9	18.5	0.26	1.62	0.45	0.94
165	11.0	36.4	31.4	21.2	0.30	1.48	0.58	1.00
200	2.2	47.7	22.5	27.6	0.05	0.81	0.58	0.41
242	8.0	42.9	29.6	19.5	0.19	1.51	0.45	0.66
282	8.8	41.3	29.2	20.8	0.21	1.41	0.50	0.64
325	9.3	45.6	24.4	20.7	0.20	1.18	0.46	0.53

Table 5.2 Down core variations in major clay minerals in core GC-4.

Depth (cm)	Smectite (%)	Illite (%)	Kaolinite (%)	Chlorite (%)	S/I	K/C	C/I
0	9.2	40.8	33.7	16.4	0.23	2.05	0.40
18	13.5	38.1	29.0	19.4	0.35	1.49	0.51
27	13.6	36.9	29.1	20.4	0.37	1.43	0.55
62	13.7	42.4	22.4	21.5	0.32	1.04	0.51
92	13.5	46.8	21.0	18.8	0.29	1.12	0.40
127	12.7	40.5	25.9	21.0	0.31	1.23	0.52
172	13.1	43.0	23.5	20.4	0.30	1.15	0.48
222	13.9	39.2	23.5	23.5	0.35	1.00	0.60
262	18.1	36.0	22.3	23.6	0.50	0.95	0.65
312	16.8	39.9	24.5	18.8	0.42	1.30	0.47
357	13.5	43.7	27.1	15.6	0.31	1.74	0.36
390	18.0	37.7	21.7	22.6	0.48	0.96	0.60

Table 5.3 Down core variations in major clay minerals in core GC-3.

Depth (cm)	Smectite (%)	Illite (%)	Kaolinite (%)	Chlorite (%)	S/I	K/C	C/I	Illite 5Å/ Illite 10Å
0	10.9	56.5	15.9	16.8	0.19	0.95	0.30	0.48
18	09.7	51.6	19.4	19.4	0.19	1.00	0.38	0.42
52	17.9	46.0	20.5	15.6	0.39	1.31	0.34	0.78
92	22.7	41.4	17.5	18.4	0.55	0.95	0.44	0.68
112	07.8	50.7	17.5	24.0	0.15	0.73	0.47	0.57
152	17.7	55.4	10.3	18.7	0.32	0.55	0.34	0.62
222	15.3	58.3	06.8	19.6	0.26	0.35	0.34	0.53
262	22.6	51.6	08.0	17.8	0.44	0.45	0.34	0.71
282	13.2	53.4	10.9	22.5	0.25	0.49	0.42	0.72
327	29.6	38.1	15.5	16.8	0.78	0.93	0.44	0.43
342	18.2	52.9	13.4	15.5	0.34	0.86	0.29	0.41
382	26.0	42.0	13.4	18.6	0.62	0.72	0.44	0.51
422	21.6	52.0	07.4	19.1	0.42	0.39	0.37	0.55
445	16.9	52.7	08.2	22.2	0.32	0.37	0.42	0.76

Table 5.4 Down core clay mineralogical variations in core GC-2.

Depth (cm)	Smectite (%)	Illite (%)	Kaolinite (%)	Chlorite (%)	S/I	K/C	C/I
0	05.9	51.3	20	22.8	0.11	0.88	0.44
10	06.9	62.7	15.5	14.9	0.11	1.04	0.24
25	16.8	49.2	15.0	19.0	0.34	0.79	0.39
55	22.2	41.7	15.7	20.5	0.53	0.77	0.49
70	15.7	52.1	13.7	18.6	0.30	0.74	0.36
110	15.6	53.8	11.6	19.0	0.29	0.61	0.35
160	14.2	53	15.7	17.1	0.27	0.91	0.32
220	15.4	58.9	10.4	15.3	0.26	0.68	0.26
265	20.8	48.7	12.3	18.2	0.43	0.68	0.37
300	15.2	51.7	15.5	17.6	0.29	0.88	0.34
365	19.2	48.1	13.9	18.7	0.40	0.74	0.39
380	21.1	46.3	14.6	18.0	0.46	0.81	0.39
405	19.3	50.3	11.1	19.2	0.38	0.58	0.38
425	25.5	45.1	13.4	16.0	0.56	0.84	0.35

Chapter 6

Chapter 6

AUTHIGENIC GREEN CLAYS FROM THE SEDIMENTS OF THE WESTERN CONTINENTAL MARGIN OF INDIA

6. 1 INTRODUCTION

Authigenic green marine clays can be distinguished from the detrital clays by their colour, morphology, mineralogy and geochemistry. These clays are light to dark green in colour; unlike detrital clays, authigenic clays usually grow within the substrates (such as faecal pellets, microfossil tests, cavities or cleavage planes of the mineral grains) and thus are granular in habit. They are iron-rich and thus can be separated magnetically from the detrital clays. Authigenic clays are useful indicators of the distinct sedimentary environment at the time of their formation (Odin, 1988).

Prior to 1985, authigenic green grains occurring in recent marine sediments were mostly referred to as glauconite. Subsequently, Odin (1985) reported a new distinct authigenic green clay facies which has been named as 'verdine facies'. Verdine facies is the result of a synsedimentary interaction between sea water and deposited sediment, near an abundant source of iron (Odin, 1990). They generally occur at depths between 5 and 60 m in the Quaternary marine sediments of the tropical oceans as infillings in microtest chambers, replacement of faecal pellets and replacement of mineral debris. It has been reported to occur only from fifteen locations in the tropical oceans of the world (Odin, 1985, 1988, 1990; Odin *et al.*, 1989; Rao *et al.*, 1993, 1995). Of these, 10 are from the Atlantic, 3 Indian and 2 western Pacific Oceans. Except the verdine from Miocene sediments of the Niger delta, all other occurrences are from recent marine sediments <15 ka-BP (Odin, 1988).

Verdine facies is characterised by a variety of green clay minerals which are different from those present in the glaucony facies as well as ironstone facies (Odin, 1985). Phyllite V and phyllite C are the two mineral phases of the verdine facies. Phyllite V is a ferric-magnesian dioctahedral-trioctahedral 1:1 clay mineral

which has been recently designated as 'odinite' (Bailey, 1988). Phyllite C has an intermediate structure between smectite and swelling chlorite (Odin, 1990).

Minerals belonging to the glaucony facies are widespread and form in areas of low sedimentation rates under suboxic to anoxic conditions and mostly at depths between 60-1000 m. Eventhough glaucony facies occur in diverse forms, the most common habit is granular. A potassium-poor glauconitic smectite is the one end member of this facies and glauconitic mica constitutes the other end member. Glauconitic smectite forms first and with continued recrystallisation, it transforms into potassium-rich glauconitic mica which require comparatively longer time (10^5 - 10^6 years) (Odin and Matter, 1981). As the verdine facies is replaced by glaucony at greater depths, their distribution can be used for the reconstruction of paleogeography of the margins.

Mallik *et al.* (1976) and Thrivikramji and Machado (1982) reported the occurrence of green grains (internal moulds of microfossils) at a few locations at depths <50 m on the continental shelf of the western India and referred to them as glauconite. Subsequently, Rao *et al.* (1993) made detailed studies on the distribution of verdine and glaucony facies on the Kerala continental shelf and slope. In this chapter, the mineralogy and geochemistry of the green grain facies is reported from a larger region i.e., between Ratnagiri and Cape Comorin on the westem continental margin of India, which represents one of the largest verdine bearing basins in the world associated with low fluvial inputs and nearly equal to that off the Amazon river mouth.

6. 2 RESULTS

6. 2. 1 Nature and distribution of green grains

Detailed sample locations in the study area are given in Figures 6.1 & 6.2 and Table 6.1. Of the 198 samples studied, 112 showed the presence of green pigment (Fig. 6.3). The content of green grains in the coarse fraction varies from 1.9 to 56% (Table 6.1; Fig. 6.4). The higher percentages (~23 to 56%) of green grains are found diametrically opposite the Periyar, Ponnani, Netravati, Mandovi-Zuari and other river mouths (Fig. 6.3; Table 6.1). Green grains are either absent or present in very low quantity in clayey sediments of the inner shelf. They are less

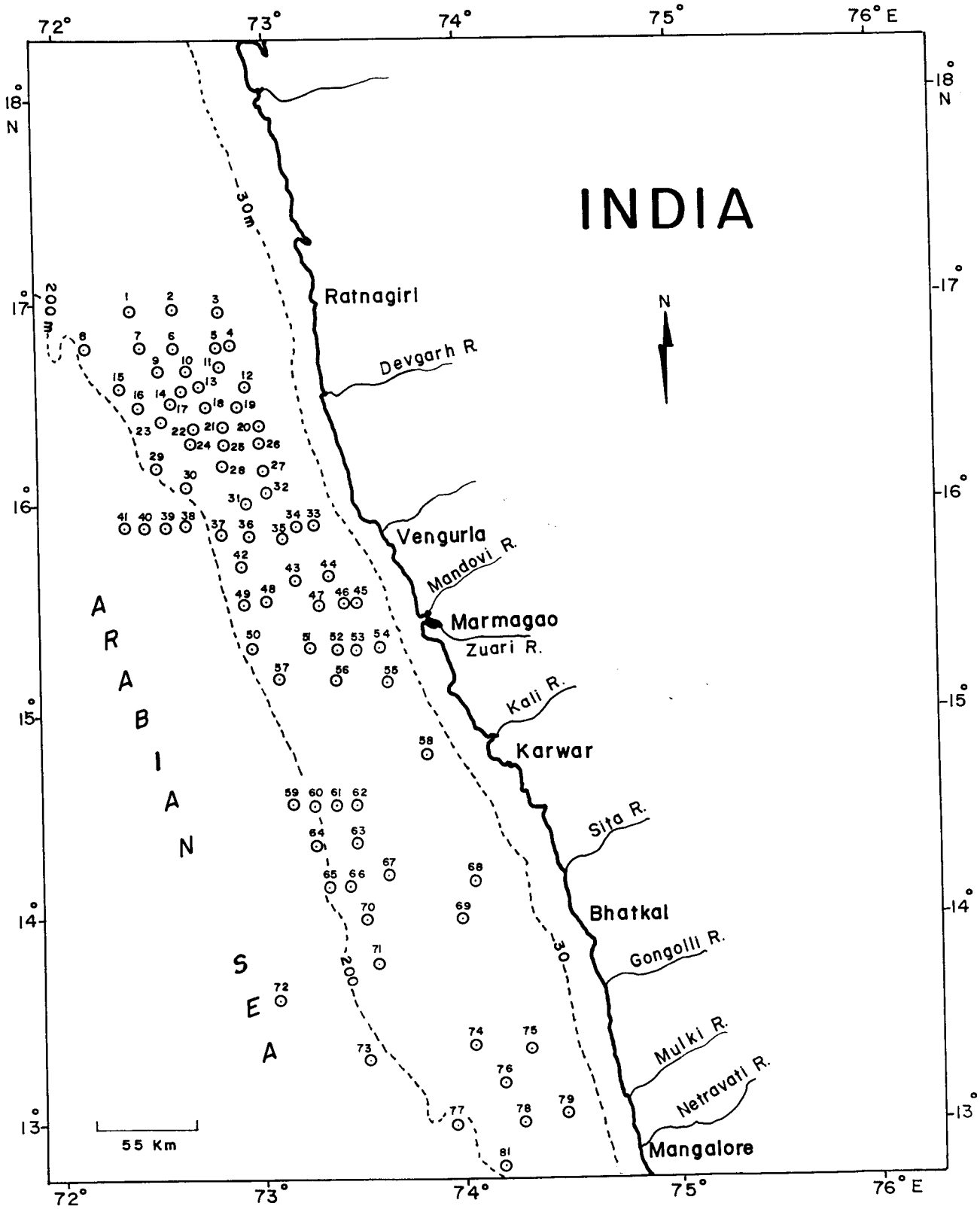

Fig. 6. 1 Detailed sample location map - between Ratnagiri and Mangalore. Orginal sample numbers are coded (see Table 6.1).

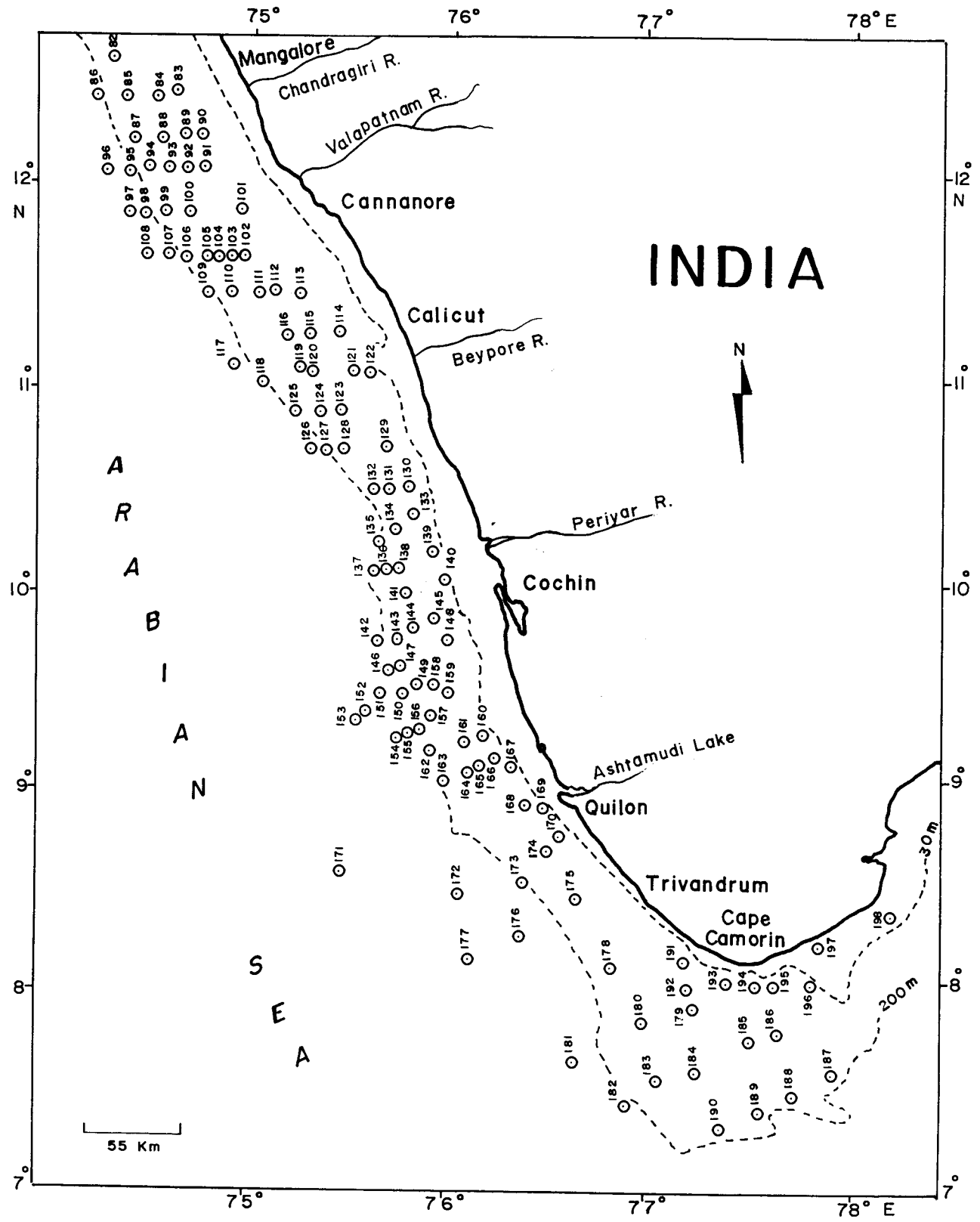

Fig. 6. 2 Detailed sample location map - between Mangalore and Cape Comorin. (see Table 6.1 for original sample numbers).

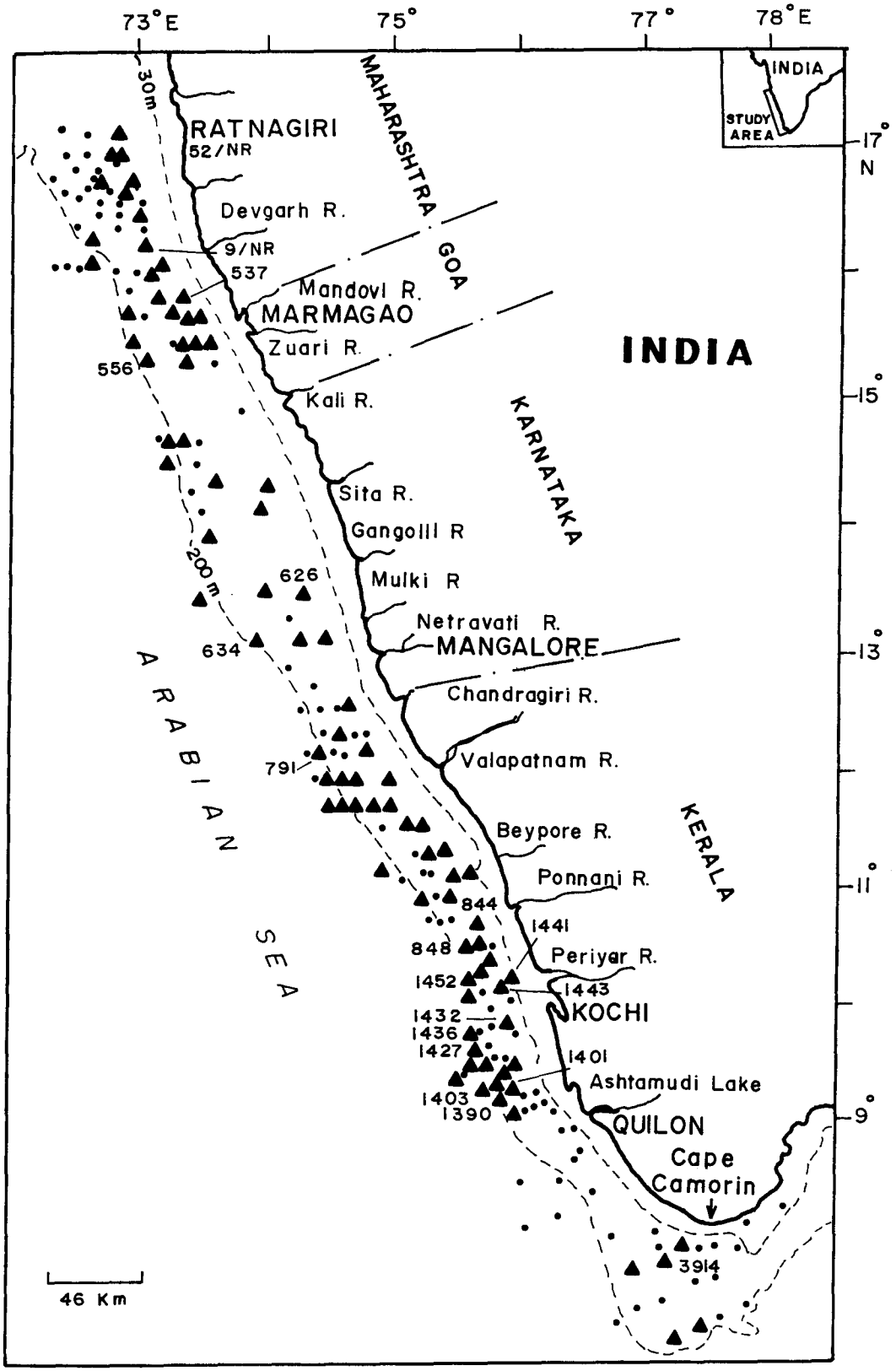

Fig. 6. 3 Sample location map (combined). Triangles indicate the samples which contain more than 5% green grains in the coarse fraction. Original station numbers are given for those samples that were used for detailed mineralogy and geochemistry.

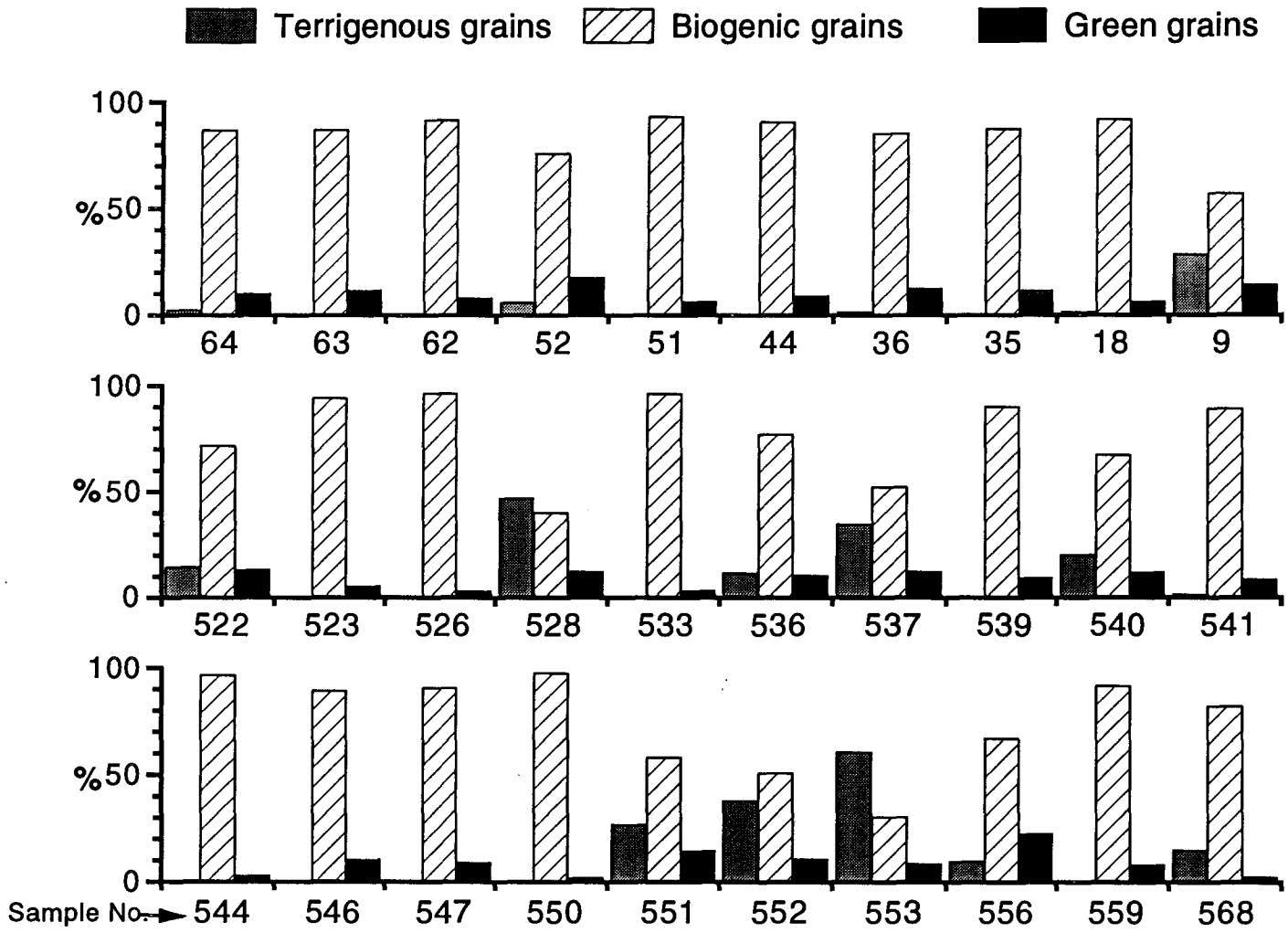

Fig. 6. 4 Percentage distribution of various components in the coarse fraction (125-250 μm) of the sediments. Sample number 1441 is not shown due to format problem. For sample details see Table 6.1.

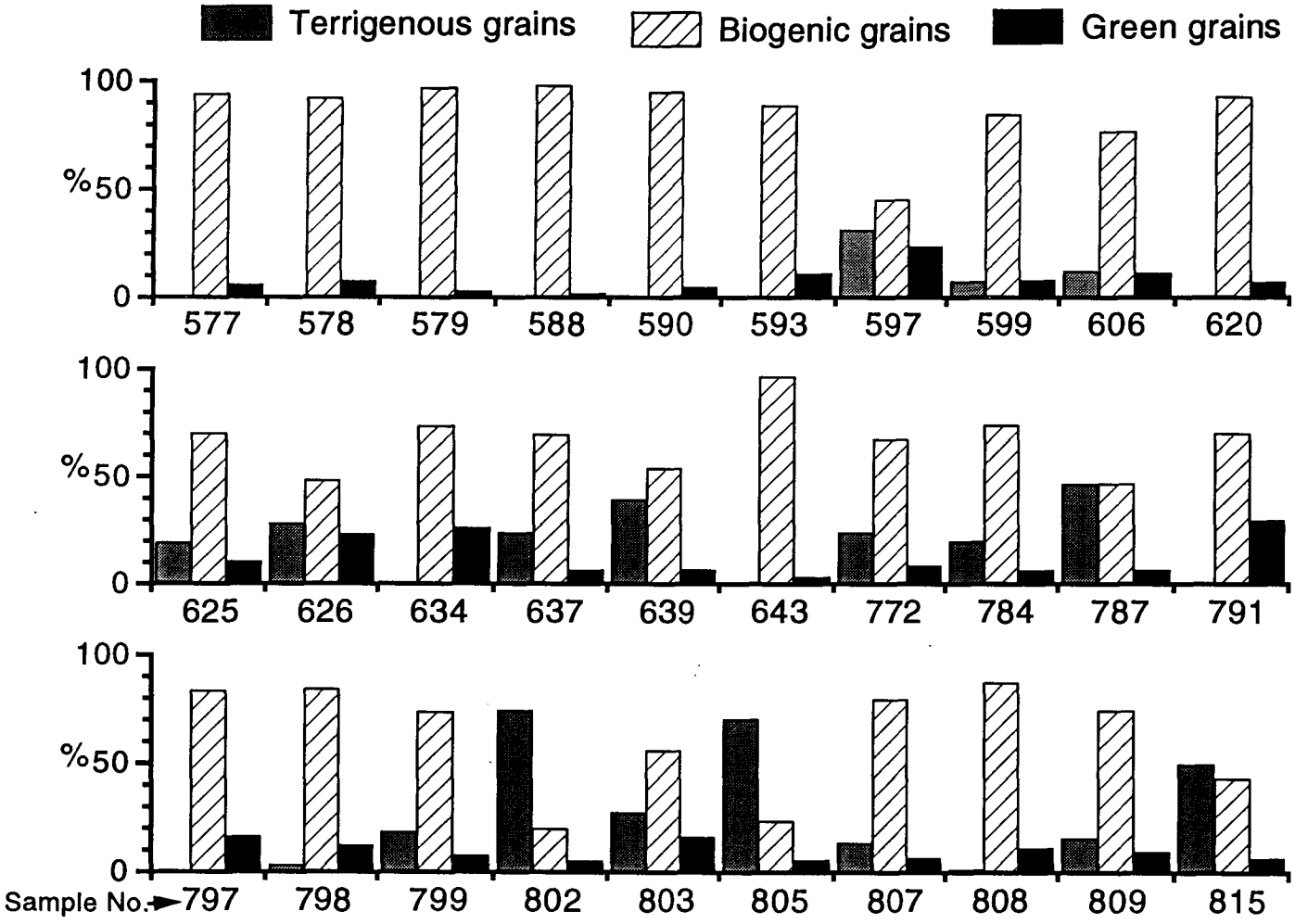

Fig. 6. 4 continued....

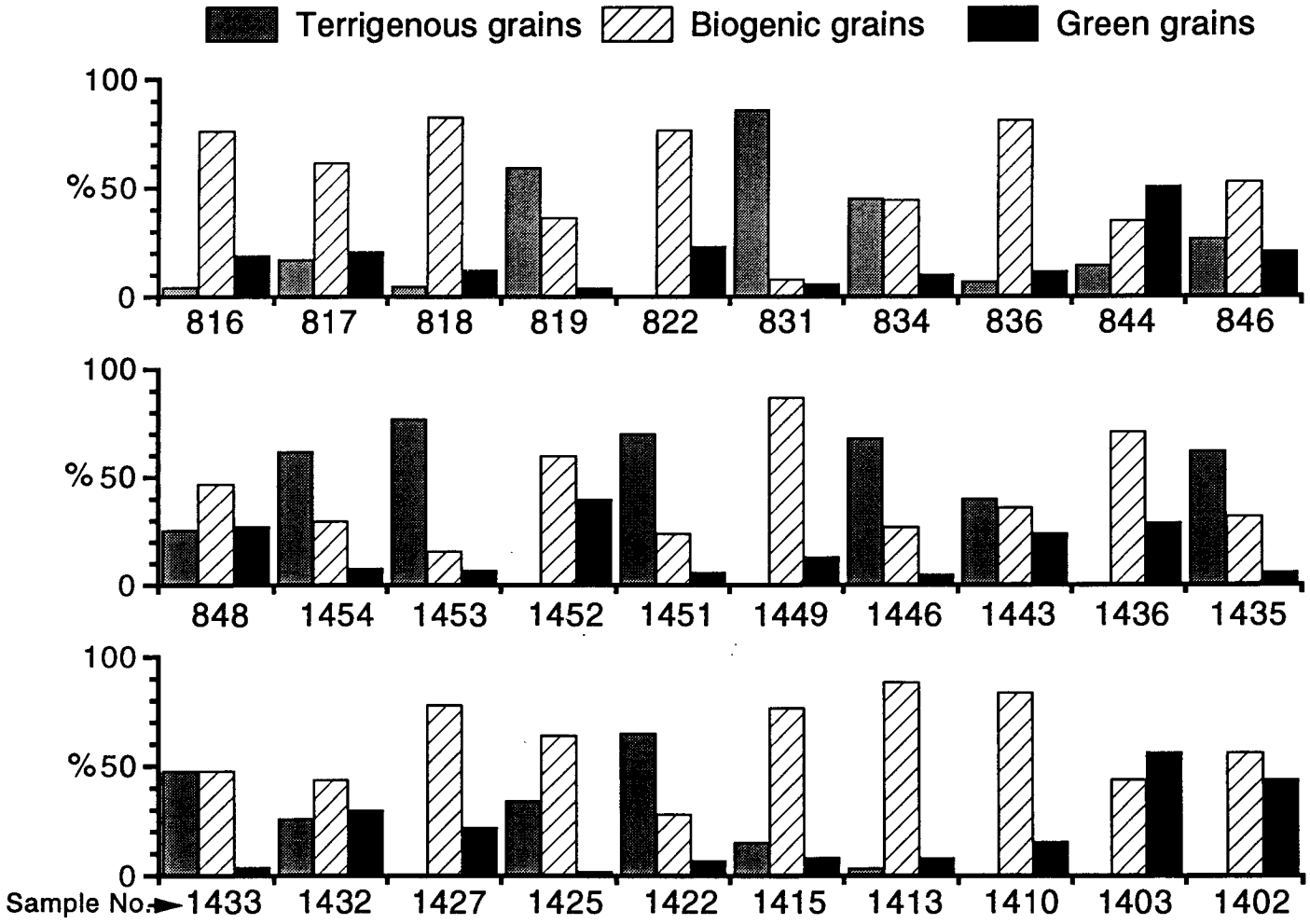

Fig. 6. 4 continued....

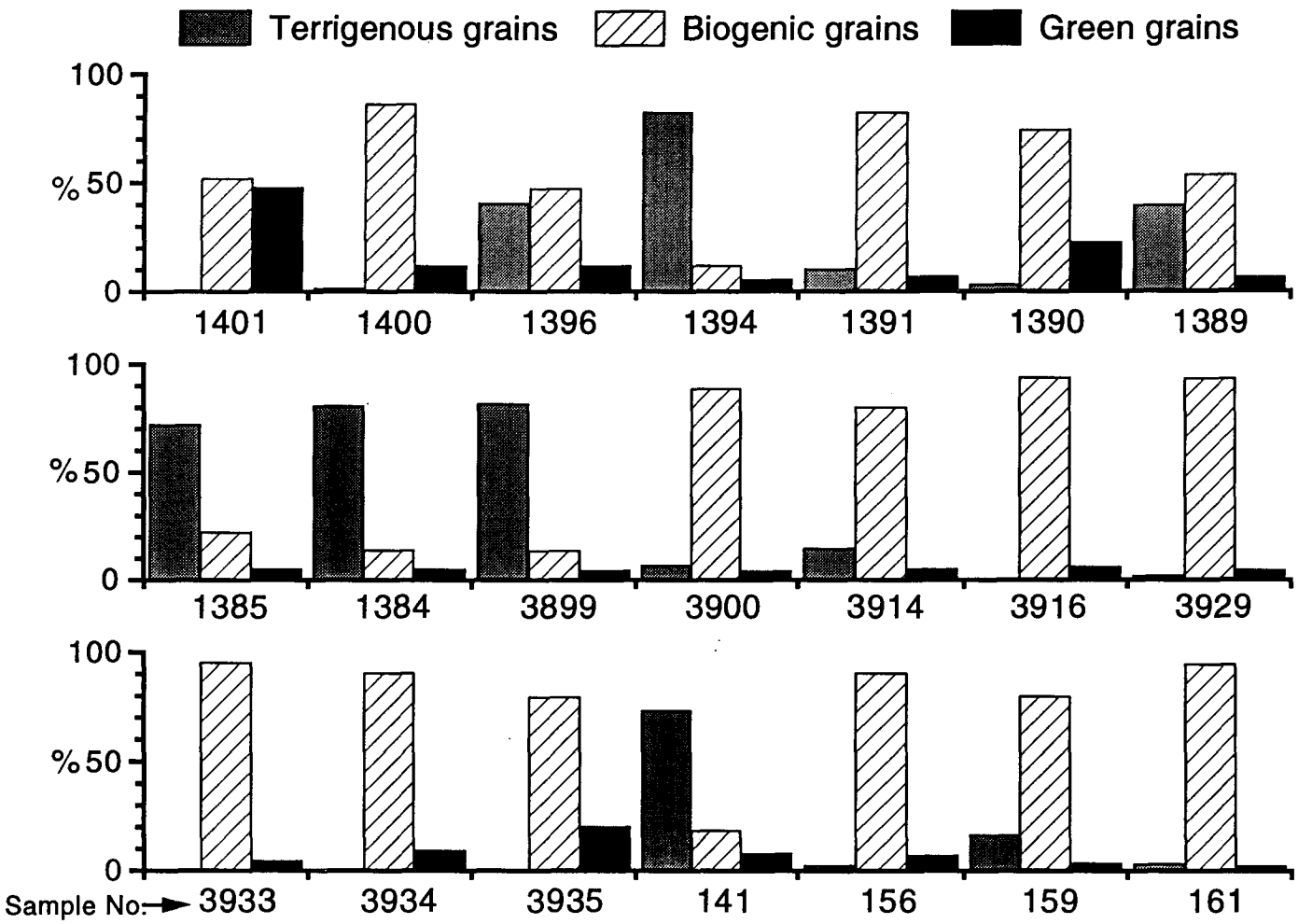

Fig. 6. 4 continued....

abundant (< 8%) in the terrigenous sand-dominated sediments and abundant (up to 56%) in bioclast-dominated sediments. In general, the green grain facies covers larger area on the continental shelf and slope of Kerala than that of Karnataka, Goa and Maharashtra (see Fig. 6.3). During magnetic separation, higher amount of heavy minerals were also obtained along with green grains from the shelf sediments of the southern tip of India.

The green grains occur in three morphologies: i). irregular free grains, ii). glossy and rough surface-textured faecal pellets, and iii). infillings and internal moulds of predominant microfossils (Fig. 6.5). Colour of the grains vary from dark green to light dull green to even brown ochre. On the shelf, irregular dark green grains with cracked outer surfaces are predominant and infillings and moulds are rare (Fig. 6.5; Table 6.2). Associated sediment components include quartz grains, shell fragments, foraminifers and ostracodes which are sometimes stained. Highly polished brown (ochre) pellets occur on the shelf (at 49 m depth) off the southern tip of India (G-167/ 3914); even irregular grains show highly smoothened surfaces. Abundant mollusc fragments and benthic foraminifers followed by quartz (stained) and heavy minerals, are associated with them (Table 6.2).

The green grains from the upper continental slope at depths between 100 m and 235 m are mostly dark green pellets and internal moulds of microfossils; irregular free grains are rare. Moulds are also dark green in colour and shiny in nature. Green grains mostly occur as infillings of foraminifers at depths >280 m. The outer tests of many green grains are still intact and appear light to pale green in colour; when the outer tests are removed, the green pigment is found to be dark in colour.

6. 2. 2 Mineralogy of the green grains

Based on the geographic location, depth and availability of sufficient material, 19 samples were selected for detailed X-ray diffraction studies. Both oriented and unoriented slides were analysed. The peaks were, however, at the noise level in unoriented slides. The peaks are slightly better in oriented slides which were used throughout the study. In order to avoid repetition and to restrict the number of illustrations, only important and representative X-ray diffractograms

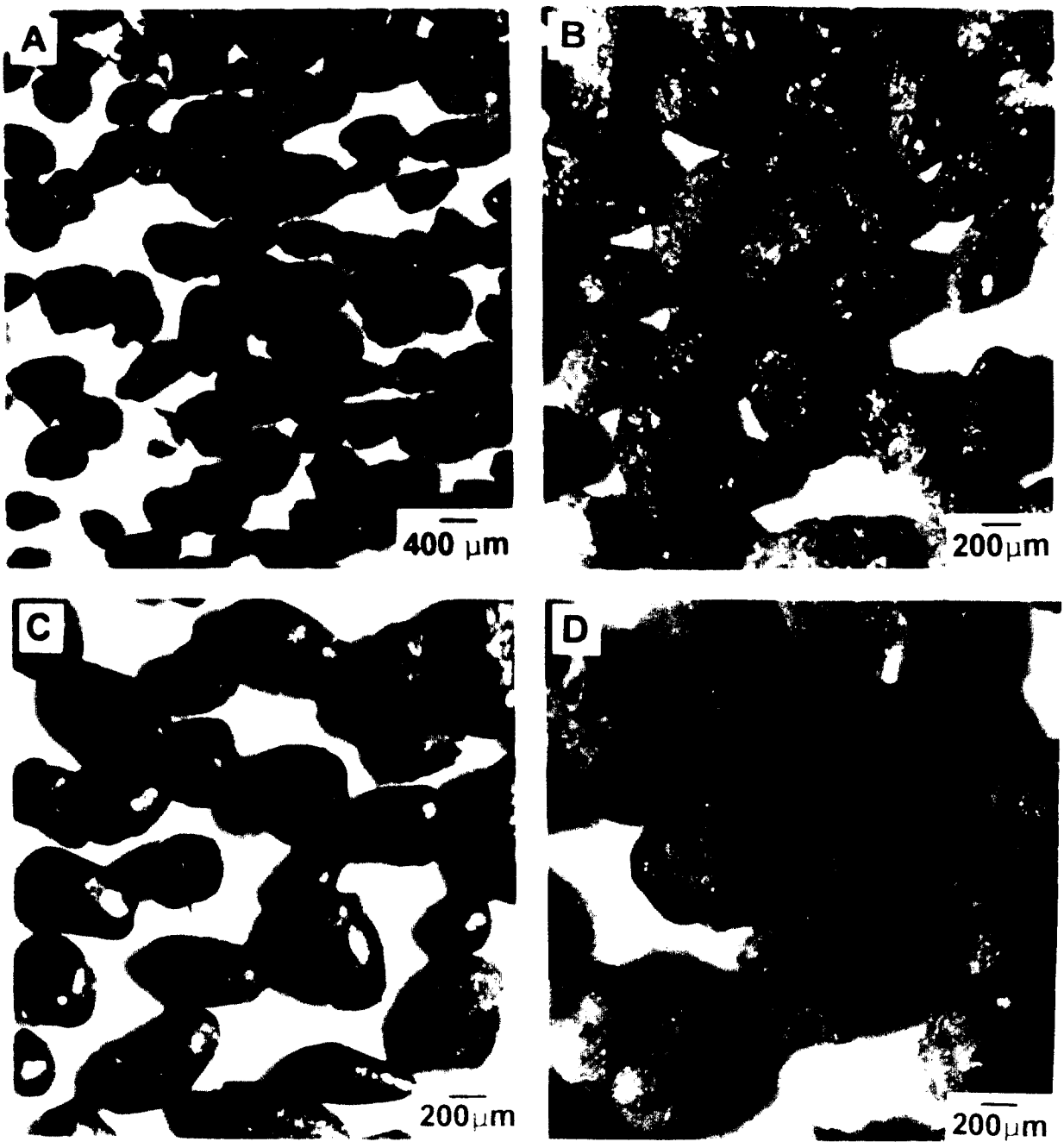

Fig. 6.5 Characteristic morphology of the green grains. (A). Irregular dark grains from the shelf; (B). Light green rugose pellets from the slope; (C). Dark green glossy pellets from the slope; (D). Green infillings and moulds from the deeper terrace.

of the green grains from the inner and outer continental shelf and upper continental slope are illustrated in Figures 6.6 - 6.12.

Green grains from the continental shelf

X-ray diffractograms of the untreated samples (irregular dark green grains) at 62-65 m water depth off Ratnagiri (NR-2A/52) exhibit a very large 14Å peak and a small dome around 7Å (Fig. 6.6). During glycolation, the 14Å peak was shifted to around 16Å. Acetic acid treatment reduces 7Å peak and marginally enhances the peak at 14Å. During heat treatment, the peaks were initially lowered (at 250°C/1 hour) and a large dome developed around 10Å (at 490°C/2 hours), which stayed there, even after heating the sample at 600°C for 4 hours. The large 14Å peak in the untreated X-ray diffractograms, its shifting to higher d- spacing during ethylene glycol solvation and its behaviour on heat treatment confirm the typical properties of phyllite C. When compared with detrital clay X-ray diffractograms from the same region (see Fig. 6.7D), the 7Å and 14Å reflections of the authigenic clays were broad and poorly crystalline region (see Fig. 6.7C), may be due to mixture of authigenic and detrital clay minerals and/or immaturity of the authigenic clay.

Irregular dark grains occurring at two stations (G-71/ 1441 and G-71/ 1443) at about 40 m depth were also analysed (see Fig. 6.3). Phyllite C is found to be the verdine mineral and is identical to that of Rao *et al.* (1993) reported from a nearby station (G-71/ 1432) (see Fig. 6.7 A). Comparison of authigenic clay and detrital clay X-ray diffractograms (Fig. 6.7A&B) suggests that the larger 7Å peak in green grains may be due to some kaolinite inherited from the substrate.

Irregular dark green grains also occur on the outer continental shelf off Karnataka, Goa and Maharashtra (see Fig. 6.3; Table 6.2) at depths between 42 m and 75 m and the X-ray diffractograms are distinctly different from that of the authigenic mineral phase discussed above. The X- ray diffractograms of the green grains from six stations reveal a large 7Å peak and a small dome around 14Å (Fig. 6.8A&B). Ethylene glycol treatment had no significant effect on these peaks. However, acetic acid treatment lowered 7Å peak and enhanced the peak at 14Å. Both peaks were distroyed after heating the samples to 250°C/1 hour. A peak at about 10Å appears in glycolated and acetic acid treated samples. The behaviour of the green grains differ from sample to sample on heat treatment at higher

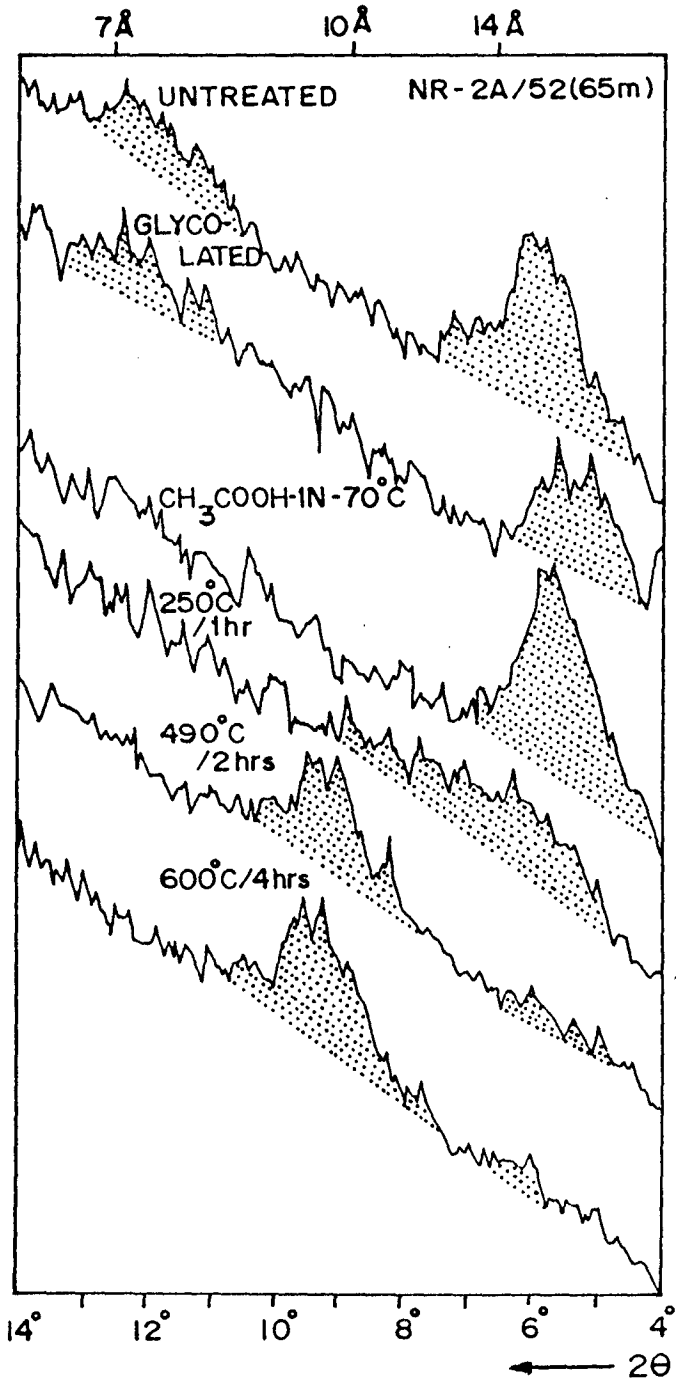

Fig. 6. 6 X-ray diffractograms of the irregular dark green grains from the inner continental shelf off Ratnagiri. Shaded portions are probable areas of authigenic clay reflections.

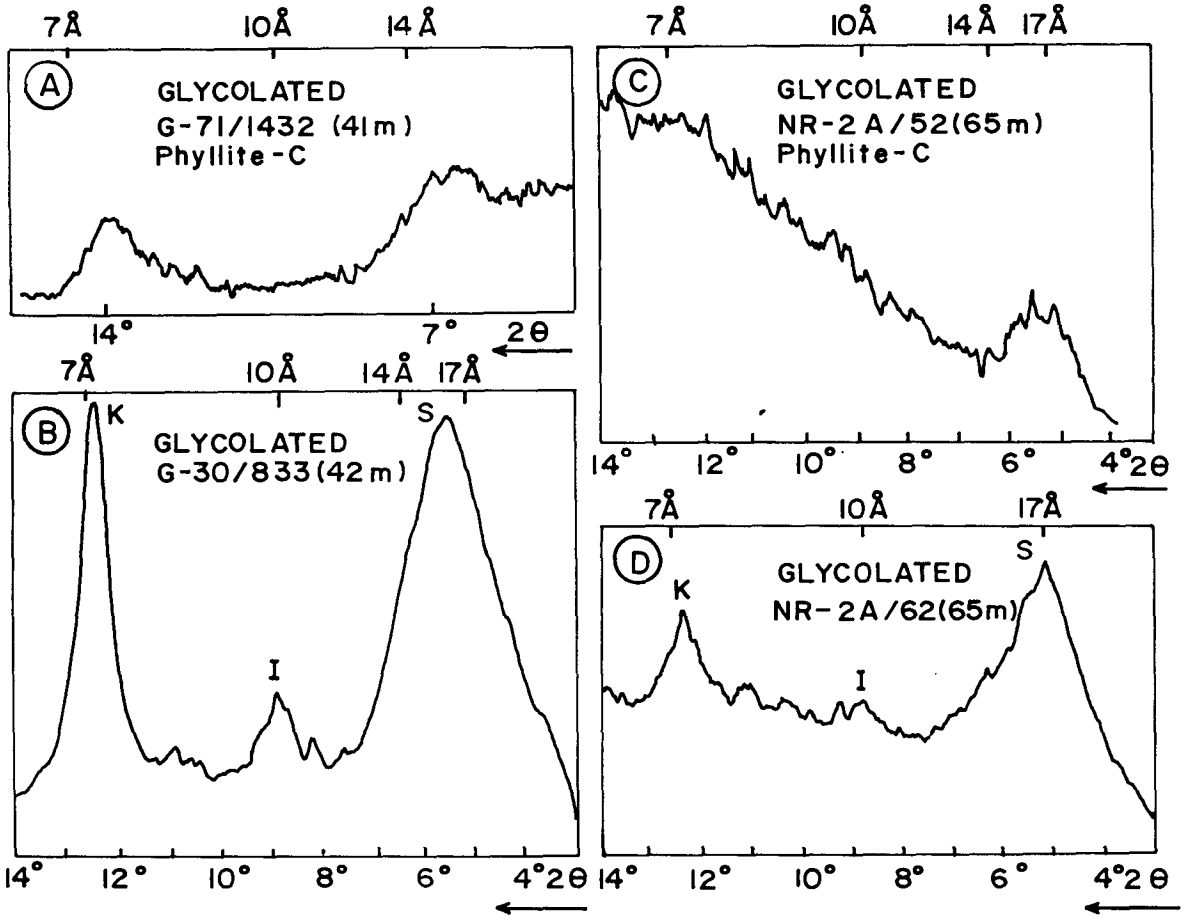

Fig. 6. 7 Representative X-ray diffractograms of authigenic green grains (A & C) and detrital clays (B & D) (in the vicinity of green grains) on the continental shelf (see Fig. 6.3 for location). S- Smectite; I- Illite and K- Kaolinite.

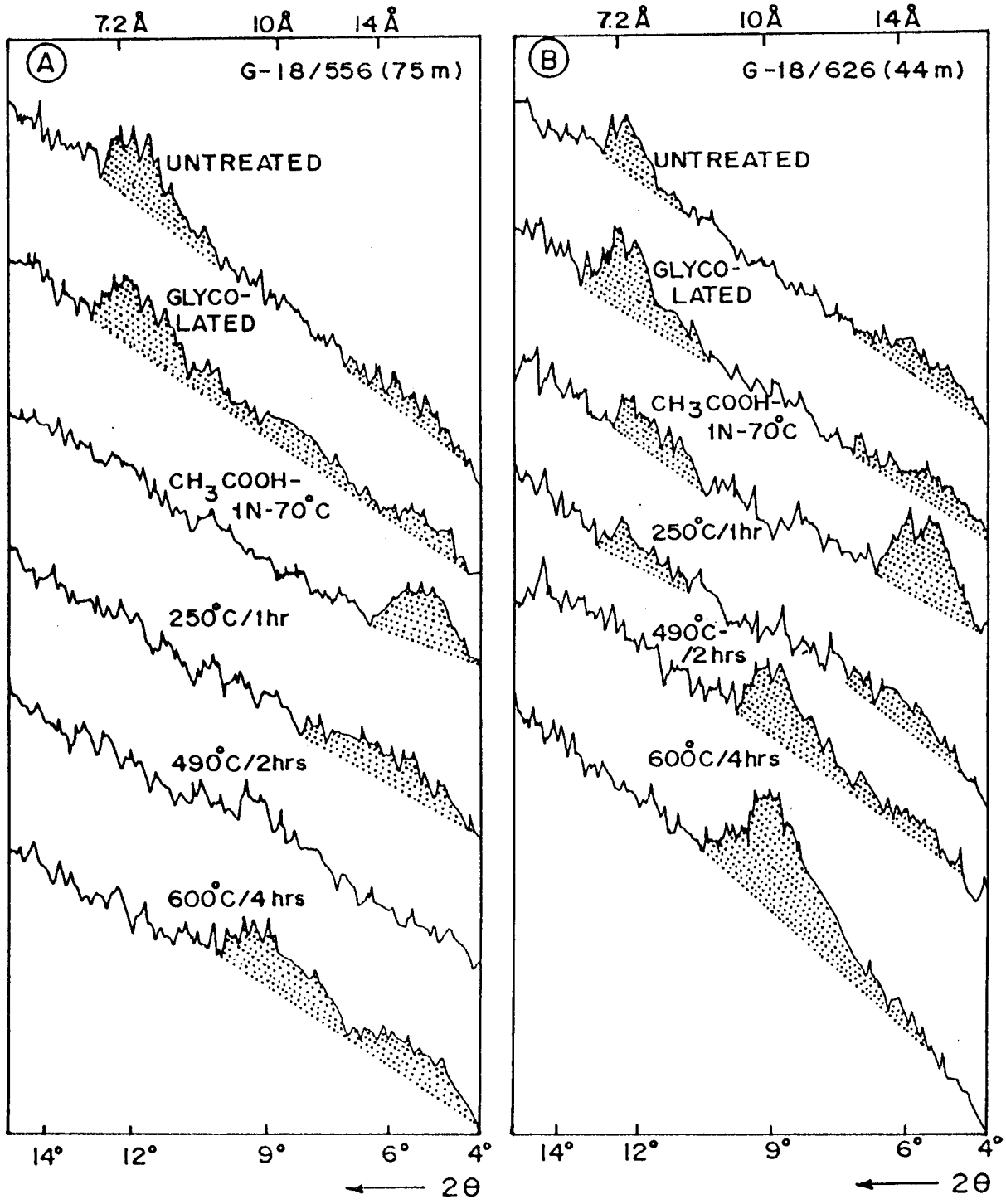

Fig. 6. 8 X-ray diffractograms of the irregular dark green grains from the outer shelf off: (A). Goa (556); and (B). Karnataka (626).

temperatures. In some samples (see sample 556 - Fig. 6.8A), the 14Å peak was slightly enhanced at 490°C/2 hours and, a portion of it shifted towards lower d-spacing with a broad dome at about 10Å at 600°C/4 hours. While in others (see sample 626 - Fig. 6.8B), the 14Å peak was completely collapsed and a broad dome was developed at around 10Å (to 490°C/2 hours) which intensified on further heating (at 600°C/4 hours).

Smectite and kaolinite are the dominant detrital clay minerals in the surficial sediments of this region (Rao and Rao, 1995). The properties of smectite (expansion of 15Å reflection on glycolation and its collapse to 10Å on heat treatment at relatively low temperatures) were not seen in the X-ray diffractograms (Fig. 6.8). Kaolinite is a non-magnetic mineral. Since magnetically separated green grains were analysed, the 7Å reflection may predominantly be due to authigenic clay. Moreover, the large 7Å and a small 14Å peak, absence of shift in 14Å peak after glycolation and enhancement of 14Å after acetic acid treatment seen in all the X-ray diffractograms (see Fig. 6.8A&B) are characteristics of young phyllite V (Odin, Bailey *et al.*, in Odin, 1988), which has been named as 'odinite' (Bailey, 1988). Development of 14Å peak and a portion of it shifting to lower d-spacing (after heat treatment) recorded in some samples (556 - Fig. 6.8A) are also characteristic of phyllite V. The complete collapse of 14Å peak to lower d-spacing at higher temperatures seen in other samples (626 - Fig. 6.8B) does not confirm phyllite V. In fact these samples were lying off the river mouths and closer to the inner shelf (see Fig. 6.3). Verdine can be destroyed quickly up on recrystallisation (Odin, 1988). It could be that the authigenic clay in these green grains was subsequently oxidised and rapidly altered destroying some original properties of authigenic minerals. So the authigenic clay is most probably phyllite V. The 10Å peak in glycolated and acetic acid treated samples and its enlargement after heat treatment may be due to the presence of detrital clays including illite, inherited from the substrate. Therefore, the green grains represent a mixture of predominant authigenic and detrital clay minerals and their alteration products.

X-ray diffractograms of untreated sample of glossy brown pellets at station G-167/ 3914 (see Fig. 6.3) did not show significant peaks at 7Å and 14Å, but showed distinct reflections (at 4.18Å, 2.45Å and 2.69Å) of goethite (Fig. 6.9). The

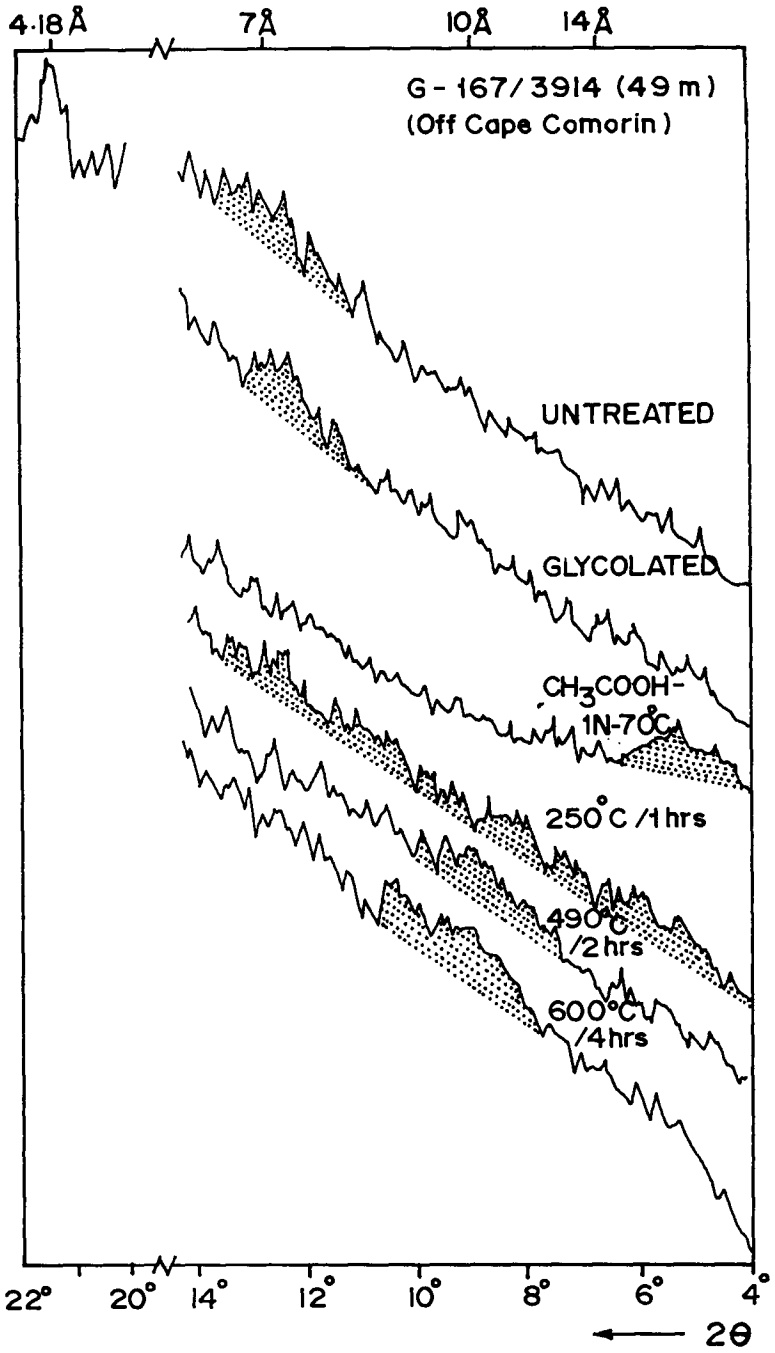

Fig. 6. 9 X-ray diffractograms of brown glossy pellets from the outer shelf off Cape Comorin (3914) (see Fig. 6.3 for location).

7Å and 14Å peaks were slightly enhanced after glycolation without shifting to higher d-spacings. The peak at 14Å was enhanced after acetic acid treatment, but centred around 16.7Å. A broad dome was developed at about 10Å, when heated to 490°C for 2 hours. Further heating did not show any significant change.

The behaviour of these grains after glycolation and acetic acid treatment (Fig. 6.9) is more or less similar to those of the grains from the outer shelf (see Fig. 6.8), suggesting the presence of verdine minerals. Abundant goethite indicate that the authigenic clay minerals existed in these grains have probably been considerably altered, following a low sea level and thus difficult to identify at present. Since the characteristics of glycolated and acid treated X-ray diffractograms resemble those of the grains of phyllite V, the authigenic green clay is most probably phyllite V of the verdine facies. The poor 7Å and 14Å reflections in these grains may be due to strong alteration.

Green grains from the continental slope

Nine samples were analysed for the present study from the continental slope of Karnataka and Kerala, at depths between 117 and 330 m. Green grains occur as dark green glossy pellets, shiny moulds and infillings of foraminifers and pteropods (Table 6.2). X-ray diffractograms show a well developed 7.2Å peak and a poorly developed dome at about 14Å (Fig. 6.10). The dome at about 14Å shifted marginally to higher d-spacings up on glycolation and intensified on acetic acid treatment. The 14Å peak completely collapsed and a large dome was developed at about 10Å up on heat treatment. The large 7Å and small 14Å reflections in untreated X-ray diffractograms and, decrease of 7Å and increase of 14Å reflections up on acetic acid treatment are characteristic of phyllite V. However, the collapse of 14Å peak on heating does not confirm phyllite V. The peak at 10Å and marginal shift of 14Å peak up on glycolation suggest the presence of detrital illite and expandable minerals like smectite, inherited from the substrate. Although the morphology of the grains differ from that of outer shelf, the X-ray diffractograms obtained after different treatments are similar, suggesting that these grains contain a mixture of authigenic and detrital clays and are altered. The authigenic green clay is most probably young phyllite V (odinite). The light green rugose pellets and dark green glossy pellets from two samples collected at 100

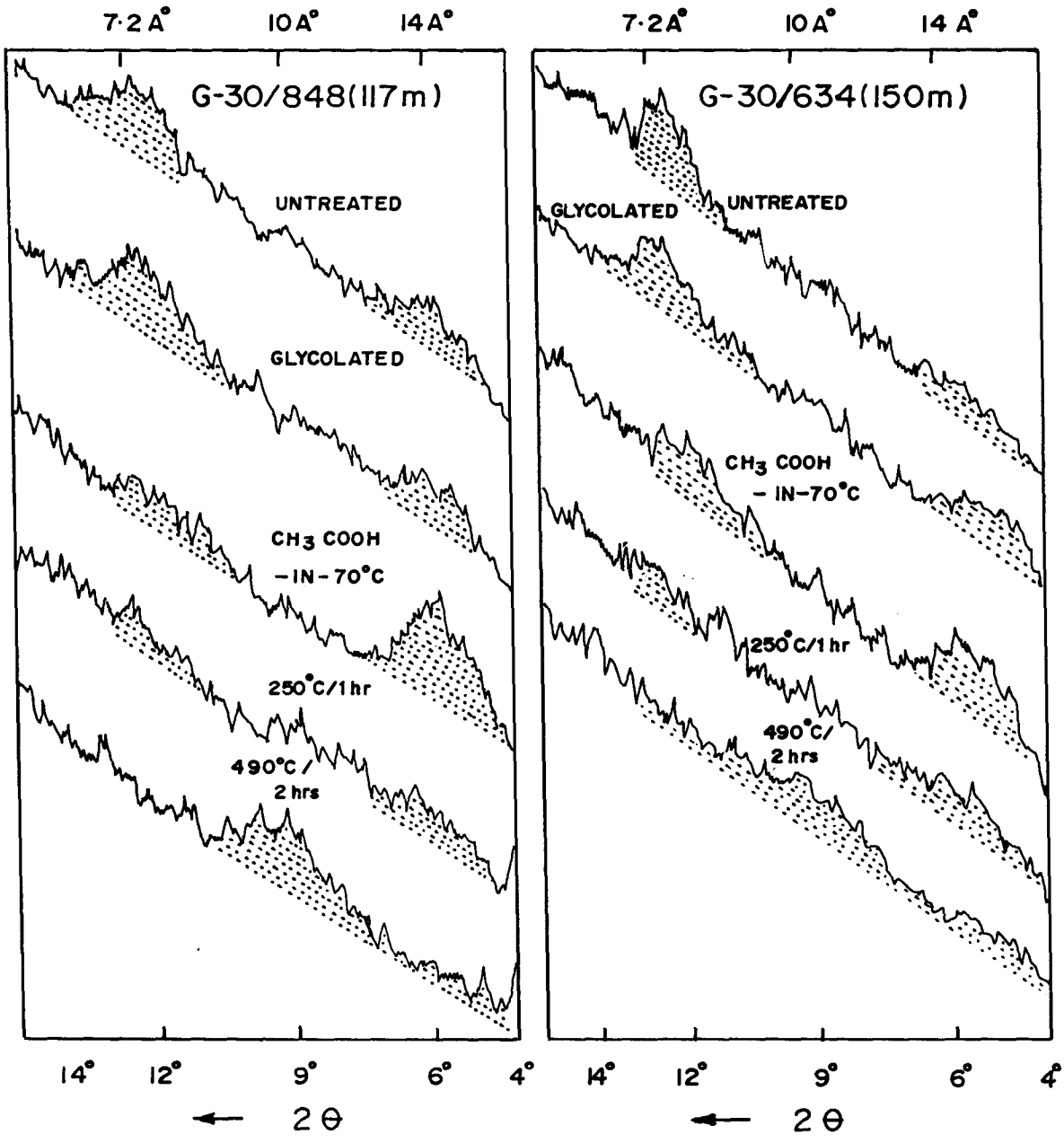

Fig. 6. 10 X-ray diffractograms of dark green grains from the continental slope of Kerala (848) and Karnataka (634).

and 205 m water depth also revealed the presence of phyllite V. Although the colour and morphology of the green grains vary at these depths (between 100 and 235 m) the verdine mineral is always young phyllite V (odinite).

Pale green infillings occurring at 280 m depth (G-71/1401) were studied. To remove the carbonate material, these infillings were treated with 1N acetic acid for 1 hour at room temperature before subjected to X-ray analysis. They are characterised by a large 14Å and a small 7Å peak (Fig. 6.11). A slight shift is observed in the 14Å reflection and in the 7Å reflection during ethylene glycol treatment. The heat treatment at 250°C/1 hour did not modify the 14Å peak from the normal peak (Fig. 6.11). The peak at 7Å disappeared and the 14Å peak modified in to a broad hump between 10 and 13Å after heating to 490°C/2 hours. The large 14Å peak and the very small 7Å peak are characteristic features of both phyllite C and glauconitic smectite. However, the shift of 14Å peak on glycolation and a partial shift of 14Å peak towards higher angles after heating to 490°C/ 2 hours are characteristic of phyllite C. The collapse of 14Å peak to lower d-spacings after heating 490°C/ 2 hours is not complete, which is not a characteristic of glauconitic smectite. It is therefore suggested that the authigenic clay is phyllite C.

Pale green infillings from the 330 m depth terrace off Cochin (G-71/ 1403) were also analysed for their mineralogy. The X-ray diffractograms of the untreated samples do not show peaks at 7Å and 14Å; instead they display a broad hump between 11 and 13Å (Fig. 6.12). This broad hump was however, shifted to low angles and centred at about 14.6Å in the acetic acid (1N) treated samples. In glycolated samples, this hump marginally shifted to low angles. The 14Å reflection was clearly shifted to high angles when heated to 250°C/1 hour and was represented by a large well defined peak at about 10Å when heated to 490°C/2 hours.

The absence of the principle reflections at 7Å and 14Å in the untreated diffractograms (Fig. 6.12) indicates that the authigenic mineral is not related to the verdine facies. The marginal shift towards lower angles identified in glycolated X-ray diffractograms is characteristic of both phyllite C of verdine facies and

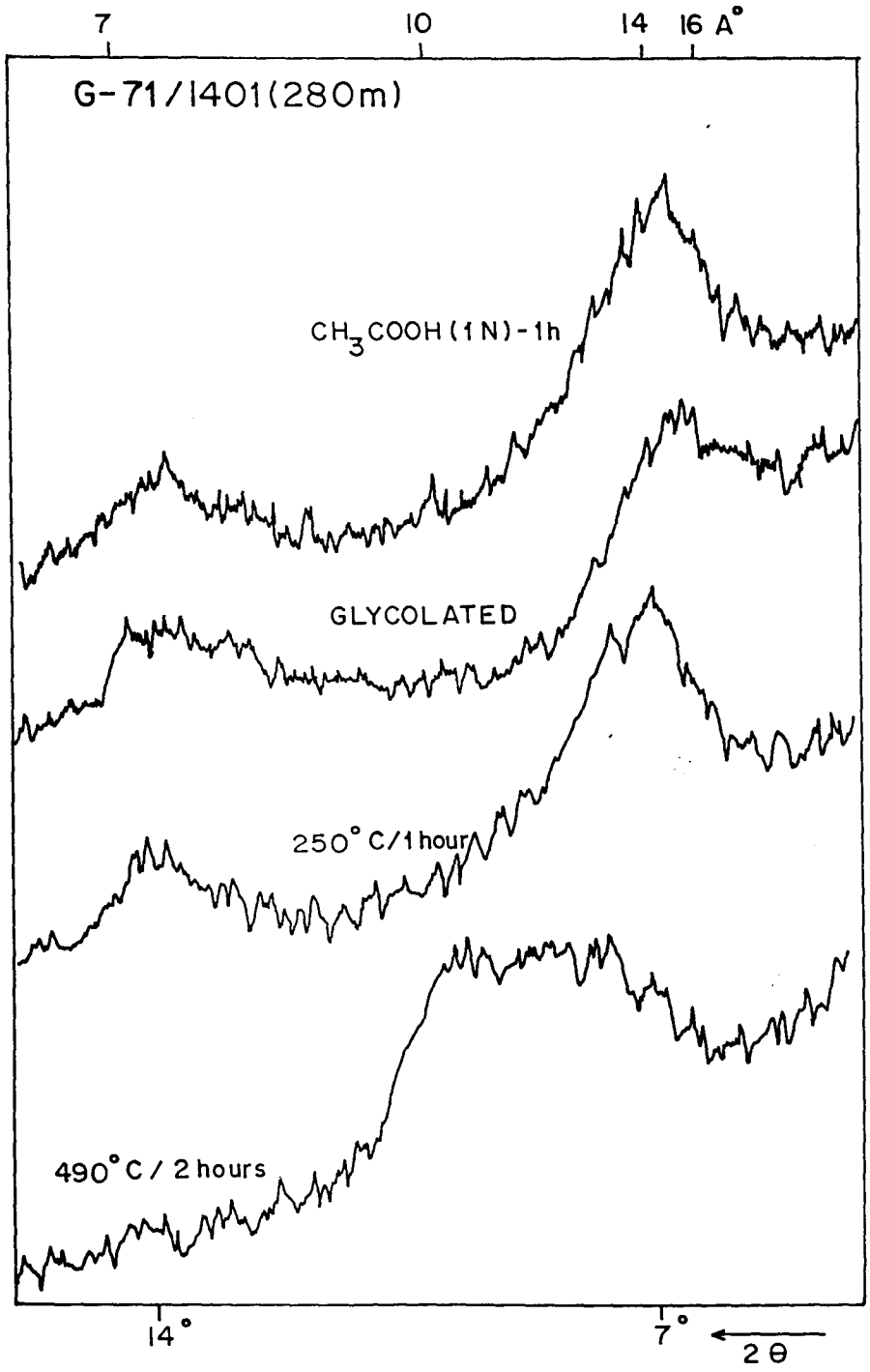

Fig. 6. 11 X-ray diffractograms of the green infillings from the slope at 280 m water depth (1401).

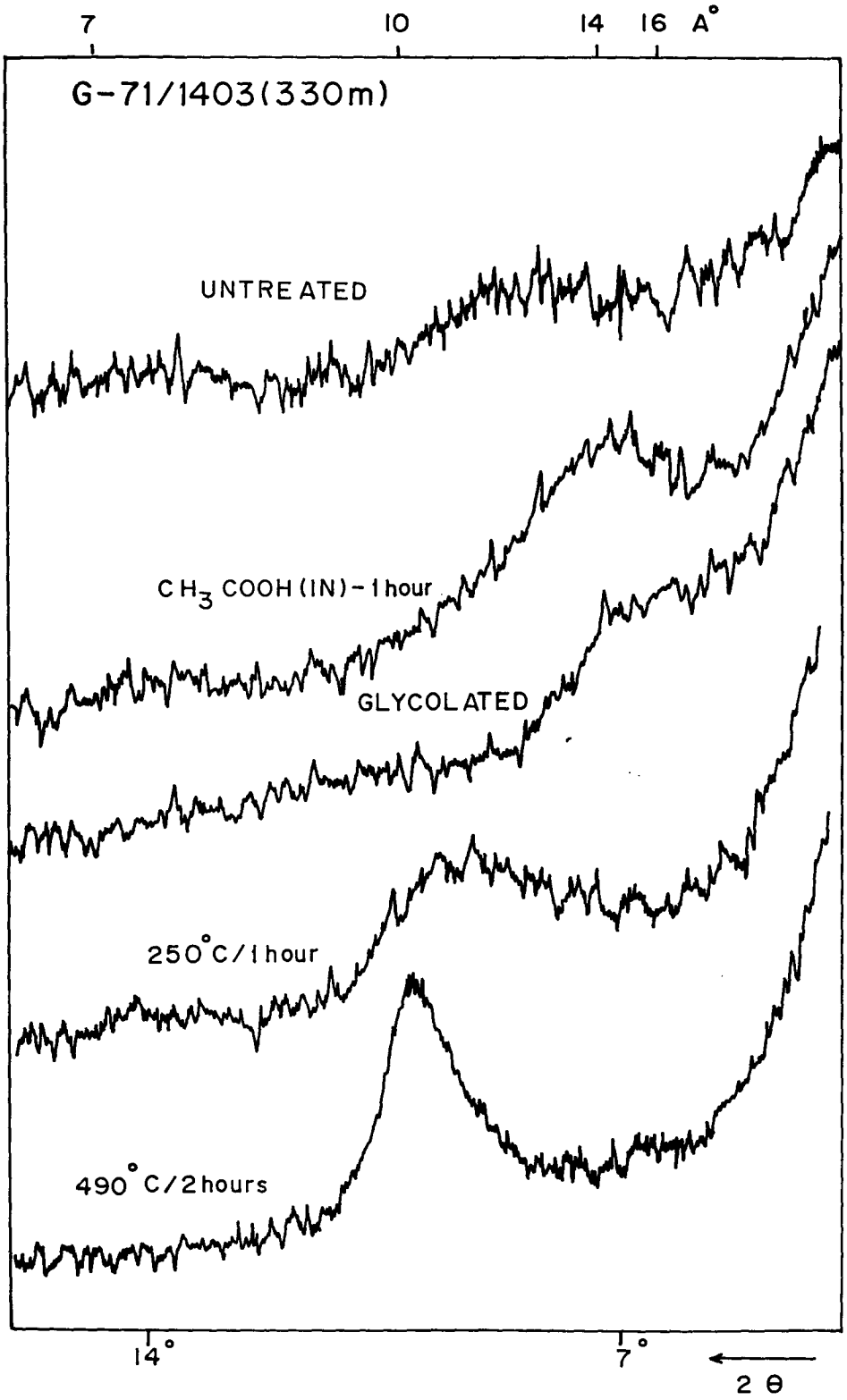

Fig. 6. 12 X-ray diffractograms of the pale green infillings from the terrace at 330 m water depth (1403).

glauconitic smectite of the glaucony facies. The complete collapse of 14Å peak to 10Å layers at 490°C/ 2 hours is characteristic of only glauconitic smectite. Therefore the authigenic clay mineral in these X-ray diffractograms clearly resembles the characteristics of glauconitic smectite. Odin (1988) reported a similar behaviour for the green grains of the glaucony facies of the Congo and Ivory coast. Therefore, the mineral is glauconitic smectite, which represents an early stage formation of glaucony minerals.

Distribution of different mineral phases

With a wide geographic coverage and sampling frequency, it is possible to reach the following conclusions: All the green grains studied here are a mixture of predominant authigenic and detrital clay minerals and are intensely altered. Both phyllite C and phyllite V associated green grains are present in the shelf sediments. The green grains associated samples showing phyllite C are located off the river mouths and occur at the transition zone between clastic inner shelf and relict outer shelf sediments. The green grains associated with relict sands and in places with reefs of the outer shelf contain phyllite V. Comparative study (Fig. 6.7) demonstrates that the authigenic clay is immature, poorly crystalline and contain detrital minerals inherited from the substrate. Brownish ochre grains contain abundant goethite and poorly crystallised phyllite V. The associated sediment constituents (abundant carbonate fragments, quartz and heavy minerals) (Table 6.2) indicate a high energy oxidising environment, which was not conducive for the formation of authigenic green clays (see Odin, 1988). It is therefore likely that part of the initially formed metastable authigenic clay (young phyllite V) has been recrystallised to goethite in the subsequent high-energy conditions. Phyllite V is the major authigenic mineral phase on the continental slope down to a depth of 235 m, followed by phyllite C at 280 m water depth. Glauconitic smectite of glaucony facies was present at 330 m water depth. Both verdine and glaucony minerals on the slope are poorly crystalline and represent minerals of early stage formation of their respective facies.

Detailed studies on the distribution and characteristics of verdine facies occurring on Senegalese, French Guiana and New Caledonian margins and from the present study (western margin of India) have given important information on

the precise nature of this facies and emphasised its significance with regard to other apparently similar facies. These studies have indicated that the colour and appearance of the verdine facies can easily be confounded with the glaucony facies. There is little difference in geochemistry of the two facies and both contain Si, Al, Fe and Mg. Since verdine occurs at the continent-ocean boundary (in shallow marine environment including lagoons and estuaries), it contain slightly higher Mg than that in glaucony (see section 6. 2. 3 'Geochemistry'). The main method of identifying the two facies is by X-ray diffractometry.

6. 2. 3 Geochemistry

Major, minor and trace elements

As mentioned above, the green grains studied here are a mixture of predominant authigenic green clay and detrital minerals and are altered. Table 6.3 shows how much the composition of the green grains of the western continental margin of India deviate from that of green grains (reported elsewhere) containing pure authigenic green clay.

SiO_2, Al_2O_3 and MgO contents of the verdine associated grains vary widely and range from 24.9 to 39.5%, 4.8 to 9.3% and 7.6 to 12.7%, respectively (Table 6.3). Higher percentages of these elements occur in green grains at shallower shelf and their concentrations decrease with increasing distance from the coast. In general, SiO_2 content is more in phyllite C associated green grains than those of phyllite V. The Al_2O_3 contents of the verdine grains from the western margin of India are lower (~7 to 9%) than in Guianese verdine deposits (Al_2O_3 ~11 to 12%), but slightly higher than that of New Caledonia and Senegal deposits (~6%; see Odin, Bailey *et al.*, in Odin, 1988). The SiO_2 content of the glaucony sample (G-71/1403) at 330 m water depth is extremely low (22.1%) compared to any other glaucony occurrences in the world oceans (SiO_2 ~ 40 to 50%; Odin and Matter, 1981; Odin and Lamboy, in Odin 1988). Glaucony developed mainly within the microfossil tests. The very high Ca (11.1%, mainly as carbonate) and possible high moisture content of the sample may be responsible for its low SiO_2 values.

Total Fe is reported here as Fe_2O_3. Because the synsedimentary iron-rich clays are more likely to be ferric than ferrous (Odin, 1988), the reported values may approximate the total iron. It varies from 14.3 to 23.6%. The green grains off the river mouths contain more Fe. Iron concentrations do not vary with depth (see Table 6.3). Calculations based on aluminium-normalised [$(Fe/Al)_{SAMPLE}$/ $(Fe/Al)_{SHALE}$ ~8.0; see Murray *et al.*, 1992] distribution indicate that the green grains contain 'excess Fe' which is not associated with the aluminosilicate matrices.

The K_2O concentrations in verdine grains range from 0.38 to 1.98% and are comparable with those reported for verdine from the world oceans. The low K_2O (~2.0%) content in the glaucony sample suggest an early stage formation of authigenic clay (Odin and Fullagar, in Odin, 1988) which is in agreement with the mineralogy. Na_2O values of the green grains range from 0.27 to 0.91% and are uniformly higher than those reported from other regions.

The CaO content varies from 2.2 to 15.5%, being highest in grains associated with the tests of microfossils and lowest in free green grains. This indicates that the Ca analysed here may not be a part of the original clay matrices, but represent the type of substrate for the authigenic clays and thus considered as impurity (see Odin, 1988).

Table 6.4 shows the distribution of minor and trace elements in the green grains studied here. The interelemental relationships among major, minor and trace elements indicate (Table 6.5) that Si shows strong positive correlation with Al ($r = 0.74$) and Mg ($r = 0.80$). Fe and K show strong correlation with each other, but do not show any significant relationship with Si, Al, Mg and Mn (see Table 6.5). Calcium (Ca) shows strong positive relation with Sr ($r = 0.8$) and is negatively correlated with Si, Al, Mg, Mn, Ba, Ni, Zr and REEs. Manganese (Mn), Ni, Co, Zr, Sc and Ba are positively correlated with Al and Mg. Barium (Ba) is also positively correlated with REEs (Table 6.5). Chromium (Cr) and V contents vary widely, being highest (Cr-610 ppm; V -234 ppm; Table 6.4) in the glaucony sample (G-71/ 1402). They correlate well with each other ($r = 0.7$) and with K and to some extent with Fe. Zinc (Zn) increases offshore and high values are found in the verdine

samples from the slope. It does not covary with the terrigenous indicators (Mg and Al). Cu values are higher in phyllite C than in phyllite V and does not show any significant relationship with other elements. High Th values at places clearly indicate a detrital source.

R-mode factor analysis of the elemental data indicates that three major factors accounts for a total of 76% variance (Fig. 6.13). Factor 1 is the major factor (41% variance) and shows high positive loadings for REEs, Y and U; and moderate to low positive loadings for Si, Al, Mg, Mn, Ba and Th; Ca, Ni and Zn shows moderate negative loadings (Fig. 6.13). Factor 2 (19% variance) shows high positive loadings for Al, Mg, Si, Mn, Cr, Co, Zr, and Sc; moderate to low positive loadings for Fe, Zn, Ba, Th, and REEs. Ca, Sr, K and Na shows moderate to high negative loadings for Factor 2. Factor 3 (15.5% variance) shows high to moderate negative loadings for Fe, K, Cr, Sc, V, Th, U, Rb and HREEs; Si, Mg, Na and Ba show moderate positive loadings (Fig. 6.13).

Moderate to high negative factor loadings for Ca and Sr in Factor 1 and 2 and moderate to high positive loadings for Si, Al, Mg, Mn, Co, Ni, Zr, Sc and Ga and moderate to low positive loadings for Fe and Zn in Factor 2 reveals that the aluminosilicate factor is being diluted by the carbonate phase.

Concentrations of different elements, their interrelationships and R- mode factor analyses indicate that Si, Al, Mg, Ba, Mn, Ni, Co, Zr, and Sc are contributed by the initial substrate. Most of the K and Fe may have derived from the water column. Ca and Sr are bio-detrital and indicate the type of substrate. The non-correspondence of Cr, V and Zn with either detrital or biogenic elements and higher values in the deeper samples may suggest their enrichment during early diagenesis from pore/ sea waters.

Rare earth elements

REE data presented here (Table 6.6) may be the first data set for the verdine minerals. Total REE content (ΣREE) in verdine grains varies from 46 to 146 ppm. These values are higher in the shallow shelf region and decrease away from the coast. The ΣREE contents are lower than they are in 'average shale'

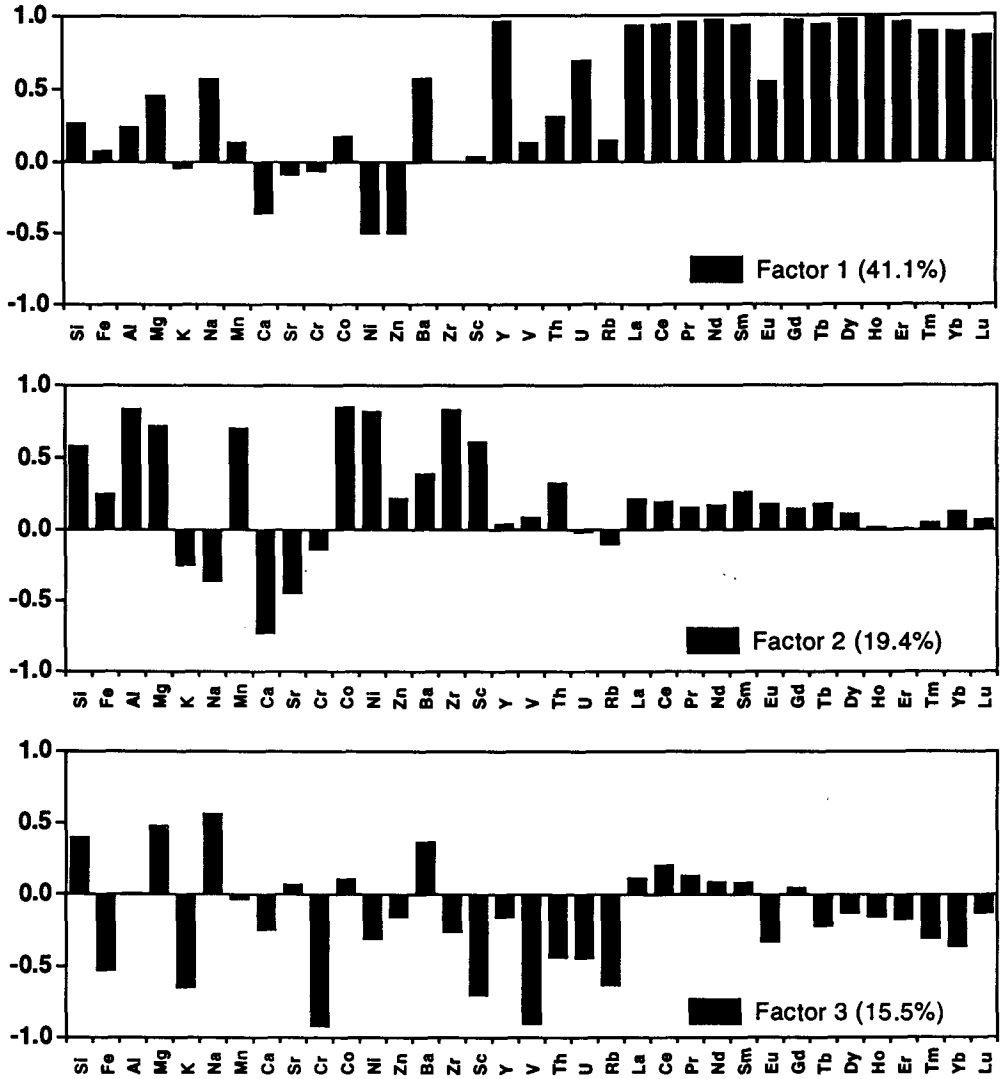

Fig. 6.13 R-mode factor analysis of the selected elemental data.

(Piper,1974a; Sholkovitz, 1988) and associated detrital clays (Table 6.6), but are comparable with that of glaucony ('glauconite') (see Fleet *et al.*, 1980). The ΣREE content correlates best with Mg and Ba (r ~0.65 in each case), least with Fe (r = 0.1) and K (r = -0.15) and show negative correlation with Ca, Sr and Zn. The REEs are highly correlated with each other (r ~0.7-0.9) revealing their coherent nature (Table 6.5).

R-mode factor analysis reveals that the Factor 1 has very high positive loadings for REEs and Y, and moderate positive loadings for other aluminosilicate elements (Si, Mg, Al, etc.) (Fig. 6.13), indicating that the REEs are mainly associated with aluminosilicate phase.

Shale-normalised REE plots of the samples are relatively 'flat' (see Fig. 6.14). The LREE to HREE enrichment, as calculated by the La_n/Yb_n ratio (Murray *et al.*, 1992) varies widely between 0.9 and 2.0 for the verdine grains. This ratio is relatively high (La_n/Yb_n ~ 1 to 2.0) in the green grains which occur closer to the land, and associated with clayey sediments of the continental slope, but lower (0.88 to 1.0) in green grains that are associated with abundant microfossils of the outer shelf/shelf break. There seems to be a moderate positive Gd and a complementary negative Tb anomalies (mean Gd_n/Gd_n^* = 1.34 and mean Tb_n/Tb_n^* = 0.75) in some samples (see Fig. 6.14).

The low ΣREE concentrations and 'flat' shale-normalised REE patterns in verdine associated green grains indicate that they retain the REE pattern of weathered aluminosilicate rocks. Verdine minerals, unlike other authigenic minerals, form in shallow marine environment where high concentrations of dissolved/ particulate elements are available and relatively high rates of sedimentation prevail. It is apparent that under these conditions the REEs are not preferentially scavenged during authigenic clay mineral formation and thus do not act as a 'sink' for REEs. Authigenic minerals such as Fe-Mn nodules, barite, authigenic montmorillonite, phillipsite, and phosphorites form in open marine environment (farther from land) where sedimentation rates are relatively low. These minerals scavenge REEs from sea water and also show fractionation of certain REEs (Ce/Eu anomalies) (Piper, 1974b).

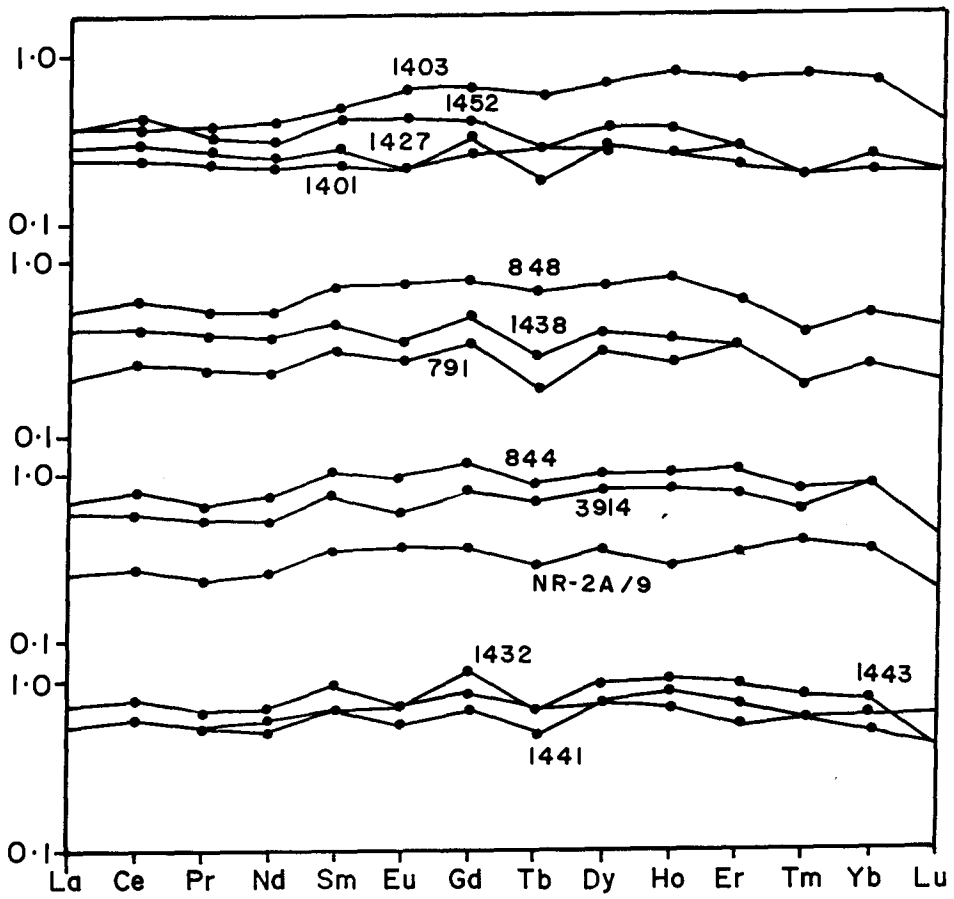

Fig. 6. 14 Shale-normalised REE patterns of the green grains (see Fig 6.3 for location).

The low REE values compared to 'average shale' (NASC) and associated detrital clays (Table 6.6) and moderate correlation of REEs with Mg (r = 0.64) (Table 6.5) imply that the sources for REEs are the detrital particles associated with the initial substrate and REE concentrations are diluted by the addition of REE-depleted authigenic clay. 'Excess Fe' indicates its source other than aluminosilicates, most probably the dissolved iron transported from the tropical weathering of laterites. No correlation of REEs with Fe indicate two different sources. Iron in the near shore mostly occurs as Fe^{3+} which is not a stable crystalline form and is readily available for the formation of synsedimentary minerals. Since verdine formation is relatively a fast process, Fe^{3+} must have been scavenged rapidly to form iron-rich clays. Fleet (1984) suggested that a substantial portion of the REE contents can be loosely held on to clays and therefore is available to take part in exchange reactions. During authigenic green clay mineral formation and recrystallisation of the host sediment (initial substrate) some REEs may have lost to sea water, a likely factor contributing towards lower REE contents in the verdine grains.

6. 3 DISCUSSION

6. 3. 1 Relationship of verdine with fluvial influx and coastal geology

Iron is a crucial element for verdine formation and is supplied to the sea by streams as detrital iron (dissolved and particulate) and by exhalations from spreading ridges and island arcs (Odin and Matter, 1981). Earlier studies have demonstrated that the size of the verdine deposit generally reflects the amount of the river runoff (Odin and Sengupta, in Odin, 1988). It is presumed that the amount of dissolved and particulate iron is related to the influx of fluvial discharge. Higher percentages of green grains on the shelf off the river mouths and their higher Fe_2O_3 values indicate that iron is largely contributed through rivers. Abundant green grains in the southern part of the study area, especially on the Kerala continental shelf and slope may be due to the large number (about 44) of west flowing streams cutting across the coastal belt and flow to the Arabian Sea through numerous lagoons and backwaters. The total annual discharge of the major and minor rivers in the study area is only about 95.6 km^3 (Rao, 1979), but

verdine facies cover an area of about 1,00,000 km^2. In contrast, the Amazon discharges about 3,187.5 km^3 water (second largest river in the world - Lisitzin, 1972) into the Atlantic and verdine bearing basin off the river mouth is about 1,00,000 km^2 (Odin, 1988). This implies that the verdine basin on the west coast of India represents an exceptionally large basin when compared to its annual (low) fluvial input and the suggestion - that the size of the verdine deposit is related to the amount of the river discharge (Odin and Sengupta, in Odin, 1988) is not valid. This also means that the amount of iron released from continental waters is more important than the volume of water discharged by the rivers and hinterland geology plays a crucial role (see Thamban and Rao, 1998). The intense chemical weathering of the extensive lateritic cappings of Western Ghat rocks and Warkala and Quilon beds with ferruginised sandstones in the coastal region (Krishnan, 1968) may have contributed abundant iron which in turn utilised for the formation of authigenic green clay minerals.

6. 3. 2 Nature of verdine grains and its relation to sediment type

The inner shelf sediments are clayey with <10% coarse fraction and high organic carbon and clay accumulation rates are also expected to be higher. Absence of green grains in these sediments may be due to the lack of suitable substrate which provides necessary microenvironments for authigenic green clay formation. High rates of sedimentation may also have inhibited the growth of authigenic clay.

The presence of phyllite C closer to the land and at the transition between inner and outer shelf suggests that the phyllite C forms where there is some contribution of fine detrital material. Manjunatha and Shankar (1992) reported minor sediment contribution at about 40-50 m water depth off Karnataka, as evidenced by the clay accumulation rates which vary from 0.56 to 0.89 mm/year. Odin (1988) recorded that phyllite C is an estuarine and nearshore facies and occurs in areas of fine-sediment contribution. The green grains occur on the outer shelf are associated with relict detrital sands and/or reefs and contain phyllite V. The reefs generally grow at shallow depths in association with warmer and clear waters. The presence of reefs at 75 m water depth and the radiocarbon dates of

the corals and algal limestones (8.3 ka-BP) (Rao and Lamboy, 1996), indicate their submerged and relict nature. The green grains associated with the reefs may have formed more or less at the same time and thus considered relict, and relate to the low sea level stands during the Holocene. Phyllite V associated green grains occur on the continental slope at depths between 100 and 235 m in clayey silt sediments. These grains most probably formed during the Last Glacial Maximum and/or during the subsequent sea level transgression. Phyllite C also occurs at 280 m depth in our study area. The different initial substrates of phyllite C for the shelf and slope occurrences rules out lateral transport. It is difficult to explain the formation of phyllite C at this depth (280 m) unless tectonic activity and subsidence of the terrace is involved (see below). The mineralogical properties of green grains on the shelf are more distinct in the northern part of the study area (sample nos. NR-2A/52 & 556; Fig. 6.6 & 6.8 A) than those in the southern part (626 & 3914; Fig. 6.8 B & 6.9) and the green grains closer to the shelf edge (848; Fig. 6.10), indicating that the latter are more altered, most probably due to high energy conditions subsequent to their formation.

Bailey (1988) and Odin (1988) interpreted that the colour of verdine grains is related to its mineralogy and morphological evolution. Verdine grains on the shelf are dark green and mostly occur as irregular grains. Both phyllite C and phyllite V are associated with them (Table 6.2). Brown glossy pellets contain poorly crystalline verdine mineral. On the other hand, young phyllite V (odinite) is invariably associated with light green rugose and dark green shiny pellets and dark green infillings on the continental slope. These results thus do not support Bailey (1988) and Odin (1988), but confirm the earlier findings from Indian margins (Rao *et al.*, 1993; Rao *et al.*, 1995; Thamban and Rao, 1998), that colour and morphology of the grains do not reflect the type of authigenic clay mineral or its evolution. The better crystallised phyllite V associated samples with microfossil tests (Fig. 6.11) and the poorly crystallised verdine with abundant goethite in brown coloured pellets (Fig. 6.9) indicate preservation of authigenic clay in the former and its alteration to neoformed minerals in the latter. It is therefore suggested that the processes leading to differences in colour may be very complex and not necessarily be related to mineralogy.

6. 3. 3 Distribution and significance of verdine facies

Once the minerals of the green grain facies are identified, their distribution can be used for understanding the palaeogeography and sediment history of the area for the following reasons: (a). Temperature and speed of formation are distinct for the two facies. For example, verdine minerals (phyllite V and phyllite C) seem to form in similar conditions and water temperature is usually higher (25°C) and the speed of reactions for the growth of verdine is very high (<1000 years). In contrast, the water temperature and growth time of glaucony minerals are 10-15°C and 10^3 to 10^5 years, respectively. In view of this and based on field observations, it has been suggested that verdine forms at depths <60 m and glaucony at deeper depths (>60 m) (Odin, 1988). (b). Verdine can easily be destroyed and thus mostly restricted to the recent sediments whose age is younger than Last Glacial maximum (18 ka-BP). (c). Traces of oxidation of verdine and its association with the relict/recent sediments are helpful to differentiate the verdine minerals of different ages on different portions of the shelf. (d). Global changes are associated with recent history of the continental margins, especially during the late Quaternary.

The present study indicates that both phyllite C and phyllite V associated green grains occur on the continental shelf, the former mostly confined to the inner shelf and latter to the outer shelf. The colour and mineralogical characters of the green grains also indicate that the grains on the outer shelf showed significant alteration and are less crystalline than those in the inner shelf. Furthermore, the sediments on the outer shelf are relict. These imply that green grains on the outer shelf are older and involve long history for their formation and subsequent alteration. It could be that the outer shelf grains are of late Holocene and inner shelf grains are forming in the present day. The age of the sediments associated with green grains on the outer shelf is early Holocene (about 8,300 years BP) (Rao and Lamboy, 1996). On the continental slope, green pigment is associated with different types of pellets, moulds and infillings of microfossils. Except the green pigment in the infillings, all the green grains showed poorly-crystalline, early stage minerals (of verdine and glaucony), irrespective of their colour and type of substrates. Therefore it is difficult to differentiate their relative age simply based on mineralogy. Verdine facies on the slope occurs at water

depths up to 280 m, followed by glaucony facies at 330 m. Detailed account on the distribution of verdine and glaucony and their comparison with other margins was given in the next chapter. Since verdine forms at <60 m and sea level was at about 120 m below the present position at LGM, it is possible to account the formation of verdine minerals on the continental slope only up to a depth of about 180 during the last glacial maxima. Two possibilities exist for the formation of verdine at depth between 110-280 water depth on this margin: (a). Transportation from shallow shelf and/or, (b). Neotectonic activity and related subsidence. Transportation of green grains from shallow slope is ruled out, because verdine mineral at depths between 110 and 235 m depth is phyllite V and at 280 m depth is phyllite C (see Fig. 7.6 of Chapter 7). Moreover the substrate for green grains is mostly pellets at 110-235 m and infillings at 280 m water depth. The alternative hypothesis is subsidence of the margin which has been reported all along the western margin of India (see Chapter 7 for comparison). Therefore, their distribution clearly suggests that the southwest margin of India has undergone neotectonic activities during the late Quaternary.

6. 4 CONCLUSIONS

1. Investigations on the authigenic green grains from the surficial sediments of the western continental margin of India, between Ratnagiri and Cape Comorin, (water depth 37 to 330 m) indicate that these occur as irregular grains, faecal pellets and infillings/ internal moulds of microfossils. Colour of the grains vary from dark green to pale green or brownish green.
2. Authigenic green grains are abundant in sediments from the continental shelf off river mouths and their distribution varies with sediment type.
3. Green grains consisting of both phyllite C and phyllite V minerals of the verdine facies occur on the continental shelf (between 37 and 100 m). On the continental slope, phyllite V occurs at depths between 100 and 235 m, followed by phyllite C at 280 m depth and glauconitic smectite of the glaucony facies at 330 m depth on the terrace.
4. The authigenic green grains studied here are composed of a mixture of predominant authigenic clay, detrital clay and some altered products.

5. The major element composition of the green grains differs from those of the green grains reported from other regions. The low REE contents and flat shale-normalised REE patterns suggest that the REEs were inherited from the substrate and diluted by the addition of authigenic clays.
6. Verdine facies occur over an area of about 100,000 km^2, representing the largest sedimentary basin in the world, associated with low fluvial inputs.
7. It appears that the size of the verdine deposit is related to the influx of iron rather than the amount of fluvial discharge. The colour and morphology of the grains do not reflect the authigenic mineral or its evolution.
8. Green grains on this margin were formed at different times when the sea level was at different depths during the late Quaternary. The distribution of verdine and glaucony facies on the southwestern margin of India appears to be anomalous.

Table 6.1 Details of surficial samples and general distribution of different components in the 250-500 μm fraction. Only samples that contain green grains are given here. Cruise short names used are: NR - M/V Nand Rachit; G - R/V Gaveshani.

Sl. No.	Nos. used in the Map	Cruise No.	Station No.	Depth (m)	Distribution of grains (%)		
					Terrigen. grains	Biogenic grains	Green grains
1	3	NR- 2A	64	65	02.6	87.1	10.3
2	4	NR- 2A	63	60	00.9	87.3	11.9
3	5	NR- 2A	62	65	00.0	91.8	08.2
4	12	NR- 2A	52	65	06.2	76.0	17.8
5	13	NR- 2A	51	75	00.0	93.4	06.6
6	19	NR- 2A	44	60	00.0	90.9	09.2
7	26	NR- 2A	36	65	01.8	85.4	12.8
8	27	NR- 2A	35	70	00.9	87.5	11.6
9	31	NR- 2A	18	80	01.7	91.9	06.4
10	32	NR- 2A	9	70	28.6	56.9	14.5
11	34	G- 18	522	68	14.6	71.9	13.4
12	35	G- 18	523	77	00.0	94.5	05.5
13	37	G- 18	526	121	00.0	96.7	03.3
14	38	G- 18	528	205	47.1	40.3	12.6
15	42	G- 18	533	115	00.0	96.5	03.5
16	43	G- 18	536	60	11.8	77.3	10.9
17	44	G- 18	537	61	34.9	52.5	12.6
18	45	G- 18	539	57	00.0	90.4	09.6
19	46	G- 18	540	58	20.3	67.5	12.2
20	47	G- 18	541	64	01.7	89.5	08.8
21	48	G- 18	544	115	00.0	96.8	03.2
22	49	G- 18	546	332	00.0	89.4	10.6
23	50	G- 18	547	186	00.0	90.8	09.2
24	51	G- 18	550	80	00.0	97.8	02.2
25	52	G- 18	551	65	27.1	58.3	14.6
26	53	G- 18	552	56	38.0	51.0	11.0
27	54	G- 18	553	55	60.7	30.6	08.7
28	56	G- 18	556	75	10.0	67.2	22.8
29	57	G- 18	559	111	00.0	91.7	08.3
30	58	G- 18	568	48	15.1	82.2	02.7
31	60	G- 18	577	140	00.0	94.1	05.9
32	61	G- 18	578	104	00.0	92.3	07.7
33	62	G- 18	579	96	00.0	96.9	03.1
34	63	G- 18	588	110	00.0	98.1	01.9
35	64	G- 18	590	218	00.0	95.0	05.0
36	67	G- 18	593	85	00.0	88.8	11.2
37	68	G- 18	597	50	31.2	45.2	23.6
38	69	G- 18	599	52	07.4	84.6	08.0
39	71	G- 18	606	84	12.1	76.6	11.3
40	73	G- 18	620	170	00.0	92.7	07.3

Table 6.1 continued...

Sl. No.	No. used in Map	Cruise No.	Station No.	Depth (m)	Distribution of grains (%)		
					Terrigen. grains	Biogenic grains	Green grains
41	74	G- 18	625	51	19.3	70.2	10.5
42	75	G- 18	626	44	28.2	48.4	23.4
43	77	G- 18	634	150	00.0	73.6	26.4
44	78	G- 18	637	62	23.8	69.7	06.5
45	79	G- 18	639	48	39.4	54.0	06.7
46	81	G- 18	643	114	00.0	96.8	03.3
47	83	G- 30	772	53	24.0	67.5	08.5
48	88	G- 30	784	75	19.9	74.0	06.3
49	91	G- 30	787	65	46.6	46.8	06.6
50	95	G- 30	791	150	00.0	70.2	29.8
51	98	G- 30	797	145	00.0	83.5	16.5
52	99	G- 30	798	110	03.2	84.3	12.4
53	100	G- 30	799	78	18.4	74.0	07.7
54	101	G- 30	802	50	74.5	20.1	05.4
55	102	G- 30	803	49	27.5	56.1	16.4
56	104	G- 30	805	56	70.5	23.7	05.8
57	106	G- 30	807	240	13.6	79.7	06.7
58	107	G- 30	808	156	01.4	87.4	11.2
59	108	G- 30	809	30	15.8	74.6	09.6
60	112	G- 30	815	45	49.7	43.5	06.8
61	113	G- 30	816	42	04.5	76.4	19.0
62	114	G- 30	817	49	17.2	61.9	20.9
63	115	G- 30	818	58	04.9	82.8	12.3
64	116	G- 30	819	64	59.5	36.4	04.1
65	117	G- 30	822	240	00.0	76.9	23.2
66	122	G- 30	831	35	86.0	08.1	05.9
67	123	G- 30	834	107	45.2	44.6	10.3
68	125	G- 30	836	112	07.0	81.3	11.7
69	129	G- 30	844	42	14.4	34.9	50.7
70	131	G- 30	846	45	26.6	52.7	20.7
71	132	G- 30	848	117	25.6	46.9	27.5
72	133	G- 71	1454	45	62.0	30.0	08.0
73	134	G- 71	1453	55	77.0	16.0	07.0
74	135	G- 71	1452	100	00.0	62.0	38.0
75	136	G- 71	1451	85	70.0	24.0	06.0
76	137	G- 71	1449	300	00.0	87.0	13.0
77	138	G- 71	1446	55	68.0	27.0	05.0
78	139	G- 71	1443	37	39.0	37.0	24.0
79	140	G- 71	1441	38	38.0	50.0	12.0
80	142	G- 71	1436	170	00.0	73.0	27.0

Table 6.1 continued...

Sl. No.	No. used in Map	Cruise No.	Station No.	Depth (m)	Distribution of grains (%)		
					Terrigen. grains	Biogenic grains	Green grains
81	143	G- 71	1435	80	62.0	32.0	06.0
82	144	G- 71	1433	50	48.0	48.0	04.0
83	145	G- 71	1432	40	25.0	48.0	27.0
84	146	G- 71	1427	235	00.0	77.0	23.0
85	147	G- 71	1425	82	34.0	64.0	02.0
86	148	G- 71	1422	40	65.0	28.0	07.0
87	150	G- 71	1415	220	15.1	76.5	08.4
88	151	G- 71	1413	360	03.5	88.3	08.2
89	153	G- 71	1410	500	01.1	83.6	15.3
90	154	G- 71	1403	330	00.0	44.0	56.0
91	155	G- 71	1402	330	00.0	56.0	44.0
92	156	G- 71	1401	280	00.0	52.0	48.0
93	157	G- 71	1400	240	01.6	86.3	12.1
94	159	G- 71	1396	57	40.7	47.4	11.9
95	160	G- 71	1394	42	82.2	12.1	05.7
96	161	G- 71	1391	85	10.5	82.3	07.2
97	162	G- 71	1390	90	03.3	74.1	22.6
98	163	G- 71	1389	105	39.7	53.6	06.7
99	165	G- 71	1385	48	72.2	22.4	05.4
100	166	G- 71	1384	40	80.8	14.0	05.2
101	174	G- 167	3899	50	81.8	13.7	04.5
102	175	G- 167	3900	78	06.9	88.7	04.4
103	179	G- 167	3914	49	14.7	80.1	05.2
104	180	G- 167	3916	74	00.0	93.8	06.2
105	186	G- 167	3929	53	02.1	93.2	04.7
106	188	G- 167	3933	123	00.0	95.4	04.6
107	189	G- 167	3934	139	00.0	90.5	09.5
108	190	G- 167	3935	163	00.0	79.6	20.5
109	191	G-17	141	25	73.2	18.6	08.2
110	193	G-17	156	43	02.5	90.3	07.2
111	195	G-17	159	30	16.5	79.9	03.6
112	196	G-17	161	33	03.4	94.3	02.4

Table 6. 2 Distribution, morphology and mineralogy of the green grains in selected samples.

Sl. No	Sample No.	Depth (m)	Distri. of grains (%) Bio.	Terri.	G.grain	Morphology of the green grains	Predominant authigenic green mineral
1	G-71/ 1441	38	50.0	38.0	12.0	Irregular, dark green grains, few infillings	Phyllite C
2	G-71/ 1443	37	39.0	37.0	24.0	Irregular dark green grains	Phyllite C
3	G-71/ 1432	40	48.0	25.0	27.0	Irregular dark green grains, cracked outer surface	Phyllite C
4	G-71/ 844	42	34.9	14.4	50.7	Irregular dark green grains, cracked outer surface	Phyllite V
5	G-18/ 626	44	48.4	28.2	23.4	Irregular dark green grains, few infillings, moulds	Phyllite V
6	G-167/ 3914	49	80.1	14.7	5.2	Brown glossy pellets	Goethite, Phyllite V
7	G-18/ 537	61	52.5	34.9	12.6	Dark green internal moulds and casts of microfauna	Phyllite V
8	NR-2A/ 52	65	76.0	6.2	17.8	Dark green moulds and pellets; few brownish grains	Phyllite C
9	NR-2A/ 9	70	56.9	28.6	14.5	Irregular dark green grains, few pellets; stained grains	Phyllite V
10	G-18/ 556	75	67.2	10.0	22.8	Dark green shiny moulds; also irregular grains	Phyllite V
11	G-30/ 848	117	46.9	25.6	27.5	Irregular dark green grains; few dark moulds	Phyllite V
12	G-71/ 1390	117	74.1	03.3	22.6	Dark green infillings and moulds of foraminifers	Phyllite V
13	G-30/ 791	150	70.2	--	29.8	Dark green moulds and infillings of microfossils	Phyllite V
14	G-30/ 634	150	73.6	--	26.4	Dark green moulds of foraminifers and ostracods	Phyllite V
15	G-71/ 1436	170	73.0	--	27.0	Dark green glossy pellets; also moulds and infillings	Phyllite V
16	G-71/ 1452	190	62.0	--	38.0	Dark shiny moulds of foraminifers and pteropods	Phyllite V
17	G-71/ 1427	235	77.0	--	23.0	Dark green glossy pellets and also irregular grains	Phyllite V
18	G-71/ 1401	280	52.0	--	48.0	Dark green pellets; Infillings of foraminifers	Phyllite C
19	G-71/ 1403	330	56.0	--	44.0	Infillings of foraminifers; few internal moulds	Glauconitic-smectite

Bio.- Biogenic ; Terri.- Terrigenous ; G.grain- Green grains

Table 6.3 Major element chemistry of the green grains from the study area and their comparison with other occurrences in world oceans. Also included are the total REE (ΣREE) contents of individual samples.

Sample No.	Depth (m)	Predomin. Authigen. Minerals	SiO_2 (%)	Al_2O_3 (%)	Fe_2O_3 (%)	MgO (%)	K_2O (%)	Na_2O (%)	MnO (%)	CaO (%)	ΣREE (ppm)
G-71/ 1441	38	Phyllite C	32. 2	7. 6	14. 4	11.0	0.6	0.5	0. 08	7. 3	110. 0
G-71/ 1443	37	Phyliite C	37. 0	8. 8	14. 3	10. 8	0.9	0.8	0. 06	4. 1	113. 0
G-71/ 1432	40	Phyllite C	39. 19	7. 7	17. 8	11. 4	0.6	0.9	0. 04	2. 8	142. 6
G-30/ 844	42	Phyllite V	39. 5	8. 9	23. 5	12. 7	1.1	0.5	0. 03	2. 2	145. 6
G-167/ 3914	49	Goethite, Phyllite V	27. 4	8. 9	17. 3	10. 4	0.5	0.3	0. 13	4. 1	111. 0
NR-2A/ 9	70	Phyllite V	38. 0	9.0	21. 8	10. 9	0.7	0.3	0. 14	3. 9	51.2
G-30/ 848	117	Phyllite V	nd	9. 3	22. 6	12. 1	1.0	0.4	0. 16	2. 7	111. 6
G-30/ 791	150	Phyllite V	30.0	4. 8	14. 7	7. 6	0.5	0.6	0. 04	6. 9	47. 6
G-71/ 1436	170	Phyllite V	24. 9	6. 6	15. 0	7. 9	0.4	0.5	0. 04	13. 5	75. 8
G-71/ 1452	190	Phyllite V	nd	7. 9	18. 6	8. 2	0.6	0.4	0. 08	4. 8	70. 9
G-71/ 1427	235	Phyllite V	27. 6	7. 1	16. 4	7. 1	0.6	0.4	0. 02	12. 9	54. 2
G-71/ 1401	280	Phyllite C	36. 1	8. 9	21. 9	8.0	2.0	0.3	0. 01	4. 5	45. 4
G-71/ 1403	330	Glauconitic smectite	22. 1	5. 3	23. 0	3. 1	2.0	0.4	0. 01	15. 5	77. 3
French Guiana*		Phyllite V	36.9 -39.1	10.8- 12.0	17.9 -19.5	8. 3 - 11. 0	1.1 - 1.4	0.2 - 0.3	na	0.3 - 0. 7	na
New Caledonia*		Phyllite V	31.2, 34.0	5.2, 6.1	22.0, 23.1	10. 8, 13. 7	0.18 , 0.16	0.02	0.02, 0.03	0. 7, 1. 1	na
Senegal Shelf *		Phyllite V	32.6, 34.8	5.9, 9.3	21.7, 25.1	12.0 ,13. 2	0.5 , 0.17	0.2	0. 02	0. 4	na
GL - $O^{@}$		---	52.1	7.47	20.7	4.39	8.48	0.14,	0. 005	0. 98	na
GL - O^{S}		---	50.9	7.55	19.4	4.45	7.95	0.10	na	0. 95	na

* Odin, Bailey *et al.*, in Odin (1988) ; nd - not determined ; na - data not available
GL-$O^{@}$ - Glauconite mineral standard values obtained in the present study ; GL - O^{S} - certified values (Odin and Matter, 1981).

Table 6. 4 Distribution of minor and trace elements (in ppm) in the green grains from the study area.

Station No.	Co	Cr	Cu	Ni	Zn	Pb	Zr	Y	Sr	Ba	V	Sc	Rb	Th	U
G-71/ 1441	19.2	166.8	81.2	57.2	130.5	24.1	28.5	20.2	261.0	91.7	71.1	9.4	30.5	6.1	4.2
G-71/ 1443	18.6	172.1	38.8	71.3	110.3	19.7	34.1	24.6	170.9	119.3	65.2	10.7	46.9	4.4	4.0
G-71/ 1432	15.2	159.3	39.4	63.6	112.5	18.6	22.8	31.8	156.1	78.6	46.2	8.2	27.6	5.3	4.1
G-30/ 844	20.9	230.3	15.4	72.3	130.6	21.1	31.8	33.0	121.0	83.1	63.3	9.6	42.3	4.1	3.2
G-167/ 3914	25.8	476.4	21.4	92.0	125.2	41.6	45.6	23.5	168.2	77.2	215.6	14.1	28.3	14.5	3.5
NR-2A/ 9	41.4	188.4	56.3	80.0	142.5	17.5	67.6	10.9	405.1	55.9	111.9	14.9	32.3	3.3	3.2
G-30/ 848	18.0	181.2	16.7	49.3	113.3	20.8	30.2	19.8	110.9	97.3	68.9	9.5	38.8	5.5	3.9
G-30/ 791	15.7	154.4	13.5	56.5	108.6	14.5	15.2	8.1	419.5	33.2	58.2	6.7	14.8	2.6	1.8
G-71/ 1436	16.7	192.8	22.4	53.0	144.8	18.1	19.1	10.7	539.9	71.3	63.6	8.5	18.2	5.9	2.1
G-71/ 1452	38.7	128.6	38.5	68.6	182.6	18.8	24.4	8.7	260.1	78.9	46.3	9.8	27.6	4.3	2.2
G-71/ 1427	13.8	186.8	33.2	53.9	151.9	18.1	17.2	7.0	468.8	72.5	35.4	7.3	22.2	3.7	2.1
G-71/ 1401	8.5	535.0	26.5	67.8	215.2	15.9	22.0	8.8	214.8	58.3	56.9	11.1	62.5	3.4	2.1
G-71/ 1403	7.2	610.3	47.6	55.2	121.8	25.4	24.9	24.9	391.6	33.5	234.0	13.2	62.1	5.3	5.1
GL - O*	16.4	109.5	4.7	37.6	42.3	10.4	34.2	14.5	21.9	6.5	56.5	8.4	252.8	3.4	0.8

* Glauconite standard (GL-O) values obtained in the present study.

Table 6. 5 Inter-elemental correlations for the selected data set.

	Si	Al	Fe	Mg	K	Na	Mn	Ca	Sr	Cr	Co	Ni	Zn	Ba	Zr	Y	Sc	V	Rb	ΣREE
Si	1.00																			
Al	0.74	1.00																		
Fe	0.26	0.33	1.00																	
Mg	0.80	0.74	-0.01	1.00																
K	0.01	0.04	0.65	-0.44	1.00															
Na	0.26	-0.15	-0.38	0.23	-0.24	1.00														
Mn	0.25	0.49	0.27	0.48	-0.24	-0.17	1.00													
Ca	-0.86	-0.73	-0.22	-0.85	0.11	-0.17	-0.46	1.00												
Sr	-0.64	-0.67	-0.32	-0.65	-0.21	-0.25	0.38	0.80	1.00											
Cr	-0.38	-0.04	0.47	-0.55	0.79	-0.49	-0.19	0.24	-0.10	1.00										
Co	0.42	0.53	0.14	0.61	-0.45	-0.30	0.67	-0.49	-0.10	-0.38	1.00									
Ni	0.42	0.72	0.25	0.53	-0.02	-0.32	0.40	-0.67	-0.53	0.21	0.62	1.00								
Zn	0.17	0.38	0.42	-0.10	0.46	-0.52	0.08	-0.04	-0.02	0.36	-0.12	-0.01	1.00							
Ba	0.50	0.66	-0.23	0.69	-0.28	0.40	0.37	-0.45	-0.58	-0.42	0.22	0.24	-0.07	1.00						
Zr	0.41	0.61	0.34	0.46	-0.07	-0.40	0.57	-0.46	-0.22	0.01	0.89	0.77	-0.03	0.16	1.00					
Y	0.29	0.26	0.24	0.41	0.12	0.46	0.07	-0.38	-0.70	0.07	-0.01	0.29	-0.48	0.41	0.12	1.00				
Sc	0.12	0.50	0.60	0.10	0.38	-0.51	0.60	-0.25	-0.30	0.50	0.53	0.65	0.20	0.03	0.79	0.17	1.00			
V	-0.47	-0.08	0.35	-0.35	0.36	-0.44	0.24	0.24	-0.05	0.71	0.12	0.38	-0.18	-0.30	0.39	0.26	0.73	1.00		
Rb	0.17	0.23	0.56	-0.25	0.95	-0.14	-0.24	-0.03	-0.34	0.71	-0.34	0.14	0.36	-0.05	0.07	0.28	0.44	0.33	1.00	
ΣREE	0.38	0.40	0.10	0.64	-0.15	0.51	0.29	-0.48	-0.75	-0.21	0.10	0.25	-0.40	0.66	0.09	0.91	0.06	0.03	0.01	1.00

n = 12 ; values > 0.66 are significant at 99% level.

Table 6. 6 Concentration of REEs in the green grains (in ppm) and their comparison with other authigenic minerals.

Station No.	La	Ce	Pr	Nd	Sm	Eu	Gd	Tb	Dy	Ho	Er	Tm	Yb	Lu	ΣREE
'average shale'*	41.0	83.0	10.1	38.0	7.5	1.6	6.35	1.23	5.5	1.34	3.75	0.63	3.53	0.61	204.0
G-71/ 1441	22.3	47.3	05.0	17.9	4.5	0.8	3.80	0.50	3.5	0.80	1.70	0.30	1.40	0.20	110.0
G-71/ 1443	21.2	46.8	04.9	19.9	4.6	1.0	4.80	0.70	3.5	1.00	2.20	0.30	1.80	0.30	113.0
G-71/ 1432	27.9	59.9	06.1	23.6	6.2	1.0	6.20	0.70	4.3	1.10	2.90	0.40	2.10	0.20	142.6
G-71/ 844	26.7	61.0	06.0	24.6	6.9	1.3	6.50	0.90	4.5	1.10	3.10	0.40	2.40	0.20	145.6
G-167/ 3914	23.3	44.0	04.9	18.0	5.0	0.8	4.40	0.70	3.8	0.90	2.40	0.30	2.30	0.20	111.0
NR-2A/ 9	10.2	20.8	02.1	08.8	2.3	0.5	2.00	0.30	1.6	0.30	1.00	0.20	1.00	0.10	051.2
G-30/ 848	21.0	48.8	05.0	17.9	4.8	1.1	4.30	0.70	3.4	0.90	1.90	0.20	1.40	0.20	111.6
G-30/ 791	08.8	20.5	02.3	07.8	2.1	0.4	1.90	0.20	1.4	0.30	1.00	0.10	0.70	0.10	047.6
G-71/ 1436	16.3	32.9	03.5	12.7	2.9	0.5	2.60	0.30	1.8	0.40	1.00	0.10	0.70	0.10	075.8
G-71/ 1452	14.3	32.8	03.1	10.8	2.8	0.6	2.30	0.30	1.7	0.40	0.90	0.10	0.70	0.10	070.9
G-71/ 1427	11.3	24.1	02.6	08.5	1.9	0.3	1.80	0.20	1.4	0.30	0.90	0.10	0.70	0.10	054.2
G-71/ 1401	09.8	18.9	02.1	07.7	1.6	0.3	1.60	0.30	1.3	0.30	0.70	0.10	0.60	0.10	045.5
G-71/ 1403	14.3	28.4	03.4	13.8	3.2	0.9	3.60	0.60	3.3	0.90	2.20	0.40	2.10	0.20	077.3
GL - O ①	21.9	56.1	06.4	25.5	5.9	1.2	5.50	0.60	3.1	0.60	1.20	0.20	0.60	0.10	na
GL - O ②	19.5	52.6	06.1	27.0	5.4	1.3	4.36	na	2.7	0.50	1.27	na	0.64	0.09	na
Sediment ③	56.0	119	na	na	9.8	2.09	na	1.22	na	na	na	na	2.34	0.42	na
Apatite pellets ④	35.0	41.0	07.8	34.0	8.1	2.2	10.4	na	na	2.6	8.4	na	8.4	1.4	na
Phillipsite ⑤	167	54.7	na	169	32.0	7.5	na	6.6	na	na	na	na	21.3	3.6	na
Fe-Mn nodule⑥	152	704	35.2	144	34.4	9.1	44.4	5.8	31.1	5.7	15.8	2.3	15.5	2.3	na

* 'average shale' values after Piper (1974a) ; ① REE values obtained in this study for Glauconite standard GL-O ; ② reported values from Jarvis and Jarvis (1985). ③ Bulk sediment values for the inner shelf samples off Western margin of India (Nath, 1993). ④Apatite pellets from Peru shelf (Piper *et al.*, 1988). ⑤ Phillipsite values are from Piper (1974b). ⑥ Fe-Mn nodule values are mean of 14 samples from Indian Ocean (Nath *et al.*, 1992) ; *na* - indicates data not available

Chapter 7

Chapter 7

AUTHIGENIC CLAYS FROM THE EASTERN CONTINENTAL MARGIN OF INDIA: THEIR DISTRIBUTION AND COMPARISON

7.1 INTRODUCTION

The occurrence of green particles from the eastern continental margin of India was reported first by Subbarao (1964). He referred to these particles as glauconitised grains without specifying its composition. However, in the year 1985, verdine, has been specifically identified as distinct facies occurring in shallow marine environments (<60 m water depth) (Odin, 1985). This has necessitated a reassessment of the green grains in the sediments of the eastern margin of India.

In this chapter, authigenic green grains occurring in the surficial sediments of the eastern continental margin of India between the Mahanadi and Godavari river mouths and at depths between 18 and 247 m, were investigated by differentiating them according to their composition. The distribution of verdine and glaucony facies on this margin has been compared with that of other world occurrences and more importantly the western continental margin of India. The main objective of this chapter is to report the verdine facies hitherto unknown from this margin and differentiate the palaeogeography of the eastern and western continental margins of India based on the distribution of verdine and glaucony facies during the late Quaternary.

7.2 PHYSIOGRAPHIC SETTING AND PREVIOUS STUDIES

The east coast of India receives an enormous amount of sediment load both from major extra-peninsular (the Ganges and Brahmaputra) and peninsular rivers (the Krishna, Godavari and Mahanadi) and numerous small rivers and streams. As a result, larger part of the shelf and slope is covered by recent clayey sediments except for a smaller region between Mahanadi and Godavari, wherein relict sediments are exposed on the outer shelf and slope (Subbarao, 1964; Murthy, 1989). This part of the continental margin is chosen for the present investigation (Fig. 7.1). The drainage areas and annual water discharges of the

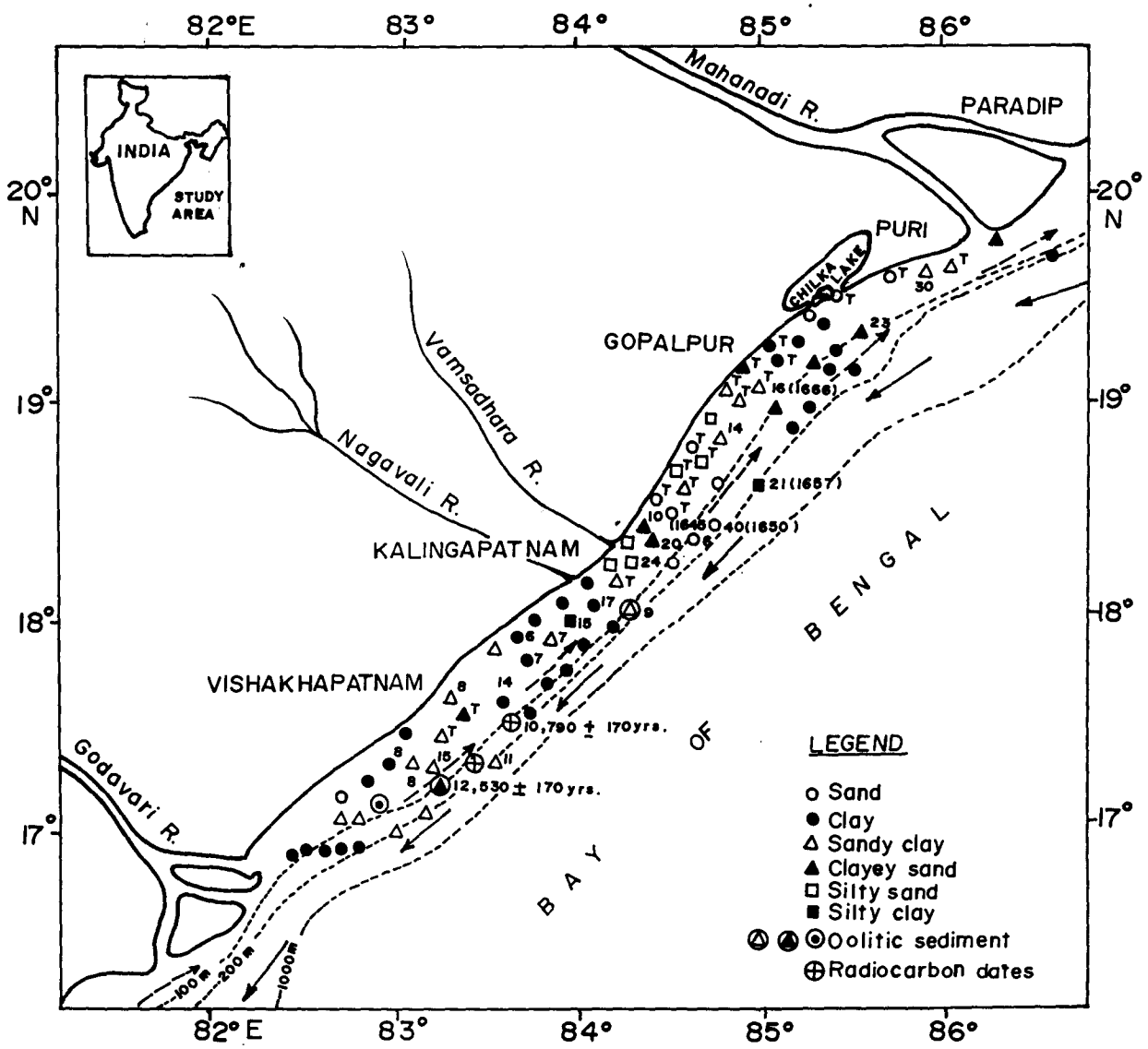

Fig. 7. 1 Sample location map. Texture of the sediments are shown with different symbols. *T* represents the samples containing abundant quartz and heavy minerals in the coarse fraction. The single and two digit numbers indicate the percentage of of green grains in the 125-250 μm fraction. The four digit numbers in parenthesis are the samples whose diffractograms are shown in Fig. 7.3 - 7.5. Dashed arrows show the direction of the currents during the SW monsoon season, and continuous arrows show the direction of currents during the NE monsoon.

Mahanadi and Godavari are about 88,320 km^2 and 313,147 km^2, and about 1726 m^3/s and 2925 m^3/s, respectively (Subramanian *et al.*, 1987). The Vamsadhara and Nagavali are seasonal rivers. The Vamsadhara drains about 7820 km^2 area and discharges about 83 m^3/s water annually. Hinterland hilly regions are mainly composed of metamorphosed gneisses.

The width of the continental shelf in the study area varies from 35 to 50 km and the shelf break occurs at water depths between 100 and 220 m with higher depths in the northern portion (Murthy *et al.*, 1993). Subbarao (1964) reported the detailed sediment distribution between Visakhapatnam and Puri: Recent sediments consisting of sands (up to 27 m depth) are succeeded in a seaward direction by clayey sand/ silty clays (up to 80 m) on the inner shelf. Mixed clastic and calcareous relict sediments with textures varying from clayey sand to sand occur between 80 and 145 m. Aragonitic oolites are reported to occur at about 100 m water depth. Clay-foraminiferal sands and silty clays occur at depths deeper than 145 m. Rao and Rao (1994) reported relict algal terraces at 80 and 100 m water depth formed during 10,790 and 12,530 yrs-BP, respectively. Kaolinite, illite and montmorillonite (in order of abundance) are present in the clay fraction of the surficial sediments (Rao, 1991).

7. 3 RESULTS

7. 3. 1 Texture and coarse fraction constituents

Clayey sediments dominate the shelf in the southern part between Godavari and Nagavali; sandy clays also occur at places, especially in the mid-shelf (Fig. 7.1). In the northern part, sandy sediments occur in the nearshore environment, silty sand to clayey sand or sandy clays on the mid and outer shelf and clayey-silty clays on the continental slope. Terrigenous minerals with abundant quartz and heavy minerals and minor skeletal remains are present in the 125-250 μm fraction of several nearshore sediments (Fig. 7.1). Sediments with a significant 250-500 μm fraction are very rare and if present, consists of abundant terrigenous minerals and a few skeletal fragments. Only 24 sediment samples contained appreciable amount (6-40%) of green grains in the 125-250 μm fraction (Fig. 7.1). Higher percentages of green grains are found near the outlets of the

Vamsadhara and Nagavali and are associated with sandy clays/ clayey sands (Fig. 7.1). Green grains are rare in clay-dominated sediments near the outlets of the Godavari and Mahanadi. Green grains in 13 sediment samples ranging from 18 to 70 m water depth are irregular and dark-coloured (Fig. 7.2 A-C) and the associated sediments are mostly terrigenous sandy clays and/or clayey sands. Green grains in 6 sediment samples at depths between 70 and 125 m occur in the form of dark-coloured green pellets (Fig. 7.2 D-F) and a few dark green internal moulds of molluscs, benthic foraminifers and pteropods. The associated sediments are calcareous sandy clays or clayey sands. Several foraminifers and ostracods in these sediments look fresh and do not contain green pigment. Green grains in 2 sediment samples at about 170 m water depth and 3 sediment samples at depths between 200 and 247 m occur as dark green internal moulds (Fig. 7.2 G&H) and dark green infillings of molluscs, pteropods and planktic and benthic foraminifers. These sediments are clayey.

7. 3. 2 X-ray diffraction studies

Shelf green grains

Although the morphology of the green grains at 55 and 100 m water depth differs, their X-ray diffraction patterns (Fig. 7.3A) (even their behaviour after different treatments) are similar. They show minor reflections at about 7Å and 14Å and are poorly crystalline. Oriented samples also show similar reflections. Ethylene glycol treatment has no or only minor effect on these reflections. The reflections at 10Å and 3.34Å also exist in some diffractograms. However, after acetic acid treatment, the intensity of 7Å reflection is reduced and 14Å reflection is slightly increased. After heating to 490°C for 2 hours and to 600°C for 4 hours, the reflection at about 7Å is destroyed and 14Å reflection is enlarged and shifted towards higher angles with a broad hump at about 10Å.

Detrital clay mineral reflections from the sediments, shown in Fig. 7.3B, are contrastingly different from those of the green grains (Fig. 7.3A) at the same station. Moreover, only magnetically separated green grains were analysed for mineralogy. So the 7Å and 14Å reflections are expected to correspond to the authigenic clay minerals of verdine (phyllite V and phyllite C) and/or glaucony (glauconitic smectite). The 14Å spacing of phyllite C and glauconitic smectite

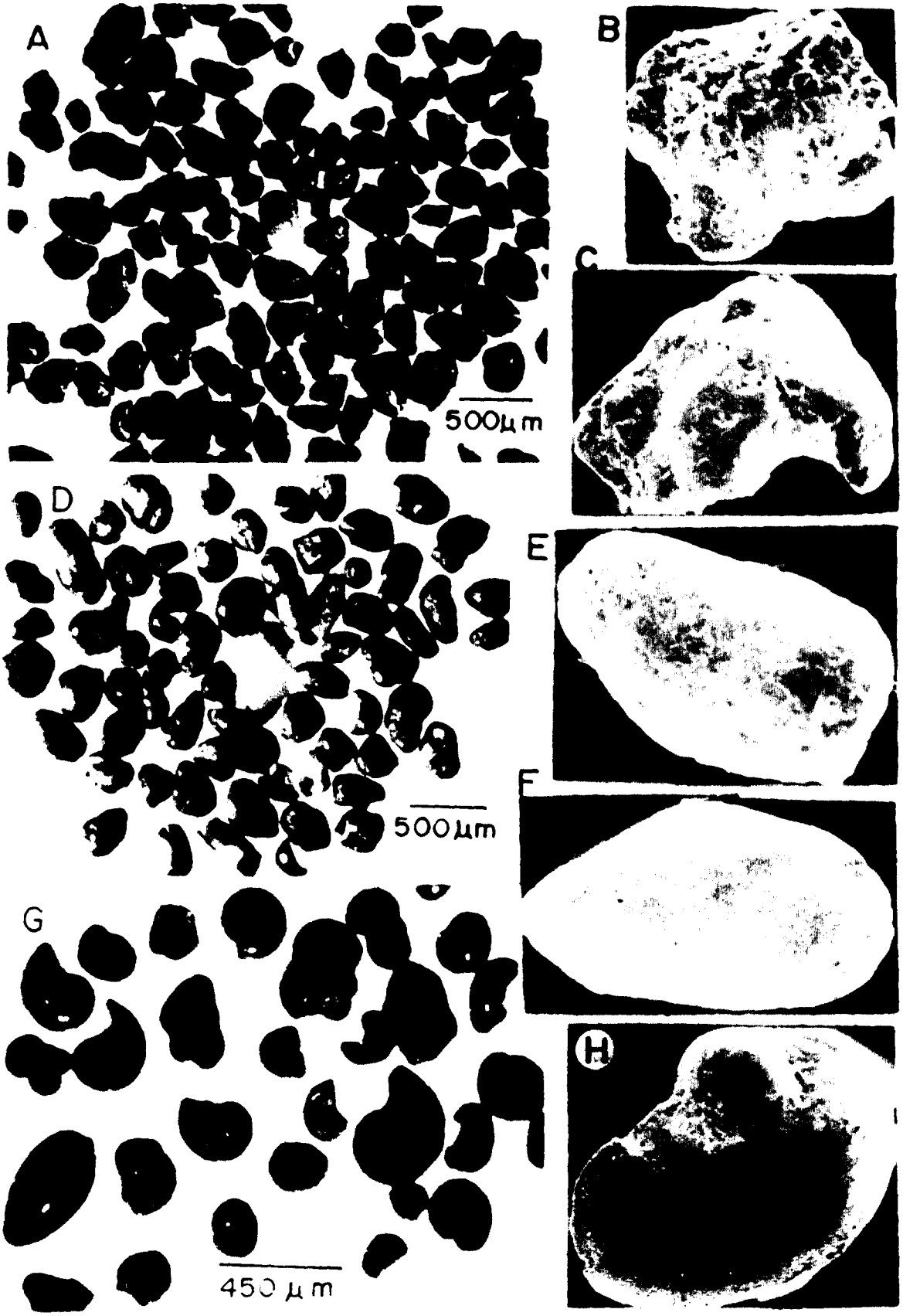

Fig. 7.2 Characteristic morphology of the green grains (A, D & G are photomicrographs; B, C, E, F & H are SEM photographs - all of same magnification). A, B & C - irregular dark grains from the inner shelf; D, E & F - dark green pellets from the outer shelf; G & H - infillings and moulds of microfossils from the slope.

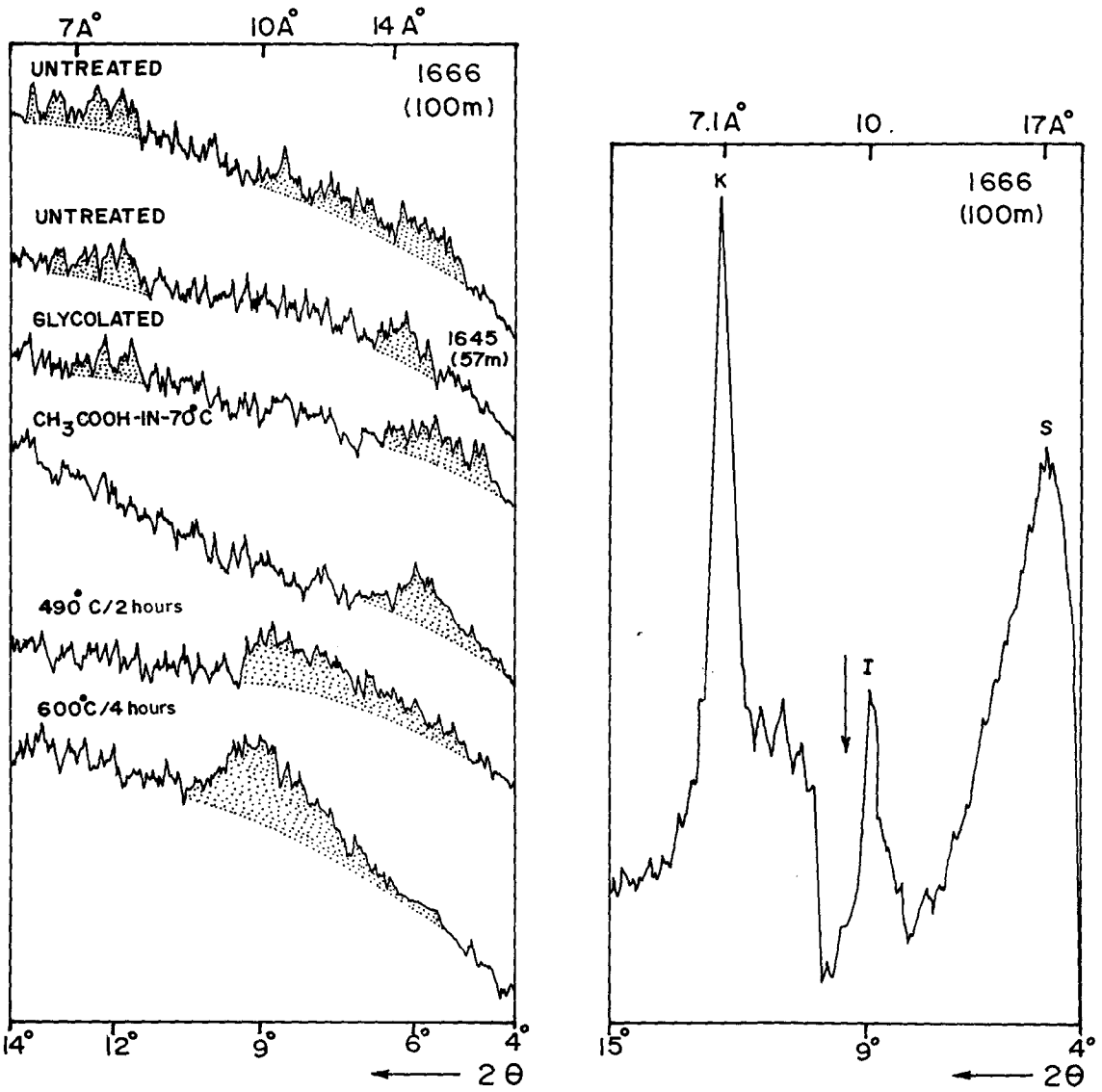

Fig. 7. 3 (A) Representative X-ray diffractograms of the shelf green grains. *I* - probable detrital illite reflections; other shaded portions are the areas of the authigenic clay reflections. (B) X-ray diffractogram of the detrital clay from the sediment sample (This particular diffractogram was taken on a Philips XRD PW 1130 Model; higher background after 10°2θ (arrow) is due to the change of divergent slit). S = Smectite, I = Illite; K = Kaolinite.

expands upon glycolation while that of phyllite V do not expand (Odin, Bailey *et al.*, in Odin, 1988). The intensification of 14Å peak to lower d- spacings (Fig. 7.3A) is characteristic of both phyllite V and phyllite C. Since the basic properties (such as higher 14Å reflection than 7Å reflection and expansion of 14Å reflection on glycolation) of phyllite C (Odin and Masse in Odin, 1988) are not observed in the samples (Fig. 7.3A), it is suggested that the authigenic clay may be poorly crystalline phyllite V. The reflections at 10Å and at 3.34Å in untreated and glycolated samples may be due to detrital illite and quartz inherited from substrate. The minor shift of 14Å reflection on glycolation may be due to some smectite. The green grains may, therefore, represent a poorly crystalline phyllite V with possibly some detrital clay minerals.

Slope green grains

The green grains at 170 m water depth show a larger and better crystalline 7Å peak and a smaller 14Å peak (Fig. 7.4). These peaks are unaffected by ethylene glycol treatment. Upon acetic acid treatment, the 7Å peak height was completely destroyed (showing easy alteration of the peak) and 14Å peak intensity was marginally increased. The heat treatment showed a moderate hump at 10Å and a small peak between 12Å and 10Å.

The strong 7Å reflection is a typical character of young phyllite V. Furthermore, the behaviour of this clay on glycolation, acid and heat treatments (see Fig. 7.4) is similar to the green grains at 55 and 100-125 m depth and supports young phyllite V, which has been named odinite (Bailey, 1988).

The green grains at 202 and 247 m water depth show broad peaks at about 14Å and 7Å (Fig. 7.5). The 14Å peak is shifted towards lower angles on glycolation. Acetic acid treatment intensified the 14Å peak and reduced the 7Å peak. The peak at 10Å is also distinct. The peak at 14Å completely collapsed to 10Å after heat treatment at 490°C for 2 hours. Subsequent heating had no effect on this peak (Fig. 7.5).

The shift of 14Å reflection after glycolation and intensification of 14Å peak after acid treatment are characteristics of phyllite C and glauconitic smectite. However, the complete collapse of 14Å reflection to 10Å after heat treatment (at 490°C/2 hours) is typical for glauconitic smectite (Odin, 1988) and thus indicates

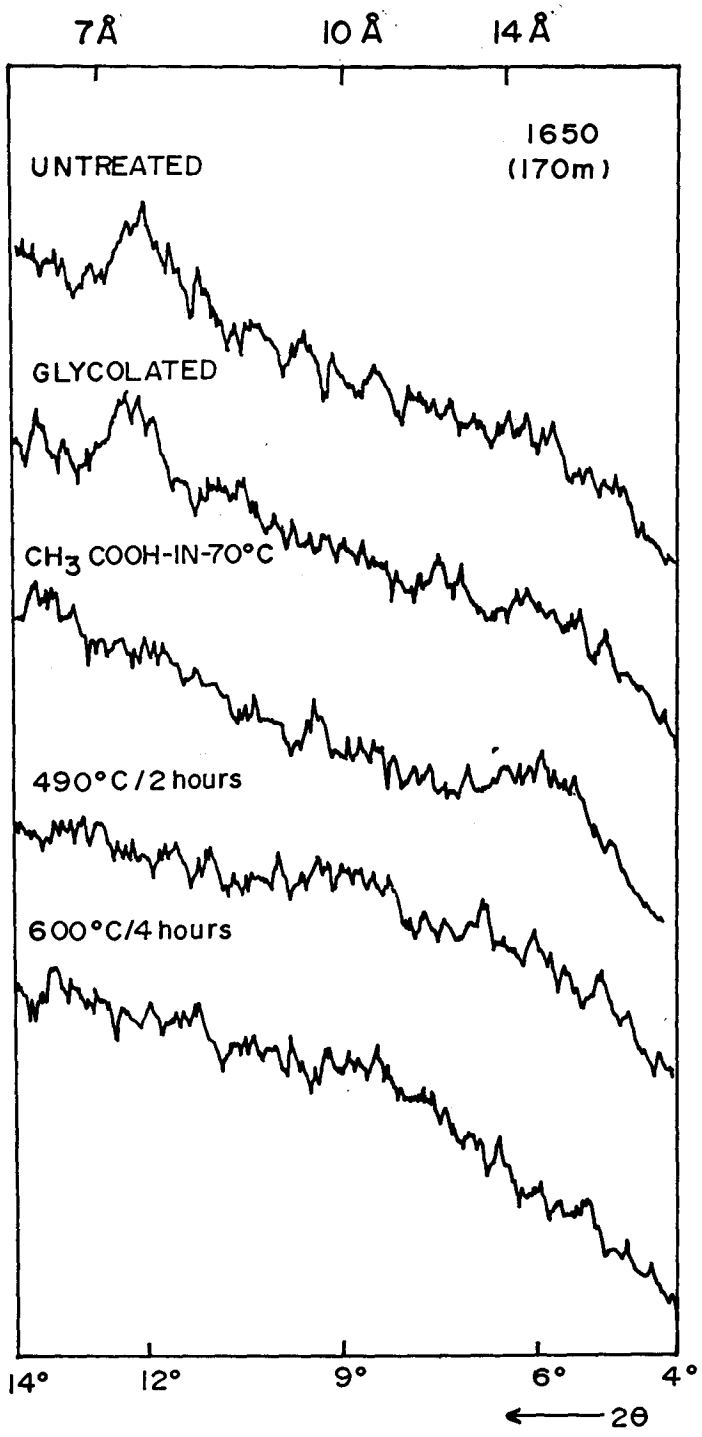

Fig. 7. 4 X-ray diffractograms of the green grains from the continental slope at 170 m water depth.

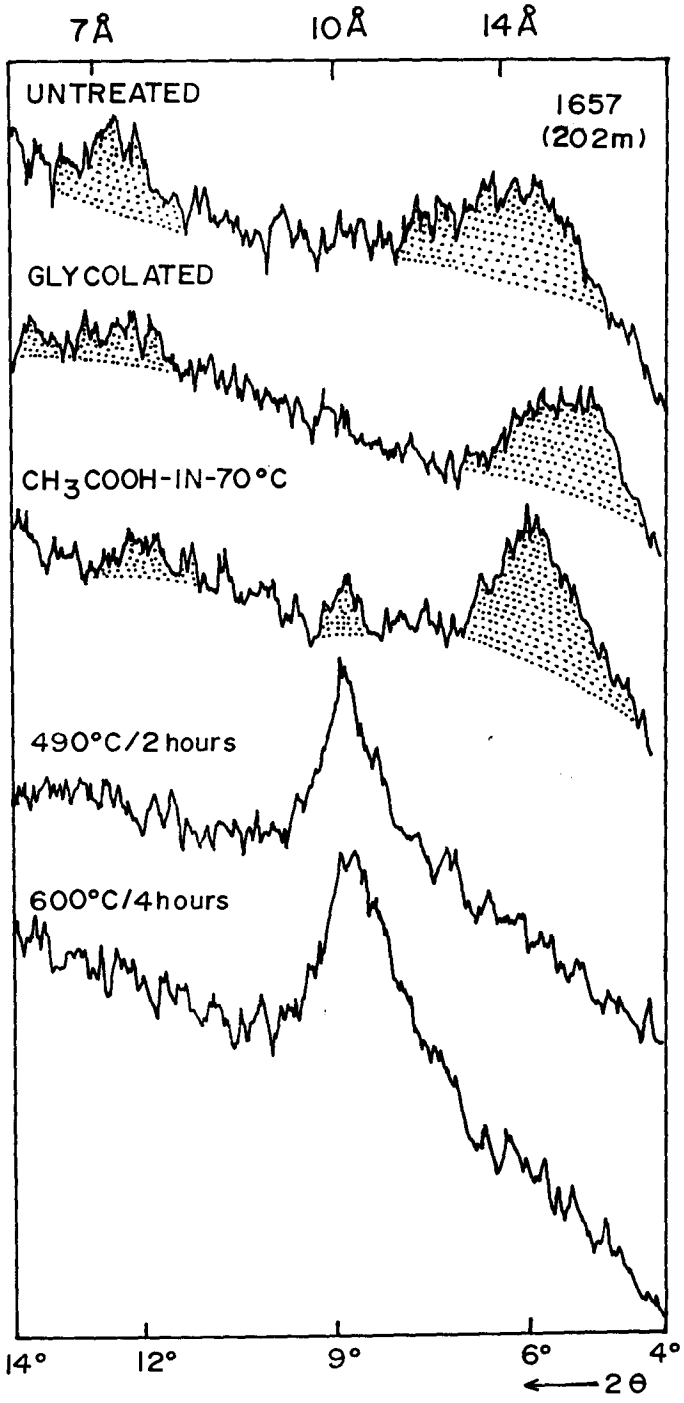

Fig. 7. 5 X-ray diffractograms of the green grains from the continental slope at 202 m water depth. *I* - probable detrital illite reflections; other shaded portions are the areas of authigenic clay reflections.

the presence of this mineral in these samples. Similar observations were reported for the glaucony grains from the Gulf of Guinea (Odin, 1988).

Synthesis of X-ray diffractograms

Phyllite V occurs down to a depth of 170 m. However, the phyllite V reflections at depths between 18 and 125 m are broader and more poorly crystalline than those at deeper depths (at about 170 m). Glauconitic smectite occurs between 202 and 247 m. These authigenic clays are poorly crystalline than any other known verdine facies in the world ocean (Odin, 1990). These samples show an early stage development of verdine and glaucony and appear to be a mixture of authigenic clays with small amounts of detrital clay.

7. 4 DISCUSSION

The colour of all green grains investigated here is dark green irrespective of the depth of occurrence, type of substrate, type of authigenic clay and its degree of crystallinity. This suggest that colour is not a true reflection of the degree of evolution of authigenic clay, as also observed along the west coast of India (see Chapter 6). The substrates hosting the authigenic green clays occurring on the outer shelf (pellets) and slope (skeletal tests) (between 70 and 247 m) are recognisable, whereas the grains on the inner shelf (18-70 m) exhibit irregular morphology. The poorly crystalline authigenic clay in irregular green grains and pellets may be due to the type of substrate and/or poor preservation. The better crystalline authigenic clay associated with planktic and benthic foraminifers, and other tests at deeper depths suggests that the biogenic tests acted as favourable substrates for the development and preservation of authigenic clay.

7. 4. 1 Age of the authigenic clay

Phyllite V occurs at depths between 18 and 170 m. Out of 13 inner shelf sediment samples (18-70 m) which contain green grains, 12 are from depths <60 m and one sample was from 70 m. As such these samples are within the depth range (<60 m) suggested for verdine formation (Odin and Sen Gupta, in Odin,

1988). It is therefore, presumed that verdine is forming at present day in the inner shelf sediments.

The radiocarbon dates of the algal terraces on the outer shelf at 80 and 100 m water depth are 10,790 and 12,530 yrs-BP, respectively (Rao and Rao, 1994). Subbarao (1964) assigned a late Pleistocene age for the skeletal constituents, bearing the authigenic clay, which occurs at depths deeper than 70 m and may have formed during glacial sea-level low stands. Many fresh looking skeletals on the outer shelf and slope have not been verdinised. It therefore, appears that verdine is relict on the outer shelf and slope. Two possibilities exist to infer its age: (1) If we assume that verdine was formed in a single event presently at depths between 70 and 170 m, it would imply that verdine generally forms at depths >60 m, and glaucony developed at depths deeper than 100 m. This contradicts the earlier suggestion of Odin and Sen Gupta (in Odin 1988) that verdine forms at depths <60 m. This would also imply that, in the same event, verdine of the outer shelf developed a poor crystallinity, whereas the verdine of the slope developed a better crystallinity, which would be difficult to explain. In this consideration, the age of 10,790 yrs-BP (the ^{14}C age of algal reef at 80 m water depth) should be accommodated as well. (2) It is most likely that the authigenic clay facies on the outer shelf and slope formed at two different periods. The slope facies might have formed during the Last Glacial Maximum (LGM ~18 ka-BP) when the sea level was at 120 m water depth below the present level. Then the actual formation depths of phyllite V at about 170 m and glauconitic smectite at about 200-247 m corresponds to 50 and 80-127 m, respectively. These depths are well within the depth range suggested for verdine and glaucony formation (Odin and Sen Gupta in Odin, 1988). The outer shelf facies might have formed during the subsequent marine transgression in the late Pleistocene. The radiocarbon dates on the outer shelf are in agreement with this.

Exposure of relict sediments on the outer shelf in the central part of the study area and poorly crystalline verdine in the shelf sediments suggest that the (low) sediment discharge coming from the Vamsadhara and Nagavali rivers to the shelf may not be sufficient enough to supply iron (both dissolved and particulate) for the faster development of authigenic clay. It also implies that iron as well as sediment discharge supplied from the major peninsular rivers such as Godavari

and Mahanadi do not reach the shelf and slope off the central part of the study area. The detrital clay mineral studies in this region (Rao, 1991) also support this argument. The study area is in tropical waters and temperature may not have influenced the authigenic clay formation. However, the maximum fluvial discharge to the shelf occurs during the SW monsoon period and the salinity of the surface waters drops down to 32‰ and water becomes turbid at this time. These factors probably contribute towards the slow development of authigenic clay at present.

7. 4. 2 Distribution and comparison of authigenic green clay facies on the east and west coasts of India

Figure 7.6 shows the depth distribution of verdine and glaucony facies on the east and west coasts of India. As discussed above, verdine facies (only phyllite V) occurs at depths between 18 and 170 m, followed by glaucony facies down to 247 m on the east coast of India. It is presumed that the green grain facies on the slope formed during the lowered sea level (see section 7.4.1). The change in green grain facies from verdine to glaucony after 170 m depth on this margin is in well agreement with the suggested depth ranges for these facies, considering the sea level low during the LGM was ~120 m. Moreover, their distribution is also similar to that of Senegalese and French Guiana margins (see Odin, 1988).

The green grain facies on the Kerala margin extends up to 330 m depth and the green grains represent both verdine and glaucony facies (see Chapter 6). Therefore, the distribution of verdine and glaucony facies along this margin is compared with that of the east coast of India. Here verdine occurs at depths between 40 and 280 m, followed by glaucony at 330 m depth (Fig. 7.6). Both phyllite V and phyllite C of verdine facies occur on the continental slope, whereas phyllite C is absent on the east coast. It has been suggested that verdine and glaucony formation on this margin is diachronous (see Chapter 6), and slope facies formed during the Last Glacial Maxima (LGM) when the sea level was at 120 m below the present level and, the shelf facies formed during the Holocene transgression. If verdine and glaucony facies on the slope formed during the lowered sea levels during LGM (~18 ka-BP), one would expect verdine up to 180

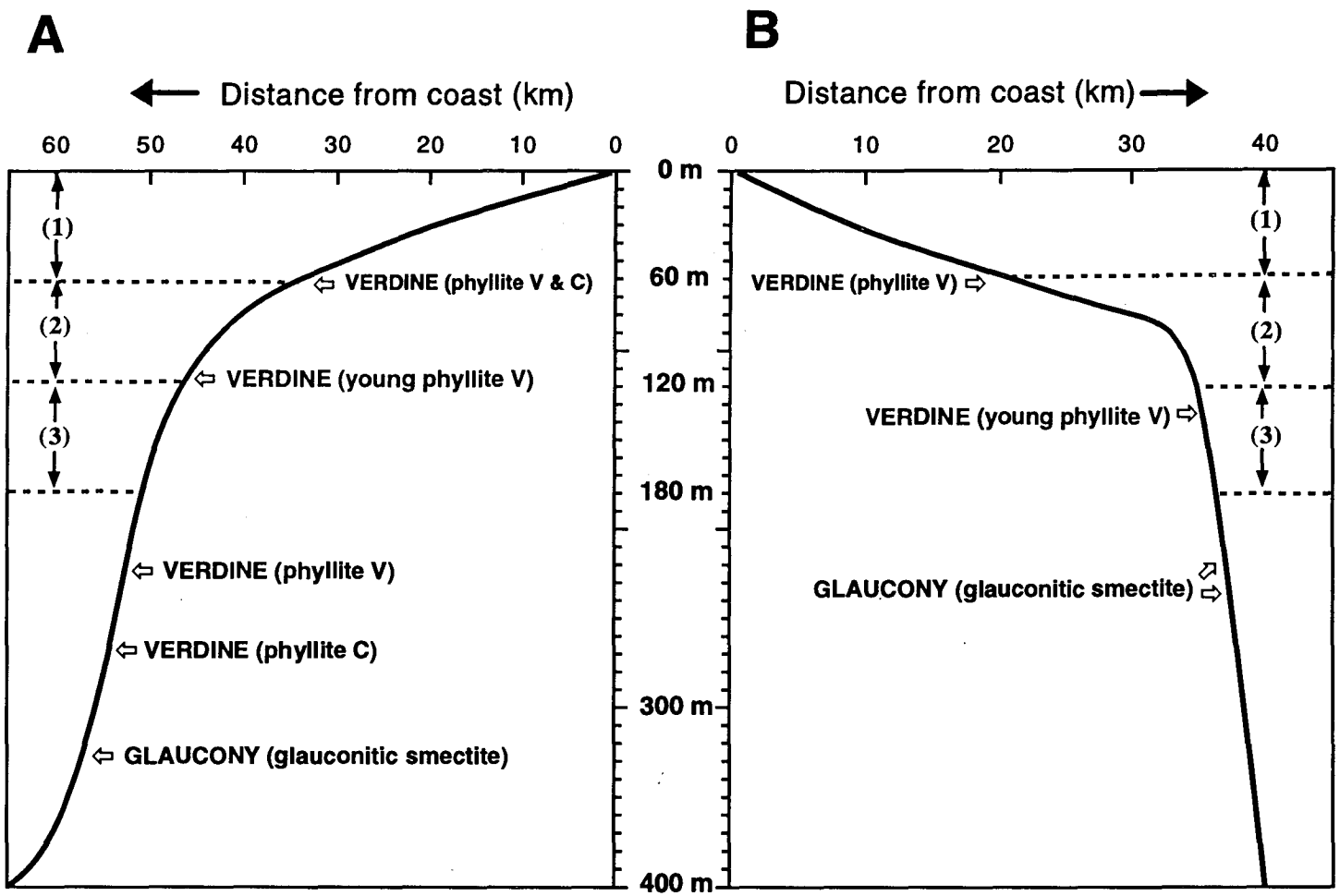

Fig. 7. 6 Distribution of verdine and glaucony facies from: (A) the western continental margin (off south of Cochin); and (B) eastern continental margin of India (off Kalingapatnam). Zone (1) - depth range (0-60 m) for the formation of present day verdine; Zone (2) - depth range (60-120 m) for verdine formed during the Holocene transgression; Zone (3) - depth range (120-180 m) for verdine formed during the Last Glacial Maximum (LGM).

m (as the depth range for verdine facies is <60 m) and the glaucony below. So the expected depth range for verdine and glaucony facies on the slope during the LGM are 120 to 180 m and >180 m, respectively. However, on the continental slope of Kerala, verdine occurs down to a depth of 280 m. The verdine mineral at 100-235 m (phyllite V) and at 280 m (phyllite C) is different. These rule out the possibility of lateral transport on the slope. It is also noticed that the substrate for the formation of verdine mineral at these depths is also different (see section 6.3.3 in Chapter 6).

The distribution of verdine and glaucony facies on the Kerala continental shelf and slope therefore appears be anomalous as its distribution does not agree with the suggested depth range for these facies on the Senegalese and French Guianese margins (Odin, 1988) and also with that of east coast of India. This suggests that the palaeogeography of the southwest coast of India was different during the late Quaternary, pointing to the subsidence of the terrace. Based on several evidences such as deeper submerged terraces on the upper continental slope, occurrence of vadose diagenetic limestones of early Holocene age on the Fifty Fathom Flat, demise of *Halimeda* bioherms after 8.3 ka-BP, and early Holocene radiocarbon dated sample on the shore, Rao *et al.* (1996) proposed late Quaternary neotectonic activity and subsidence along the western continental margin of India. The contrasting distribution of authigenic green marine clays on either side of the Indian margins reported here may also support the influence of neotectonic activity and subsidence along the western continental margin of India during the late Quaternary.

7. 5 CONCLUSIONS

1. Studies on the authigenic green grains from the surficial sediments along the eastern continental margin of India revealed that phyllite V of the verdine facies occurs at depths between 18 and 170 m followed by glauconitic smectite of the glaucony facies down to 247 m water depth.
2. The verdine formation on the shelf and slope of this margin is also diachronous. The distribution of verdine and glaucony facies on the continental slope of this margin is in agreement with the proposed depth ranges for the formation of

these mineral facies and eustatic sea level variations during the late Quatemary. Moreover, their distribution is also in accordance with that of the Senegalese and French Guiana margins, where palaeogeography of the margin has been constructed.

3. Comparison of the distribution of green grain facies of this margin with that of west coast of India, especially Kerala continental shelf and slope, reveals that the palaeogeography of the western margin of India was different and influenced by neotectonic activity and subsidence during the late Quaternary.

Chapter 8

Chapter 8

SUMMARY AND CONCLUSIONS

Sedimentological and palaeoceanographical studies were carried out on six sediment cores and one hundred and ninety eight surficial sediment samples along the western continental margin of India between Ratnagiri and Cape Comorin (between 17° and 7°N latitudes). A variety of studies conducted on the sediment cores using multiple geological proxies are integrated and palaeoclimatic conditions during the late Quaternary have been suggested. Surficial sediments along the western continental margin of India were used for the composition and distribution of authigenic green grain facies. In addition, eighty two surficial sediment samples from the eastern continental margin of India were studied for the distribution of green grain facies and compared with that of western margin of India and discussed their differences in terms of palaeogeography of the margins. A summary of the work carried out and salient findings of this study are described below:

1. Studies on organic carbon (C_{org}), grain size parameters and $CaCO_3$ in six sediment cores collected from the Oxygen minimum Zone (OMZ) between 280 and 350 m depths reveal that the relationship of C_{org} with $CaCO_3$ and sand content is diverse in the cores collected from different topographic domains.

2. The C_{org}, $CaCO_3$ and sand contents are high on core tops in the cores from the slope and terrace and progressively decrease from surface to base of the Holocene and exhibits strong correlation with each other; this implies that productivity played a major role for the enhanced organic carbon content in the sediments.

3. The low C_{org} content in the Pleistocene sediments may be due to the low productivity and dilution by skeletal constituents from the shelf during the lowered sea levels. Reworking of the sediments played an important role for the enhanced C_{org} content at certain intervals of the core from the terrace.

5. The very high C_{org} content in the Holocene sediments of the topographic highs is related to the combined influence of productivity, fine-grained sediments and suboxic conditions. The low C_{org} content in the Pleistocene sediments may be due to coarser sediments and winnowing in oxidising conditions.

6. Rock-Eval pyrolysis results reveal that the C_{org} is marine and immature in the Holocene sediments and reworked marine and/or terrestrial in the Pleistocene sediments.

7. The distinct variations in C_{org} content in different cores suggest that C_{org} distribution in the Holocene sediments is mainly controlled by primary productivity in combination with texture and reworking of sediments.

8. The stable isotope record of planktic and benthic foraminifers and organic matter in four sediment cores from the western continental margin of India indicates that the intensity of monsoons and related oceanic productivity fluctuated widely during the late Quaternary.

9. Down core oxygen isotope records of planktic foraminifers *Globigerinoides ruber* and *Globigerinoides sacculifer* exhibit a step-wise feature and are comparable with the deglacial warming stages reported in other regions of the Arabian Sea. The general trend of $\delta^{18}O$ record suggests that the Arabian Sea summer monsoon responded strongly to the fluctuations in solar insolation during the late Quaternary.

10. The amplitude of $\delta^{18}O$ values between the Last Glacial Maximum (LGM) and Holocene ($\Delta\delta^{18}O$ ~2.1‰) exceeds the global 'ice volume effect' (~1.2‰) significantly; this is best explained by a combination of decrease in sea surface temperature (SST) and increase in salinity during LGM.

11. The abrupt fluctuations in the high resolution $\delta^{18}O$ record during the last deglacial period in a core off Cochin appear to correspond to the abrupt climatic reversals reported from the continental records during this period. Changes in tropical land surface conditions (soil moisture feedback and changes in methane production from wet lands) may explain these abrupt reversal events.

12. The $\delta^{18}O$ record of benthic foraminifer *U. peregrina* shows that $\delta^{18}O$ amplitude ($\Delta\delta^{18}O$) (~0.9‰) is lower than the 'ice volume effect' (~1.2‰) and is not represented in any other regional record. This has been attributed to local temperature effect caused by the apparent shallowing of the core site during LGM.
13. The down core carbon isotope ($\delta^{13}C$) records of planktic foraminifers (*G. ruber* and *G. sacculifer*) are very complex and many factors (like variations in upwelling intensity, productivity, nutrient availability and variations in $\delta^{13}C$ of atmospheric CO_2) could have contributed to the past variations in the total $\delta^{13}C$ values.
14. The $\delta^{13}C$ records of benthic foraminifer *U. peregrina* closely correlate with the C_{org} record and are thus against the established hypothesis that enhanced productivity leads a decrease in $\delta^{13}C$ of the organic matter produced. The $\delta^{13}C$ variations can be attributed to the glacial-interglacial variations in oceanic denitrification rate and/or sea water alkalinity.
15. The down core variations in the carbon isotope ratios of bulk organic matter ($\delta^{13}C_{org}$) in two cores indicate that the C_{org} is dominantly marine in nature. The observed $\delta^{13}C_{org}$ variations may correspond to the varying supply of organic matter from terrestrial and marine sources.
16. Clay mineral studies on four sediment cores along the western continental slope of India reveal that the detrital flux transported through rivers is the main process supplying lithogenic material to the sediments.
17. Illite and chlorite are the dominant clay minerals on the topographic highs and are apparently derived from the Indus discharge. Kaolinite and gibbsite associated clay minerals in the sediments of the cores from the upper continental slope indicate abundant detrital flux from the hinterlands of the Peninsular India.
18. Down core variations in clay mineral proxies reveal that the K/C (kaolinite/chlorite) and S/I (smectite/illite) ratios (humidity indicators) were low and the aridity indicator C/I (chlorite/illite) ratio was high during LGM. These indicate that the continental climate was dry and less amount of terrigenous material reached the Arabian Sea during this period.

19. Marked increase in K/C and S/I ratios and decrease in C/I ratio and abundant clay accumulation in the cores between ~12 and 7 ka-BP suggest intense humid conditions. Monsoonal intensity during this period was maximum, when the northern hemisphere summer insolation was at its maximum. The clay mineral proxies also indicate a late Holocene arid period around ~4.5 ka-BP.
20. The climatic variations deduced based on clay mineral proxies are in agreement with the interpretations based on $\delta^{18}O$ and C_{org} variations in the same cores and also with the climatic variations reported from the monsoon-dominated areas around the Arabian Sea and Indian subcontinent.
21. Investigations on the authigenic green grains from the surficial sediments of the western continental margin of India, between Ratnagiri and Cape Comorin, (water depth 37 to 330 m) indicate that these grains occur as irregular grains, faecal pellets and infillings/ internal moulds of microfossils. Colour of the grains vary from dark green to pale green or brownish green.
22. Authigenic green grains are abundant in sediments from the continental shelf off river mouths and their distribution varies with sediment type.
23. Green grains consisting of both phyllite C and phyllite V minerals of the verdine facies occur on the continental shelf (between 37 and 100 m). On the continental slope, phyllite V occurs at depths between 100 and 235 m, followed by phyllite C at 280 m depth and glauconitic smectite of the glaucony facies at 330 m depth on the terrace.
24. The authigenic green grains studied here are composed of a mixture of predominant authigenic clay, detrital clay and some altered products.
25. The major element composition of the green grains differs from those of the green grains reported from other regions. The low REE contents and flat shale-normalised REE patterns suggest that the REEs were inherited from the substrate and were diluted by the addition of authigenic clays.
26. Verdine facies occur over an area of about 100,000 km^2, representing the largest sedimentary basin in the world, associated with low fluvial inputs.
27. It appears that the size of the verdine deposit is related to the influx of iron rather than the amount of fluvial discharge. The colour and morphology of the grains do not reflect the authigenic mineral or its evolution.

28. Green grains on this margin were formed at different times when the sea level was at different depths during the late Quaternary. The distribution of verdine and glaucony facies on the southwestern margin of India appears to be anomalous.
29. Studies on the authigenic green grains from the surficial sediments along the eastern continental margin of India revealed that phyllite V of the verdine facies occurs at depths between 18 and 170 m followed by glauconitic smectite of the glaucony facies down to 247 m water depth.
30. The verdine formation on the shelf and slope of this margin is also diachronous. The distribution of verdine and glaucony facies on the continental slope of this margin is in agreement with the proposed depth ranges for the formation of these mineral facies and eustatic sea level variations during the late Quaternary. More over, their distribution is also in accordance with that of the Senegalese and French Guiana margins, where palaeogeography of the margins have been constructed.
31. Comparison of the distribution of green grain facies of this margin with that of western margin of India, especially Kerala continental shelf and slope, reveals that the palaeogeography of the western margin of India was different and influenced by neotectonic activity and subsidence during the late Quaternary.

References

REFERENCES

Ahmad, S. M. and Labeyrie, L., 1994. Glacial to Holocene $\delta^{13}C$ variations in intermediate depth water masses of North Indian Ocean. *Geo-Marine Letters*, 14: 36-40.

Altabet, M. A., Francois, R., Murray, D. W. and Prell, W. L., 1995. Climate-related variations in denitrification in the Arabian Sea from sediment $^{15}N/^{14}N$ ratios. *Nature*, 373: 506-509.

Altenbach, A. V. and Sarnthein, M., 1989. Productivity record in benthic foraminifera. *In*: Productivity of the Ocean: Present and Past, Berger, W. H., Smetacek, V. S. and Wefer, G. (Eds.), Dahlem Konferenzen, *John Wiley & Sons*, pp. 255-269.

Anderson, D. M., Prell, W. L. and Barrat, N. J., 1989. Estimates of sea surface temperature in the coral sea at the last glacial maximum. *Paleoceanography*, 193-208.

Bailey, S. W., 1988. Odinite: A new dioctahedral-trioctahedral Fe-rich 1:1 clay mineral. *Clay Minerals*, 23: 237 - 247.

Balaram, V. and Saxena, V. K., 1988. Determination of rare earth elements (REE) in standard geological reference samples by Inductively Coupled Plasma-Mass Spectrometry (ICP-MS) using Indium as internal standard. *Ist International Conference on Plasma Source Mass Spectrometry*. Durham Univeristy, UK (Abstract), pp. 44.

Bard, E., Rostek, F. and Sonzogni, C., 1997. Interhemispheric synchrony of the last deglaciation inferred from the alkenone paleothermometry. *Nature*, 385: 707-710.

Barnola, J. M., Raynaud, D., Korotkerich Y. S. and Lorius, C., 1987. Vostok ice core: a 160, 000 years record of atmospheric CO_2. *Nature*, 329: 408-414.

Beck, J. W., Récy, J., Taylor, F., Edwards, R. L. and Cabioch, G., 1997. Abrupt changes in early Holocene tropical sea surface temperature derived from coral records. *Nature*, 385: 705-707.

Berger, W. H., Diester-Haas, L. and Killingley, J. S., 1978. Upwelling off Northwest Africa: the Holocene decrease as seen in carbon isotopes and sedimentological indicators. *Oceanologica Acta*, 1: 1-7.

Bhattathiri, P. M. A., Pant, A., Sawant, S., Gauns, M., Matondkar, S. G. P. and Mohanraju, R., 1996. Phytoplankton production and chlorophill distribution in the eastern and central Arabian Sea in 1994-1995. *Current Science* (JGOFS- India Special Section), 71(11): 857-862.

Biscaye, P. E., 1965. Mineralogy and sedimentation of deep sea clay in the Atlantic Ocean and adjacent sea and oceans. *Bulletin Geological Society of America*, 76: 803-832.

Brassel, S. C., Eglinton, G., Marlowe, I. T., Pflaumann, U. and Sarnthein, M., 1986. Molecular stratigraphy: a new tool for climatic assessment. *Nature*, 320: 129-133.

Brummer, G. -J. A. and Kroon, D., 1988. Planktonic foraminifers as tracers of ocean-climate history. *Free University Press*, Amsterdam, pp. 346.

Calvert, S. E. , Bustin, R. M. and Pedersen, T. F., 1992. Lack of evidence for enhanced preservation of sedimentary organic matter in the oxygen minimum of the Gulf of California. *Geology,* 20: 757-760.

Calvert, S. E., Douglas, F., Cowie, G. L., Schubert, C., von Rad, U., Schulz, H., Berner, U. and Erlenkeuser, H., 1996. Late Pleistocene record of organic carbon accumulation in the northeastern Arabian Sea. *International Symposium on Geology and Geophysics of the Indian Ocean*, Goa (Abstract), pp. 60-61.

Calvert, S. E. and Pedersen, T. F., 1992. Organic carbon accumulation and preservation in marine sediments: how important is anoxia? *In*: Organic carbon productivity, accumulation and preservation in Recent and Ancient sediments. Whelan, J. K. and Farrington, J. W. (Eds.), *Columbia University Press*, pp. 231-263.

Calvert, S. E. , Pedersen, T. F., Naidu, P. D. and von Stackelberg, U., 1995. On the organic carbon maximum on the continental slope of the eastern Arabian Sea. *Journal of Marine Research* 53: 269-296.

Chamley, H., 1989. Clay Sedimentology, *Springer-Verlag*, Berlin, 623 pp.

Clemens, S. and Prell, W. L., 1990. Late Pleistocene variability of Arabian Sea summer monsoon winds and continental aridity; eolian records from the lithogenic component of deep-sea sediments. *Paleoceanography*, 5(2): 109-145.

Clemens, S., Prell, W.L., Murray, D., Shimmield, G. B. and Weedon, G., 1991. Forcing mechanisms of the Indian Ocean monsoon. *Nature*, 353: 720-725.

CLIMAP, 1976. The surface of the ice-age earth. *Science*, 191: 1131-1137.

CLIMAP Project Members, 1981. Seasonal reconstruction of the Earth's Surface at the Last Glacial Maximum. *Geological Society of America Map and Chart series,* MC-36.

Codispoti, L. A., 1983. On nutrient variability and sediments in the upwelling regions. *In*: Coastal upwelling, its sediment record, Part A, Suess, E. and Thiede, J. (Eds.), *Plenum*, New York, 10A: 99-121.

Craig, H., 1953. Carbon-13 in plants and the relationships between carbon-13 and carbon-14 variations in nature. *Geology*, 62: 115-149.

Craig, H., 1957. Isotopic standards for carbon and oxygen and correction factors for mass-spectro-metric analysis of carbon dioxide. *Geochimica et Cosmochimica Acta*, 12: 133-149.

Curry, W. B., Ostermann, D. R., Guptha, M. V. S. and Ittekkot, V., 1992. Foraminiferal production and monsoonal upwelling in the Arabian Sea: evidence from sediment traps. *In*: Upwelling systems: evolution since the early Miocene, Summerhayes, C. P., Prell, W. L. and Emeis, K. C. (Eds.), *Geological Society Special Publication* No. 64, pp. 93-106.

Dawson, A. G., 1992. Ice Age Earth - Late Quaternary geology and climate. Physical Environment Series, *Routledge*, London New York, 293 pp.

Dean, W. E., Gardner, J. V. and Anderson, R. Y., 1994. Geochemical evidence for enhanced preservation of organic matter in the oxygen minimum zone of the continental margin of northern California during the late Pleistocene. *Paleoceanography* 9: 47-61.

Degens, E. T. and Ittekkot, V., 1984. A new look at clay-organic interactions. *Mitteilungen Geologisch Paläontologishes Institut der Universität Hamburg*, Festband Georg Knetsch, Heft 56: 229-248.

Demaison, G. and Moore, G. T., 1980. Anoxic environments and oil source bed genesis. *American Association of Petroleum Geologists Bulletin,* 64: 1179-1209.

Descolas-Gros, C. and Fontugne, M. R., 1985. Carbon fixation in marine phytoplankton: carboxylase activities and stable carbon isotope ratios; physiological and paleoclimatological aspects. *Marine Biology*, 87: 1-6.

Deuser, W. G., Ross, E. H., Hemleben, C. and Spindler, M., 1981. Seasonal changes in species composition, numbers, mass, size, and isotopic composition of planktonic foraminifera settling into the deep Sargasso Sea. *Palaeogeography, Palaeoclimatology, Palaeoecology*, 33: 103-127.

Duplessy, J. -C., 1982. Glacial to interglacial contrast in the northern Indian Ocean. *Nature*, 295: 494-498.

Duplessy, J. -C., Blanc, P. L. and Bé, A. W. H., 1981. Oxygen-18 enrichment of planktonic foraminifera due to gametogenic calcification below the euphotic zone. *Science*, 213: 1247-1250.

Dürkoop, A., Hale, W., Mulitza, S., Pätzold, J. and Wefer, G., 1997. Late Quaternary variations of sea surface salinity and temperature in the western tropical Atlantic: Evidence from $\delta^{18}O$ of *Globigerinoides sacculifer*. *Paleoceanography*, 12(6): 764-772.

El Wakeel, S. K. and Riley, J. P. 1957. Determination of organic matter in marine muds. *Journal du Conseil International pour l' Exploration de la Mer*, 22: 180-183.

Emiliani, C., 1955. Pleistocene temperatures. *Journal of Geology*, 63(6): 538-578.

Emrich, K., Ehhalt, D. H. and Vogel, J. C., 1970. Carbon isotope fractionation during the precipitation of calcium carbonate. *Earth and Planetary Science Letters*, 8: 363-371.

Epstein, S., Buchsbaum, R., Lowenstam, H. A. and Urey, H. C., 1953. Revised carbonate, water isotopic temperature scale. *Geological Society of America Bulletin*, 64: 1315-1326.

Erez, J., 1978. Vital effect on stable-isotope composition seen in foraminifera and coral skeletons. *Nature*, 273: 199-202.

Erez, J. and Honjo, S., 1981. Comparison of isotopic composition of planktic foraminifera in plankton tows, sediment traps and sediments. *Palaeogeography, Palaeoclimatology, Palaeoecology*, 33: 129-156.

Espitalié, J., Deroo, G. and Marquis, F., 1985. Rock-Eval pyrolysis and its applications. *Revue de l'Institut Francais du Petrol*, 40: 755-784.

Espitalié, J. and Joubert, L., 1987. Use of T_{max} as a maturation index in petroleum exploration. *In*: Petroleum Geochemistry and Exploration in the Afro-Asian Region. Kumar, R. K., Dwivedi, P., Banerji, V. and Guptha, V. (Eds.), *Rotterdam, A. A. Balkema,* pp. 67-73.

Fairbanks, R. G., 1989. A 17,000 year glacio-eustatic sea level record: Influence of glacial melting rates on the Younger Dryas event and deep-ocean circulation. *Nature*, 342: 637-642.

Fairbanks, R. G., Sverdlove, M., Free, R., Wiebe, P. H. and Bé, A. W. H., 1982. Vertical distribution and isotopic fractionation of living planktonic foraminifera from the Panama Basin. *Nature*, 298: 841-844.

Fleet, A. J., 1984. Aqueous and sedimentary geochemistry of the rare earth elements. *In*: Rare Earth Element Geochemistry, P. Henderson (Editor). (Developments in Geochemistry, 2) *Elsevier,* Amsterdam, 510 pp.

Fleet, A. J., Buckley, H. A. and Johnson, L. R., 1980. The rare earth element geochemistry of glaucony and celadonites. *Journal of Geological Society of London*, 137: 683 - 688.

Folk, R. L., 1968. Petrology of sedimentary rocks, *Hemphills*, Austin. 177 pp.

Fontugne, M. R. and Duplessy, J. -C., 1981. Organic carbon isotopic fractionation by marine plankton in the temperature range -1 to 31ºC. *Oceanologica Acta*, 4(1): 85-90.

Fontugne, M. R. and Duplessy, J. -C., 1986. Variations of the monsoon regime during the upper Quaternary: evidence from carbon isotopic record of organic matter in north Indian Ocean sediment cores. *Palaeogeography, Palaeoclimatology, Palaeoecology*, 56: 69-88.

Ganeshram, R. S., Pedersen, T. F., Calvert, S. E. and Murray, J. W., 1995. Large changes in oceanic nutrient inventories from glacial to interglacial periods. *Nature*, 376: 755-758.

Ganssen, G. and Sarnthein, M., 1983. Stable-isotope composition of foraminifers: the surface and bottom water record of coastal upwelling. *In*: Coastal upwelling, its sediment record, Suess, E. and Thiede, J. (Eds.). *Plenum*, New York, 10A: 99-121.

Gasse, F. and van Campo, E., 1994. Abrupt post-glacial climate events in West Asia and North Africa monsoon domains. *Earth and Planetary Science Letters*, 126: 435-456.

Gibbs, R. J., 1977. Clay mineral segregation in the marine environment. *Journal of Sedimentary Petrology*, 47: 237-243.

Gingele, F. X., 1996. Holocene climatic optimum in Southwest Africa- evidence from the marine clay mineral record. *Palaeogeography, Palaeoclimatology, Palaeoecology*, 122: 77-87.

Gingele, F. X., Müller, P. J., Schneider, R. R., 1998. Orbital forcing of freshwater input in the Zaire Fan area- clay mineral evidence from the last 200 kyr. *Palaeogeography, Palaeoclimatology, Palaeoecology*, 138: 17-26.

Goldberg, E. D. and Griffin, J. J., 1970. The sediments of the northern Indian Ocean. *Deep Sea Research*, 17: 513-537.

Griffin, J. J., Windson, H. and Goldberg, E. D., 1968. The distribution of clay minerals in the World Ocean. *Deep-Sea Research*, 15: 433-459.

Grimm, R. E., 1968. Clay Mineralogy, *McGraw Hill Book Company*, New York, 600 pp.

Grossman, E. L., 1987. Stable isotopes in modern benthic foraminifera: a study of vital effect. *Journal of Foraminiferal Research*, 17(1): 48-61.

Hartnett, H. E., Keil, R. G., Hedges, J. I. and Devol, A. H., 1998. Influence of oxygen exposure time on organic carbon preservation in continental margin sediments. *Nature*, 391: 572-574.

Hashimi, N. H., Nair, R. R., Kidwai, R. M. and Rao, V. P., 1982. Carbonate mineralogy and faunal relationship in tropical shallow water marine sediments. *Sedimentary Geology*, 32: 89-98.

Hastenrath, S. and Greischar, L., 1991. The monsoonal current regimes of the tropical Indian Ocean: Observed surface flow fields and their geostrophic and wind-driven components. *Journal of Geophysical Research*, 96: 12619-12633.

Hedges, J. I., 1992. Global biogeochemical cycles: progress and problems. *Marine Chemistry*, 39: 67-93.

Hedges, J. I. and Keil, R. G., 1995. Sedimentary organic matter preservation: an assessment and speculative synthesis. *Marine Chemistry*, 49: 81-115.

Hoefs, J., 1987. Stable Isotope Geochemistry, 3rd edition, *Springer-Verlag*, Berlin Heidelberg, 237 pp.

Hülsemann, J., 1966. On the routine analysis of carbonates in unconsolidated sediments. *Journal of Sedimentary Petrology,* 36: 622-625.

Imbrie, J., Hays, J. D., Martinson, D. G., McIntyre, A., Mix, A. C., Morley, J. J., Pisias, N. G., Prell, W. L. and Shackleton, N. J., 1984. The orbital theory of of Pleistocene climate: support from a revised chronology of the marine $\delta^{18}O$ record. *In*: Milankovitch and Climate - Part I, Berger, A., Imbrie, J., Hays, J., Kukla, G. and Saltzman, B. (Eds.). *D. Reidal Publ. Company*, Dordrecht, Netherlands, pp. 269-305.

Jacobs, M. B., and Hays, J. D., 1972. Palaeoclimatic events indicated by changes in deep sea sediments. *Journal of Sedimentary Petrology*, 42: 889-989.

Jarvis, I. and Jarvis, K. E., 1985. Rare earth element geochemistry of standard sediments: A study using Inductively Coupled Plasma Spectrometry. *Chemical Geology*, 53: 335-344.

Jasper, J. P. and Gagosian, R. B., 1990. The sources and deposition of organic matter in the Late Quaternary Pigmy basin, Gulf of Mexico. *Geochimica et Cosmochimica Acta*, 54: 1117-1132.

Katz, B. J., 1983. Limitations of "Rock-Eval" pyrolysis for typing organic matter. *Organic Geochemistry,* 4 :195-199.

Kolla, V., Henderson, L. and Biscaye, P. E., 1976. Clay mineralogy and sedimentation in the western Indian Ocean. *Deep Sea Research*, 23: 946-961.

Kolla, V., Kostecki, J. A., Robinson, F., Biscaye, P. and Ray, P. K., 1981. Distribution and origin of clay minerals and quartz in surface sediments of the Arabian Sea. *Journal of Sedimentary Petrology*, 51: 563-569.

Konta, J., 1985. Mineralogy and chemical maturity of suspended matter in major rivers samples under the SCOPE/UNEP Project. *Mitteilungen Geologisch Paläontologishes Institut, Universität Hamburg*, Heft 58: 557-568.

Krishnan, M. S., 1968. Geology of India and Burma, *Higginbothoms Ltd.*, Madras, 536 pp.

Kroopnick, P., 1974. Correlations between ^{13}C and ΣCO_2 in surface waters and atmospheric CO_2. *Earth and Planetary Science Letters*, 22: 397-403.

Kroopnick, P., 1985. The distribution of carbon-13 in the world oceans. *Deep Sea Research*, 32: 57-84.

Kumar, S. P. and Prasad, T. G., 1996. Winter cooling in the northern Arabian Sea. *Current Science* (JGOFS-India Special Section), 71: 834-841.

Kutzbach, J. E., 1981. Monsoon climate of the Early Holocene: climate experiment with the Earth's orbital parameters for 9,000 years ago. *Science*, 214: 59-61.

Kutzbach, J. E. and Street-Perrot, F. A., 1985. Milankovitch forcing of fluctuations in the level of tropical lakes from 18 to 0 kyr B. P. *Nature*, 317: 130-134.

Labeyrie, L. D., Duplessy, J. -C. and Blank, P. L., 1987. Variations in mode of formation and temperature of oceanic deep waters over the past 125,000 years. *Nature*, 327: 477-482.

Lal, D., 1994. Biogeochemistry of the Arabian Sea: Present information and gaps. *In*: Biogeochemistry of the Arabian Sea, Lal, D. (Ed.), *Proceedings of Indian Academy of Sciences* (Earth and Planetary Sciences), 103(2): 99-106.

Langford, F. F. and Blanc-Valleron, M. M., 1990. Interpreting Rock-Eval pyrolysis data using graphs of pyrolysable hydrocarbons vs. total organic carbon. *American Association of Petroleum Geologists Bulletin*, 74: 799-804.

Lisitzin, A. P., 1972. Sedimentation in the world oceans. *SEPM Special Publication*, Tulsa, 17: 218 pp.

Longhurst, A. R. and Wooster, W. S., 1990. Abundance of oil sardine (*Sardinella longiceps*) and upwelling on the southwest coast of India. *Canadian Journal of Fisheries and Aquatic Sciences*, 47: 2407-2419.

Maldonado, A. and Stanley, D. J., 1981. Clay mineral distribution as influenced by depositional processes in the southeastern Levantine Sea. *Sedimentology*, 28: 21-32.

Mallik, T. K., Venkatesh, K. V., Sen Gupta, R., Rao, B. R. and Ramamurty, M., 1976. Heavy mineral distribution patterns in the northern part of the Arabian Sea, Western continental shelf of India. *Indian Journal of Earth Sciences*, 3: 178-187.

Manjunatha, B. R. and Shankar, R., 1992. A note on the factors controlling the sedimentation rate along the western continental shelf of India. *Marine Geology*, 104: 219-224.

McArthur, J. M., Tyson, R. V., Thomson, J. and Matey, D., 1992. Early diagenesis of marine organic matter: alteration of the carbon isotopic composition. *Marine Geology*, 105: 51-61.

McCorkle, D. C., Keigwin, L. D., Corliss, B. H. and Emerson, S. R., 1990. The influence of microhabitats on the carbon isotopic composition of deep-sea benthic foraminifera. *Paleoceanography*, 5(2): 161-185.

Milliman, J. D., Quraishee, G. S. and Beg, M. A. A., 1984. Sediment discharge from the Indus River to the Ocean: Past, present and future. *In*: Marine Geology and Oceanography of the Arabian Sea and Coastal Pakistan, Haq, B. U. and Milliman, J. D. (Eds.). *Van Nostrand Reinhold*, New York, pp. 65-70.

Millot, G., 1970. Geology of the clays. *Springer-Verlag*, New York, 375 pp.

Mix, A. C., Pisias, N. G., Zahn, R., Rugh, W., Lopez, C. and Nelson, K., (1991). Carbon-13 in Pacific deep and intermediate water, 0-370 ka: Implications for ocean circulation and Pleistocene CO_2. *Paleoceanography*, 6: 205-226.

Müller, P. J., Schnieder, R. R. and Ruhland, G., 1994. Late Quaternary PCO_2 variations in the Angola Current: evidence from organic carbon $\delta^{13}C$ and alkenone temperatures. *In*: Carbon cycling in the glacial ocean: constraints on the ocean's role in global change. R. Zahn *et al.* (Eds.). NATO ASI Series, *Springer-Verlag*, Berlin-Heidelberg, Vol. 117: 343-366.

Murray, R. W., Buchholtz-Ten Brink, M. R., Gerlach, D. C., Price Russ III, G. and Jones, D. L., 1992. Interoceanic variation in the rare earth, major and trace element depositional chemistry of chert: Perspectives gained from the DSDP and ODP records. *Geochimica et Cosmochimica Acta*, 56: 1897-1913.

Murthy, K. S. R., 1989. Seismic stratigraphy of Ongole-Paradip continental shelf, east coast of India. *Indian Journal of Marine Sciences*, 16: 47-58.

Murthy, K. S. R., Rao, T. C. S., Subramanyam, A. S., Rao, M. M. M. and Lakshminarayana, S., 1993. Structural lineaments from the magnetic anomaly maps of the eastern continental margin of India (ECMI) and NW Bengal fan. *Marine Geology*, 114: 171-183.

Naidu, A. S., Mowatt, T. C., Somayajulu, B. L. K. and Rao, K. S., 1985. Characteristics of the clay minerals in the bed loads of major rivers of India. *Mitteilungen Geologisch Paläontologishes Institut Universität Hamburg*, SCOPE/UNEP Sonderband, 58: 559-568.

Naidu, P. D., 1996. Onset of an arid climate at 3.5 ka in the tropics: Evidence from monsoon upwelling record. *Current Science*, 71 (9): 715-718.

Naidu, P. D., 1995. High-resolution studies of Asian Quaternary monsoon climate and carbonate records from the equatorial Indian Ocean. *Ph.D Thesis*, Göteborg University, A7, 36 pp.

Naidu, P. D. and Malmgren, B. A., 1995. Monsoon upwelling effects on test size of some planktonic foraminiferal species from the Oman Margin, Arabian Sea. *Paleoceanography*, 10: 117-122.

Nair, R. R., 1975. Unique mud banks, Southwest India. *American Association of Petroleum Geologists Bulletin*, 60: 616-621.

Nair, R. R., Hashimi, N. H. and Rao, V. P., 1982a. On the possibility of high velocity tidal streams as dynamic barriers to longshore sediment transport: Evidence from the continental shelf off the Gulf of Kutch, India. *Marine Geology*, 47: 77-86.

Nair, R. R., Hashimi, N. H. and Rao, V. P., 1982b. Distribution and dispersal of clay minerals on the western continental shelf of India. *Marine Geology*, 50: M1-M9.

Nair, R. R., Ittekkot, V., Manganini, S. J., Ramaswamy, V., Haake, B., Degens, E. T., Desai, B. N. and Honjo, S., 1989. Increased particle flux to the deep ocean related to monsoon. *Nature*, 338: 749-751.

Nair, R. R. and Pylee, A., 1968. Size distribution and carbonate content of the sediments of the western shelf of India. *Bulletin of National Institute of Sciences, India*, 38: 411 - 420.

Naqvi, W. A., 1987. Some aspects of the oxygen deficient conditions and denitrification in the Arabian Sea. *Journal of Marine Research*, 45: 1049-1072.

Naqvi, W. A. and Fairbanks, R. G., 1996. A 27,000 year record of Red Sea Outflow: Implications for timing of post-glacial monsoon intensification. *Geophysical Research Letters*, 23(12): 1501-1504.

Nath, B. N., 1993. Rare earth element geochemistry of the sediments, ferromanganese nodules and crusts from the Indian Ocean. *Ph.D Thesis* (Unpublished), Goa University, Goa, India, 176 pp.

Nath, B. N., Balaram, V., Sudhakar, M. and Plüger, W. L., 1992. Rare earth element geochemistry of ferromanganese deposits from the Indian Ocean. *Marine Chemistry*, 38: 185 - 208.

National Geographic Society, 1981. *Atlas of the World*, Fifth Edition, National Geographic Society, Washington, D. C., 383 pp.

NOAA, 1994. World Ocean Atlas: 1x1 Degree Seasonal Means. *http://www.ferret.wrc.noaa.gov/fbin/climate_server.*

O'Hare, G., 1997. The Indian monsoon, Part 1: The wind system. *Geography*, 82(3): 218-230.

Odin, G. S., 1985. La verdine, faciès granulaire vert, marin et côtier, distinct de la glauconie: distribution actuelle et composition. *Comptes Rendus de l' Académie des Sciences de Paris*, 301: 105-108.

Odin, G. S., 1988. Green Marine Clays. (Developments in Sedimentology, 45) *Elsevier*, Amsterdam, 445 pp.

Odin, G. S., 1990. Clay mineral formation at the continent-ocean boundary: the verdine facies. *Clay Minerals*, 25: 477 - 483.

Odin, G. S., Amouric, M., Bailey, S. W. and Mackinnon, D. R., 1989. Minéralogie du faciès verdine. *Comptes Rendus de l' Académie des Sciences de Paris*, 308: 395 - 400.

Odin, G. S. and Matter, A., 1981. De glauconiarum origine. *Sedimentology*, 28: 611 - 641.

Oppo, D. W. and Fairbanks, R. G., 1989. Carbon isotope composition of tropical surface water during the past 22,000 years. *Paleoceanography*, 4 (4): 333-351.

Pant, G. B. and Maliekal, J. A., 1987. Holocene climatic changes over northwest India: an appraisal. *Climate Change*, 10: 183-194.

Paropkari, A. L., Babu, C. P. and Mascarenhas, A., 1992. A critical evaluation of depositional parameters controlling the variability of organic carbon in Arabian Sea sediments. *Marine Geology*, 107: 213-226.

Paropkari, A. L., Babu, C. P. and Mascarenhas, A., 1993. New evidence for enhanced preservation of organic carbon in contact with oxygen minimum zone on the western continental slope of India. *Marine Geology*, 111: 7-13.

Paropkari, A. L., Iyer, S. D., Chauhan, O. S. and Babu, C. P., 1991. Depositional environments inferred from variations of calcium carbonate, organic carbon and sulfide sulfur: A core from southwestern Arabian Sea. *Geo-Marine Letters*, 11: 96-102.

Paropkari, A. L., Rao, Ch. M. and Murty, P. S. N., 1987. Environmental controls on the distribution of organic matter in recent sediments of the western continental margin of India. *In*: Petroleum Geochemistry and Exploration in the Afro-Asian Region. Kumar, R. K., Dwivedi, P., Banerji, V. and Guptha, V. (Eds.). *Rotterdam, A. A. Balkema*, pp. 347-361.

Pedersen, T. F. and Calvert, S. E., 1990. Anoxia vs. productivity: What controls the formation of organic carbon-rich sediments and sedimentary rocks? *American Association of Petroleum Geologists Bulletin*, 74: 454-466.

Pedersen, T. F., Shimmield, G. B. and Price, N. B., 1992. Lack of enhanced preservation of organic matter in sediments under the oxygen minimum in the Oman margin. *Geochimica et Cosmochimica Acta*, 56: 545-551.

Pierce, J. W. and Siegel, F. R., 1969. Quantification in clay mineral studies of sediments and sedimentary rocks. *Journal of Sedimentary Petrology*, 39: 187-193.

Piper, D. Z., 1974a. Rare earth elements in the sedimentary cycle: a summary. *Chemical Geology*, 17: 287 - 297.

Piper, D. Z., 1974b. Rare earth elements in ferromanganese nodules and other marine phases. *Geochimica et Cosmochimica Acta*, 38: 1007-1022.

Piper, D. Z., Baedecker, P. A., Crock, J. G., Burnett, W. C. and Leobner, B. J., 1988. Rare earth elements in the phosphatic- enriched sediment of the Peru Shelf. *Marine Geology*, 80: 269-285.

Prahl, F. G., Muehlhausen, L. A. and Zahnle, D., 1988. Further evaluation of long-chain alkenones as indicators of paleoceanographic conditions. *Geochimica et Cosmochimica Acta*, 52: 2303-2310.

Prell, W. L., 1984a. Variation of monsoonal upwelling: A response to changing solar radiation. *In*: Climate Processes and Climate Sensitivity. Hansen, J. E. and Takahashi, T. (Eds.). *Geophysical Monograph Series*, AGU, Washington D.C., 29: 48-57.

Prell, W. L., 1984b. Monsoonal climate of the Arabian Sea during the Late Quaternary: A response to changing solar radiation. *In*: Milankovitch and climate-Part I, Berger, A., Imbrie, J., Hays, J., Kukla, G. and Saltzman, B. (Eds.). *D. Reidal Publishing Company*, Dordrecht, The Netherlands, pp. 349-366.

Prell, W. L. and Curry, W. B., 1981. Faunal and isotopic indices of monsoonal upwelling: Western Arabian Sea. *Oceanologica Acta*, 4(1): 91-98.

Prell, W. L., Hutson, W. H., Williams, D. F., Bé, A. W. H., Geitsennauer, K. and Molfino, B., 1980. Surface circulation of the Indian Ocean during the Last Glacial Maximum, approximately 18,000 year B. P. *Quaternary Research*, 14: 309-336.

Prell, W. L., Imbrie, J., Martinson, D. G., Morley, D. G., Pisias, N. G., Shackleton, N. J. and Streeter, H. F., 1986. Graphic correlation of oxygen isotope stratigraphy application to the late Quaternary. *Paleoceanography*, 1: 137-162.

Prell, W. L. and Kutzbach, J. E., 1987. Monsoon variability over the past 150,000 years. *Journal of Geophysical Research*, 92: 8411-8425.

Prell, W. L., Nitsuma, N. *et al.*, 1991. *Proceedings of ODP Scientific Results*, Vol. 117, College Station, Texas.

Prell, W. L. and van Campo, E., 1986. Coherent response of Arabian Sea upwelling and pollen transport to late Quaternary monsoonal winds. *Nature*, 323: 526-528.

Qasim, S. Z., 1977. Biological productivity of the Indian Ocean. *Indian Journal of Marine Sciences*, 6: 122-137.

Rajagopalan Geeta, Sukumar, R., Ramesh, R., Pant, R. K. and Rajagopalan, G., 1997. Late Quaternary vegetational and climatic changes from tropical peats in southern India- an extended record up to 40,000 years BP. *Current Science*, 73(1): 60-63.

Rao, K. L., 1979. India's water wealth: It's assessment, uses and projections. *Orient Longman Ltd.*, New Delhi (2nd Edition), 267 pp.

Rao, K. M. and Rao, T. C. S., 1994. Holocene sea levels of Vishakapatnam shelf, East Coast of India. *Journal of Geological Society of India*, 44: 685-689.

Rao, V. P., 1989. Some mineralogical investigations on the sediments of the continental margins of India and the Central Indian Basin and phosphorites of Error Seamount, Northwestern Arabian Sea. *Ph.D Thesis* (Unpublished), Andhra University, Waltair, 141 pp.

Rao, V. P., 1991. Clay mineral distribution in the continental shelf sediments from Krishna to Ganges river mouth, east coast of India. *Indian Journal of Marine Sciences*, 20: 7-12.

Rao, V. P. and Lamboy, M., 1996. Genesis of apatite in the phosphatized limestones of the western continental shelf of India. *Marine Geology*, 136: 41-53.

Rao, V. P., Lamboy, M. and Dupeuble, P. A., 1993. Verdine and other associated authigenic (glaucony, phosphate) facies from the surficial sediments of the southwestern continental margin of India. *Marine Geology*, 111: 133 - 158.

Rao, V. P. and Rao, B. R., 1995. Provenance and distribution of clay minerals in the sediments of the western continental shelf and slope of India. *Continental Shelf Research*, 15: 1757-1771.

Rao, V. P. and Wagle, B. G., 1997. Geomorphology and surficial geology of the western continental shelf and slope of India: A review. *Current Science*, 73(40): 330-350.

Rao, V. P., Rao, Ch. M., Thamban, M., Natarajan, R. and Rao, B. R., 1995. Origin and significance of high grade phosphorite in a sediment core from the continental slope off Goa, India. *Current Science*, 69: 1017-1022.

Rao, V. P., Thamban, M. and Lamboy, M., 1995. Verdine and glaucony facies from surficial sediments of the eastern continental margin India. *Marine Geology*, 127: 105-113.

Rao, V. P., Veerayya, M., Thamban, M., and Wagle, B. G., 1996. Evidences of Late Quaternary neotectonic activity and sea-level changes along the western margin of India. *Current Science,* 71: 213-219.

Rau, G. H., Froelich, P. N., Takahashi, T. and Des Marais, D. J., 1991. Does sedimentary organic $\delta^{13}C$ record variations in Quaternary ocean [CO_2(aq)]? *Paleoceanography*, 6(3): 335-347.

Sacket, W. M., 1964. The depositional history and isotopic organic carbon composition of marine sediments. *Marine Geology*, 2: 173-185.

Sarkar, A. and Bhattacharya, S. K., 1992. Glacial to interglacial isotopic changes in planktonic and benthic foraminifera from the western Arabian Sea. *In*: Oceanography of the Indian Ocean, B. N. Desai (Ed.). *Oxford & IBH*, New Delhi, pp. 417-425.

Sarkar, A., Ramesh, R., Bhattacharya, S. K. and Rajagopalan, G., 1990. Oxygen isotope evidence for a stronger winter monsoon current during the last glaciation. *Nature*, 343: 549-551.

Sarma, V. V. S. S., Kumar, M. D. and George, M. D., 1998. The central and eastern Arabian Sea as a perennial source of atmospheric carbon dioxide. *Tellus*, 50: 179-184.

Sarnthein, M., Winn, K., Duplessy, J. -C and Fontugne, M., 1988. Global variations of surface ocean productivity in low and mid latitudes: influence on CO_2 reservoirs of the deep ocean and atmosphere during the last 21,000 years. *Paleoceanography*, 3(3): 361-399.

Savin, S. M. and Yeh, H. -W., 1981. Stable isotopes in ocean sediments. *In*: Emiliani, C. (Ed.). The Sea, Vol. 7, *Wiley-Inter Science*, pp. 1521-1554.

Schneider, R. R., Dahmke, A., Kölling, A., Müller, P. J., Schulz, H. D. and Wefer, G., 1992. Strong deglacial minimum in the $\delta^{13}C$ record from planktonic foraminifera in the Benguela upwelling region: palaeoceanographic signal or early diagenetic imprint? *In*: Upwelling systems: evolution since the early Miocene, Summerhayes, C. P., Prell, W. L. and Emeis, K. C. (Eds.). *Geological Society Special Publication* No. 64, pp. 285-297.

Schneider, R. R., Müller, P. J. and Ruhland, G., 1995. Late Quaternary surface circulation in the east equatorial South Atlantic: Evidence from alkenone sea surface temperature. *Paleoceanography*, 10: 197-220.

Schott, F. 1983. Monsoon response of the Somali Current and associated upwelling. *Progress in Oceanography*, 12: 357-381.

Sen Gupta, R. and Naqvi, W. A., 1984. Chemical oceanography of the Indian Ocean, north of the equator. *Deep Sea Research*, 31: 671-706.

Shackleton, N. J., 1977. Carbon-13 in *Uvigerina*: Tropical rainforest history and and the equatorial Pacific carbonate dissolution cycles. *In*: The fate of fossil fuel CO_2 in the Oceans, Anderson, N. R. and Malhoff, A. (Eds.). *Plenum*, New York, pp. 401- 428.

Shackleton, N. J., 1987. Oxygen isotopes, ice volume and sea level. *Quaternary Science Reviews*, 6: 183-190.

Shackleton, N. J., Hall, M. A., Line, J. and Shuxi, C., 1983. Carbon isotope data in core V19-30 confirm reduced carbon dioxide concentration in the ice age atmosphere. *Nature*, 306: 319-322.

Shackleton, N. J. and Vincent, E., 1978. Oxygen and carbon isotope studies in recent foraminifera from the southwest Indian Ocean. *Marine Micropaleontology*, 3: 1-13.

Shapero, L. and Brannock, W. W., 1962. Rapid analysis of silicate, carbonate and phosphate rocks. *United States Geological Survey Bulletin*, 1144: A21-A22.

Shetye, S. R., Gouveia, A. D. and Shenoi, S. S. C., 1994. Circulation and water masses of the Arabian Sea. *In*: Biogeochemistry of the Arabian Sea, Lal, D. (Ed.). *Proceedings of Indian Academy of Sciences* (Earth and Planetary Sciences), 103 (2): 107-123.

Shetye, S. R., Gouveia, A. D., Shenoi, S. S. C., Michael, G. S., Sundar, D., Almeida, A. M. and Santanam, M., 1990. Hydrography and circulation off the west coast of India during the southwest monsoon. *Journal of Marine Research*, 48: 359-378.

Sheu, D. D. and Huang, C. Y., 1989. Carbonate and organic carbon sedimentation on the continental margin off southwestern Taiwan. *Geo-Marine Letters*, 9: 45-51.

Shimmield, G. B., Mowbray, S. R. and Weedon, G. P., 1990. A 350 ka history of the Indian southwest monsoon- evidence from deep sea cores, northwest Arabian Sea. *Transactions of the Royal Society of Edinburgh (Earth Sciences)*, 81: 289-299.

Shimmield, G. B., Price, N. B. and Pedersen, T. F., 1990. The influence of hydrography, bathymetry and productivity on sediment type and composition on the Oman Margin and in the northwestern Arabian Sea. *In*: Geology and Tectonics of the Oman Region, Robertson, A. H. F. *et al.* (Eds.). *Geological Society Special Publication*, 49: 759-769.

Sholkovitz, E. R., 1988. Rare earth elements in the sediments of the North Atlantic Ocean, Amazon delta and East China Sea: Reinterpretation of terrigenous input patterns to the oceans. *American Journal of Science*, 288: 236 - 281.

Singer, A., 1984. The palaeoclimatic interpretation of clay minerals in sediments- a review. *Earth-Science Reviews*, 21: 251-293.

Singh, G., Joshi, R. D. and Singh, A. B., 1972. Stratigraphic and radiocarbon evidence for the age and development of three salt lake deposits in Rajasthan, India. *Quaternary Research*, 2: 496-505.

Singh, G., Wasson, R. J., and Agrawal, D. P., 1990. Vegetational and seasonal climatic changes since the full glacial in the Thar Desert, northwestern India. *Review of Palaeobotany and Palynology*, 64: 351-358.

Sirocko, F., Garbe-Schönberg, D., McIntyre, A. and Molfino, B., 1996. Teleconnections betweeen the subtropical monsoons and high-latitude climates during the last deglaciation. *Science*, 272: 526-529.

Sirocko, F. and Lange, H., 1991. Clay accumulation rates in the Arabian Sea during the late Quaternary. *Marine Geology*, 97: 105-119.

Sirocko, F. and Sarnthein, M., 1989. Wind-borne deposits in the Northwestern Indian Ocean: record of Holocene sediments versus modern satellite data. *In*: Palaeoclimatology and Palaeometeorolgy: Modern and Past Patterns of Global Atmospheric Transport, Leinen, M. and Sarnthein, M. (Eds.). NATO ASI Series C282, *Kluwer*, Dordrecht-Boston-London, pp. 401-433.

Sirocko, F., Sarnthein, M., Erlenkeuser, H., Lange, H., Arnold, M. and Duplessy, J. -C., 1993. Century scale events in monsoon climate over the past 24,000 years. *Nature*, 364: 322-324.

Sirocko, F., Sarnthein, M., Lange, H. and Erlenkeuser, H., 1991. Atmospheric summer circulation and coastal upwelling in the Arabian Sea during the Holocene and last glaciation. *Quaternary Research*, 36: 72-93.

Slater, R. D. and Kroopnick, 1984. Controls on dissolved oxygen distribution and organic carbon deposition in the Arabian Sea. *In*: Marine Geology and Oceanography of the Arabian Sea and Coastal Pakistan, Haq, B. U. and Milliman, J. D. (Eds.). *Van Nostrand Reinhold*, New York, 305-313 pp.

Smith, S. L., Banse, K., Cochran, J. K., Codispoti, L. A., Ducklow, H. W., Luther, M. E., Olson, D. B., Peterson, W. T., Prell, W. L., Surgi, N., Swallow, J. C. and Wishner, K., 1991. U. S. JGOFS: Arabian Sea Process Study, U. S. JGOFS Planning Report No. 13, *Woods Hole Oceanographic Institution*, Woods Hole, Massachusetts, 164 pp.

Sonzogni, C., Bard, E. and Rostek, F., 1998. Tropical sea surface temperatures during the last glacial period: a view based on alkenones in Indian Ocean sediments. *Quaternary Science Reviews* (in press).

Spero, H. J., Bijma, J., Lea, D. W. and Bemis, B. E., 1997. Effect of sea water carbonate concentration on foraminiferal carbon and oxygen isotopes. *Nature*, 390: 497-500.

Spero, H. J. and Williams, D. F., 1988. Extracting environmental information from planktonic foraminiferal $\delta^{13}C$ data. *Nature*, 335: 717-719.

Steinmetz, J. C., 1994. Stable isotopes in modern coccolithophores. *In*: Coccolothophores, Winter, A. and Seisser, W. G. (Eds.). *Cambridge University Press*, pp. 219-229.

Stewart, R. A., Plikey, O. H. and Nelson, B. W., 1965. Sediments of the northern Arabian Sea. *Marine Geology*, 3: 413-427.

Street, F. A. and Grove, A. T., 1979. Global maps of lake-level fluctuations since 30,000 years BP. *Quaternary Research*, 12: 83-118.

Street-Perrott, F. A., Huang, Y., Perrott, R. A., Eglinton, G., Barker, P., Khelifa, L. B., Harkness, D. D. and Olago, D. O., 1997. Impact of lower atmospheric carbon dioxide on tropical mountain ecosystems. *Science*, 278: 1422-1426.

Subbarao, M., 1964. Some aspects of continental shelf sediments off the east coast of India. *Marine Geology*, 1: 59-87.

Subramanian, V., 1980. Mineralogical input of suspended matter by Indian rivers into the adjacent areas of the Indian Ocean. *Marine Geology*, 36: M29-M34.

Subramanian, V., Biksham, G. and Ramesh, R., 1987. Environmental geology of peninsular river basins of India. *Journal of Geological Society of India*. 30: 393-401.

Sukumar, R., Ramesh, R., Pant, R. K. and Rajagopalan, G., 1993. A $\delta^{13}C$ record of late Quaternary climate change from tropical peats in southern India. *Nature*, 364: 703-706.

Summerhayes, C. P., 1981. Organic facies of middle Cretaceous Black shales in deep north Atlantic. *American Association of Petroleum Geologists Bulletin*, 65: 2364-2380.

Swain, A. M., Kutzbach, J. E. and Hastenrath, S., 1983. Estimates of Holocene precipitation for Rajasthan, India, based on pollen and lake-level data. *Quaternary Research*, 19: 1-17.

Thamban, M., 1998. Changing depositional environments during the Late Quaternary along the western continental margin of India. *Journal of Indian Association of Sedimentologists* (in press).

Thamban, M. and Rao, V. P., 1998. Distribution and composition of verdine and glaucony facies from the sediments of the western continental margin of India. *In*: Marine Authigenisis: From Global to Microbial, Glenn, C. R., Lucas, J. and Prévöt, L. (Eds.), *SEPM Special Publication*, (in press).

Thamban, M., Rao, V. P. and Raju, S. V., 1997. Controls on organic carbon distribution in the sediment cores from the eastern Arabian Sea. *Geo-Marine Letters*, 17 (3): 20-27.

Thrivikramji, K. P. and Machado, T., 1982. Autochthonous glauconite in the sediments off Trivandrum coast, Kerala. *Indian Journal of Marine Sciences*, 11: 336 - 337.

Thunnel, R. C., Anderson, D., Gellar, D. and Miao, Q., 1994. Sea-Surface Temperature estimates for the Tropical Western Pacific during the last glaciation and their implications for the Pacific warm pool. *Quaternary Research*, 41: 255-264.

Tissot, B. P., Demaison, G., Masson, P., Delteil, J. R. and Combaz, A., 1980. Palaeoenvironment and petroleum potential of middle Cretaceous black shales in Atlantic basins. *American Association of Petroleum Geologists Bulletin*, 64: 2051-2063.

Tissot, B. P. and Welte, D. H., 1984. Petroleum formation and occurrence. Berlin, *Springer-Verlag*: 538 pp.

van Campo, E., 1986. Monsoon fluctuations in two 20,000 yr B. P. oxygen-isotope/ pollen records off southwest India. *Quaternary Research*, 26: 376-388.

van Campo, E., Duplessy, J. C. and Rossignol-Strick, M., 1982. Climatic conditions deduced from a 150 kyr oxygen isotope-pollen record from the Arabian Sea. *Nature*, 296: 56-59.

von Rad, U., Schulz, H. and SONNE 90 Scientific Party, 1995. Sampling the oxygen minimum zone off Pakistan: glacial-interglacial variations of anoxia and productivity (preliminary results, SONNE 90 Cruise). *Marine Geology*, 125: 7-19.

von Stackelberg, U. V., 1972. Faziesverteilung in Sedimentendes Indich-Pakistanischen Kontinental-Randes (Arabisches Meer). *Meteor Forschungsgebn.*, Reiche C. 9: 1-73.

Walsh, J. J., Rowe, G. T., Iverson, R. L. and McRoy, C. P., 1981. Biological export of shelf carbon is a sink for the global CO_2 cycle. *Nature*, 291: 196-201.

Warren, B. A., 1987. Ancient and medieval records of the monsoon winds and currents of the Indian Ocean. *In*: Monsoons, Fein, J. and Stephens, P. (Eds.). *John Wiley*, New York, pp. 137-158.

Webb III, T., Ruddiman, W. F., Street-Perrot, F. A., Markgraf, V., Kutzbach, J. E., Bartlein, P. J., Wright Jr., H. E. and Prell, W. L., 1993. Climatic changes during the past 18,000 years: Regional syntheses, mechanisms, and causes. *In*: Global climates since the last glacial maximum, Wright Jr., H. E., Kutzbach, J. E., Webb III, T., Ruddiman, W. F., Street-Perrot, F. A. and Bartlein, P. J. (Eds.). *University of Minnesota Press*, Minneapolis, USA, pp. 514-535.

Wefer, G. and Berger, W. H., 1991. Isotope paleontology: growth and composition of extant calcareous species. *Marine Geology*, 100: 207-248.

Whitehouse, G., Jeffrey, L. M. and Debbrecht, J. D., 1960. Differential settling tendencies of clay minerals in saline waters. *Clays, Clay Minerals*, 7: 1-79.

Williams, M. A. J. and Clarke, M. F., 1984. Late Quaternary environments in north-central India. *Nature*, 308: 633-635.

Wyrtki, K., 1971. Oceanographic Atlas of the International Indian Ocean Expedition. Washington. D.C., *National Science Foundation*, 531 pp.

Wyrtki, K., 1973. Physical Oceanography of the Indian Ocean. *In*: The Biology of the Indian Ocean, Zeitzschel, B. and Gerlach, S. A. (Ed.). *Springer-Verlag*, New York, pp. 18-36.

You, Y., 1997. Seasonal variations of thermocline circulation and ventilation in the Indian Ocean. *Journal of Geophysical Research*, 102(C5): 10,391-10,422.

You, Y. and Tomczak, M., 1993. Thermocline circulation and ventilation in the Indian Ocean derived from water mass analysis. *Deep Sea Research*, 40: 13-56.

Zahn, R., 1994. Fast flickers in the tropics. *Nature*, 372: 621-622.

Zahn, R. and Pedersen, T. F., 1991. Late Pleistocene evolution of surface and mid-depth hydrography at the Oman margin: planktonic and benthic isotope records at Site 724. *In*: *Proceedings of the Ocean Drilling Program,* Prell, W. L., Niitsuma, N., *et al.* (Eds.). College station, Texas, 117: 291-308.

Zahn, R., Winn, K. and Sarnthein, M., 1986. Benthic foraminiferal $\delta^{13}C$ and accumulation rates of organic carbon: *Uvigerina peregrina* group and *Cibicidoides wuellerstorfi*. *Paleoceanography*, 1(1): 27-42.

Zonneveld, K. A. F., Ganssen, G., Troelstra, S., Versteegh, G. J. M. and Visscher, H., 1997. Mechanisms forcing abrupt fluctuations of the Indian Ocean summer monsoon during the last deglaciation. *Quaternary Science Reviews*, 16: 187-201.

List of Publications of the Author

LIST OF PUBLICATIONS OF THE AUTHOR

1. V. Purnachandra Rao, **M. Thamban** and M. Lamboy (1995). Verdine and glaucony facies from surficial sediments of the eastern continental margin of India. **MARINE GEOLOGY**, 127: 105-113.

2. V. Purnachandra Rao, Ch. M. Rao, **M. Thamban,** R. Natarajan and B. R. Rao (1995). Origin and significance of high-grade phosphorite in a sediment core from the continental slope off Goa, India. **CURRENT SCIENCE**, 69: 1017-1022.

3. **M. Thamban** , K. Reghunadh and K. Sajan (1996). Distribution of Organic matter, Iron and Manganese in the estuarine clay of mangrove sediments, Tellicherry, Kerala. **JOUR. GEOL. SOC. INDIA**, 48: 183-188.

4. V. Purnachandra Rao, M. Veerayya, **M. Thamban** and B. G. Wagle (1996). Evidences of Late Quaternary neotectonic activity and sea-level changes along the western continental margin of India. **CURRENT SCIENCE**, 71: 213-219.

5. V. Purnachandra Rao and **M. Thamban** (1997). Dune associated calcretes, rhizoliths and palaeosols from the western continental shelf of India. **JOUR. GEOL. SOC. INDIA,** 49: 297-306.

6. **M. Thamban**, V. Purnachandra Rao and S. V. Raju (1997). Controls on organic carbon distribution in the sediment cores from the eastern Arabian Sea. **GEO-MARINE LETTERS,** 17 (3): 20-27.

7. **M. Thamban** and V. Purnachandra Rao (1998). Distribution and composition of verdine and glaucony facies from the sediments of the western continetal margin of India. *In*: ***Marine Authigenesis: From Global to Microbial.*** C. R. Glenn, J. Lucas and L. Prévöt (Editors), **SEPM Special Publication** (*in press*).

8. **M. Thamban** (1998). Changing depositional environments during the Late Quaternary along the western continental margin of India. **JOUR. INDIAN ASSOC. OF SEDIMENTOLOGISTS** (*in press*).